UNIVERSITÉ PARIS-SUD 11

ECOLE DOCTORALE :
INNOVATION THÉRAPEUTIQUE : DU FONDAMENTAL A L'APPLIQUÉ
PÔLE : PHARMACOLOGIE ET TOXICOLOGIE

ANNÉE 2011 SÉRIE DOCTORAT N°

THÈSE DE DOCTORAT
soutenue le 15 décembre 2011

Influence of a chronic ^{90}Sr contamination by ingestion on the hematopoietic, immune and bone systems

Influence d'une contamination chronique par ingestion de ^{90}Sr sur les systèmes hématopoïétique, immunitaire et osseux

par

Nicholas SYNHAEVE

Composition du jury :

Rapporteurs :	Pr. Marie-Hélène HENGE	INSTN (Bagnols-sur-Cèze, France)
	Dr. Francis HERODIN	CRSSA (La Tronche, France)
Examinateurs :	Dr. Saadia KERDINE-RÖMER	PARIS 11 (Châtenay-Malabry, France)
	Dr. Louis DE SAINT-GEORGES	SCK-CEN (Mol, Belgique)
	Dr. Jean-Marc BERTHO	IRSN (Fontenay-aux-Roses, France)

ECOLE DOCTORALE ED425
PÔLE : PHARMACOLOGIE ET TOXICOLOGIE

UNIVERSITÉ PARIS-SUD 11
UFR «FACULTÉ DE PHARMACIE DE CHATENAY-MALABRY »
5, rue Jean Baptiste Clément
92296 CHÂTENAY-MALABRY Cedex

Institut de Radioprotection et Sûreté Nucléaire (IRSN)
DRPH/SRBE/Laboratoire de Radiotoxicologie Expérimentale (LRTOX)
31, Av de la Division Leclerc
92262 Fontenay-aux-Roses

Remerciements

En premier lieu, je tiens à remercier sincèrement les membres du jury d'avoir accepté d'évaluer mon travail de thèse: Madame Marie-Hélène Henge et Monsieur Francis Herodin en tant que rapporteurs et Madame Saadia Kerdine-Römer et Monsieur Louis de Saint-Georges en tant qu'examinateurs. Merci pour le temps qu'ils ont bien voulu me consacrer.

J'exprime ma plus sincère gratitude à Monsieur Jean-Marc Bertho qui a su guider cette thèse avec compétence, efficacité et enthousiasme. Je suis très reconnaissant de la confiance qu'il m'a accordée, sa grande disponibilité et son soutient constant. Merci pour sa bonne pédagogie et tout ce qu'il m'a apporté d'un point de vue scientifique et non scientifique. C'était un grand plaisir travailler avec lui durant ces trois années.

Je tiens à remercier Monsieur Patrick Gourmelon, Madame Jocelyne Aigueperse, Messieurs Philippe Voisin et Patrick Laloi et Madame Isabelle Dublineau de m'avoir accueilli au sein de leurs équipes à l'IRSN et de m'avoir donné les moyens nécessaires à la réalisation de cette thèse.

Mes remerciements vont également au chercheurs Mesdames Teni Ebrahimian, Céline Dinocourt, Chrystelle Ibanez, Christine Linard, Valérie Holler, Noelle Mathieu, Christine Granotier et Aurélie Desbrée et Messieurs Yann Gueguen, Philippe Lestaevel, Mamaâr Souidi, Eric Blanchardon et François Boussin pour leurs nombreux et précieux conseils, aide et encouragements pendant nos discussions et collaborations. Merci pour leur sympathie et gentillesse.

Je remercie infiniment Mesdames Johanna Stefani et Line Grandcolas et Monsieur Stéphane Grison pour leur aide excellent à la paillasse et leurs conseils techniques. Merci pour votre grande disponibilité, discussions ouvertes et bonne humeur. Un grand merci en particulier à Madame Johanna Stefani, qui a partagé son bureau avec moi pendant trois ans, qu'elle soit assurée de ma sincère reconnaissance.

Mes remerciements s'adressent aussi à l'ensemble des thésards, stagiaires et post-doctorants que j'ai croisés pendant ces trois ans et qui m'ont apporté conseils, aide et amitié: Marième, Caroline, Radjini, Hélène, Carine, Clémentine, Clélia, Raphaëlle, Jean-Victor, Mohammad,

Thibault, Awatif, Karl, Rym, Marco, Baptiste, Stefania, Patricia, Hanane, Youssra, Fabrice, Ouarda, Yseult, Audrey, Anaïs et Fatoumata.

Je remercie également les membres du LRTOX de Pierrelatte pour leur accueil et leur aide. En particulier je remercie les zootechniciens Frédéric Voyer et Thierry Loiseau pour toute l'attention qu'ils ont portée aux animaux au cours de nos nombreuses expérimentations.

Je remercie également tous mes collègues des autres laboratoires du SRBE pour leur sympathie.

Merci à Mesdames Veronique Joffres, Keltoum Mediana et Delphine Lurmin pour leur aide administrative et leur gentillesse.

Je remercie vivement la famille Carrel pour l'accueil chaleureux dans leur gîte de la Baume-de-Transit pendant nos nombreux déplacements à Pierrelatte. Merci pour tous les bons moments que nous avons passé ensemble.

Je tiens à remercier Messieurs Peter Hoet, Benoit Nemery de Bellevaux et Jorge Boczkowski et Madame Franceline Marano qui m'ont transmis leur passion en toxicologie environnementale et qui m'ont motivé pour poursuivre mes études en France.

Je n'oublie pas mon frère, mes amis à Paris et en Belgique, qui sont des amis précieux.

Je remercie naturellement mes parents et mon grand-père, qui ont su me transmettre leur passion du travail et leur persévérance. Merci d'avoir toujours cru en moi et de m'avoir soutenu en permanence. Dank jullie voor alle steun.

Je tiens à remercier particulièrement Roser. Je la remercie très sincèrement pour sa très grande gentillesse, son attention, ses encouragements, et sa patience admirable pendant mes quatre ans à Paris. Merci à elle et sa famille de m'avoir toujours accueilli à bras ouverts à Barcelone. Els meus sincers agraïments pel seu suport.

A toutes et tous mille mercis.

Table of contents

Figures

Tables

Abbreviations

AA	ascorbid acid
ALI	annual limit on intake
ALP	alkaline phosphatase
ALT	alanine aminotransferase
APC	antigen presenting cell
AST	aspartate aminotransferase
BCR	B cell receptor
BFU	burst forming unit
BglyP	beta-glycerophosphate
BMP	bone morphogenetic protein
Bq	becquerel
BSA	bovine serum albumin
BSP	bone sialoprotein
BV	bone volume
Ca	calcium
CaSR	calcium sensing receptor
CD	cluster of differentiation
CFC	colony forming cell
CFU	colony forming unit
CNS	central nervous system
cpm	counts per minute
Cs	cesium
CTX	C-telopeptide from type 1 collagen
DCF	dose converting factor
DNA	deoxyribonucleic acid
DSB	double strand break
ELISA	enzyme linked immunosorbant assay
EPO	erythropoietin
EU	European Union
FGF	fibroblast like growth factor
GAPDH	glyceraldehyd 3-phosphate dehydrogenase
Gata3	Gata binding protein 3
GI	gastrointestinal
GM-CSF	granulocyte macrophage colony stimulating factor

Gy	gray
HES	hematoxylin eosin safran
HSC	hematopoietic stem cell
IAEA	International Atomic Energy Agency
ICRP	International Commission on Radiological Protection
IFN	interferon
Ig	immunoglobulin
IGF	insulin like growth factor
IL	interleukin
IRSN	Institut de Radioprotection et Sûreté Nucléaire
KLH	keyhole lympet hemocyanin
LDH	lactate dehydrogenase
LET	linear energy transfer
M-CSF	macrophage colony stimulating factor
MEM	minimum essential medium
MHC	major histocompatibility complex
min	minutes
MMP	matrix metalloproteinase
MNC	mononuclear cell
MSC	mesenchymal stem cell
NCX	natrium calcium exchanger
NISA	Nuclear and Industrial Safety Agency of Japan
NK	natural killer cell
NOAEL	no observed adverse effect level
OCN	osteocalcin
OD	optical density
OPG	osteoprotegerin
OPN	osteopontin
P	phosphorus
PBS	phosphate buffer saline
PCR	polymerase chain reaction
PHA	phytohemagglutinin
PINP	procollagen 1 N-terminal propeptide
ppm	parts per million
PTH	parathyroid hormone
RANK	receptor activator of nuclear factor kappa beta

RNA	ribonucleic acid
rpm	rounds per minute
RT	reverse transcriptase
RTG	radioisotope thermoelectric generator
Runx2	runt related transcription factor 2
SAF	specific absorption fraction
Sca-1	stem cell antigen 1
SCF	stem cell factor
SD	standard deviation
SDF-1	stem cell derived factor 1
Sr	strontium
Sv	sievert
T-bet	T-box expressed in T cells
TBS	tris buffer saline
TCR	T cell receptor
TGF-β	transforming growth factor beta
Th	T helper cell
TNF	tumor necrosis factor
TNT	trinitrotoluene
TPO	thrombopoietin
TRAP5b	tartrate resistant acid phosphatase 5b
TREC	TCR rearrangement excision circle
Treg	T regulatory cell
TT	tetanus toxin
TV	tissue volume
USSR	Union of Soviet Socialist Republics
VDR	vitamin D receptor
WBC	whole body counter
WHO	World Health Organization

Résumé

Introduction

Le questionnement sur les conséquences sanitaires des essais nucléaires aériens et des accidents d'installations nucléaires reste toujours d'actualité. En effet, des dizaines d'années après ces événements, différents radionucléides, en particulier le ^{137}Cs et le ^{90}Sr, sont toujours présents dans l'environnement du fait de leur demi-vie longue (Fairlie 2007; Kashparov et al. 2001). Ces radionucléides ont progressivement intégré les écosystèmes et les chaînes alimentaires menant à l'homme, et encore aujourd'hui des populations importantes ingèrent quotidiennement de faibles quantités de ces radioéléments, bien que des études aient montré une réduction de l'ingestion de radionucléides avec le temps (Assimakopoulos et al. 1995; Cooper 1992; Paasikallio et al. 1994; UNSCEAR 2000). Ces deux radionucléides sont principalement retrouvés dans les champignons, mais aussi dans le lait et les produits laitiers pour le ^{90}Sr (de Ruig and van der Struijs 1992; Hoshi et al. 1994). Les effets sanitaires non cancéreux de l'ingestion de ces petites quantités de radionucléides pendant de longues périodes restent mal connus. Des études chez les populations vivant sur les territoires contaminés de Tchernobyl ont montré des déséquilibres des systèmes hématopoïétique et immunitaire: par exemple une augmentation des immunoglobulines G et M circulantes chez des enfants (Titov et al. 1995), une diminution de l'activité du thymus et du nombre de lymphocytes chez les liquidateurs (Yarilin et al. 1993), une modification des populations lymphocytaires sanguines (Vykhovanets et al. 2000) ou une diminution de la réponse proliférative des lymphocytes après activation par différents mitogènes chez les liquidateurs (Kuzmenok et al. 2003). Cependant, ces études n'ont pas permis d'établir un lien direct entre l'ingestion chronique de radionucléides et les effets observés.

Notre laboratoire a lancé le programme de recherche ENVIRHOM, dans le but d'étudier les modifications non cancéreuses des grandes fonctions physiologiques de l'organisme à la suite d'une telle contamination. Dans un premier temps, des études ont été centrées sur le ^{137}Cs. Ces études ont montré que la contamination induit quelques modifications dans différents systèmes physiologiques des modèles de rongeurs utilisés. Par exemple, une modification des cycles veille-sommeil chez des rats (Lestaevel et al. 2006) a été démontrée, ce qui peut être associé à une réaction neuro-inflammatoire (Lestaevel et al. 2008). Également des

modifications du système cardio-vasculaire (diminution de la pression artérielle) (Gueguen et al. 2008), du métabolisme de la vitamine D (diminution de la vitamine D3 active dans le plasma) (Tissandie et al. 2006; Tissandie et al. 2009), du métabolisme du cholestérol (augmentation de différents cytochromes intervenant dans la transformation du cholestérol et des acides biliaires) (Racine et al. 2009; Racine et al. 2010b; Souidi et al. 2006) et du métabolisme des hormones stéroïdiennes (Grignard et al. 2008)ont été montrées. Cependant, la plupart des modifications observées sont au niveau moléculaire (telles que des modifications d'expression génique ou la variation de la synthèse des protéines) sans conséquences majeures sur l'état de santé des animaux (Lestaevel et al. 2010).

En revanche, d'autres études n'ont montré aucune modification des systèmes hématopoïétique et immunitaire après l'ingestion chronique de ^{137}Cs (Bertho et al. 2011; Bertho et al. 2010). Ceci suggère que le ^{90}Sr pourrait être impliqué dans les effets des systèmes hématopoïétique et immunitaire observés chez l'homme. Ce radionucléide est d'origine exclusivement anthropogénique et du fait de ses propriétés physico-chimiques, persiste à long terme dans l'environnement, ce qui a notamment conduit à la contamination chronique par ingestion de populations humaines en Russie, Ukraine et Biélorussie. L'induction de tumeurs osseuses liées à la fixation du ^{90}Sr dans les os après une contamination interne a été largement décrite dans différents modèles animaux (Galle 1982, 1997; Raabe et al. 1981b). Par contre, l'occurrence d'effets non cancéreux est beaucoup moins bien connue.

Son accumulation privilégiée au niveau de l'os pourrait conduire à une modification de la physiologie de la moelle osseuse et du fait de la proximité entre l'os et la moelle osseuse (Calvi et al. 2003; Taichman 2005), il est possible que l'irradiation localisée par les rayonnements β^- induise des effets sur la différenciation hématopoïétique et sur le développement du système immunitaire.

L'objectif de cette étude est donc de déterminer quelles sont les modifications fonctionnelles des systèmes hématopoïétique, immunitaire et osseux après une contamination chronique par ingestion à faible niveau de ^{90}Sr. L'étude est menée en parallèle sur deux modèles: *in vivo* (souris Balb/c) comme modèle de la situation des populations humaines, et *in vitro* (pré-ostéoblastes et cellules souches mésenchymateuses) pour étudier les mécanismes d'actions du ^{90}Sr.

Biocinétique de ^{90}Sr et doses absorbées

Pour le modèle *in vivo*, nous avons d'abord déterminé la biocinétique de ^{90}Sr après une contamination chronique par ingestion de l'eau de boisson (20 kBq/l, correspondant à une ingestion ciblée de 120 Bq/jour par animal à l'âge adulte) dans un modèle murin juvénile et adulte. La concentration utilisée a été utilisée dans les études précédentes (Bertho et al. 2011; Bertho et al. 2010) et correspond à différentes mesures de contenu en radionucléides dans le bol alimentaire des populations exposées. Pour le modèle juvénile, la contamination a débuté chez les parents avant l'accouplement et s'est poursuivi *via* l'eau de boisson après sevrage. Les descendants ont été sacrifiés entre la naissance et l'âge de 20 semaines, que ce soit pour la détermination de la concentration en ^{90}Sr dans les os ou pour les différents tests des fonctions hématopoïétique, immunitaire et osseuse.

La première étape a consisté à déterminer la biocinétique de ^{90}Sr. Aucune modification significative du poids des animaux n'a été observée entre les animaux témoins et contaminés, en tenant compte du sexe. Les animaux contaminés ont ingéré entre 40 et 91 Bq de ^{90}Sr par animal et par jour, selon l'âge et le sexe. Cette ingestion quotidienne de ^{90}Sr correspond aux estimations de présence de ^{90}Sr dans un bol alimentaire moyen dans les territoires contaminés (de Ruig and van der Struijs 1992; Hoshi et al. 1994). L'excrétion était plus importante par les féces que par les urines, ce qui montre que le ^{90}Sr n'est pas absorbé en totalité durant le transit intestinal.

Les résultats ont montré l'accumulation de ^{90}Sr dans les os. Ceci est en accord avec d'autres études expérimentales dans divers modèles animaux (Gillett et al. 1992; Lloyd et al. 1976; Raabe et al. 1981a), y compris des rats (Gran 1960; Nilsson 1970) et conformément avec le modèle biocinétique de strontium précédemment proposé par la CIPR (ICRP 1993; Leggett 1992; Lloyd et al. 1976). Les modèles juvéniles et adultes ont montré des tendances très différentes de l'accumulation du ^{90}Sr dans les os. Pour le modèle juvénile, le taux d'absorption du ^{90}Sr dans les os a été rapide pendant les premières semaines, puis atteint un niveau plateau à l'âge adulte. Ce niveau plateau d'accumulation de ^{90}Sr à l'âge adulte a également été observée dans une étude avec des beagles qui ont ingéré chroniquement du ^{90}Sr *in utero* jusqu'à 1,5 ans (Parks et al. 1984). Comme Book et al. l'ont montré, ce taux élevé d'accumulation de ^{90}Sr est corrélée avec la croissance osseuse (Book et al. 1982). Par ailleurs,

il a été décrit que le niveau d'absorption du strontium est limitée par la disponibilité de calcium. En effet le strontium et le calcium partagent les mêmes mécanismes de transport à travers la paroi intestinale et sont donc absorbés de façon compétitive (Apostoaei 2002; Hollriegl et al. 2006a; Hollriegl et al. 2006b; Hoshi et al. 1994). Une étude menée par Sugihira et al. a montré que le ratio de l'accumulation strontium vs. calcium dans les os était plus élevée au cours des âges jeunes, probablement à cause à une plus grande efficacité de l'absorption de strontium par l'intestin grêle au début de la vie (Sugihira et al. 1990). Ces mécanismes peuvent expliquer à la fois l'augmentation rapide de l'accumulation du ^{90}Sr à un jeune âge et le niveau plateau observé à l'âge adulte.

En revanche, pour le modèle adulte, une augmentation continue du taux de ^{90}Sr dans les os a été trouvée au cours des 20 semaines de l'ingestion chronique. Cela est probablement dû au faible niveau d'ingestion quotidienne qui ne permet pas d'atteindre l'équilibre entre l'ingestion, l'excrétion et l'accumulation dans l'os, mais aussi à la limitation de 20 semaines de durée d'ingestion. Le taux réduit de l'accumulation de ^{90}Sr dans le modèle adulte est conforme avec d'autres études montrant que l'accumulation de ^{90}Sr dans les os adultes est principalement liée au remodelage osseux (Dahl et al. 2001; Momeni et al. 1976a; Momeni et al. 1976b).

Par ailleurs, pour les deux modèles, l'accumulation du ^{90}Sr est systématiquement plus élevée dans les os des femelles que chez les mâles, ce qui pourrait être lié à la régulation hormonale de la physiologie osseuse (Chiu et al. 1999; Hotchkiss and Brommage 2000; Kalyan and Prior 2010), essentiellement à cause des œstrogènes impliqués dans la régulation de la physiologie osseuse. En effet, une étude a montré que les ostéoblastes expriment des récepteurs d'œstrogènes qui, une fois activés, favorisent la différenciation des ostéoblastes (Marie 2001).

De plus, des différences ont été observées selon les différents sites du squelette. Ceci a été également observé dans d'autres modèles animaux suite à une ingestion chronique de ^{90}Sr et pourrait dépendre des différences dans le remodelage osseux local et le débit sanguin régional (Dahl et al. 2001; Momeni et al. 1976a; Momeni et al. 1976b).

Dans tous les autres organes testés (sang, foie, rate, reins, thymus, cœur, poumons, système nerveux central, muscle, peau), le taux de ^{90}Sr était inférieur à la limite de détection. Néanmoins, de petites quantités de ^{90}Sr ont été trouvées dans le tube digestif. La mesure du taux de ^{90}Sr dans les différents segments du tube digestif (estomac, grêle, caecum et colon)

d'animaux a montré que les quantités de ^{90}Sr étaient uniquement détectables dans l'intestin grêle mais pas dans les autres segments. Cela suggère plutôt une rétention faible de ^{90}Sr dans les villosités de la muqueuse intestinale qu'une accumulation vraie dans le tissu intestinal, comme décrit précédemment pour l'ingestion d'uranium (Dublineau et al. 2007; Dublineau et al. 2005).

Les doses absorbées au corps entier qui résultent de cette accumulation osseuse de ^{90}Sr ont été calculées en utilisant des facteurs de conversion de dose (FCD) pour un modèle de rat publié par la CIPR. Il en résulte que les animaux du modèle juvénile recevaient une faible dose absorbée au corps entier variant de 0.3 ± 0.1 mGy à la naissance à 10.6 ± 0.1 mGy à l'âge de 20 semaines, avec des différences entre mâles et femelles. Le calcul des doses absorbées par des DCF a été vérifié en utilisant une méthode de calcul de dose basée sur des fractions d'absorption spécifique (FAS) pour un fantôme de souris voxelisé de Stabin et al. (Stabin et al. 2006) et une simulation Monte Carlo avec un fantôme de souris voxelisé du Laboratoire d'Evaluation de la Dose Interne (LEDI) de l'IRSN. Une bonne corrélation entre les doses estimées par les méthodes FCD, FAS et LEDI ont été retrouvées. De plus, le LEDI a calculé que la dose absorbée pour le squelette a été beaucoup plus élevée que les autres tissus et atteint 55 mGy pour le modèle juvéniles après 20 semaines d'ingestion chronique de ^{90}Sr.

Par conséquent, des effets éventuels de l'ingestion chronique de ^{90}Sr pourraient être observés sur la physiologie osseuse et le système hématopoïétique, en raison de la localisation des cellules souches hématopoïétiques (CSH) près de l'os (Calvi et al. 2003; Howard and Jannke 1970; Taichman 2005). En effet, un modèle dosimétrique a décrit que des doses de rayonnement beaucoup plus élevées peuvent atteindre les cellules souches hématopoïétiques en raison de la proximité de l'os (Eckerman and Stabin 2000). Comme la moelle osseuse est le site anatomique principal de la différenciation des lymphocytes B, des effets pourraient également être observés sur le système immunitaire.

L'utilisation du modèle juvénile pour étudier les effets potentiels de la contamination par l'ingestion chronique de ^{90}Sr sur la physiologie osseuse et les systèmes hématopoïétique et immunitaire semble être d'un intérêt particulier parce que le rayonnement absorbé est plus élevé que dans le modèle adulte. En effet, les systèmes hématopoïétique et immunitaire se développent essentiellement pendant la vie fœtale et postnatale et les juvéniles montrent une

sensibilité accrue envers de nombreux composés toxiques, y compris les radionucléides (Blakley 2005; Hoyes et al. 2000; Lindop and Rotblat 1962; Preston 2004).

Effets sur la physiologie osseuse

Pour la physiologie osseuse, nous n'avons pas observé une modification des taux plasmatiques de calcium et de phosphate pour les animaux contaminés par rapport aux animaux témoins. Ni les concentrations plasmatiques des hormones calciotropiques (vitamine D3 active et hormone parathyroïdienne) ni les marqueurs de la formation osseuse (alkaline phosphatase spécifique (bALP), protéine morphogénétique osseuse 2 (BMP2) et procollagène 1 propeptide N-terminal (PINP)) n'ont été modifiés. En revanche, une augmentation significative du taux plasmatique du marqueur de la résorption osseuse C-télopeptide du collagène de type 1 (CTX) a été observée chez des mâles contaminés. De plus, l'ingestion de ^{90}Sr et son accumulation dans l'os a induit une modification de l'expression des gènes impliqués dans la formation et la résorption osseuse, avec un déséquilibre favorisant la résorption osseuse. Nous avons donc examiné la morphologie osseuse chez les animaux à l'âge de 20 semaines. Nous n'avons pas observé de modification significative de l'épaisseur de la plaque de croissance ni de la surface osseuse. Ceci suggère donc que le déséquilibre induit par le ^{90}Sr dans le remodelage osseux ne conduit pas à l'apparition des modifications morphologiques. Cependant, nous ne pouvons pas exclure qu'à un temps plus tardif (au-delà de 20 semaines), des modifications morphologiques au niveau du tissu osseux puissent être observées pour les animaux contaminés.

Comme nous avons observé une modification de l'équilibre de la formation et la résorption osseuse au niveau de l'expression des gènes et des concentrations plasmatiques après une contamination chronique de ^{90}Sr, il serait intéressant d'étudier les effets morphologiques à des temps plus tardifs et de compléter l'étude par de l'immunohistologie et des mesures de la microarchitecture osseuse et de la solidité des os.

Effets sur le système hématopoïétique

Pour le système hématopoïétique, différents paramètres ont été étudiés et les effets sur le système hématopoïétique étaient limités. Le Flt3-ligand était significativement diminué à la

naissance chez des femelles contaminées. Ce résultat pourrait indiquer une hématopoïèse modifiée mais ceci n'a pas été confirmé ni par l'analyse phénotypique des cellules $Lin^{-}C\text{-}kit^{+}SCA\text{-}1^{+}$ dans la moelle osseuse, ni par la fréquence des progéniteurs dans la moelle osseuse et la rate. En revanche, des différences significatives au cours du temps (sans influence de l'état de la contamination des animaux) ont été observées pour certains paramètres, liés au développement normal du système hématopoïétique au cours de la vie post-natale (Tavian and Peault 2005).

Nos résultats suggèrent que l'ingestion chronique de ^{90}Sr à des faibles concentrations ne provoque pas un changement significatif dans la moelle osseuse de souris. Toutefois, des méthodes plus sensibles devraient être utilisées afin de confirmer cette hypothèse. Par exemple en regardant *in situ* les cellules souches hématopoïétiques (CSH) dans la niche ou d'effectuer des dosages plasmatiques des facteurs de croissance spécifiques de l'hématopoïèse, comme SDF-1 (facteur 1 dérivé des cellules stromales), EPO (érythropoïétine), TPO (thrombopoïétine) ou SCF (facteur des cellules souches) (Tarasova et al. 2011; Wognum et al. 2003).

Effets sur le système immunitaire

Mis à part quelques différences ponctuelles, nous n'avons pas observé d'effets sur le système immunitaire à l'état d'équilibre chez les animaux contaminés par le ^{90}Sr. Bien que nous n'ayons pas observé une modification majeure sur les populations des lymphocytes T et B, nous ne pouvons pas exclure l'induction d'un vieillissement accéléré du système immunitaire qui pourrait être observé à des temps plus tardifs.

Par ailleurs, des augmentations significatives dans le pourcentage des $CD3^{+}CD4^{+}CD25^{+}$ lymphocytes T régulateurs (Treg) ont été observées pour les animaux contaminés à l'âge de 16 et 20 semaines. Ces cellules sont connues pour leur régulation négative sur la réponse immunitaire des lymphocytes T et B et des cellules NK (natural killer) et le contrôle de la réponse auto-immunitaire (Jager and Kuchroo 2010). En tant que tel, une augmentation du pourcentage de Tregs pourrait suggérer une réponse réduite aux antigènes. Ainsi, bien qu'aucun changement majeur n'ai été observé dans le système immunitaire à l'état d'équilibre,

nous avons supposé que la contamination au ^{90}Sr pourrait induire des changements fonctionnels du système immunitaire.

Afin de répondre à cette question, nous avons étudié la réponse vaccinale. Nous avons effectué ce test fonctionnel avec des antigènes spécifiques soit de la toxine tétanique (TT) soit de l'hémocyanine de patelle (KLH), qui sont classiquement utilisés dans des expériences de toxicologie (Luster et al. 1993; Luster et al. 1992).

Nous avons observé une diminution significative des immunoglobulines G spécifiques à la TT pour les animaux contaminés et vaccinés TT en comparaison aux animaux témoins et vaccinés TT. De plus, l'analyse phénotypique des cellules de la rate ont révélé une diminution significative du pourcentage des lymphocytes T $CD3^{+}CD4^{+}$ et lymphocytes B $CD45^{+}CD19^{+}$ pour ces animaux. Basé sur ces faits, nous avons évalué si la balance Th1/Th2 de la réponse immunitaire avait été modifiée. Nous avons observé dans la rate des diminutions significatives des gènes T-bet (T-box exprimé dans les cellules T, Th1), Gata3 (protéine 3 liée à Gata, Th2) et FoxP3 (Forkhead box P3, Treg) pour les animaux contaminés et vaccinés TT ou KLH en comparaison aux animaux témoins et vaccinés TT ou KLH. Au niveau protéique, la diminution significative de l'expression de T-bet pour les animaux contaminés et vaccinés TT a été confirmée.

En conclusion de cette expérience avec les antigènes TT et KLH pour évaluer la capacité du système immunitaire à répondre à une stimulation antigénique a montré une diminution significative des immunoglobulines spécifiques, une différenciation lymphoïde B perturbée et un changement possible dans la balance Th1/Th2 de la réponse immunitaire dans la rate chez les animaux vaccinés. Cela suggère un effet indirect de l'accumulation du ^{90}Sr dans les os des animaux sur leur système immunitaire et cet effet pourrait être dû à l'irradiation par le ^{90}Sr des cellules stromales médullaires.

Pour compléter cette étude, il serait intéressant d'effectuer une analyse phénotypique et histologique des cellules de la moelle osseuse, d'évaluer les cellules B dans la rate et la moelle osseuse par histologie et de confirmer les résultats par mesure des taux de cytokines de la balance Th1/Th2 dans la rate.

Mécanismes du ^{90}Sr

Afin d'examiner *in vitro* les mécanismes d'action de ^{90}Sr, nous avons utilisé la lignée des cellules pré-ostéoblastiques MC3T3-E1, qui était auparavant utilisé pour explorer les mécanismes moléculaires de la prolifération, maturation et différenciation des ostéoblastes (Davis et al. 2000; Gal et al. 2000; Wang et al. 1999). Plusieurs techniques ont été mises au point afin d'étudier les effets du ^{90}Sr sur la mortalité cellulaire, la prolifération et la différenciation des pré-ostéoblastes. Aux concentrations de ^{90}Sr utilisées (jusqu'à 100 kBq/ml dans le milieu de culture) aucun effet n'a été observé. En revanche, il a été montré précédemment par des irradiations externes γ que les cellules MC3T3-E1 sont sensibles aux radiations ionisantes, et que leur survie et leur prolifération peuvent en conséquence être affectées (Dudziak et al. 2000; Gevorgyan et al. 2008; Szymczyk et al. 2004).

Cependant, une étude préliminaire a montré l'induction de foci γ-H2AX dans des cellules souches mésenchymateuses (CSM) contaminées avec les mêmes concentrations de ^{90}Sr, indiquant l'induction des cassures d'ADN double brin par le ^{90}Sr. Des expériences complémentaires seront nécessaires pour confirmer ce résultat et il serait intéressant de détecter des protéines de réparation des cassures d'ADN double brin tels qu'ATM et MRE11 (Czornak et al. 2008; Garner and Costanzo 2009).

Conclusion et perspectives

Nos résultats suggèrent qu'après ingestion chronique à faible concentration de ^{90}Sr, l'accumulation de ^{90}Sr dans l'os, essentiellement durant la phase de croissance osseuse, est à l'origine de modifications de la physiologie osseuse et immunitaire. Nous ne pouvons pas exclure que l'ingestion chronique de ^{90}Sr pourrait par exemple provoquer une accélération du vieillissement hématopoïétique qui pourrait être observée à des temps plus tardifs. Cependant, le choix d'une durée de 20 semaines de contamination chronique dans notre modèle juvénile était basé sur l'hypothèse que cette durée serait suffisante pour observer des effets éventuels dus à l'exposition précoce. En effet, pendant la vie fœtale et post-natale les systèmes hématopoïétique et immunitaire sont très sensibles à de nombreux agents toxiques, y compris des radionucléides (Blakley 2005; Gran 1960; Hoyes et al. 2000; MacDonald 1962; Preston 2004; Ruhmann et al. 1963; von Zallinger and Tempel 1998).

Nous avons supposé que nos modèles de souris utilisés sont représentatifs de la situation des personnes vivant sur des territoires contaminés. Néanmoins, dans le contexte de la radioprotection, il serait intéressant d'effectuer une étude dose-réponse afin de déterminer à quelle concentration d'ingestion de ^{90}Sr la dose sans effet nocif observé (NOAEL) est atteinte. Par ailleurs, du point de vue toxicologique, une étude dose-réponse avec des doses plus élevées de ^{90}Sr serait intéressante pour confirmer les conclusions formulées sur la base des résultats obtenus. De plus, il serait intéressant d'utiliser un mélange de radionucléides dans l'eau potable pour nos modèles de souris, éventuellement en combinaison avec des métaux lourds ou d'autres polluants chimiques, afin d'être plus pertinent par rapport à la situation à la suite d'un accident nucléaire.

Les mécanismes par lesquels l'accumulation de ^{90}Sr dans les os mène à une diminution de la capacité du système immunitaire à réagir aux stimuli extérieurs restent à élucider. Cependant, on peut proposer un mécanisme hypothétique basé sur le fait que les CSM et les ostéoblastes, qui sont tous deux des régulateurs clés de l'hématopoïèse, sont situés à proximité du site de l'accumulation du ^{90}Sr. Ainsi, nous ne pouvons pas exclure que l'irradiation locale des MSC et/ou des ostéoblastes conduisent non seulement à une dérégulation de la physiologie osseuse, mais aussi à une dérégulation de l'hématopoïèse. Ceci est soutenu par notre observation préliminaire de foci γ-H2AX dans des MSC et ostéoblastes *in vitro* en présence de ^{90}Sr. De même, on ne peut pas exclure que le ^{90}Sr irradie des CSH dans la niche endostéale. En conséquence, l'irradiation localisée à faible dose par le ^{90}Sr pourrait induire des changements sur la différenciation des cellules B et/ou de la différenciation précoce des cellules T. Bien que dans notre étude ceci n'est pas visible sur les principaux paramètres du système immunitaire, tel que l'analyse phénotypique, des changements fonctionnels dans la réponse immunitaire pourraient être induits.

Les effets mécanistiques du ^{90}Sr pourraient être élucidés par une étude des dommages à l'ADN *in situ* sur des coupes de moelle osseuse avec la détection des foci γ-H2AX, ATM et MRE11 phosphorylés (Czornak et al. 2008; Garner and Costanzo 2009; Suzuki et al. 2006). De plus une étude de l'apoptose induite dans les cellules stromales de la moelle osseuse, un examen histologique de la niche endostéale par quantification des CSM nestine^{+} ou SDF-1^{+} et des CSH exprimant CXCR4 (Martin et al. 2003; Nagasawa et al. 2011), et le suivi de la

différenciation des lymphocytes B selon l'âge des animaux par la quantification des cellules pré-B IgM^+, IgD^+ et $CD20^+$ dans la moelle osseuse et la rate (Chu et al. 2006).

En conclusion, nos résultats suggèrent que l'accumulation de ^{90}Sr dans les os après ingestion chronique de ^{90}Sr est responsable de changements dans l'os et le système immunitaire. Nos résultats contribuent à améliorer les connaissances sur les conséquences non cancéreuses après une exposition chronique à de faibles quantités de radionucléides rejetés accidentellement. Selon les systèmes physiologiques testés nous avons observé différents niveaux de réponse, de la moelle osseuse dans laquelle aucun effet significatif n'a été observé et du système immunitaire dans lequel un effet majeur a été observé. Ainsi les effets biologiques de la contamination chronique peuvent varier non seulement en fonction de la concentration en radionucléides, mais aussi selon le système physiologique étudié. Il est important de poursuivre ce travail car il est d'un intérêt majeur pour la santé publique. Ceci est montré par l'accident nucléaire de Tchernobyl et plus récemment de Fukushima, au cours desquels de nombreux radionucléides, y compris le ^{90}Sr, ont été libérés dans l'environnement. Aujourd'hui des questions sur les conséquences sanitaires de ces accidents demeurent, même 25 ans après l'accident de Tchernobyl.

Foreword

Nuclear weapon tests and nuclear power plant accidents caused the release of many radionuclides in the environment. Most of these radionuclides decayed during the transport in the atmosphere or have decayed in the months following after their deposition on the ground. However, two radionuclides remain above all in the environment due to their long half-life: cesium-137 (^{137}Cs) and strontium-90 (^{90}Sr). These two radionuclides have in the course of time progressively integrated the ecosystems and the food chains conducting to humans. Consequently, large populations living on contaminated territories ingest on a daily basis small quantities of them. The effects on the human health of long term ingestion of small quantities of these radionuclides remains until now unclear.

Some data obtained for populations living on contaminated territories around Chernobyl, where a major nuclear accident happened in 1986 with a massive release of radionuclides, suggest that ^{137}Cs accumulates in skeletal muscles, heart muscles and the thyroid after chronic ingestion. Experimental studies showed on the other hand showed that ^{90}Sr accumulates preferentially in the skeleton and teeth after chronic ingestion.

Other studies showed changes in the immune system of liquidators and inhabitants of contaminated territories of Chernobyl as a consequence of the accumulation of these radionuclides in the human body. Although it is difficult to make a link between the nature and amount of radionuclides ingested and the observed changes in the immune system, it is suggested that chronic ingestion of radionuclides could significantly alter the immune system and induce changes in the frequency of allergic or opportunistic diseases among these contaminated populations.

As part of the program ENVIRHOM, the Laboratory of Experimental Radiotoxicology (LRTOX) of the french National Institute of Radioprotection and Nuclear safety (IRSN) developed over the past years a research program to study functional changes in the hematopoietic and immune system after chronic ingestion of ^{137}Cs at small amounts. Obtained results for the mouse model used suggest that chronic ingestion of small amounts of ^{137}Cs in drinking water in the long term does not have any biologically relevant effect on the hematopoietic or immune system.

However, while ^{137}Cs is predominantly found in the environment, other radionuclides might be involved in the effects observed in populations living on contaminated territories. Of these radionuclides ^{90}Sr is an interesting candidate. Indeed, ^{90}Sr can be found in significant amounts on contaminated territories even 25 years after the Chernobyl accident. It is a β emitter and induces a high local energy deposition in its accumulation site, the bone tissue. In fact, several experimental studies showed the appearance of osteosarcoma in animals following a chronic contamination by ^{90}Sr. Moreover, a close interaction between bone cells and the hematopoietic niche in the bone marrow was shown in other studies. Therefore it is possible that the local accumulation of ^{90}Sr in bone tissue induces changes in the bone physiology as well as in the homeostasis of the hematopoietic and immune system.

While ^{137}Cs has previously been investigated, little information on the non-cancerous effects after ^{90}Sr long term chronic ingestion at small quantities is available up to now. The aim of this thesis is to determine what changes can appear as a result of such ^{90}Sr chronic ingestion to the bone physiology, and what are the possible functional consequences of these changes to the hematopoietic and immune system.

Introduction

Introduction

1. Release of radionuclides in the environment

Radionuclides found in the environment can be of natural or anthropogenic origin. In this chapter we focus on ^{90}Sr, an anthropogenic radionuclide released in the environment after nuclear weapon tests and power plant accidents. In this chapter, these events will be discussed in detail. However, one has to note that these events released large amounts of also other radionuclides in the environment, with the nature of the radionuclides being variable and the mixture complex.

1.1. Nuclear weapon tests and power plant accidents

Atmospheric nuclear weapon tests and different accidents at nuclear installations have lead to the release of ^{90}Sr in significant amounts in the environment (Christodouleas et al. 2011). Small amounts of ^{90}Sr are also be released by the normal operation of nuclear power and reprocessing plants and are as such found in airborne and water effluents. However, these releases are considered insignificant when compared to the amounts of ^{90}Sr released from atmospheric nuclear weapon tests and accidents at nuclear installations. Effluents of the plants are mostly arriving at waterways or the sea and as such an important dilution takes place. It is considered that the dilution is such that the accumulation of ^{90}Sr in marine species is very low and that the accumulation takes mainly place in the skeleton of fish or shells of crustaceans and molluscs, which are not consumed by humans. So these releases are considered to contribute only for a very small part to the ^{90}Sr found in the environment and will not be further discussed (Muck et al. 2001).

A description and the main consequences for both the environment and contaminated populations of some events in the past that lead to major releases of ^{90}Sr in the environment are given in this chapter. Recently, on March 11, 2011, a natural disaster caused substantial damage to the Fukushima Daiichi nuclear power plant at Japan. The Nuclear and Industrial Safety Agency (NISA) of Japan estimates that the release of radionuclides in the atmosphere was approximately 10 % of the Chernobyl accident, the major nuclear accident ever occurred. The exact levels of radionuclides released by the Fukushima accident in the environment are

until now not certain and the impact of this accident on the population's health is so far unknown (Bolsunovsky and Dementyev 2011; Christodouleas et al. 2011).

1.1.1. Atmospheric nuclear weapon tests

Above ground testing of nuclear weapons resulted in the wide dispersal of ^{90}Sr and other radionuclides in the environment. Te bulk of the nuclear fission products that were released into the atmosphere from the past until now was as a result of tests taking mainly place in the northern hemisphere during the 1950s and 1960s **(Table 1)**. In function of the power of the nuclear weapons, the altitude and place of explosion, radioactive particles were spread in different layers of the atmosphere (Balonov 1997; Comar et al. 1957; Muck et al. 2001).

Country	Time period	Number	Power (Mt)
ex-USSR	1945-1962	193	138.6
USA	1949-1962	142	357.5
United Kingdom	1952-1962	21	16.7
France	1960-1974	45	11.9
China	1964-1980	22	20.7

Table 1. Distribution of atmospheric nuclear weapon tests between 1945 and 1980. 1 Mt is the equivalent of the power released by an explosion of 1 10^6 ton of trinitrotoluene (TNT) (data from Balonov 1997; Comar et al. 1957; Lawson 1994; Muck et al. 2001; Stamoulis et al. 1999).

A detailed table of nuclear explosions was published by Lawson et al. for the period 1945-1994. According to the authors, during this period, 881 nuclear weapon tests were performed above ground and in the atmosphere. It is estimated that about 10^{18} Bq of ^{90}Sr were released in the atmosphere and subsequently deposited on the earth and in the oceans by the tests during the first half of this period (1945-1965), (Froidevaux et al. 2006; Lawson 1994; Stamoulis et al. 1999). Another study showed that the release of ^{90}Sr in the atmosphere reached a maximum in 1963, with declining levels afterwards (**Figure 1**) (Galle 1997).

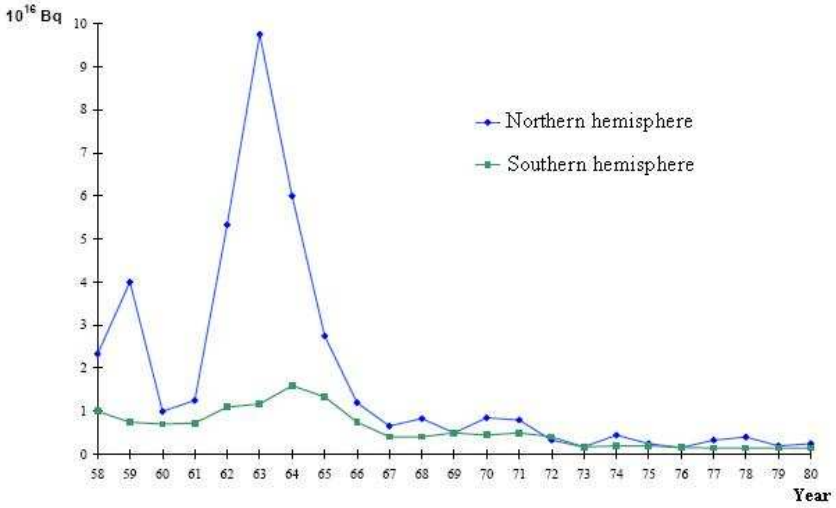

Figure 1. Annual release of ^{90}Sr in the atmosphere by above ground nuclear weapon testing, the blue line represents the northern hemisphere and the green line the southern hemisphere (from Galle 1997).

At the end of 1963, the so-called "Nuclear Test Ban Treaty" was signed by the United States, the former Soviet Union (USSR) and the United Kingdom. This meant the prohibition of all test detonations of nuclear weapons above ground and was made to slow the arms race between the different nations and to stop the excessive release of radionuclides into the planet's atmosphere. Since the signing of the "Nuclear Test Ban Treaty", the airborne concentrations of ^{90}Sr have dropped steadily due to deposition and radioactive decay.

The ^{90}Sr released by these atmospheric nuclear weapon tests was transferred to humans predominantly via the consumption of contaminated milk (Balonov 1997) which will be discussed further in detail.

1.1.2. Techa river

One of the main military plutonium production plants of the former Soviet Union (USSR) for the fabrication of nuclear weapons was situated in the Ural Mountains and included the so called "Mayak" production plant. This plant had a surface over 100 km^2 and was located between the cities of Chelyabinsk and Ekatrinbourg about 1200 km east of Moscow. People living along the banks of the nearby Techa River were exposed to contaminated drinking water and food following discharges of radioactive waste into the river between 1949 and 1956 from this production plant (Balonov 1997; Tolstykh et al. 2011b).

Technical flaws and lack of expertise in radioactive waste management led to the contamination of vast areas and the population was not informed about the releases. Protective measures as evacuations, restrictions on the use of flood lands and river water for agricultural and domestic purposes were implemented too late. As such, during the years of the releases, 39 settlements, with a total population of about 28 000 people, located along the banks of the Techa River were exposed (Balonov 1997; Degteva et al. 1994; Tolstykh et al. 2011b). The peak of most releases of radionuclides was during 1950-1951 (Kossenko et al. 1997) with an estimated release of 1 to 2 PBq of ^{90}Sr during this period (Apostoaei and Miller 2004; Balonov 1997).

The radioecological situation in the riverside settlements was followed by Peremyslova et al. They showed that the specific activity of ^{90}Sr in the water below the river mouth was 44.4 Bq/l in 1961 and decreased to 3.2 Bq/l in 2002. ^{90}Sr in fish muscles was 18 Bq/kg in 1977 and decreased to 2 Bq/kg in 2002. An average ^{90}Sr specific activity in milk was 10.2 Bq/l in 1961 and 1.2 Bq/l in 2001 (Peremyslova et al. 2009). Shutov et al. performed in 2002 environmental measures in the two villages closest to the Mayak production plant and showed that soils were contaminated with 100 to 1000 kBq/m^2 of ^{90}Sr. What concerns the foodstuff collected, vegetables were rather weakly contaminated (1 to 2 Bq/kg). However, milk (0.1 to 20 Bq/kg of ^{90}Sr) and fish (from the Techa river, 2 to 130 Bq/kg of ^{90}Sr) contained higher levels of ^{90}Sr (Shutov et al. 2002).

It was estimated that the riverside residents ingested an average of 3 MBq of ^{90}Sr, with 95 % of the ^{90}Sr being ingested in the short period of time from September 1950 to October 1951 (Shagina et al. 2003b; Tolstykh et al. 2011b). In another study, ^{90}Sr intake for breast-fed infants of the riverside settlements was calculated and a ^{90}Sr intake between 60 and 80 Bq for the period 1950-1951 was found (Tolstykh et al. 2008). The same authors measured also ^{90}Sr body burden of approximately 15 000 individuals between 1974 and 1997 with use of a special whole body counter (WBC). They found that almost the entire amount of ^{90}Sr had been deposited in the cortical part of the skeleton by 25 years following intake (Tolstykh et al. 2011a). This result was confirmed by Shagina et al. by direct measurements of ^{90}Sr concentration in different types of bones of riverside residents (Shagina et al. 2003b). Moreover, Tolstykh et al. found a significant negative relationship between the cortical bone resorption rate and ^{90}Sr body burden or doses absorbed by the riverside residents. The observed decrease in bone remodelling rate can be a cause of the increased degenerative

dystrophic bone pathologies observed in the exposed persons (Tolstykh et al. 2011a). Furthermore Degteva et al. estimated absorbed doses for the bone marrow of riverside residents. It was estimated that the mean dose to the bone marrow was about 0,4 Gy and for about 5 % of the individuals a dose to the bone marrow was in excess of 1 Gy was estimated (Degteva et al. 1994).

1.1.3. Kyshtym accident

A major nuclear accident took place in the winter of 1957-1958 at a nuclear weapon production plant near the city of Kyshtym at the Ural Mountains in the USSR. At that time period, the city of Kyshtym counted about 32 000 inhabitants. It is supposed that an explosion took place of a stored nuclear waste container. A surface of about 1500 km^2 around Kyshtym was contaminated with radioactive strontium and cesium. About 12 PBq of ^{90}Sr was released in the environment. Populations were contaminated by the consumption of contaminated milk and vegetables. Balonov et al. estimated that the average effective dose in the most exposed group of residents reached 0.5 Sv (Balonov 1997).

1.1.4. Chernobyl accident

The most severe accident ever occurred in the nuclear industry took place in Chernobyl, Ukraine, about 20 km south of the border with Belarus. After atmospheric nuclear weapon tests, this accident is the most significant source of environmental contamination by radioactive materials. The impact of this accident on the workers and local residents has been both serious and enormous (Balonov 1997).

On April 25th, 1986, operators of the Chernobyl nuclear power plant shut down the graphite-moderated light water reactor number 4 to test the emergency power system in the event of a power loss. After a series of failures and human errors, the reactor number 4 exploded in the early morning of April 26th. The explosion completely destroyed the reactor, sheared pressure tubes and water coolant channels, and dislodged the upper shield of the reactor, weighing 1400 tons. The explosion ejected a large cloud of radioactive fission products and debris from the core and reactor 7 to 9 kilometres into the atmosphere. About a day later, combustible gases from the disrupted core caught fire, and this ignited the graphite moderator, which burned for the next 10 days (Fairlie 2007). The fire continued the massive release of radionuclides in the environment. The quantity of radionuclides released after 10 days

following the accident was estimated, based on the inventory of the nuclear core of the reactor and measures of radionuclide deposition in the environment, to be 12 000 Pbq. About 85 PBq of ^{137}Cs and 8 PBq of ^{90}Sr were released in the atmosphere (UNSCEAR 2011). In terms of Becquerel, the total radioactivity released from Chernobyl was 200 times higher than that released by the atomic bombs at Hiroshima and Nagasaki (Fairlie 2007).

After the accident, hundreds of thousands measurements of ^{137}Cs levels in the environment were carried out by low altitude flights and analyses of soil samples. The obtained data have been mapped (**Figure 2**) and indicated a very widespread ^{137}Cs contamination. Over 40 % of the surface of Europe was contaminated by ^{137}Cs at levels higher than 4 kBq/m^2. A smaller area, about 2.3 % of the surface of Europe, was even more contaminated, to levels higher than 40 kBq/m^2. Particularly large areas of Belarus, Ukraine and Russia were contaminated with high levels of radionuclides (Fairlie 2007; Moller and Mousseau 2006).

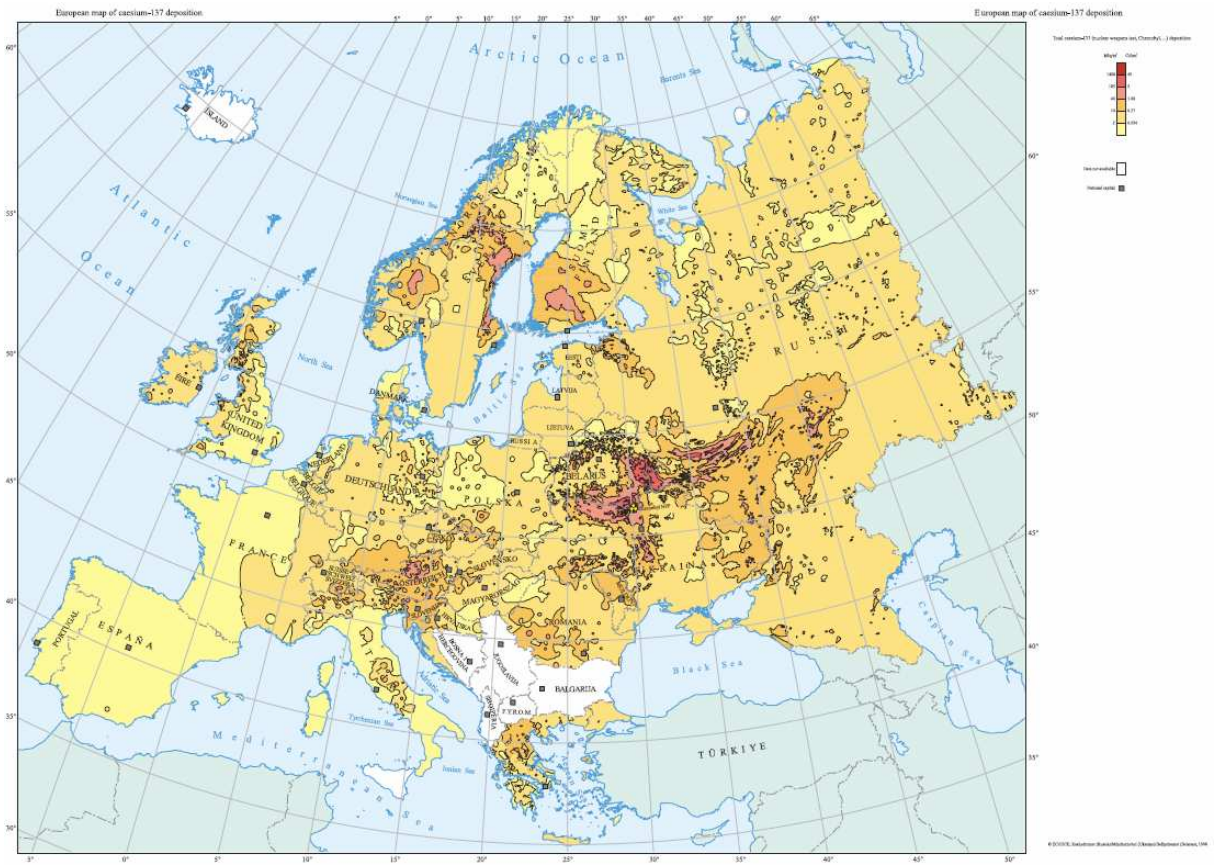

Figure 2. Distribution of ^{137}Cs deposition (kBq/m^2) in May 1986 as a result of the Chernobyl disaster (from UNSCEAR 2000).

Being less volatile than ^{137}Cs particles, ^{90}Sr particles had a greater deposition near the source of the accident (Hirose et al. 1993; Outola et al. 2009). The largest part of the ^{90}Sr released was deposited in the former Soviet Republics in Eastern Europe (**Figure 3**) and the rest was blown northwest by winds and dispersed as fallout over Northern Europe (Fairlie 2007; Muck et al. 2001). Measures for instance in France after the passage of the radioactive plume showed a mean density of ^{90}Sr deposition between 1 and 600 Bq/m^2 for ^{90}Sr and between 120 Bq/m^2 and 3560 Bq/m^2 for ^{137}Cs (Renaud et al. 1999).

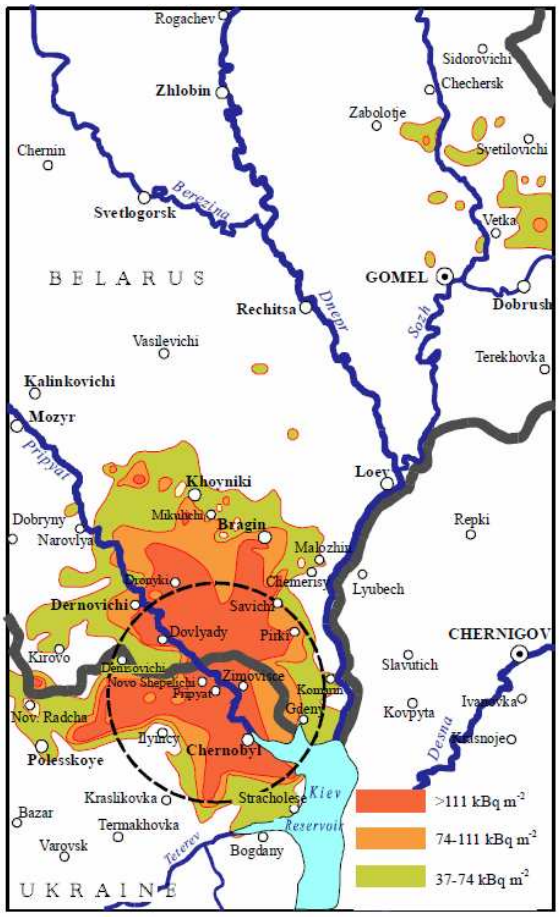

Figure 3. Distribution of ^{90}Sr deposition (kBq.m^{-2}) in May 1986 as a result of the Chernobyl disaster (from UNSCEAR 2000).

Several years after the accident Kashparov et al. did large-scale soil sampling (at about 1300 sampling sites) in the 30 km exclusion zone around the destroyed nuclear reactor of Chernobyl. The total content of ^{90}Sr on the ground surface of this zone (without the reactor site and the radioactive storages) was estimated to be 8.1 10^{14} Bq in 1997 (Kashparov et al. 2001).

Furthermore, Fairlie et al. did an estimation of residual amounts of radioactive radionuclides in the environment around Chernobyl over a period of 50 years until 2056 and the results are shown in **Table 2** for ^{90}Sr and ^{137}Cs (Fairlie 2007).

Nuclide	PBq released in 1986	PBq remaining in 1996	PBq remaining in 2006	PBq remaining in 2056
^{90}Sr	8	6	4.9	1,5
^{137}Cs	85	68	54	17

Table 2. Estimation of residual radionuclides in the environment of Chernobyl (from Fairlie 2007).

Over 600 000 people have been registered as being involved in the clean up operation during and after the accident. Of this total, about 200 000 recovery operation workers were employed in the 30 km exclusion zone. A total of 100 000 residents from 75 settlements were evacuated from the area and relocated (Balonov 1997; Cherenko et al. 2004; Moysich et al. 2011).

Since 1987, populations still living on contaminated territories around Chernobyl have on the long term essentially been contaminated by ^{137}Cs and ^{90}Sr, either by external exposure of these radionuclides deposited on the ground and internal exposure due to the contamination of local foodstuff. For foodstuff, the highest levels of radionuclides were mainly found in milk, dairy products, mushrooms and wild berries of the forest (Balonov 1997). The most significant radionuclide found in contaminated food was ^{137}Cs, with lower levels of ^{90}Sr. ^{90}Sr radioactivity measurements by de Ruig et al. on food products sampled in 1990 in the contaminated areas ranged between 1.8 and 340 $Bq.kg^{-1}$ wet mass. Mushrooms were very highly contaminated: from 7.8 up to 340 $Bq.kg^{-1}$. Milk products had a content of 3.6 $Bq.kg^{-1}$. The authors conclude that the contamination of all food products was below stated limits, except for mushrooms (de Ruig and van der Struijs 1992). Measures of ^{90}Sr in foodstuff in 1991 by Hoshi et al. showed levels of 118 $Bq.kg^{-1}$ in fresh mushrooms and 6.5 $Bq.kg^{-1}$ in powder milk (Hoshi et al. 1994). Furthermore, the International Atomic Energy Agency (IAEA) performed in the 1990s in selected settlements in three former USSR republics a study of radioactivity in food estimate internal doses. The ^{90}Sr concentration ranged form 0.1 to 7.9 $Bq.kg^{-1}$ wet mass in foodstuff. In mushrooms a maximum ^{90}Sr concentration was measured of 165 $Bq.kg^{-1}$ dry mass. Calculated internal doses due to ^{90}Sr in the diet, ranged from 0.01 to 0.08 mSv per year (Cooper 1992). Other studies showed that 270 000 people in

the most contaminated areas received internal doses between 5 and 50 mSv during the first year after the accident (Balonov 1997; Cherenko et al. 2004; Moysich et al. 2011).

Although the consumption of local foodstuff in contaminated areas around Chernobyl has been banned, there is evidence suggesting that contaminated milk, dairy products and forest products (i.e. mushrooms) are still widely consumed by important populations (Sekitani et al. 2010).

1.2. Radionuclides released in the environment

The events described above show that large amounts of different nuclear fission products were released in the environment after nuclear weapon tests and power plant accidents. The most important for human health are the long term remnants ^{137}Cs and ^{90}Sr, which will be described further in detail, and short-lived radioactive iodine isotopes.

The major long-lived radionuclide detected is ^{137}Cs with a half-life of 30.1 years. Its high solubility in water and high mobility in the environment results in a wide distribution in plants and animals. ^{137}Cs has a biological behaviour close to that of potassium (Leggett et al. 2003). Although it was demonstrated that ^{137}Cs competes with potassium and may induce a blockade of K^+ channels in smooth muscle cells (Cecchi et al. 1987), ^{137}Cs is considered to be a radionuclide with low toxicity, mainly linked to the emission of β (514 keV) and γ (662 keV) rays during its disintegration (Balonov 1997).

The major short-lived iodine isotope released during these events is ^{131}I. The half-life of this γ emitter is 8 days and therefore once released in the environment, it is dissipated fairly soon. However, it is demonstrated that after its accumulation in the thyroid, ^{131}I can cause thyroid cancer (Moysich et al. 2011). Indeed, different studies on the Chernobyl population found evidence for an increased thyroid cancer incidence in young people in the aftermath of the accident (Moysich et al. 2011; Prysyazhnyuk et al. 2007).

2. Post accidental situation and consequences on human health

The below described health effects in humans after oral exposure to ^{90}Sr are based mostly on long term studies of the Techa riverside population. One has to note that although this

population was mainly exposed to ^{90}Sr, they were also exposed to ^{137}Cs and lower levels (Tolstykh et al. 2008).

Riverside residents were reported to have immunological changes, which included granulocytopenia, decreased antigen expression of differentiating T-lymphocytes, and decreased T-lymphoblast transformation (Akleyev et al. 2010). Furthermore, a slight increase in lethal chromosomal anomalies and a significant increase in the incidence of leukaemia were observed in this population (Kossenko 1996; Kossenko et al. 1994).

Furthermore, several scientific groups did immunological monitoring of persons affected by the Chernobyl accident, as little was known of the effects of chronic exposure of low radiation doses to the immune system,.

A study evaluated T-cell immunity in 134 clean up workers. Peripheral blood mononuclear cells (MNCs) were used to analyze their phenotype and proliferative response to mitogens in vitro. Evaluation of the MNC phenotype did not reveal a significant disturbance in the T-cell subpopulations content except for an increase in $CD3^+CD16^+CD56^+$ natural killer cells. Phenotyping of phytohemagglutinin (PHA)-activated MNCs demonstrated suppression of $CD4^+$ T-cell propagation and augmentation of $CD8^+$ T-cell propagation in vitro compared to control individuals (Kuzmenok et al. 2003). T-cell number and serum concentrations of thymic hormones were studied by Yaralin et al. in 71 people 5 years after they were affected by the Chernobyl accident, either working at the power plant during the accident or taking part in the clean up operation. Total T-cell number and serum α_1-thymosin concentration were decreased in all groups of affected persons and $CD8^+$ or $CD4^+$ cell number were decreased in the low dose and the high dose exposed people respectively (Yarilin et al. 1993). Peripheral blood MNCs were also examined of 23 clean up workers by Chumak et al. The percentage of $CD4^+$ cells was significantly increased in heavily irradiated men, whereas the percentage of $CD8^+$ cells tented to decrease with higher doses (Chumak et al. 2001).

The immediate and long term effects (from 1986 to 1992) of radiation on the B-system immunity of children affected by the Chernobyl accident were studied by Titov et al. They carried out a complete clinical and immunological examination of more than 6000 children. Decreased levels of B-cells and immunoglobulins (Ig) M and G were observed short after the disaster. Long term effects of low doses of radiation showed increased concentrations of IgM

and IgG (Titov et al. 1995). Furthermore, in children, lymphocyte subsets in the peripheral blood were assessed by Chernyshov et al. in 120 children of 6 to 13 years old with recurrent respiratory diseases and living on highly contaminated areas around Chernobyl. Significantly lower percentage of $CD3^{+}CD4^{+}$ T-helper cells was observed for these children compared to control children also having recurrent respiratory diseases (Chernyshov et al. 1997). Vykhovanets et al. also analysed blood lymphocyte subsets in children with recurrent respiratory diseases living around Chernobyl and they observed significantly lower percentage of T-cells and higher percentage of NK cells compared to control children with recurrent respiratory diseases (Vykhovanets et al. 2000).

In a study by Senyuk et al. peripheral blood of 124 men working at the "shelter" object of the demolished nuclear reactor number 4 at Chernobyl was investigated. An increased manifestation of signs of common inflammatory reactions was observed, such as increased number of leukocytes, an unproportionally high number of monocytes and neutrophiles, and increased in plasma cytokine levels, such as interferon-α (IFN- α) and tumor necrosis factor-β (TNF- β) (Senyuk et al. 2002).

The above described studies showed that in the 10 to 15 years after the Chernobyl accident many clean up workers and children had quantitative changes in their cellular and humoral immunity. These changes were mainly expressed by a decrease in the general number of T- and B-lympocytes, changes in the ratio of subpopulations of T-lymphocytes, a decrease in the levels of serum IgG and IgM immunoglobulins, impaired production of cytokines and an activation of neutrophilic granulocytes.

Apart from the events described above, several hundred thousand people were exposed to radioactive fallout from atmospheric nuclear weapon detonations at nuclear test sites carried out in the 1950s and 1960s. A study by Taooka et al. observed increased T-cell receptor (TCR) mutations in peripheral blood from radiation exposed residents near such a former nuclear test site in the ex-USSR (Taooka et al. 2006).

Little or no association between oral exposure to ^{90}Sr from worldwide fallout and cancer incidence has been found in epidemiological studies. For example, a study by Hole et al. used data collected between 1959 and 1970 from a ^{90}Sr monitoring program in Scotland to identify risk cohorts for leukaemia, non-Hodgkin's lymphoma, acute myeloid leukaemia and bone

cancer. Based on the degree of fallout, three cohorts were identified and included: a high risk group born between 1963 and 1966 (exposed to high levels of fallout, i.e. ^{90}Sr at young age), a medium risk group born between 1959 and 1962 (exposed to high levels at an older age) and a low risk group born after 1966. The study found no evidence for increased risk of leukaemia, non-Hodgkin's lymphoma or acute myeloid leukaemia for cohorts born during the highest radioactive fallout period (between 1963 and 1966). The few cases of bone cancers showed a statistically non significant increase for children born during the high risk period (Hole et al. 1993).

Finally, there is little information concerning specific ^{90}Sr toxicity in humans. One study describes effects for workers in paint factories in Czechoslovakia, Switzerland and Poland that were exposed to luminescent colours containing ^{90}Sr and ^{226}Ra. No significant clinical changes could be observed in the exposed persons, except the signs of radiation dermatitis in some cases. An increase in the frequency of chromosomal aberrations in blood lymphocytes was observed, and was correlated with absorbed doses at the bone marrow (Müller 1966). On the other hand, more information is available on non radioactive strontium effects in humans. Non radioactive strontium under the form of strontium ranelate has namely been reported to enhance bone formation and to decrease bone loss in osteoporosis patients (Dahl et al. 2001).

3. What are the respective roles of each of the radionuclides ingested?

As can be deduced from the above described studies, it is unclear if the human health consequences of chronic ingestion of radionuclides are due to either internal radionuclide contamination or external irradiation exposure and which radionuclides are exactly responsible for the observed effects. Thus, our laboratory launched the research program ENVIRHOM, which is dedicated to the study of non-cancerous effects of chronic ingestion of low quantities of radionuclides. The type of contamination used for the ENVIRHOM program, i.e. chronic ingestion, is representative to the mode of contamination for populations living on contaminated territories after nuclear accidents.

The first studies conducted at our laboratory were focused on the effects of chronic ^{137}Cs contamination by ingestion. A rat model of chronic ingestion of ^{137}Cs by drinking water (at 6500 Bq/l, corresponding to 150 Bq/rat/day) was used. Results showed that the contamination

induced some modifications in various physiological systems. A modification of sleep-wake cycles in rats (Lestaevel et al. 2006) was demonstrated, which may be associated with a neuro-inflammatory reaction (Lestaevel et al. 2008). Also modifications on the cardio-vascular system (decrease in arterial pressure) (Gueguen et al. 2008), the vitamin D metabolism (decrease of active vitamin D3 in plasma) (Tissandie et al. 2006; Tissandie et al. 2009), the cholesterol metabolism (increase in different cytochromes intervening in the transformation of cholesterol and bile acids) (Racine et al. 2010a; Racine et al. 2009; Souidi et al. 2006) and the steroid hormone metabolism (Grignard et al. 2008) were shown. Obtained results showed thus that the chronic ingestion of low quantities of ^{137}Cs over a long period of time induced some non-cancerous modifications in the physiology of animals, however without major consequences on their general health status.

Furthermore, the effects of this ^{137}Cs chronic intake on the hematopoietic and immune system were studied, as earlier mentioned studies suggested that in humans chronic ingestion of long-lived radionuclides may be responsible for modifications in thymic physiology (Yarilin et al. 1993), in blood Ig levels (Titov et al. 1995) and in blood lymphocyte subsets (Vykhovanets et al. 2000). In order to detect non-cancerous modifications in these physiological systems during the course of a chronic ingestion of ^{137}Cs, our laboratory used a mouse model, at which Balb/c mice were chronically contamined by ^{137}Cs through contaminated drinking water (at 20 kBq/l). The obtained results showed however no biologically relevant effect on the hematopoietic or immune system (Bertho et al. 2011; Bertho et al. 2010).

Thus, the modifications of the immune system observed within contaminated human populations may be due to other causes. In fact, we used a single contaminant in a controlled environment and we cannot exclude that another radionuclide, or a combination of different radionuclides, may have different effects on the hematopoietic and immune systems. Precisely ^{90}Sr presents in this context interesting properties. This radionuclide accumulates preferentially in bone tissue and there exist a close interaction between bone cells and the hematopoietic niche in the bone marrow. The properties of this radionuclide will now be discussed in detail.

4. Strontium-90

4.1. Origin and utilisation

Strontium is named after Strontian, a village in Scotland near the lead mine where this element was first discovered in 1790. The rate of strontium in the earth crust is rather weak (0.034 %). Natural strontium is non radioactive and is a mixture of four stable isotopes: ^{84}Sr (0.56%), ^{86}Sr (9.86%), ^{87}Sr (7.02%) and ^{88}Sr (82.56%). For the first time it was isolated from its mineral form in 1808 in England and it occurs mostly in the mineral forms of strontium sulphate (celestite, $SrSO_4$) and strontium carbonate (strontianite, $SrCO_3$) (Galle 1997; Pors 2004).

The first large scale application of non radioactive strontium was in the production process of sugar from sugar beet, this by a crystallisation process using strontium hydroxide. Nowadays, stable strontium is used in combination with ranelic acid as a pharmaceutical agent to prevent osteoporosis, as it has been shown to stimulate bone growth.

Radioactive strontium on the other hand is artificial and, like many other radionuclides, was discovered in the 1940s in nuclear experiments connected to the development of the atomic bomb. Of the sixteen unstable isotopes known, the most important are ^{85}Sr, ^{89}Sr and ^{90}Sr. During the 1960s and 1970s, ^{85}Sr was used for research of the skeleton. However, due to its half-life of 65 days and its relatively high γ energy emission of 0.51 MeV, this radionuclide was no longer used after the 1970s as it caused consequent irradiation of patients. Nowadays ^{85}Sr is replaced by other bone tracers like labelled pyrophosphates and ^{99m}Technetium. The isotope ^{89}Sr has also a short half life and is still used as a treatment to alleviate bone pain secondary to metastatic bone tumors. As strontium acts like calcium, which will be discussed further, the administration of ^{89}Sr results in the delivery of radioactive emissions directly to bone sites with increased osteogenesis (Galle 1997).

The isotope ^{90}Sr is a by-product of the fission reaction of uranium and plutonium. As ^{90}Sr is one of the best long-lived high energy β emitters known, the heat generated by ^{90}Sr radioactive decay can be converted to electricity for long lived portable power supplies. Indeed, ^{90}Sr is often used for remote locations, such as navigational beacons, remote weather stations and spacecraft. Moreover, it is also used as a heat source in many Russian

radioisotope thermoelectric generators (RTGs), usually in the form of strontium chloride. ^{90}Sr is also used as a radioactive tracer in medical and agricultural studies, as a radiation source in industrial thickness gauges, in luminous signs and ice detection devices of airplane wings. Finally, controlled amounts of ^{90}Sr have been used a treatment for bone cancer and ophthalmic diseases (Galle 1982, 1997).

4.2. Physicochemical and radiological characteristics

Strontium, like calcium, magnesium, barium and radium, belongs to group 2 of the periodic classification table of elements. In **Table 3** one can find the properties of the most biologically important elements of this group (i.e. calcium, magnesium and strontium) and their distribution in the body of a 70 kg standard man (Pors 2004).

Element	Atomic number	Atomic weight	Amount (g) in man	% of body mass in man
Ca	20	40.08	1000	1.4
Mg	12	24.32	19	0.027
Sr	38	87.63	0.32	0.00044

Table 3. Physical properties of the most biologically important elements of group 2 of the periodic system and their distribution in the body of a 70 kg standard man.

Strontium is a silver-white alkaline earth metal and turns yellow when exposed to air. It has atomic number 38 and its standard atomic weight is 87.63 $g.mol^{-1}$. Because of its high reactivity, the element strontium alone is not found in nature. Strontium exists only as molecular compound with other elements, mostly as oxide, hydroxide, nitrate or chloride salt, which are soluble in water, or as sulphate or phosphate salts, which are relatively insoluble.

As mentioned before, the most important radioactive isotopes of strontium are ^{85}Sr, ^{89}Sr and ^{90}Sr **(Table 4)**. ^{85}Sr is a γ emitter with a half life of 65 days, while ^{89}Sr and ^{90}Sr are β^- emitters with half-lives of 50 days and 28.8 years respectively.

Radioisotope	Half life	Principal emissions
^{85}Sr	65 days	γ (0.51 MeV)
^{89}Sr	50 days	β^- (1.49 MeV)
^{90}Sr	28.8 years	β^- (0.54 MeV)

Table 4. Characteristics of the principal radioactive isotopes of strontium.

^{90}Sr has 52 neutrons and 38 protons and results from a fission chain reaction of ^{90}Br **(Figure 4)**. By β^- disintegration, in the form of an energetic electron of maximum 0.54 MeV, ^{90}Sr will conduct to the ytrium 90 (^{90}Y), which is also an unstable radioisotope. ^{90}Y is a β^- emitter (2.26 MeV) with a short half-life of 64 hours and decays itself to stable zirconium 90 (^{90}Zr). The long half-life period of ^{90}Sr and the short half-life period of ^{90}Y make that these two radionuclides reach a secular equilibrium within three weeks.

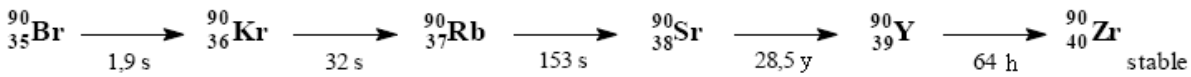

Figure 4. Fission chain reaction of ^{90}Br and disintegration of ^{90}Sr.

The two successive β^- emissions of ^{90}Sr and ^{90}Y deposit their energy within a small volume in the vicinity of the decaying nuclei. The route of the β^- emission depends of its energy. It is in the order of a meter in air and some micrometers in water and tissue. An aluminium paper of some micrometers thickness can block the particle. The energy of β^- particles is sufficient to produce ionizations and excitations of molecules in their path. However, due to a rather weak linear energy transfer (LET), the β^- emission is not highly ionizing.

4.3. Transfer of ^{90}Sr in the environment

^{90}Sr is mainly found in the environment after atmospheric nuclear weapon tests or nuclear accidents as described earlier. For all radionuclides released in the atmosphere, their dispersion and ground deposition are governed by many factors. Apart from the characteristics of the explosion, the size of particles emitted, topography of surrounding territories and weather conditions are decisive. What concerns the weather conditions, speed and wind direction and temperature gradient condition the movement of the radioactive

plume. Furthermore, rainfall causes leaching of the air and increases the rate of deposition of radionuclides on the ground (Galle 1997).

The radionuclides deposited on the ground will be able to penetrate the soil, migrate and settle there, more or less rapidly, at depth. Once in the soil, radionuclides are absorbed by soil constituents with whom they form complexes. The rate of migration of radionuclides depends on the nature and stability of these complexes, as well as physical and chemical properties of the soil, such as its composition, pH, permeability and water holding capacity (Comar et al. 1957). Strontium shows rather a moderate mobility in soils and sediments. It has been shown that the absorption of strontium is highest in grounds with weak levels of calcium and that the migration rate is about 0.2 to 0.4 $cm.year^{-1}$. Some studies in contaminated territories showed that radioactive strontium is mainly found in the superior layers of the soil, about fifty percent in the first four centimetres and the rest up to thirty centimetres deep (Balonov 1997; Galle 1982, 1997).

Rather lowly fixed by soil constituents, strontium is easily transferred to plants. The penetration of strontium in plant tissues can be foliar or by root. Foliar uptake of strontium is low but once retained by the leaves, strontium is very mobile in the plant. Root uptake from soil is more important and the absorption is dependent on the mineral composition of the soil. Indeed, it has been shown that there can be up to 50 fold differences among the transfer factors of plants in different soils. Furthermore, the competition between radioactive isotopes and stable isotopes or chemically similar stable elements in the soil limits the uptake by the roots. For this reason the absorption of strontium by plant roots is inversely proportional to the concentration of exchangeable calcium in the soil. Of course, root uptake is also dependent on the type of plant. After uptake by the roots, strontium is distributed in the plants and fixed in their stems and leaves (Balonov 1997; Paasikallio et al. 1994; Putyatin et al. 2006).

4.4. Exposure pathways

Animals like cattle can be contaminated by ingestion of these ^{90}Sr contaminated plants and also, but to a lesser extent, by inhalation of ^{90}Sr particles. The duration of contamination by inhalation is usually short and only contamination by ingestion continues on the long term. Given the long half-life of ^{90}Sr, its accumulation in the soil and its mode of transfer to plants,

animals mostly become contaminated for long periods. In these animals, strontium will follow calcium metabolism and distribution in different organs and body fluids and will be excreted primarily in urine and milk (Assimakopoulos et al. 1995; Balonov 1997; Fabbri et al. 1994).

Human exposure to ^{90}Sr can result from consumption of contaminated food, drinking water, or the incidental ingestion of soil or dust contaminated with ^{90}Sr. As for animals, the exposure by inhalation seems to be for humans only a minor pathway (Comar et al. 1957; Putyatin et al. 2006). The primary route of exposure to ^{90}Sr is considered through ingestion of contaminated food and drinking water. Contaminated vegetation consumed by animals such as cows, goats, reindeer may eventually transfer ^{90}Sr to the human food chain through the human consumption of beef, milk or other dairy products. As the transfer of ^{90}Sr throughout the food chain is similar to that of calcium, milk and dairy products are the main food in which ^{90}Sr will be found (Assimakopoulos et al. 1995; Fabbri et al. 1994).

Studies show that global populations consume daily varying amounts of strontium, depending on the source of food and water, leading to the natural presence of small amounts of it in their soft tissues, blood and bones. One study showed that a normal diet contains between 0.023 and 0.046 mmol of strontium per day (Marie et al. 2001) and another study showed that a normal diet in Western countries contains 2 to 4 mg of strontium per day, mostly derived from vegetables and cereals (Pors 2004). Furthermore, a study showed that the average daily intake of ^{90}Sr in North America is less than 0.05 Bq per day (ATSDR 2004). For populations living on contaminated territories around Chernobyl on the other hand, the daily ingestion of ^{90}Sr was estimated to be up to 100 Bq per day, mainly by the consumption of contaminated local dairy products and mushrooms (de Ruig and van der Struijs 1992; Hoshi et al. 1994).

4.5. ^{90}Sr intake recommendations

An annual limit on intake (ALI) of 10^6 Bq for ^{90}Sr ingestion intake and $7\ 10^5$ Bq for ^{90}Sr inhalation intake was proposed by the International Commission on Radiological Protection (IRCP) (ICRP 1979).

In drinking water, a maximum value 10 Bq of ^{90}Sr per litre was recommended by the World Health Organisation (WHO) (WHO 2011). On the other hand, the European Union (EU) recommended 0.06 Bq of ^{90}Sr per litre (Euratom 2000).

Furthermore, the EU recommended 0,2 Bq of ^{90}Sr per litre in milk and 0,1 Bq of ^{90}Sr per person per day in a mixed diet (Euratom 2000).

4.6. ^{90}Sr levels in bone and teeth

One study has recorded the levels of activity of ^{90}Sr in the milk teeth of children from different regions of Switzerland since the first atomic explosions in the atmosphere from 1950 to 2002. It is assumed that teeth are an extension of the skeleton and accumulate stable and radioactive bone seeking metals that enter the body. The ^{90}Sr activity peaked at 0.421 Bq/g of calcium (Ca) at the beginning of the sixties, coinciding with the detonation of many large nuclear devices. Following the "Nuclear Test Ban Treaty", a steady and significant decrease in ^{90}Sr activity in milk teeth was observed (down to 0.03 Bq/g of Ca for children born in 1994). The effect of the ^{90}Sr deposition from the Chernobyl accident was barely measurable in the milk teeth. Furthermore, no effect was observed from nearby Swiss nuclear power plants (**Figure 5**) (Froidevaux et al. 2006).

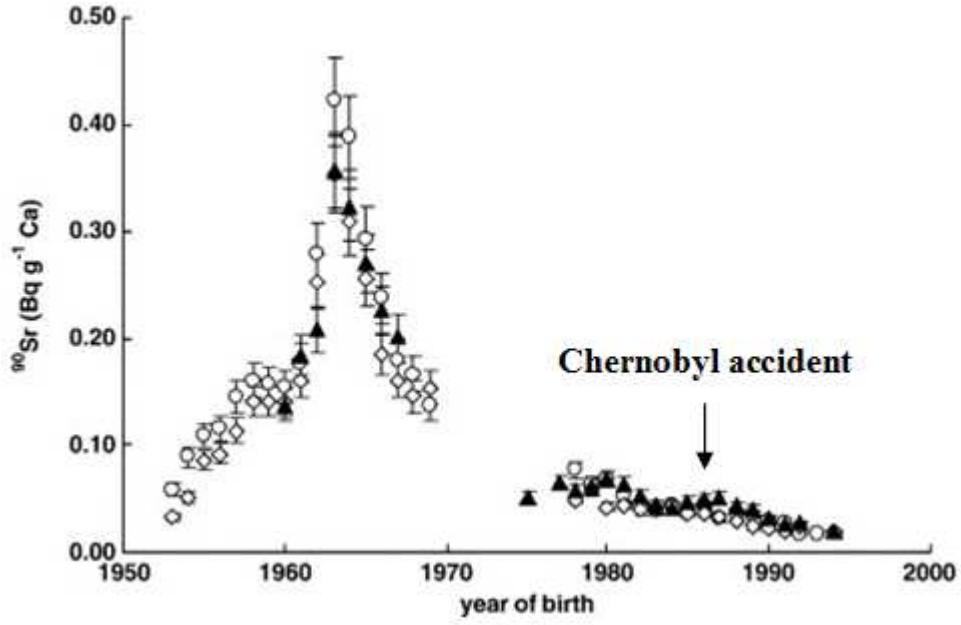

Figure 5. ^{90}Sr activity in milk teeth extracted from Swiss children since 1950 for three different regions in Switzerland (n>5 teeth for each point, from Froidevaux et al. 2006).

A similar study performed in the United States confirms the peak of ^{90}Sr concentration in milk teeth at the beginning of the sixties (**Figure 6**). However, in this study an increase in ^{90}Sr has been observed in the milk teeth of children living close to nuclear power plants (Mangano et al. 2003). In another study by the same authors milk teeth of only people born during the

atmospheric nuclear weapon testing years were analysed. Interestingly the authors showed that average ^{90}Sr levels in milk teeth of persons who died from cancer were significantly greater than for matched controls (Mangano and Sherman 2011).

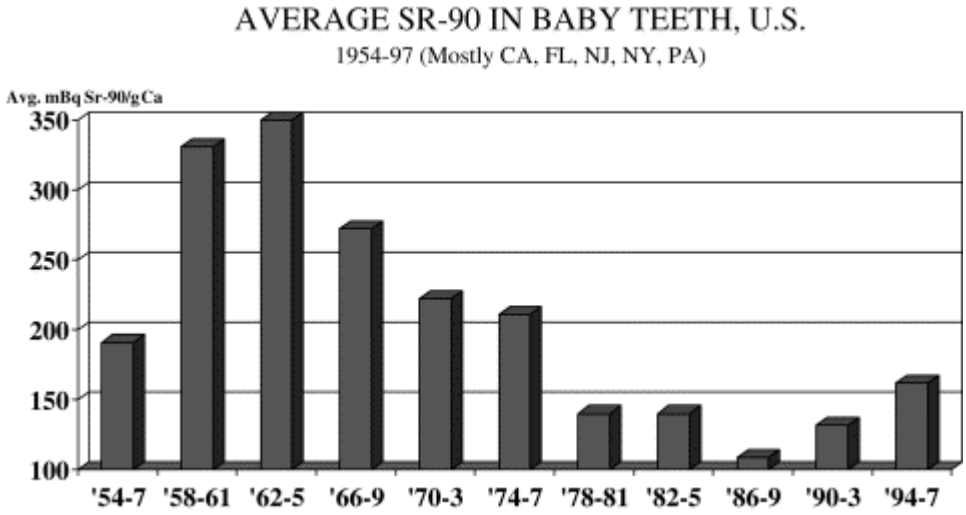

Figure 6. ^{90}Sr activity in milk teeth extracted form United States children (n=6-836 for the different time periods, from Mangano et al. 2003).

Others collected adult teeth in Ukraine for measurements of ^{90}Sr activity. The teeth were grouped according to the age and sex of donors. ^{90}Sr activity was lower by a factor of 10 for teeth in the 1990s compared to teeth in the 1960s and 1970s. An interesting feature of the data was a 3 fold increase of ^{90}Sr levels for teeth in the 1990s in the 25-45 year old age group of the male population compared to the female population of the same age. The authors suggested that this age group contained a significant number of men who were mobilized immediately after the Chernobyl accident for cleanup operations within the 30 km zone around the damaged nuclear power plant (Kulev et al. 1994).

Stamoulis et al. have compiled data from more than 20 studies to show mean values of ^{90}Sr concentration in bones throughout the world as a function of the calendar year (**Figure 7**) (Stamoulis et al. 1999).

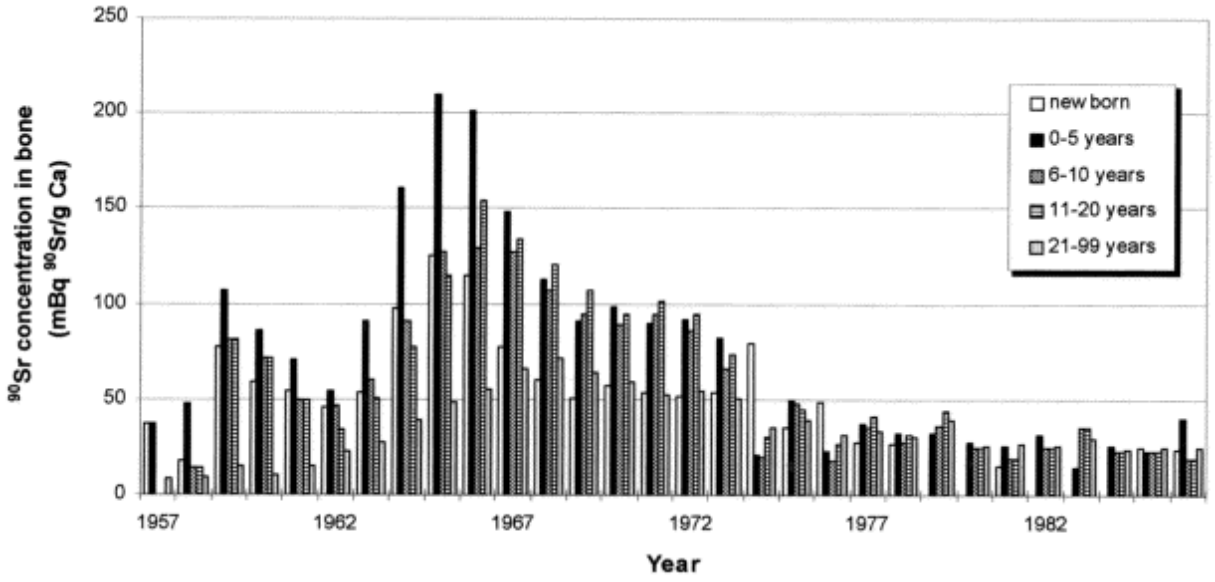

Figure 7. World-wide mean annual values of ^{90}Sr concentration in bones grouped by age. Data are a compilation of more than 20 studies from the period 1957-1986 (from Stamoulis et al. 1999).

Since the start of nuclear weapon tests in the 1950s several studies have been conducted to measure ^{90}Sr concentration levels in bone and teeth. In conclusion, the studies discussed here indicate that the ^{90}Sr environmental contamination which resulted from the atmospheric nuclear weapon tests exceed by far the ^{90}Sr environmental contamination caused by the Chernobyl accident (Stamoulis et al. 1999).

Shagina et al. measured over a period of 24 years (from 1974 to 1997) ^{90}Sr levels in bones of 15 000 individuals living near the Techa river. The authors showed that almost all of the ^{90}Sr was in the cortical part of the skeleton by 25 years after initial intake (Shagina et al. 2003b). Retrospective analysis of post-mortem measurements of ^{90}Sr levels in bones from riverside residents was performed by Tolstykh et al. from 1960 to 1982. It was shown that ^{90}Sr levels in bones of residents that lived in settlements located downstream from the river mouth was 5 times higher than average ^{90}Sr levels in bones of general Russian residents. Moreover, dietary ^{90}Sr intake was reconstructed by the authors from these measurements. The mean total ^{90}Sr dietary intake for the period 1950 to 1975 was about 68 kBq and the mean absorbed dose in the red bone marrow after 25 years accumulated to 14 mGy (Tolstykh et al. 2010).

Other studies used the radionuclide contamination measurements in soil and food samples in order to reconstruct population exposure doses. For ^{137}Cs for instance, there is a good correlation between the radioactivity measured in soil and food samples of contaminated

territories of Chernobyl and human whole body counting results (Sekitani et al. 2010; Takatsuji et al. 2000). One study on the other hand showed a good correlation (**Figure 8**) between soil contamination levels of villages near the "Mayak" nuclear production plant and ^{90}Sr levels measured in teeth of cows living on those soils (Toyoda et al. 2010).

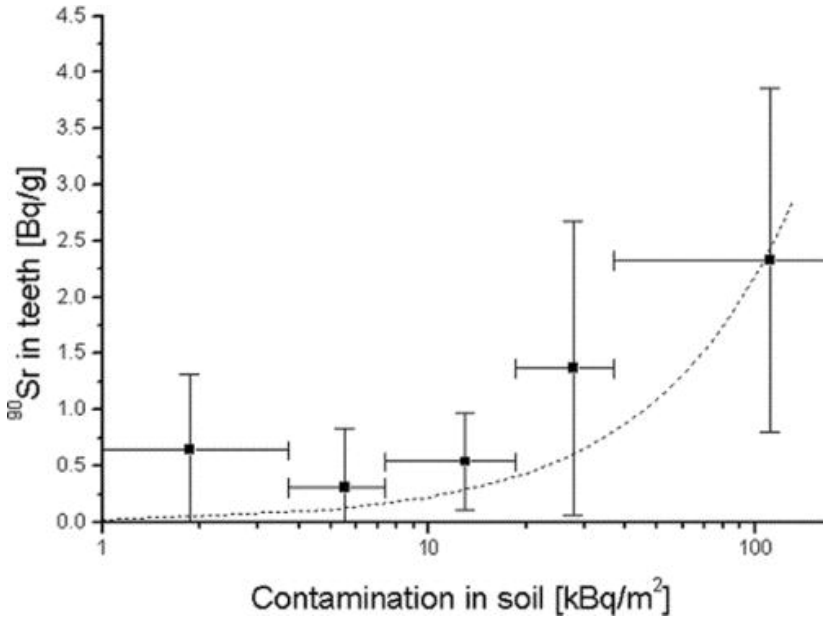

Figure 8. Correlation between soil ^{90}Sr levels and ^{90}Sr levels measured in teeth of cows living on those soils. The curve shown is the best fit line for all 64 samples (from Toyoda et al. 2010).

Another study by Ryabokon et al. measured ^{90}Sr levels in soil and bank voles captured using live traps at five monitoring sites with different ground deposition of radionuclides at different distances from the destroyed Chernobyl nuclear reactor. Investigations were started in the year of the accident and continued until 10 years later. The ^{90}Sr levels in the bank voles increased in the period 5 to 10 years after the accident and correlated well with the ^{90}Sr levels of the soil (Ryabokon et al. 2005).

5. Biokinetics of strontium(-90)

The biokinetics of strontium have mostly under the form of strontium chloride been examined in different species after oral administration, injection or inhalation. These studies will are discussed in detail in this chapter as well as the strontium biokinetics model proposed by the ICRP.

5.1. Absorption

It is recognized that the absorption of calcium and strontium occurs mostly in the small intestine, especially in the jejunum and ileum, and that little absorption takes place in the stomach or large intestine. Some data indicate that a constant ratio of calcium and strontium absorption exist throughout the small intestine (Li et al. 2006, 2008; Wasserman 1963; Wiseman 1964). Dahl et al. reported gender differences in the gastrointestinal absorption of strontium as in experimental studies with rats and monkeys, plasma strontium levels were higher in males than females (Dahl et al. 2001).

The transport of strontium through the enteral cells seems to be mediated by the same membrane carriers used for calcium (Hollriegl et al. 2006a; Hollriegl et al. 2006b; ICRP 2006; Sugihira et al. 1990). It is assumed that the gastrointestinal absorption of strontium takes place, at least partly, by an active transport mechanism involving calcium-binding proteins (Dahl et al. 2001). However, although the chemical behaviour of strontium is similar to that of calcium, strontium is not as efficiently absorbed or retained as calcium (Comar et al. 1957; Gran 1960; Sugihira et al. 1990; Wasserman 1963). It is estimated that the ratio of intestinal absorption of calcium to strontium is 2 for humans and 3 for rats (ICRP 2006). One hypothesis of the preferential absorption of calcium is attributed to its relatively smaller size (Cohn et al. 1963; Pors 2004).

On the basis of available human data, the ICRP adopted an average gut to blood transfer factor (f_1 value) of 0.3 for adults, with ranges from 0.15 to 0.45 (ICRP 1993). Values from studies with animal species are generally similar (Fujita 1965; Hollriegl et al. 2006a; ICRP 1993, 2006; Li et al. 2006).

Data on a possible elevated absorption of strontium during growth period are contradictory. A study with 7 day old infants fed with cow's milk showed an intestinal absorption greater than 0.73 (Widdowson et al. 1960). On the other hand, a study with 5 to 15 year old children showed same intestinal absorption ratios for children as for adults (Bedford et al. 1960). Anyhow, based on the available information, the ICRP set higher gut to blood transfer factors of 0.4 to 0.6 for infants (ICRP 1993).

In **table 5** ^{90}Sr ingestion dose coefficients proposed by the ICRP are shown for different age groups. The dose coefficients are significantly higher for children and teenagers (Balonov 1997; ICRP 1993).

	Age (years)					
Radionuclide	**<1**	**1-2**	**2-7**	**7-12**	**12-17**	**>17**
^{90}Sr	230	72	47	60	79	28

Table 5. ^{90}Sr ingestion dose coefficients for different age groups (nSv of effective dose per Bq intake) (data from Balonov 1997; ICRP 1993).

It has been shown that the intestinal absorption of ^{90}Sr is better when ^{90}Sr is taken in with an aqueous solution than with food. Alginate, a specific nutrional factor and food additive, reduces significantly strontium absorption (Hollriegl et al. 2006b; Li et al. 2006, 2008). On the other hand, some studies show that milk diets may increase strontium absorption (Hollriegl et al. 2006b; ICRP 2006; Li et al. 2006; Wasserman 1963). A number of factors have furthermore been found to increase strontium intestinal absorption, including low dietary levels of calcium, magnesium and phosphorus; fasting; vitamin D; lactose and some amino acids (i.e. L-lysine and L-arginine) (Apostoaei 2002; Gran 1960; Hollriegl et al. 2006b; ICRP 2006; Kargacin and Kostial 1982; Li et al. 2006; Pors 2004; Wasserman 1963; Wiseman 1964). A study with human volunteers showed that overnight fasting resulted in an increase in strontium absorption from about 25 % to 55 % and a decrease in calcium content of the diet by 75 % raised strontium absorption from 20 % to 40 % (ICRP 2006). Another study showed that a low calcium diet enhances the expression of all genes involved in the transcellular pathway for calcium absorption in the intestine probably by activation of the vitamin D endocrine system (Perez et al. 2008). Indeed, it has been shown that the active form of vitamin D, calcitriol (1,25-dihydroxyvitamin D3), regulates the transcellular pathway of calcium absorption, through the activation of intestinal channels TRPV6 and TRPV5, $PMCA_{1b}$ and the Na^+/Ca^{2+} exchanger (NCX1). Calcitriol molecules bind to their nuclear receptors and this complex interacts with specific DNA sequences inducing the transcription and increasing the expression levels of TRPV5 and TRPV6, calbindins and the extrusion systems (**Figure 9**) (Apostoaei 2002; Perez et al. 2008).

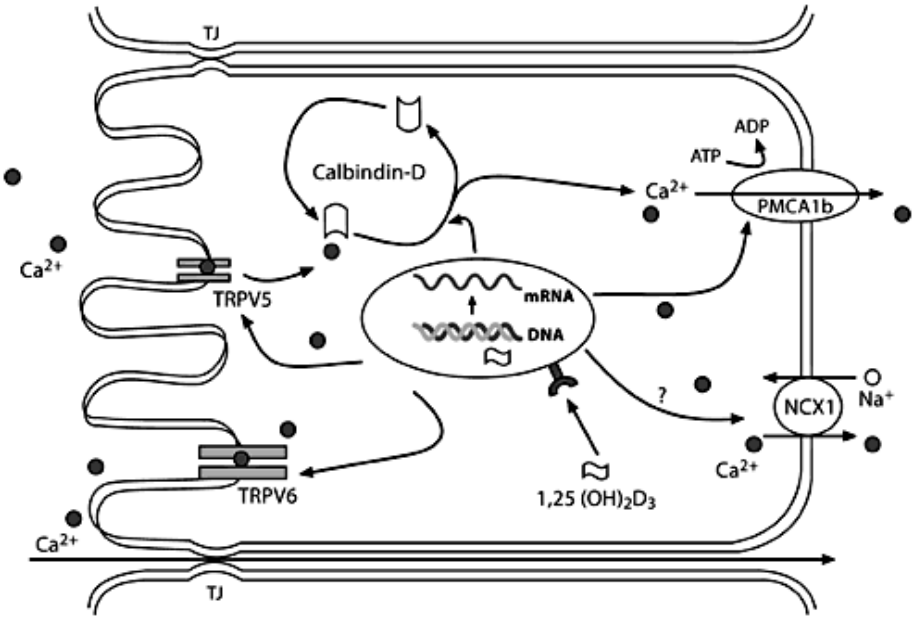

Figure 9. Schematic representation of mechanisms involved in the intestinal calcium (Ca^{2+}) absorption. Calcitriol (1,25-$(OH)_2$ vitamin D3) stimulates the individual steps of transcellular Ca^{2+} transport (from Perez et al. 2008).

Under the condition of an increased absorption it has been shown that the degree of discrimination between strontium and calcium ions in the small intestine is often reduced (Wasserman 1963). Different studies showed that for young animals and humans, the intestinal absorption is very effective and that no discrimination between strontium and calcium exist (Comar et al. 1957; Galle 1997; ICRP 2006; Kulp et al. 1960; Wiseman 1964). It has been suggested that the mechanisms discriminating the uptake of strontium and calcium develop gradually during maturation, and as such that the high efficiency of strontium absorption by the small intestine early in life may be due to a deficiency in this discrimination (Dahl et al. 2001; Sugihira et al. 1990).

Finally, what concerns inhalation exposure, experimental studies with beagles showed that ^{90}Sr is rapidly translocated from the lung to the blood (Benjamin et al. 1975; Gillett et al. 1987a).

5.2. Distribution

It is assumed that strontium follows the movement of calcium in the body with slight differences in the pattern of distribution. Where there is a metabolically controlled passage of

ions across a biological membrane in the living organism, calcium seems to be transported more efficiently than strontium (Cohn et al. 1963; Dahl et al. 2001; Harrison et al. 1967).

After passage of the intestinal or pulmonary barrier, ^{90}Sr enters the blood circulation and binds to plasma proteins. The plasmatic half life is estimated to be a couple of hours (Leeuwenkamp et al. 1990). Experimental studies in animals and humans indicated that only very low concentrations of strontium can be found in blood and that there is no evidence for the accumulation of ^{90}Sr in the erythrocytes (Li et al. 2008).

According the ICRP, 99 % of absorbed ^{90}Sr is accumulated in the skeleton and teeth (ICRP 1993; Leggett et al. 1982). Marie et al. suggested that the distribution of strontium in the skeleton seems to be directly proportional to plasma levels (Marie et al. 2001).

Bone mineral consists mainly of a crystalline fraction made of apatite and crystalline calcium phosphate complexes and strontium is incorporated into it by two mechanisms: surface exchange and ionic substitution (Dahl et al. 2001). It is assumed that ^{90}Sr is predominantly fixated in metabolic active regions of bones and this in function of the bone growth and remodelling rate. Indeed, autoradiography of tibia and femurs of young rats, who were contaminated with ^{90}Sr at 148 kBq/g by single intramuscular injection, showed that ^{90}Sr was fixated in metabolic active regions of bone growth (Graf and Lafuma 1963). However, strontium seemed to be less incorporated into new bone than calcium (Cohn et al. 1963).

The skeletal repartition of strontium seems to be related to the relative cortical and trabecular proportions of bone, because bone turnover is higher in trabecular than in cortical bone, and newly formed bone is more abundant in trabecular than cortical bone (Dahl et al. 2001). A study measured ^{90}Sr levels in human femurs and vertebrae. Calculations showed that of the ^{90}Sr that reached the skeleton, half went to the cortical bone and half to the trabecular bone. Furthermore, it has been shown in the same study that uptake and turnover varied with age (Papworth and Vennart 1984). On the other hand, Shagina et al. measured over a long period of 24 years ^{90}Sr levels in bones of 15 000 individuals living near the Techa river and almost all of the ^{90}Sr was in the cortical part of the skeleton by 25 years after initial ^{90}Sr intake. The authors explained the fact that ^{90}Sr remained mainly in cortical bones by a more rapid elimination of ^{90}Sr from trabecular bone, as the rate of trabecular bone remodelling is six times higher than for cortical bone (Shagina et al. 2003b).

Experimental animal studies suggested that the incorporation of strontium in bone is gender and skeletal site dependent and varies in function of dose, duration and mode of administration (Dahl et al. 2001; Gran 1960; Marie et al. 2001; Parks et al. 1984). Administration of strontium to rats at 5 to 500 parts per million (ppm) in drinking water for 12 weeks showed a dose dependent increase in strontium and decrease in calcium in bones (Xu et al. 1997). Rats given strontium up to 0.5 % in their feed for about four weeks beginning at weaning showed dose dependent effects on calcium in femurs. At the highest dose, corresponding to 0.875 micromoles per day of strontium, calcium was markedly decreased in both serum and femur (Morohashi et al. 1994). In a study by Ruhmann et al., pregnant rats received ^{90}Sr by injection and the offspring showed a continued increase in strontium burden from birth until weaning (Ruhmann et al. 1963).

Dahl et al. showed in rats that after repeated administration for a sufficient period of time (at least 4 weeks), strontium concentration in bone reached a plateau level. The strontium levels in bone varied according to the anatomical site and bone structure. Higher levels were found in trabecular bone than in cortical bone (Dahl et al. 2001). In another study, this time with beagles exposed to ^{90}Sr beginning in utero and by continuous ingestion up to 540 days of age, the continuous ingestion of ^{90}Sr resulted in a ^{90}Sr burden that steadily increased with age. However, a plateau level was reached at the time of skeletal maturity. When the ^{90}Sr intake was stopped after 540 days of age, the ^{90}Sr levels in bone decreased due to mineral exchange and skeletal remodelling (Parks et al. 1984).

Overall, these experimental data have suggested that strontium levels in bone increase with the administered dose and at higher administered doses, the strontium levels in bone tend to reach a plateau level. One likely explanation for this plateau effect is a saturation of the gastrointestinal absorption mechanisms. Sugihira et al. showed that higher strontium to calcium ratios in all tissues of young rats could be found compared to old rats and assigned this fact to the high efficiency of strontium absorption by the small intestine early in life (Sugihira et al. 1990).

What concerns the distribution of strontium through the placental barrier, it is assumed that once administered to the mother, strontium traverses rapidly the placental barrier. As for the intestinal barrier, there exists a preferential transfer of calcium (Gran 1960; MacDonald 1962; Ruhmann et al. 1963). Mice experiments evaluated this discrimination and showed a

maximum discrimination early in pregnancy while at the end of pregnancy strontium and calcium were transported at almost equal proportions across the placenta (von Zallinger and Tempel 1998).

5.3. Metabolism

In animal experimental studies strontium showed similar metabolism action in bone like calcium. In fact, the chemical properties of strontium seem to be similar enough to calcium so that it can exchange with calcium in bone and other cellular components. However, specific biological effects for strontium exist. For example, non radioactive strontium at pharmacological doses may affect the rate of bone turnover by increasing osteoblastic activity and decreasing osteoclastic activity (Marie 2006). The biological effects of non radioactive strontium and radioactive ^{90}Sr are described further in this thesis.

5.4. Elimination

It is assumed that elimination of strontium from bone happens by different processes: clearance from exchangeable pools in bone, displacement of strontium (presumably by calcium) from sites within the bone matrix by long term exchange processes, and volume removal from the bone matrix by osteoclastic resorption. Theoretical models of strontium elimination from the skeleton revealed an initial rapid elimination followed by a slower elimination (Dahl et al. 2001).

Shagina et al. measured over a long period of 24 years ^{90}Sr levels in bones of 15 000 Techa riverside residents and calculated the rate of ^{90}Sr elimination from bone. The authors showed that women had higher rates of elimination than men over the entire range of observation, and for both sexes the elimination of ^{90}Sr increased with increasing age (Shagina et al. 2003b).

In comparison with other elements, strontium seems to be excreted rather slowly from the body. The urine appears to be the major route of excretion of strontium from the plasma. A study showed that urinary excretion was maximal the day of administration and decreased progressively afterwards (Hollriegl et al. 2006a). It is assumed that calcium and strontium share a common tubular transport path in the renal tubes (ICRP 2006; Pors 2004). It was shown that the mammalian kidney excretes strontium more rapidly than calcium. Studies suggest that the renal clearance of strontium is around 3 times higher than for calcium. The

discrimination between both elements seems to be principally situated at the tubular re-absorption, with a smaller tubular re-absorption of strontium, probably due to the larger size of the strontium elements (Dahl et al. 2001; Hollriegl et al. 2006b; ICRP 2006; Pors 2004).

Apostoaei et al. showed that in the first days after a single ingestion of $^{85}SrCl_2$, most of the strontium eliminated in feces was of exogenous origin (i.e. not absorbed into the body fluids). However, small amounts of strontium of endogenous origin (i.e. absorbed into the blood fluids and been returned to feces) were also excreted. Five to six days after a single ingestion, the entire amount of strontium eliminated in feces was of endogenous origin (Apostoaei 2002). Another experimental animal study confirmed that strontium was secreted in tiny amounts directly from the plasma into the intestine (Palmer and Thompson 1961). Other studies indicated that biliary secretion accounted for only a small portion of the total secretion of strontium, calcium, into the alimentary tract (ICRP 2006; Wasserman 1963; Wiseman 1964).

In a study with strontium chronically fed mice, elimination of strontium happened mainly by the feces (Wiseman 1964). In a study with ^{90}Sr chronically fed rats, ^{90}Sr levels in feces increased over time. On the other hand, the urinary levels of ^{90}Sr were low and stayed constant over time (Gran 1960).

^{90}Sr could be found in milk of lactating rats. However, preferential transfer for calcium from blood to milk was observed (Gran 1960).

5.5. ICRP strontium biokinetics model

A biokinetic model mathematically characterizes the movement, transfer, fate, deposition and excretion of a substance in a living system. Such a model predict where a substance goes in the body, how long it there remains, and as such permits the calculation of internal doses and risk to specific tissues and organs as well as the whole body.

The ICRP developed a such a biokinetic compartimental model for alkaline earth elements, including strontium, which is applicable to children, adolescents and adults (**Figure 10**) (ICRP 1993). This model is based on a nearly identical model previously developed by Leggett et al. (Leggett 1992). The model is designed to simulate oral exposures and cannot be

applied to other routes of exposure without modification. As well it is designed for human applications and cannot be applied to other species without modification.

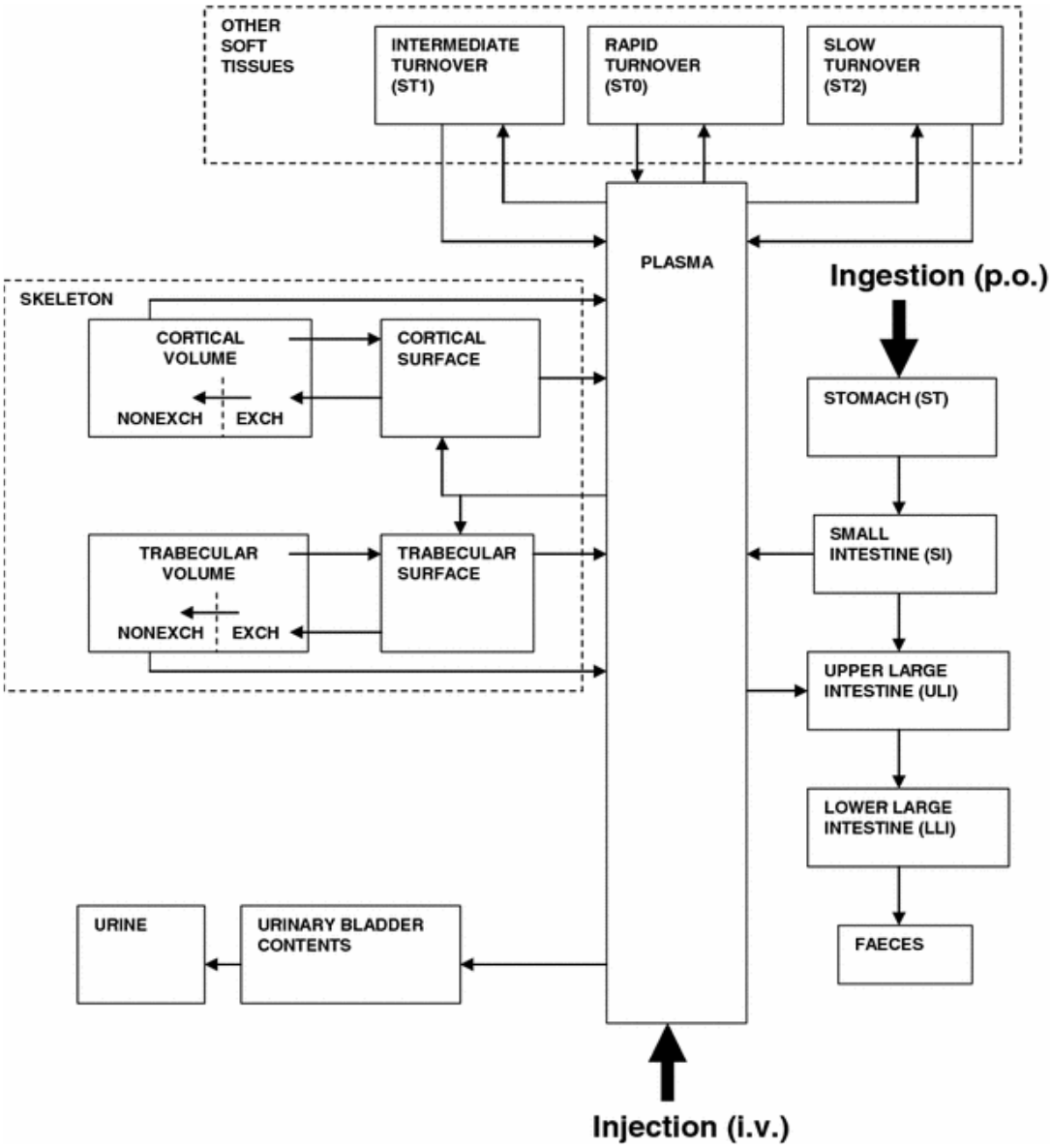

Figure 10. ICRP model of strontium biokinetics (from Li et al. 2006).

The fraction of ingested strontium that is absorbed by the small intestine is assumed to vary with age and has values of 0.6 in children up to 12 months of age, 0.4 from 12 months of age through 15 years, and 0.3 from 15 years of age through adulthood. Once absorbed, strontium that enters the blood plasma is assumed to distribute to the skeleton, liver and other tissues. Blood plasma in the model is treated as a uniformly mixed pool. Since the alkaline earth elements have little affinity for red blood cells, this compartment is not considered explicitly.

Liver and kidneys are treated separately from other soft tissues, because these organs show sometimes higher concentrations of radionuclides than the average soft tissue (Leggett 1992).

In the ICRP model, bone is divided into cortical and trabecular components, each of which is further divided into bone surface and bone volume. The model assumes that 99 % of the strontium that enters the body and not being excreted is ultimately transferred to the skeleton and only 1% to soft tissues. Skeletal deposition is assumed to distribute initially to the bone surface of either cortical or trabecular bone, from which it can exchange relatively rapidly with plasma or more slowly with the bone volume. Two pools are assumed to exist within the bone volume, an exchangeable pool that communicates with the surface bone, and a non exchangeable pool from which strontium can be returned to plasma only as a result of bone resorption (Leggett 1992).

Excretion is assumed to occur only in urine and feces. Strontium in urine is assumed to have passed directly from plasma to the urinary bladder, and strontium in feces is assumed not been absorbed or have passed directly form plasma to the gastrointestinal tract. The biliary excretion pathway is considered of limited importance. Furthermore, it is assumed that strontium secreted into the gastrointestinal tract is not reabsorbed (Leggett 1992).

The transfer rate coefficients between compartments are assumed to be age and gender specific (Apostoaei and Miller 2004; Shagina et al. 2003a). However, originally the ICRP (ICRP 1993) did not account for age dependence of strontium elimination in elderly persons. Indeed, because the model was created for a standard human of undefined sex, gender dependence was not taken into account either. Apostoaei et al. calculated on the basis of available human metabolic data that transfer rates of strontium from plasma to cortical and trabecular bone and subsequent elimination rates are age dependent. Moreover they calculated that the elimination rate of strontium from the trabecular bone is slightly gender dependent (Apostoaei and Miller 2004).

Besides the above described systemic biokinetics model, the ICRP developed also a gastrointestinal model (GI) for strontium. This GI model is used to describe the movement of swallowed or endogenously secreted strontium through the stomach and intestines. The GI model developed divides the GI tract into four compartments: stomach, small intestine, upper

large intestine and lower large intestine. Like the systemic biokinetics model, the GI model assumes that absorption of strontium occurs only through the small intestine (ICRP 2006).

6. Biological effects of non radioactive strontium

6.1. Generalities

The processes of bone formation and resorption are tightly regulated by a variety of systemic and local regulatory agents, of which calcium is one of them. Strontium, which is chemically related to calcium, is also found to exert effects on bone cells (Marie et al. 2001).

Many studies showed that non radioactive strontium has a positive effect on bone formation. In an *in vitro* study with human bone derived cells (HOB), it was demonstrated that strontium ($5\ 10^5$ M $SrCl_2$) increased the expression of type 1 collagen mRNA and reduced the production of matrix metalloproteinases (MMP) (Braux et al. 2011). Another study observed that strontium (1mM $SrCl_2$) enhanced the ability of osteoblasts to form mineralized nodules *in vitro* and increased the expression of Runx2, one of the earliest osteoblast specific transcription factors (Lymperi et al. 2008). Moreover, in a study by Boanini et al., the response of primary cultures of rat osteoblasts to strontium substituted hydroxyapatite was investigated. Increased levels of cell proliferation, alkaline phosphatase (ALP) and collagen 1 were observed (Boanini et al. 2011). *In vivo* studies in normal rats and mice indicate that low doses of strontium (up to 4 mmol/kg/day $SrCl_2$) may increase bone mass at different skeletal sites by increasing bone formation and reducing bone resorption (Marie 1984; Marie et al. 2001). Lymperi et al. showed that strontium treated mice had increased number of osteoblasts, increased bone volume and trabecular thickness, with the trabeculae having more interconnections within the bone marrow cavity (Lymperi et al. 2008). On the other hand, a study with mice fed with a high concentration of strontium (2 % $SrCO_3$ in rodent chow) throughout pregnancy, showed inhibited bone development in the offspring, presumably by affected bone calcification (Shibata and Yamashita 2001).

Given its potential beneficial effect on bone formation, the use of strontium has been thought to have an interest as a treatment for osteoporosis. This bone disorder of mainly post-menopausal women is characterized by low bone mass, enhanced bone fragility and fracture risk. This may be due to oestrogen deficiency, causing an imbalance between bone resorption and bone formation, and impaired intestinal absorption of calcium (Dahl et al. 2001). As such,

this led to the development of the drug strontium ranelate, which has been proven its efficiency to reduce the bone fracture incidence of osteoporotic patients (Cortet 2010; Pors 2004).

6.2. Strontium ranelate

Most *in vitro* studies used the anti-osteoporotic drug strontium ranelate (5-[bis(carboxymethyl) amino]-2-carboxy4-cyano-3-thiopheneacetic acid distrontium salt, S12911, Protelos®, Servier, France) (**Figure 11**) to investigate the effects of strontium. However, until now cellular and molecular mechanisms of action have not yet been fully elucidated. This drug, composed of two atoms of stable strontium (Sr^{2+}) and an organic part (ranelic acid) was found to stimulate bone growth, increase bone density, and lessen vertebral, peripheral and hip fractures (Dahl et al. 2001).

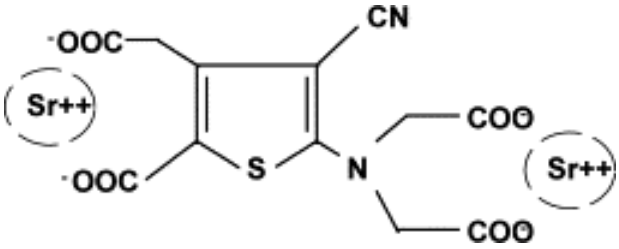

Figure 11. Chemical structure of strontium ranelate (S12911-2, from Baron and Tsouderos 2002).

Different *in vivo* studies suggested that strontium ranelate reduces bone resorption and increases bone mineral density and some markers of bone formation (Ahmet-Camcioglu et al. 2009; Ammann 2006; Marie 2006). A study with female rats showed that a 2 year period of exposure to strontium ranelate significantly increased bone mechanical properties of vertebrae and femurs. All the determinants of bone strength measured were positively influenced by the treatment, like bone mass and microarchitecture (Ammann 2006). Results of another study by histomorphometric analysis demonstrated that long term administration (104 weeks) of strontium ranelate at dose levels up to 1800 mg/kg/day increased bone formation and reduced bone resorption in normal male and female mice, and increased bone volume without deleterious effect induced on bone metabolism (Delannoy et al. 2002).

Moreover, strontium ranelate showed its anti-fracture efficacy in a study with mice overexpressing Runx2, which is a model of severe developmental osteopenia associated with spontaneous vertebral fractures. Strontium ranelate was able to decrease vertebrae fracture

through an improvement of bone microarchitecture (Geoffroy et al. 2010). Treatment with strontium ranelate prevented also the effect of ovariectomy on bone strength (Ammann 2006). Strontium ranelate (625 mg/kg/day for 52 weeks) treatment showed improved bone strength in ovariectomized rats (Bain et al. 2009).

In vitro studies showed that strontium ranelate reduced osteoclast differentiation and induced even apoptosis of these cells (**Figure 12**) (Baron and Tsouderos 2002; Marie et al. 2001). Moreover, it was shown that strontium ranelate dose dependently decreased osteoclastic activity *in vitro* (Ammann 2006). Another study showed a decreased area of resorption pits of osteoclasts (Takahashi et al. 2003).

On the other hand, strontium ranelate induced replication of pre-osteoblasts, synthesis of collagen and ALP activity (Barbara et al. 2004; Canalis et al. 1996; Marie 2006; Marie et al. 2001). A study suggested that interaction of strontium with the G-protein-coupled calcium-sensing receptor (CaSR), might be one of the explanations of the mechanism of action. More precisely, strontium ranelate has been shown to increase the accumulation of inositol phoshatase (which derives from phospholipase C (PLC) activity) in the cultured cell lines, an effect that might occur through CaSR activation (Coulombe et al. 2004). However, this potential mechanism and eventual other mechanisms independent of the CaSR remain to be fully eludicated (Ammann 2006; Pi et al. 2005; Pi and Quarles 2004).

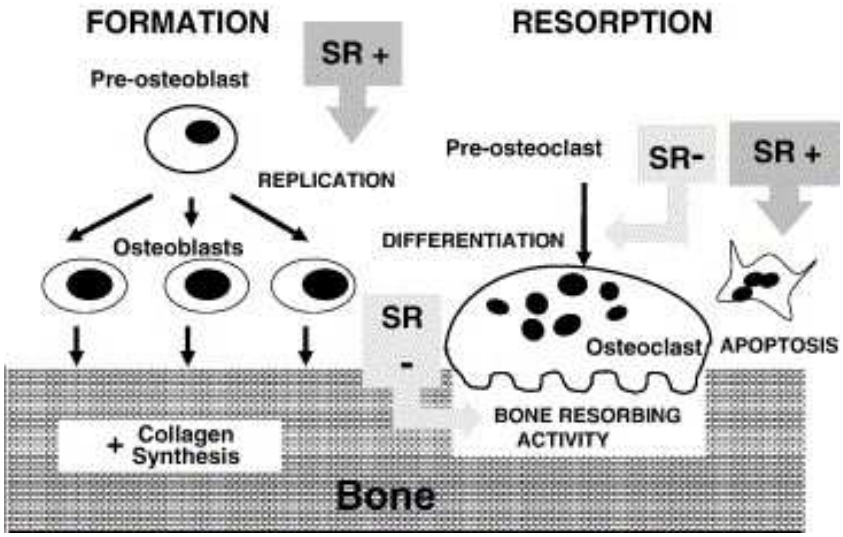

Figure 12. Strontium ranelate exerts antiresorbing and bone forming effects which results in bone gain *in vivo* (from Marie 2006).

7. Biological effects of ^{90}Sr

7.1. Generalities

^{90}Sr is chemically similar to calcium and as such, this radionuclide is capable to exchange for calcium in tissues, especially in bone which has a high calcium content, and consequently exert there biological effects. Moreover, ^{90}Sr may affect other calcium utilizing processes including enzymes, secondary messenger systems and transporter systems. The stable forms of strontium might not pose a significant health treat but the radioactive isotope ^{90}Sr, which emits high energetic β^- particles, can lead to various bone disorders and even other adverse health effects. ^{90}Sr that incorporates into bone and irradiate bone cells may also irradiate hematopoietic tissue in the bone marrow or other surrounding soft tissues. As such, hematopoietic and immune cells located in the bone marrow may be susceptible to injury as well. These facts, coupled with the proven carcinogenic effects of ionizing radiation and ^{90}Sr long half-life, make it a potential toxic hazard for exposed humans. At equal levels, children may even exhibit an enhanced response to ^{90}Sr exposure. Due to a higher intake of strontium during growth, younger organisms could be more susceptible to the toxic effects of ^{90}Sr.

Considerable animal experimental work has been performed in order to predict the radiobiological effects of ^{90}Sr once absorbed in the human body. Animal studies included acute and chronic exposures in dogs, rodents, pigs, cows and monkeys. Particularly a wide range of studies have been conducted since the 1960s using beagles. Growing concern about health effects after radioactive fallout exposure from atmospheric nuclear weapon tests conducted in the 1950-60s was the starting shot of these studies. Beagles were chosen because of the physiological similarities of their skeleton and lungs to these of humans, and for their relatively long life span, which is roughly comparable to the time required for the latent effects of radiation exposure to become manifest in humans (Gillett et al. 1987a). Of particular interest are studies at the University of California at Davis and at the University of Utah at Salt Lake City involving beagles that received ^{90}Sr chronically both in utero and by daily ingestion in their feed afterwards (Book et al. 1982; Dungworth et al. 1969; Momeni et al. 1976a; Nilsson and Book 1987; Parks et al. 1984; Raabe et al. 1981b; Raabe et al. 1981a; White et al. 1993).

The observed adverse effects included bone and kidney damage, hematological, immunological and developmental effects, cancer and death. All the observed effects could be directly correlated to the ^{90}Sr doses used. Especially young animals have been shown to be vulnerable to ^{90}Sr exposure, which was linked to their immature skeleton having a higher rate of bone remodelling.

7.2. Acute toxicity of ^{90}Sr

In experiments with young and adult rats, Casarett et al. reported a 80 % reduction in survival at five months when young rats were given at least 11 MBq of ^{90}Sr per kg per day for 10 days by drinking water. The survival of adult rats on the other hand was unaffected. The increased mortality of the young rats, which was 20 times higher than for adults, was attributed to the increased skeletal burden of ^{90}Sr in the young rats. Approximately 19 % of adult rats ingesting 2.4 MBq per day in drinking water for 10 days developed chronic interstitial nephritis. Rats drinking water for five days at doses higher than 3.7 MBq per day suffered from bone malformations, cartilage detachments, and bone fractures (Casarett et al. 1962). Another study with rhesus monkeys given daily oral doses of 37 MBq of ^{90}Sr showed that the animals died within four months from pancytopenia (Casarett et al. 1962). Cragle et al. reported deaths in four out of six young cows given 2 GBq of ^{90}Sr orally for five days. Deaths occurred from radiation sickness including severely decreased leukocytes and platelet counts after 80 days (Cragle et al. 1969).

A study showed the appearance of bone tumours in mice after single injection at high doses (up to 59.2 kBq/g) of ^{90}Sr. It was shown furthermore that not only latency time and tumor frequency but also the type and location of tumors were related to the dose (Nilsson 1970). Also a study with beagles showed the appereance of osteosarcomas after single injection at high doses of ^{90}Sr (Nilsson and Book 1987). A single injection of 22 kBq/g in rabbits at the time of weaning led to a significant reduction in the length of tibias (Galle 1997).

Hematological effects after a single administration of ^{90}Sr by inhalation was examined in adult beagles by Gillett et al. Dogs were observed throughout their life span and showed bone marrow hypoplasia, pancytopenia, thrombocytopenia and neutropenia (Gillett et al. 1987b). A single high dose injection of ^{90}Sr (300 to 740 kBq/g) by rat induced leucopenia, short period

neutropenia, transitory reticulopenia, fluctuating variations in thrombocyte numbers and finally blood anemia (Galle 1997).

7.3. Chronic toxicity of ^{90}Sr

7.3.1. Life expectancy

Several studies showed a decrease in survival of rodents orally exposed on the long term to ^{90}Sr. Hopkins et al. reported a 36 % reduction in survival of young rats ingesting 3.8 MBq/kg per day of ^{90}Sr for 30 days (Hopkins et al. 1966). In rats fed with 18.5 up to 74 kBq/kg per day of ^{90}Sr for their postweaning lifetimes, Zapol'skaya et al. reported that lifespans shortened by 18 to 30 % compared to control rats (Zapol'skaya et al. 1974). Regular administration of ^{90}Sr at 0.74 kBq/kg per day during 3 years in mice conducted to perturbations in the development of offspring and a decrease in life expectancy (Galle 1997). In another study, mice were fed up to 1147 kBq/kg per day of ^{90}Sr from the time of conception through the rest of their life. Their parents received the same amount through conception to lactation. No effects on litter size, survival of offspring or increase in malformations were noted. However, survival of offspring was shortened at doses above 111 kBq/kg per day and was attributed to an increased incidence of bone marrow cancers (Finkel 1960).

A study with beagles by White et al. reported that beagles given up to 1.3 MBq/kg of ^{90}Sr per day for 540 days and maintained until death had reduced survival of 18, 64, and 85 % at the three highest dose levels (0.1 ; 0.4 and 1.3 MBq/kg per day respectively) when compared with control dogs. Concentrations of ^{90}Sr in feed at or below 1.6 kBq/kg per day had no apparent effect on survival and there were no reported bone sarcoma deaths in these dose groups, whereas bone sarcomas were noted in the higher dose groups (White et al. 1993). In another study, Book et al. exposed 15 beagle dogs from gestational age day 21 throughout their lifetime to 0; 0.05; 0.15 or 0.44 MBq of ^{90}Sr/kg per day. The median survival times of the groups were 15; 12.5; 6.5 and 5.2 years respectively. Osteodystrophy was observed in the highest dose group. The two main causes of radiation induced mortality were myeloproliferative syndrome and skeletal sarcomas (Book et al. 1982).

Multigenerational effects were studied by Clarke et al. in swine fed with 0.037 up to 114.7 MBq of ^{90}Sr per day only during the period of mating. No effect on fertility or fecundity was observed. Some sows receiving the highest dose did not survive gestation. Offspring of sows

fed 23.13 MBq per day showed reduced weight at weaning and did not survive to nine months when fed with ^{90}Sr after birth, even though parent sows fed the same doses survived well past breeding age (Clarke et al. 1970). In another study by McClellan et al., sows ingesting 115 MBq per day from the age of nine months did not survive their first pregnancy, succumbing from the destruction of hematopoietic tissue in the bone marrow. Sows exposed to 0.9, 4.6 and 23 MBq per day, showed increased mortality after 11, 5 and 1 year respectively. Effects on the F1 generation females exposed from time of conception were more severe. None of these females exposed to the highest dose survived more than nine months (McClellan et al. 1963).

7.3.2. Bone cancers

Bone injury and bone cancers were frequent in studies with beagles chronically fed with ^{90}Sr. Momeni et al. evaluated beagles exposed to different concentrations of ^{90}Sr with as highest dose 1.3 MBq/kg of ^{90}Sr per day. Increased skeletal changes, i.e. endosteal and periosteal cortical sclerosis and thickening, were noted for dogs exposed at doses above 49 kBq/kg per day (Momeni et al. 1976b). White et al. reported that beagles fed between 4 and 125 kBq/kg per day of ^{90}Sr developed bone sarcoma, chondrosarcoma, hemangiosarcoma, fibrosarcoma and leukemia. Multiple tumors occurred only at the highest dose levels. Of the 66 sarcomas reported in this study, 75 % were osteosarcomas (White et al. 1993). Nilsson et al. showed that among beagles fed ^{90}Sr during skeletal development, the incidence of bone tumors was dose dependent. Bone tumors appeared sooner and were more often multiple in animals receiving higher doses. Long bones were the sites where most of the tumors appeared after the highest dose level (Nilsson and Book 1987). Gillett et al. showed that beagles that were exposed to ^{90}Sr by inhalation, chronic ingestion or injection developed bone tumors, which were different in their skeletal distribution and histological phenotype, dependant of the route of exposure. Furthermore, bone tumors tended to occur at later times after exposure in dogs exposed to ^{90}Sr by chronic ingestion (Gillett et al. 1992).

Other animal studies also showed that oral ^{90}Sr exposure increased the incidence of bone tumors. Adult rats developed osteosarcomas in a study when fed 1.2 up to 2.4 MBq per day of ^{90}Sr over 10 days. Rats given 29.2 MBq of ^{90}Sr over 30 days showed a 27 % increase in the incidence of osteosarcoma, hypoplasia of the bone marrow, a 11 % increase in skin sarcoma and a 6 % increase in leukemia incidence (Casarett et al. 1962). Rats fed 18.5 up to 74 kBq/kg

per day during lifetime showed an 18 % increase in malignancies compared to control rats. The malignancies included osteosarcoma and leukaemia (Zapol'skaya et al. 1974). In a study with young rabbits fed with 218 kBq/kg per day on average for 224 to 280 days, multiple osteosarcomas developed in the skull and the rapidly growing ends of long bones within 6 to 8 months (Downie et al. 1959). In a study with miniature swine, Howard et al. showed that most bone tumors occurred in the skull, including the mandible and maxilla, and arose near or within the periosteal surface of the bone (Howard et al. 1969).

In a multigenerational study with miniature swine fed with ^{90}Sr up to 114.7 MBq per day for life developed different cancers. In the parents, myeloid neoplasms were observed but no bone cancer developed. The F1 and F2 offspring exposed from conception developed myeloid metaplasia and osteosarcoma. The osteosarcoma had a longer latency period and occurred at the higher doses. The myeloid metaplasia developed sooner and were more frequent in the F1 and F2 generations (Clarke et al. 1970).

7.3.3. Hematologic malignancies

Dungworth et al. reported that beagles chronically exposed up to 530 kBq/kg per day of ^{90}Sr by ingestion showed myeloproliferative disorders in the highest dose groups. Other effects seen were abnormal erythrocyte morphology, drop in hematocrit levels, leukopenia, an abnormal amount of immature granulocytes, reduction in platelets, and splenomegaly (Dungworth et al. 1969). In a six year chronic study in which beagles were fed with ^{90}Sr at 14.8 kBq/kg per day, Dungworth et al. reported that about 1 % of the exposed animals developed myeloid metaplasia of the spleen (Dungworth et al. 1969).

Howard et al. demonstrated the induction of hematopoietic disorders, such as myeloid metaplasia, myeloid leukaemia, lymphocytic leukaemia and stem cell leukaemia, in miniature swine after chronic ^{90}Sr feeding up to 114 MBq/day (Howard and Clarke 1970). Osteonecrosis, hematopoietic disorders and bone marrow hyperplasia were commonly found by Clarke et al. among swine that died after ingesting a diet containing ^{90}Sr levels of 1 or 114 MBq/day (Clarke et al. 1972).

In rabbits, chronic administration by ingestion of low concentrations of ^{90}Sr (100 Bq/g per day) led to an instability of the erythrocyte system and weakening of the hematopoietic function (Galle 1982). Hypoplasia of the bone marrow leading to anemia and

thrombocytopenia developed in rabbits fed with 218 kBq of ^{90}Sr/kg per day for 31 to 280 days. Moreover, reduced osteocyte numbers after 48 days were reported (Downie et al. 1959). Another study showed that rats receiving chronically more than 18,5 kBq/kg per day had significantly depressed hematopoiesis (Zapol'skaya et al. 1974).

Long term exposures to ^{90}Sr resulted also in impaired immune function in animals. Howard et al. reported that pigs fed with 23,13 MBq per day for nine months had significantly reduced antibody response to Brucella bacteria or phytohemagglutinin stimulation (Howard and Jannke 1970).

8. Physiological systems studied

As explained in the foreword we decided to study the non-cancerous effects on the bone physiology and hematopoietic and immune systems after chronic ^{90}Sr ingestion at low dose for this thesis. These physiological systems are described in this chapter with particular attention for the parameters evaluated.

8.1. Bone physiology

8.1.1. Generalities

The skeleton provides structural support for the rest of the body, permits movement and locomotion by providing levers for the muscles, protects vital internal organs and structures, provides maintenance of mineral homeostasis, serves as a reservoir of growth factors and cytokines and provides the environment for hematopoiesis within the bone marrow spaces (Taichman 2005).

The four general categories of bones of the skeleton are long bones, short bones, flat bones and irregular bones. Flat bones are formed by membranous bone formation, whereas long bones are formed by a combination of endochondreal and membranous bone formation (Clarke 2008; Marie 2001). The long bones are composed of a hollow shaft, or diaphysis; cone-shaped metaphyses below the growth plates; and rounded epiphyses above the growth plates (**Figure 13**).

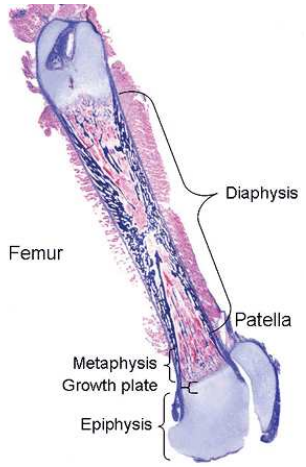

Figure 13. The long bone (here represented by a femur) is composed of the proximal and distal epiphyses, metaphyses, growth plates and the diaphysis.

It is assumed that the adult human skeleton is composed of 80 % cortical bone and 20 % trabecular bone (Clarke 2008). The diaphysis is composed primarily of dense cortical bone, whereas the metaphysic and epiphysis are composed of trabecular meshword bone surrounded by a relatively thin shell of dense cortical bone. Cortical bone is dense and solid, whereas trabecular bone is composed of a network of trabecular plates and rods. Both cortical and trabecular bone are composed of osteons (**Figure 14**). Cortical osteons are called Haversian systems. Haversian systems are cylindrical in shape, and form a branching network within the cortical bone. Trabecular osteons are called packets, and composed of concentric lamellae. Cortical bone and trabecular bone are normally formed in a lamellar pattern, in which collagen fibrils are laid down in alternating orientations. The normal lamellar pattern is absent in woven bone, in which collagen fibrils are laid down in a disorganized manner. As such, woven bone is weaker than lamellar bone. Woven bone is normally produced during formation of primary bone (Clarke 2008). The collagen fibril diameter is regulated by osteonectin (Clarke 2008). It is a glycoprotein abundantly expressed in bone undergoing active remodeling (Sila-Asna et al. 2007).

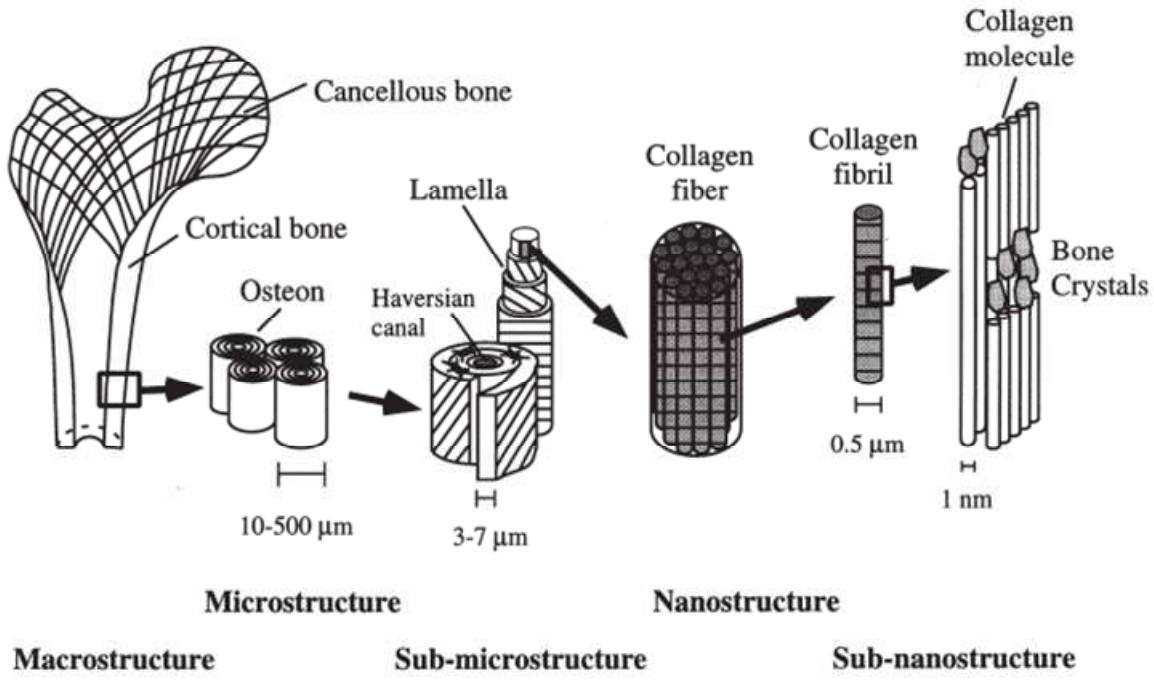

Figure 14. Hierarchical structural organization of bone: cortical and trabecular (cancellous) bone; osteons with Haversian systems; lamellae; collagen fiber assemblies of collagen fibrils; bone mineral crystals, collagen molecules, and non-collagenous proteins (from http://biomechanism.com/mechanical-properties-and-the-hierarchical-structure-of-bone).

The periosteum is a fibrous connective tissue sheath that surrounds the outer cortical surface of bone, except at joints where bone is lined by cartilage. The endosteum is a membranous structure covering the inner surface of cortical bone, trabecular bone and the blood vessel canals (Volkman's canals) present in bone (Clarke 2008).

Bone is a heterogeneous and complex tissue made up of various proportions of cellular content, extracellular matrix and mineral content. Depending on the species, age of the species, the type and location of bone, these contents can vary. The inorganic fraction makes up to 70 % of tissue weight of the mature bone, the organic fraction up to 20 % and water accounts for the remaining 10 %. Calcium phosphate minerals are present in the matrix as hydroxyapatite [$Ca_{10}(PO_4)_6(OH)_2$]. Bone crystals provide mechanical rigidity and load-bearing strength to bone, whereas the organic matrix provides elasticity and flexibility (Clarke 2008). The organic matrix of bone is composed of many diverse materials but collagen makes up to 90 % of the matrix of the tissue. Collagen type 1 fibres constitute the majority of the matrix and are arranged generally as parallel fibrils of even diameter. Their orientation changes through the thickness of the tissue. The remaining 10 % of the matrix consists of

noncollagenous material and is made up of proteins, proteoglycans, lipids and other substances with the bulk being noncollagenous proteins (Clarke 2008; Sila-Asna et al. 2007).

A main noncollagenous protein present in bone is alkaline phosphatase (ALP). This protein plays a role in the mineralization process of bone. It hydrolyzes mineral deposition inhibitors such as extracellular pyrophosphate and cleaves phosphate groups into inorganic phosphate ions, which are used for mineral deposition (Al-Jallad et al. 2006; Clarke 2008; Mackie et al. 2008). The upregulation of ALP activity is used as a marker for differentiation of pre-osteoblasts in mature osteoblasts. The final phase of osteoblast development is characterized by the formation of mineralized extracellular matrix and once this mineralization starts, ALP activity decreases significantly (Coetzee et al. 2009).

Osteopontin (OPN) is another abundant noncollagenous protein in the bone. It is produced by osteoblasts and osteoclasts. OPN plays a key controlling role both in cell attachment and bone resorption (Yoshitake et al. 1999). Moreover, OPN has a critical role in the regulation of the physical location and proliferation of HSCs. *In vitro* studies suggested that OPN inhibits HSC proliferation (Haylock and Nilsson 2006; Nilsson et al. 2005).

Furthermore, bone sialoprotein (BSP) is also a major noncollagenous matrix protein and is produced by osteoblasts, osteoclasts, osteocytes and hypertrophic chondrocytes. It mediates cell attachment. Its role is furthermore associated with the formation of the hydroxyapatite crystal on one hand and osteoclastogenesis and bone resorption on the other hand (Boudiffa et al. 2010; Clarke 2008; Sila-Asna et al. 2007; Valverde et al. 2008).

8.1.2. Mesenchymal stem cells and osteoblasts

Bone marrow contains a small population of mesenchymal stem cells that are able to give rise to several cell types such as osteoblasts, chondroblasts and adipocytes (**Figure 15**) (Bonfield and Caplan 2010; Disthabanchong et al. 2007; Pittenger et al. 1999; Thompson et al. 1998).

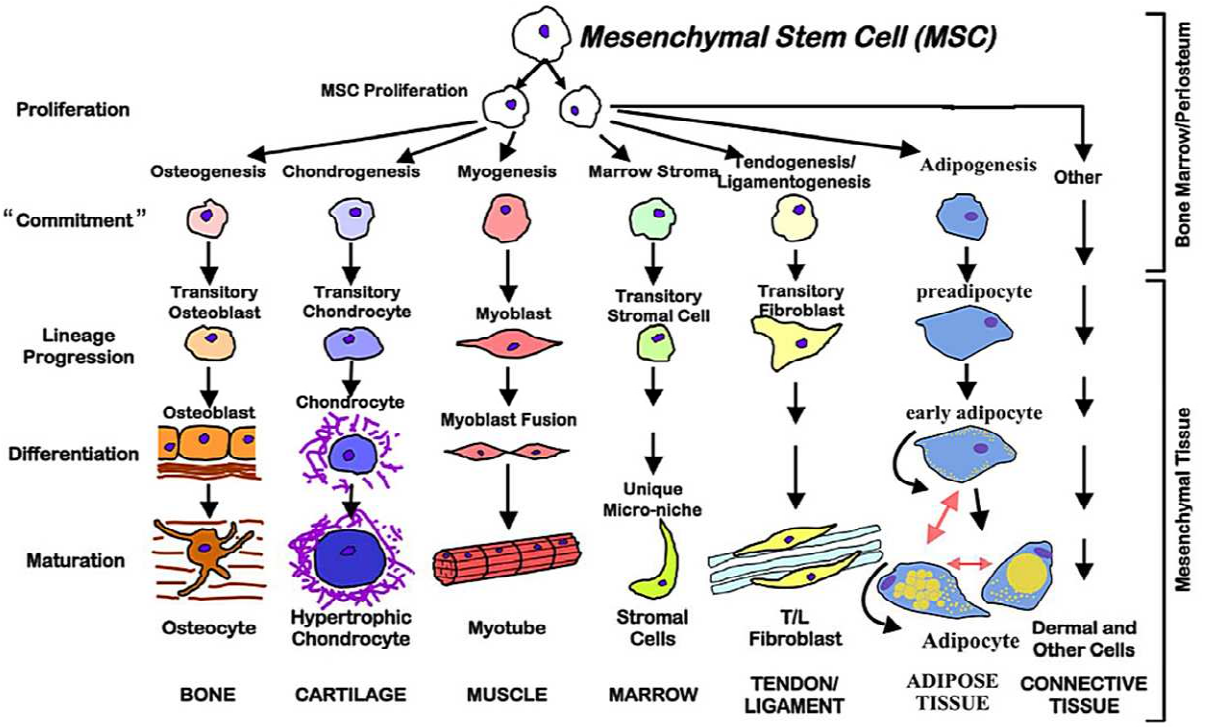

Figure 15. Mesenchymal stem cell differentiation (from Bonfield and Caplan 2010).

Mesenchymal stem cells can differentiate into immature osteoblasts through the action of Runt-related transcription factor 2 (Runx2), osterix and β-catenin. Runx2, also known as Core-binding factor alpha 1 (Cbfα1), is a transcription factor of the Runt domain gene family that is essential for bone formation. Runx2 directs multipotent mesenchymal cells to an osteoblastic lineage, and inhibits them from differentiating into the adipocytic and chrondrocytic lineages (Geoffroy et al. 2010). After MSC differentiation to pre-osteoblasts, Runx2, β-catenin and osterix direct these cells to immature osteoblasts, which produce bone matrix proteins, blocking their potential to differentiate into the chondrocytic lineage. Moreover, Runx2 inhibits osteoblast maturation and the transition into osteocytes, keeping as such osteoblasts in an immature stage (Komori 2006, 2009).

The immature pre-osteoblasts are spindle-shaped and express high levels of OPN. Pre-osteoblasts that are found near functioning osteoblasts are usually recognizable because of their expression of ALP. They differentiate into mature large cuboidal differentiated osteoblasts, which express high levels of osteocalcin (OCN). This is a major noncollagenous protein of the matrix, synthesized and secreted exclusively by osteoblastic cells in the late stage of maturation and is considered as a late indicator of osteoblast differentiation. OCN expression is modulated by parathyroid hormone (PTH) and other factors. OCN binds with

high affinity to hydroxyapatite crystals and regulates bone crystal growth (Sila-Asna et al. 2007).

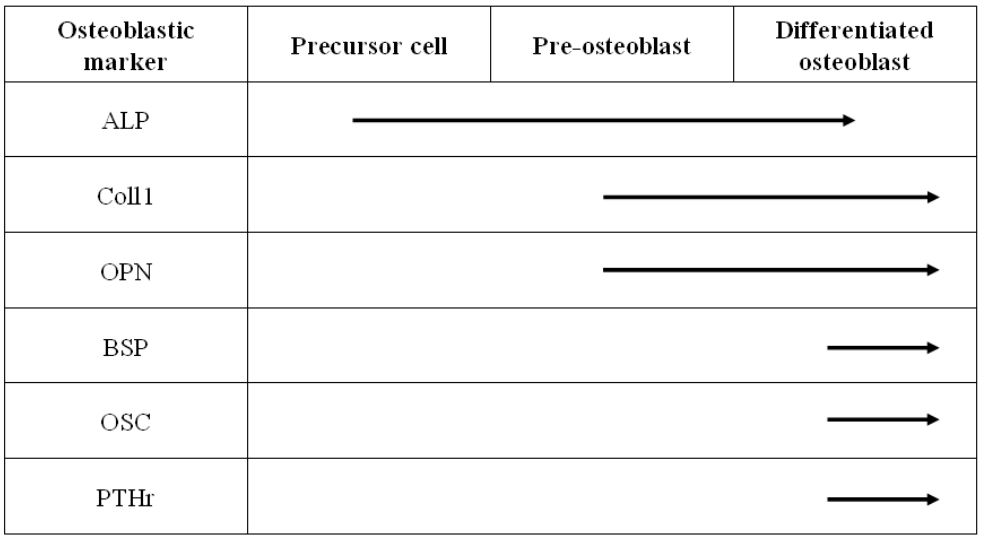

Figure 16. Some principal expressed genes during osteoblast differenciation (ALP: alkalin phosphatase, Coll 1: collagen 1, OPN: osteopontin, BSP: bone sialoprotein, OSC: osteocalcin, PTHr: parathyroid hormone receptor) (from Marie 2001).

Active mature osteoblasts that synthetize bone matrix have large nuclei, enlarged Golgi structures, and extensive endoplasmatic reticulum. These osteoblasts secrete type 1 collagen and other matrix proteins (fibronectin, OPN, osteonectin, OCN and BSP) vectorially towards the bone formation surface. Osteoblasts and bone lining cells are found in close proximity and joined by adherent junctions (Marie 2001).

Growth factors produced by osteoblasts, including insulin-like growth factor (IGF), fibroblast growth factor (FGF), bone morphogenetic protein (BMP) and transforming growth factor-β (TGF-β), are important for bone growth and osteogenesis. They are capable of stimulating both osteoblast cell proliferation and differentiation (Baek and Kang 2009; Tsumaki and Yoshikawa 2005). BMP signalling for instance is required for normal rates of onset and progression of chondrocyte hypertrophy (Mackie et al. 2008).

The mature osteoblasts are embedded in the bone matrix to become osteocytes (Komori 2006). Osteocytes represent terminally differentiated osteoblasts and support bone structure and metabolism. They do not express ALP but do express OCN. It is suggested that osteocytes may undergo apoptosis (Clarke 2008). It has been shown that osteocytes in bone

produce FGF-23, a 1,25-$(OH)_2$ vitamin D3 regulating hormone, and as such bone participates in the regulation of vitamin D and mineral homeostasis (Quarles 2008).

8.1.3. Osteoclasts

Osteoclasts are specialized cells for bone resorption via ruffled borders and clear zones (**Figure 17**) (Shibata and Yamashita 2001). They are multinucleated cells formed by cytoplasmic fusion of their mononuclear precursors, which are in the myeloid lineage of hematopoietic cells that also give rise to macrophages. The switch to osteoclast differentiation requires expression in osteoclast precursors of c-Fos, a RANKL activated transcription factor (Baron and Tsouderos 2002; Boyce and Xing 2007).

Osteoclasts bind to bone matrix via integrin receptors. Binding of osteoclasts to bone matrix causes them to become polarized, with the bone resorbing surface developing a ruffled border. The ruffled border secretes H^+ ions via H^+-ATPase and chloride channels and causes exocytosis of cathepsin K and other enzymes like MMP-9 in the acidified vesicles. Upon contact with bone matrix, the fibrillar cytoskeleton of the osteoclast organizes into an actin ring, which promotes formation of a sealing zone around the periphery of osteoclast attachment to the matrix. As such, the sealing zone surrounds and isolates the acidified resorption compartment from the surrounding bone surface (Boyce and Xing 2007). The low pH of the so called resorption pit activates the proteolytic enzymes and promotes dissolution of crystalline calcium phosphate of the bone matrix (Wu et al. 2008).

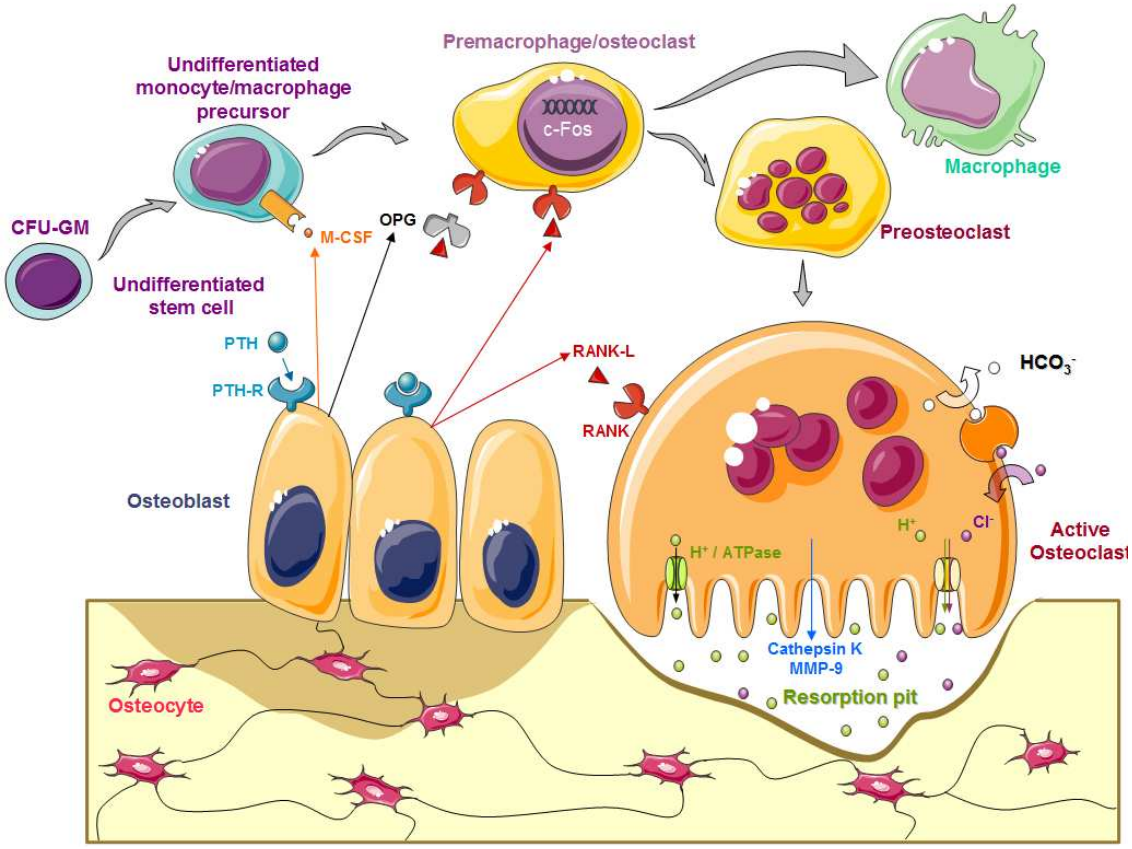

Figure 17. Diagram of the formation of osteoclasts and their relationship to osteoblasts. CFU-GM: colony-forming unit for the granulocyte-macrophage series, M-CSF: monocyte-macrophage colony-stimulating factor, Cl^- : chloride ion, H^+: hydrogen ion, H^+ ATPase: H^+-adenosine triphosphatase, HCO_3^-: carbonate ion, OPG: osteoprotegerin, PTH: parathyroid hormone, PTH-R: Parathyroid Hormone Receptor, RANK: receptor activator factor of nuclear factor-κB, RANKL: RANK ligand.

Osteoblasts regulate osteoclast maturation and proliferation by cytokines such as macrophage colony-stimulating factor (M-CSF) (Baek and Kang 2009) and receptor activator of nuclear factor-κB ligand (RANKL) (**Figure 18**) (Boyce and Xing 2007; Lymperi et al. 2008; Wu et al. 2008). RANKL belongs to the tumor necrosis factor (TNF) superfamily and is produced by osteoblasts and osteoblast precursors to stimulate osteoclast recruitment and activation. It interacts with membrane-bound molecules on nearby (by secreted RANKL) or adjacent (by membrane-bound RANKL) osteoclasts and its precursors (Baek and Kang 2009; Boyce and Xing 2007). The effects of RANKL are counterbalanced by osteoprotegerin (OPG), which protects the skeleton from excessive bone resorption by binding to RANKL and preventing it from binding to its receptor RANK (Baek and Kang 2009; Boyce and Xing 2007).

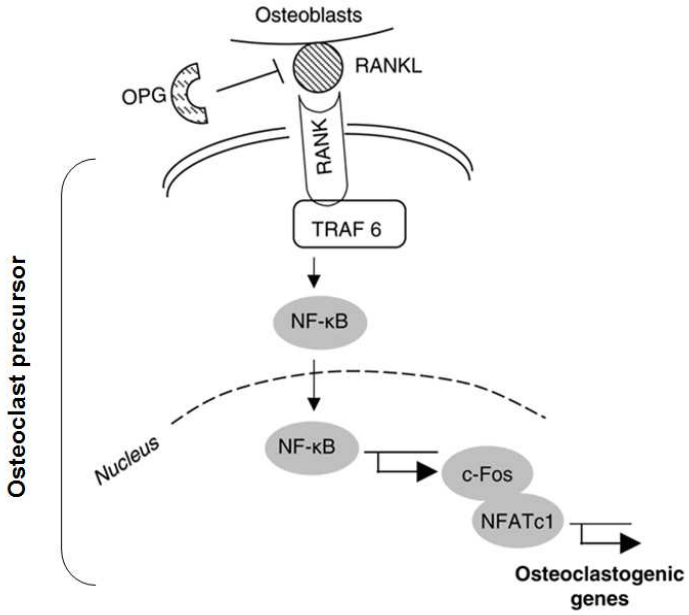

Figure 18. Signaling pathway for normal osteoclastogenesis. RANKL produced by osteoblasts binds to RANK on the surface of osteoclast precursors and recruits the protein TRAF6, leading to NF-κB activation and translocation to the nucleus. NF-κB increases c-Fos expression and c-Fos interacts with NFATc1 to trigger the transcription of osteoclastogenic genes. OPG inhibits the initiation of the process by binding to RANKL. NFAT, nuclear factor of activated T cells; NF-κB, nuclear factor-κB; OPG, osteoprotegerin; RANKL, receptor activator of nuclear factor-κB ligand; TRAF, tumor necrosis factor receptor associated factor from (Boyce and Xing 2007).

8.1.4.Bone growth, modelling and remodelling

Bone undergoes longitudinal and radial growth, modelling and remodelling during life. Longitudinal and radial growth occurs during childhood and adolescence. At growth plates, longitudinal growth occurs before subsequently undergoing mineralization to form primary new bone (Clarke 2008). Bone modelling on the other hand is the process by which bone changes its overall shape in response to physiologic influences or mechanical forces, leading to the gradual adjustment of the skeleton to the forces that it encounters (Clarke 2008).

The main recognized functions of bone remodelling include preservation of bone mechanical strength by replacing older micro-damaged bone with newer healthier bone and calcium and phosphate homeostasis (Clarke 2008). Remodelling begins before birth and continues until death. Remodelling involves continuous removal of discrete packets of old bone, replacement of these packets with newly synthesized bone matrix, and subsequent mineralization of the matrix to form new bone. The bone remodelling unit is composed of a tightly coupled group

of osteoblasts and osteoclasts that sequentially carry out resorption of old bone and formation of new bone (Clarke 2008). At skeletal maturity, the process of bone remodelling occurs less intensively than previously. Later on with age, the intensity of osteoclastic resorption begins to increase, leading to a net loss of bone mass (Riis 1996).

Studies with female humans and animals showed changes in bone remodelling during the menstrual cycle with monthly episodes of increased bone resorption (Chiu et al. 1999; Gass et al. 2008; Hotchkiss and Brommage 2000; Kalyan and Prior 2010). Women undergo significant bone mass loss during menopause which is linked to oestrogen deficiency leading to increased bone remodelling with an excess of resorption over formation (Windahl et al. 2009; Xing and Boyce 2005). *In vitro* studies have shown that oestrogen enhances the proliferation and differentiation of osteoblasts and promotes osteoclast apoptosis (Hughes et al. 1996; Marie 2001). Moreover, oestrogen decreased the production of M-CSF and tumor necrosis factor α (TNF-α), two cytokines involved in osteoclast formation (Marie 2009; Srivastava et al. 1999; Srivastava et al. 1998). Furthermore, oestrogens increase the expression of 1,25-$(OH)_2$ vitamin D3 receptor in osteoblasts, which was linked to an anti-apoptotic effect of these cells (Duque et al. 2002). Oestrogen also decreased the production of RANKL and increased the production of OPG, which prevents osteoclast differentiation (Zallone 2006). Cao et al. showed *in vitro* that oestrogen activates BMP, and as such favours the differentiation of pre-osteoblasts and osteoblasts (Cao et al. 2003). Finally, it has been shown that testosterone has some antiresorptive effects and helps maintain bone formation (Baek and Kang 2009).

8.1.4.1. Intramembranous and endochondreal bone formation

Intramembranous bone formation happens mostly in flat bones. With intramembranous bone formation, bone arises directly from mesenchymal cells which condense and directly differentiate into osteoblasts to deposit bone matrix (Chung et al. 2004; Cohen 2006).

Endochondreal bone formation happens on the other hand mostly in long bones (**Figure 19**). It involves a cartilaginous precursor template from which bone and bone marrow develops. At the onset of endochondreal bone formation, MSC differentiate into chrondrocytes. Chondrocytes then proliferate and produce a matrix to form primordial cartilage (**A**). Shortly after formation of the primordial cartilage, proliferating chrondrocytes in the central region of

the cartilage undergo differentiation into hypertrophic chondrocytes . These exit the cell cycle and synthesize another matrix. The hypertrophic cartilage is invaded by blood vessels, osteoblasts, osteoclasts and hematopoietic cells, resulting in the formation of primary ossification centers (**B**). The hypertrophic cartilage matrix is degraded by chondroclasts, the hypertrophic chondrocytes die and bone marrow and endochondreal bone replaces the disappearing cartilage (**C**). A collar of bone surrounding the surface of the cartilage model results from intramembranous ossification. As the front nears the end of the long bone, distal chondrogenesis elaborates a cartilaginous growth plate (**Figure 20**) that serves as a continual source of cartilage conversion to bone, resulting in linear growth of the long bone. Secondary centres of ossification at the ends of the long bone appear during late fetal life and early childhood. Articular-epiphyseal growth cartilage (AEGC) remains under the permanent articular cartilage (**D**). Long bones cease growing at the end of puberty and with time the growth plates are replaced by bone and the only remaining cartilage is the permanent articular cartilage at each end of bone (**E**) (Chung et al. 2004; Cohen 2006; Mackie et al. 2008; Pratt 1957; Tsumaki and Yoshikawa 2005).

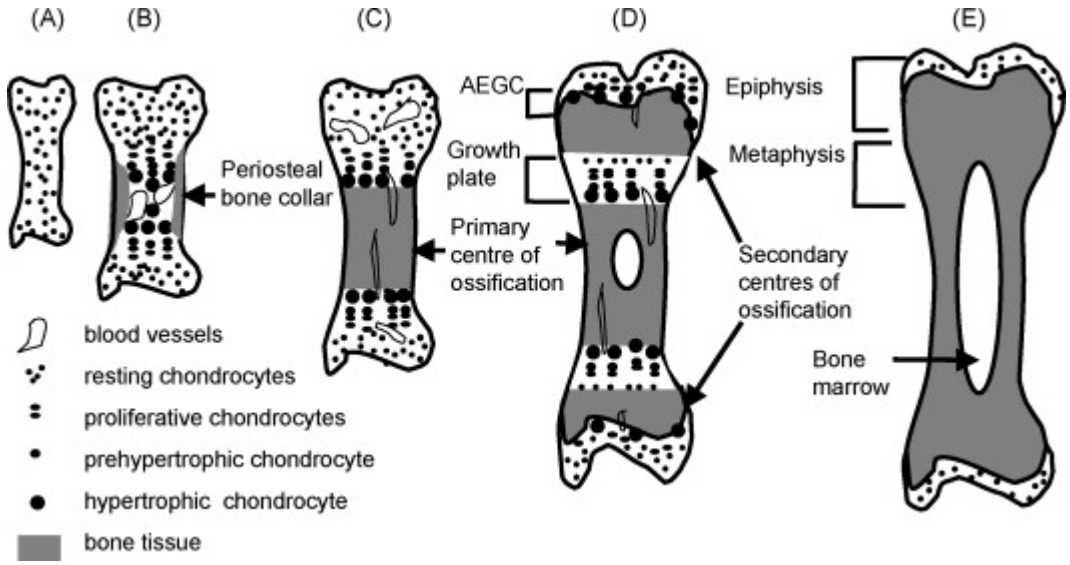

Figure 19. Development of an endochondreal bone (from Mackie et al. 2008).

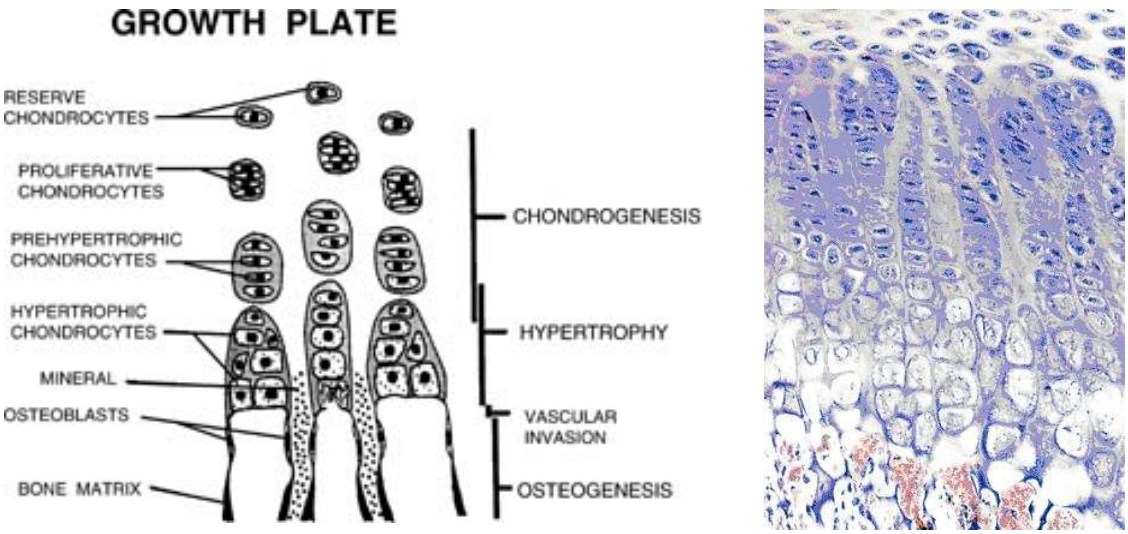

Figure 20. Schematic representation and photomicrograph of the growth plate of an endochondreal bone demonstrating chondrogenesis, hypertrophy of chondrocytes, vascular invasion, and osteogenesis (from Cohen 2006).

8.1.4.2. Bone remodelling cycle

The bone remodelling cycle (**Figure 21**) starts with resorbing osteoclasts secreting hydrogen ions via H^+-ATPase proton pumps and chloride channels in their cell membranes into the resorption pit to lower the pH within at 4,5 which helps mobilize bone mineral. Resorbing osteoclasts secrete tartrate-resistant acid phosphatase (TRAP5b), cathepsin K, MMP-9 and gelatinase from cytoplasmic lysosomes to digest the matrix (Baek and Kang 2009; Clarke 2008). TRAP5b has two distinct enzymatic activities to participate in the degradation of matrix components. It can function as a phosphatase at acidic pH and as a generator of reactive oxygen species (ROS) at neutral pH. Matrix degradation products are endocytosed together with cathepsin K into osteoclasts and transported through the cell in transcytotic vesicles. Vesicles containing TRAP5b are fused in these vesicles. When the vesicles move away from the resorption lacuna their pH is changed to neutral, providing an optimal environment for the ROS generating activity of TRAP5b. ROS finalize degradation of the matrix components during their transcytosis. Finally, the matrix degradation products are released from the osteoclast into the blood circulation together with TRAP5b (Vaaraniemi et al. 2004). During osteoclastic bone resorption, C-telopeptide degradation products from type 1 collagen (CTX) are released into the circulation. Indeed, in a rat model, it was shown that an increased concentration of CTX in the serum is associated to an enhanced degradation of the bone matrix (Brzoska and Moniuszko-Jakoniuk 2005a, b).

During a reversal phase, bone resorption transitions to bone formation. At the completion of bone resorption, resorption pits contain a variety of mononuclear cells, including pre-osteoblasts recruited to begin new bone formation. One coupling signal linking the end of bone resorption to the beginning of bone formation is TGF-β, which is released form the bone matrix and decreases osteoclast resorption by inhibiting RANKL production by osteoblasts (Clarke 2008). The osteoblasts synthesize new collagenous organic bone matrix. During collagen synthesis, procollagen 1 N-terminal propeptide (PINP) is released. This propeptide is ultimately secreted into the blood circulation. Osteoid formed is the unmineralized, organic portion of the bone matrix that forms prior to the mature mineralized bone tissue.

The end result of each bone remodelling cycle is the production of a new osteon. The remodelling process is essentially the same in cortical and trabecular bone (Clarke 2008). At the completion of bone formation, osteoblasts undergo apoptosis or become osteocytes or bone lining cells. Bone-lining cells may regulate influx and efflux of mineral ions into and out of bone extracellular fluid, thereby serving as a blood-bone barrier. They can redifferentiate into osteoblasts upon exposure to PTH or mechanical forces (Clarke 2008).

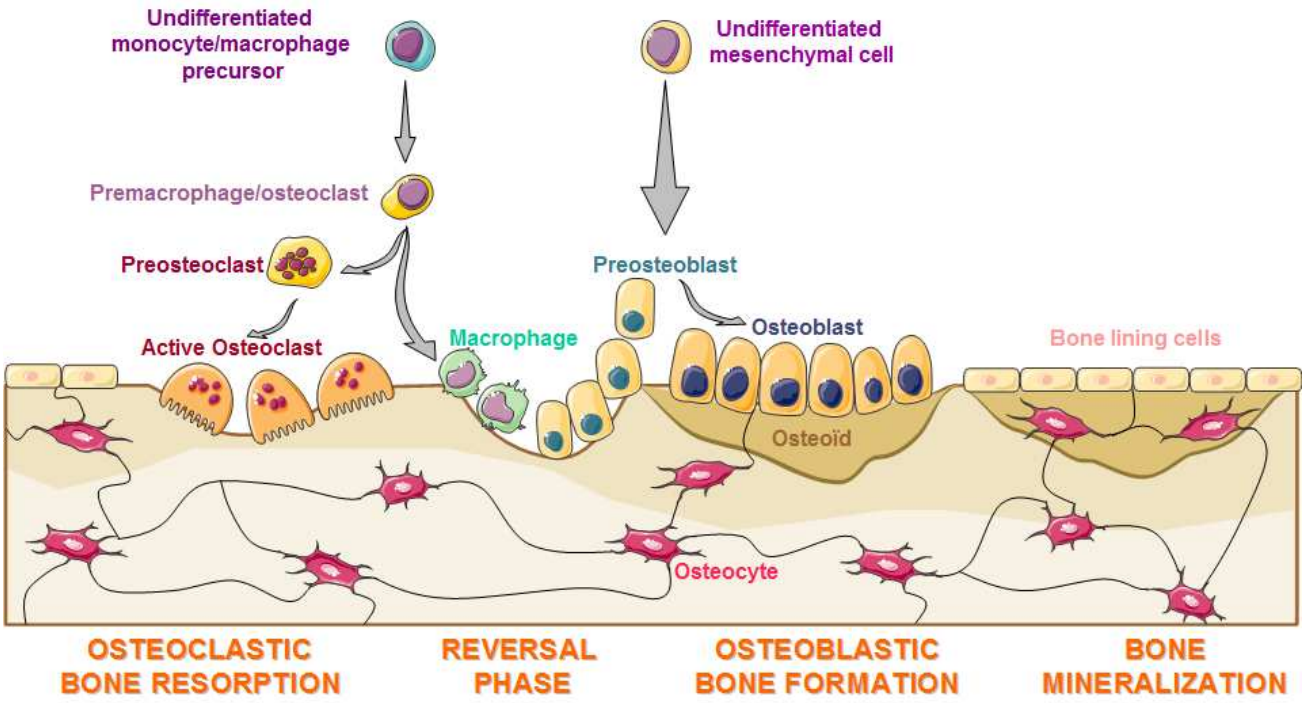

Figure 21. The bone remodelling cycle.

8.1.5. Vitamin D and bone metabolism

The process of osteogenesis is controlled by systemic hormones and growth factors. Two of the main regulators of calcium homeostasis are 1,25-$(OH)_2$ vitamin D3 and parathyroid hormone (PTH) (Baek and Kang 2009).

Vitamin D is crucial to the overall health and has important functions in calcium homeostasis and bone metabolism. After absorption or skin production of vitamin D, the liver synthesizes 25-OH vitamin D and the kidneys subsequently produce biologically active 1,25-$(OH)_2$ vitamin D3, also called calcitriol (**Figure 22**). 1,25-$(OH)_2$ vitamin D3 functions through the binding with a vitamin D receptor (VDR) in target cell nuclei, regulating gene expression in these cells, including osteoblasts and chondrocytes (Masuyama et al. 2006). Serum 1,25-$(OH)_2$ vitamin D3 is responsible for maintaining serum calcium and phosphorus and does this primarily by stimulating intestinal absorption of calcium and phosphorus (Samadfam et al. 2008; Tissandie et al. 2006). The effect of vitamin D on bone is complex and many studies conducted both *in vitro* and *in vivo* have brought conflicting results. It is suggested that 1,25-$(OH)_2$ vitamin D3 exert both anabolic and catabolic effects on the skeleton (Duque et al. 2005; Samadfam et al. 2008).

On one hand 1,25-$(OH)_2$ vitamin D3 seems to be an osteotropic hormone that stimulates bone resorption. *In vitro* experiments showed that VDR signalling in chondrocytes directly regulates osteoclastogenesis by inducing RANKL expression (Baron and Tsouderos 2002; Masuyama et al. 2006). *In vivo*, 1,25-$(OH)_2$ vitamin D3 inhibited osteoclastogenesis by decreasing the pool of osteoclast precursors in the bone marrow and removal of osteoclasts from the resorption site by apoptosis (McKenna et al. 2000; Shibata et al. 2002). On the other hand, vitamin D seems to stimulate mineralization of the bone matrix. Several studies showed that vitamin D deficiency leads to impairment of bone mineralization. Vitamin D promoted differentiation of osteoblasts and stimulated osteoblastic expression of OPN and OCN and regulated collagen post-translational modifications and maturation in an osteoblastic cell culture system (Clarke 2008; Marie 2001; Nagaoka et al. 2008). An *in vivo* study with rats showed that 1,25-$(OH)_2$ vitamin D3 improved mechanical strength in an ovariectomized rat model (Fu et al. 2009).

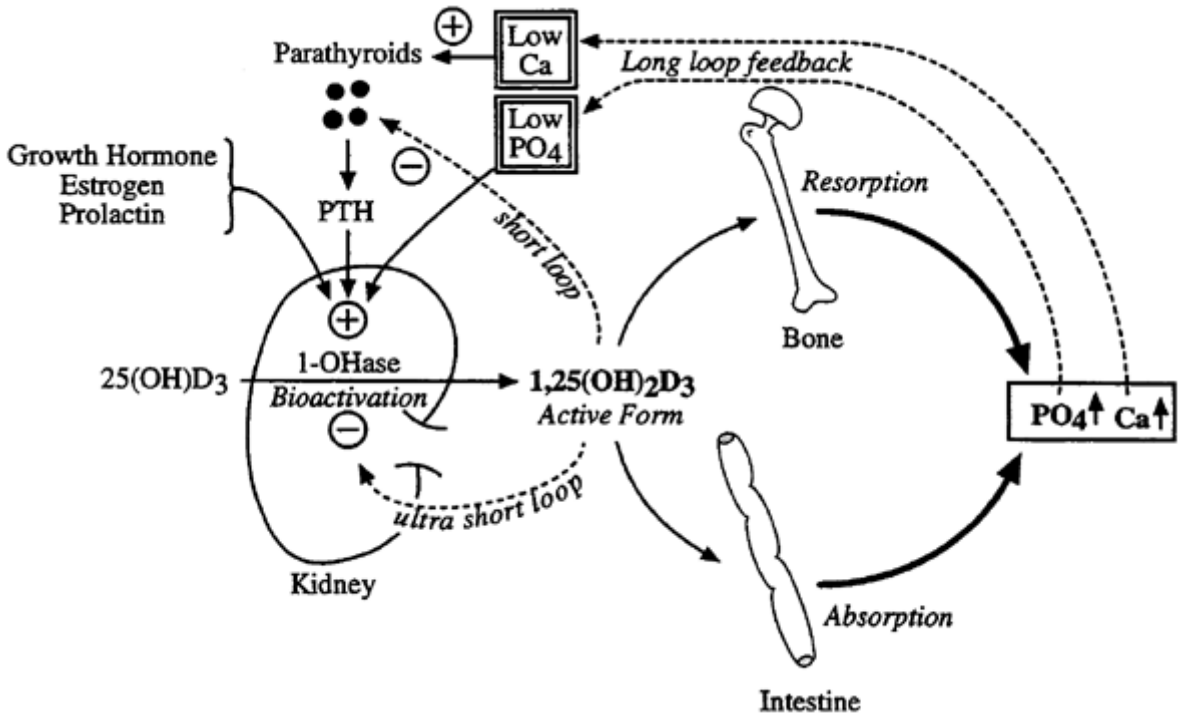

Figure 22. 1,25-$(OH)_2$ vitamin D3 production (from http://chemistry.gravitywaves.com/CHE452/).

Generally, it is assumed that 1,25-$(OH)_2$ vitamin D3 at lower doses seems to have predominantly an anabolic effect on bone, whereas at high doses seems to stimulate bone resorption (Suda et al. 2003). Furthermore, 1,25-$(OH)_2$ vitamin D3 inhibits PTH production both by direct action on the parathyroid glands and indirectly by raising serum calcium levels. PTH is recognized as being a major regulator of calcium homeostasis and bone remodelling. *In vivo*, PTH exerted both anabolic and catabolic effects on bone. Intermittent injections of PTH increased bone mass, while continuous infusion of PTH caused bone loss (Choudhary et al. 2008; Dempster et al. 1993; Lymperi et al. 2008; Marie 2001; Samadfam et al. 2008). It has been shown that PTH has direct effects on bone via PTH receptors in osteoblasts and increases calcium and phosphate efflux from the exchangeable bone compartiment (Quarles 2008).

1,25-$(OH)_2$ vitamin D3 production is itself stimulated by PTH, thus providing an effective control loop (**Figure 22**). Indeed, some studies showed a compensatory response to vitamin D deficiency by the stimulation of PTH secretion, and that hyperparathyroidism increased bone turnover and bone loss (Baek and Kang 2009).

Finally, glucocorticoids inhibit calcium absorption from the gut by opposing the actions of vitamin D and by decreasing the expression of specific calcium channels in the duodenum

(Baek and Kang 2009). Furthermore it has been shown that glucocorticoids increase the expression of RANKL, inducing osteoclastic differentiation. Some studies showed that glucocorticoid dexamethasone inhibits proliferation of pre-osteoblasts and induces on the long term reduction of bone formation (Marie 2001; Xing and Boyce 2005). Another study on the other hand showed that dexamethasone inhibits bone resorption by indirectly inducing apoptosis of osteoclasts (Warabi et al. 2001).

8.2. Hematopoietic system

8.2.1. Generalities

Hematopoiesis is defined as the whole of mechanisms leading to the continuous and regulated production of functional and mature blood cells (**Figure 23**) (Ceredig et al. 2009). The hematopoietic tissue is situated mainly in the bone marrow for adult humans and in the bone marrow and spleen for adult mice. In adult humans, bone marrow can be found in short bones and long bones, in particular femurs, hip bones, vertebrae, ribs and the skull (Cristy 1981). The hematopoietic tissue includes four cellular compartments: the hematopoietic stem cells (HSC), progenitors, precursors and mature cells. The HSC proliferate and are capable to differentiate in progenitors, then precursors and finally mature cells. This process is strictly controlled by stromal cells of the bone marrow and the medullar micro-environment through growth factors and adhesion molecules.

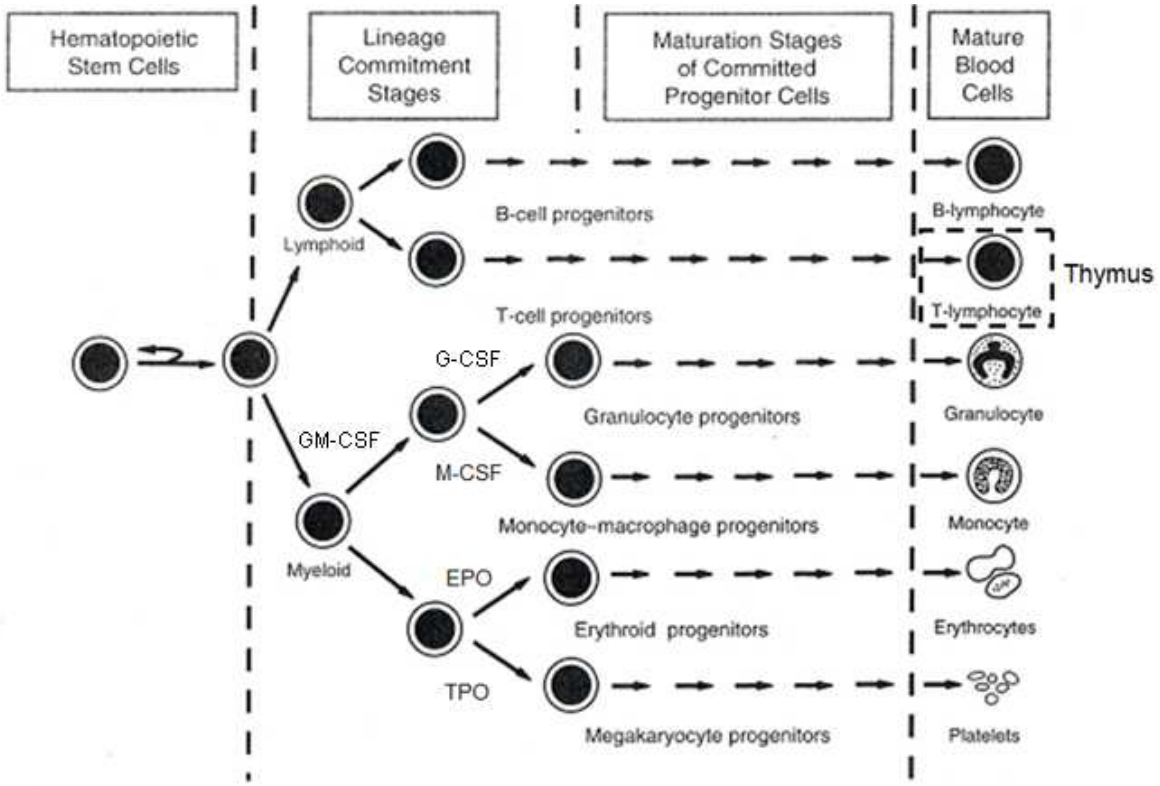

Figure 23. Diagram of hematopoietic cell differentiation. Myeloid progenitor differentiation is stimulated by granulocyte macrophage colony stimulating factor (GM-CSF), granulocyte differentiation by granulocyte colony stimulating factor (G-CSF), monocyte-macrophage differentiation by macrophage colony stimulating factor (M-CSF), erythrocyte differentiation by erythropoietin (EPO) and platelet differentiation by thrombopoietin (TPO).

8.2.2.Hematopoietic stem cell

The HSC have an auto-renewal capacity and as they are multipotent, are capable to differentiate in medullar, blood and thymic cells. One strategy by which HSC can accomplish these two tasks is asymmetric cell division, whereby each stem cell divides to generate one daughter with a stem cell fate (self-renewal) and one daughter that differentiates. HSC can also use symmetric divisions to self-renew and to generate differentiated progeny. Symmetric divisions are defined as the generation of daughter cells that are destined to acquire the same fate, i.e. two daughter stem cells or two differentiated cells. As such, these symmetric divisions can expand the HSC number. HSC seem to divide asymmetrically under steady-state conditions and divide symmetrically to restore stem cell pools depleted by injury or disease (Martinez-Agosto et al. 2007; Morrison and Kimble 2006; Morrison et al. 1997).

The existence of HSC has been put in evidence by Till and McCulloch in a mouse model fifty years ago in which a lethal medullar aplasia consecutive to an irradiation of 10 Gy was treated with bone marrow transplantation (Till and Mc Culloch 1961). Furthermore, this work put in evidence the existence of clones in the spleen, which are called colony forming units-spleen (CFU-S), that contain progenitors capable to generate erythroid, granulocyte, monocyte and megacaryocyte colonies.

Even if the existence of HSC is known for some while, their characterisation stays difficult. Indeed, these cells are not frequent in the bone marrow and present no specific morphologic characteristics recognizable by cytological coloration methods. On the other hand, these cells can be characterized by functional engraftment tests such as the competitive repopulation assay (for mouse cells) and the severe combined immuno deficient (SCID) repopulation assay (for human cells) (Dick et al. 1997; Harrison 1980; Szilvassy and Cory 1993; Yahata et al. 2003).

The absence of markers of differentiation of HSC (lineage negative) makes them difficult to identify. However, certain markers, which are species specific, can be expressed during early hematopoiesis. By men, the most important marker is the cluster of differentiation 34 (CD34), which is expressed during differentiation (Civin et al. 1984). However, as CD34 can also be found on the surface of some medullar stromal cells and endothelial cells (Fina et al. 1990; Simmons and Torok-Storb 1991), other positive or negative selection markers are used in association with CD34 in order to characterize HSC. For example, the absence of CD38, CD33 (myeloid marker) and CD19 (B lymphocyte marker) markers (Andrews et al. 1989; Terstappen et al. 1991) and the presence of CD133, CD90 and C1qRp markers can be used (Baum et al. 1992; Bonnet 2003; Boxall et al. 2009; Danet et al. 2002). Moreover, HSC express a certain number of receptors for cytokines and chemokines. KDR, CD184 (CXCR4) and CD117 (c-Kit) for example, with the latter a receptor for stem cell factor (SCF) (Wright et al. 2002; Ziegler et al. 1999). SCF is known to promote stem cell proliferation (Wognum et al. 2003). By mice, the markers are a bit different, but the way to characterize HSC is similar, with the positive and negative selection of specific markers. Stem cell antigen-1 (Sca-1) is a murine cell surface antigen identified on HSC that is expressed at varying levels throughout HSC differentiation and plays a role in HSC proliferation (Okada et al. 1992). To conclude, mouse HSC can be defined as Lin^- c-Kit^+ Sca-1^+ $CD45^+$ (Li and Li 2006; Osawa et al. 1996; Ramos et al. 2003).

8.2.3. Hematopoietic progenitors, precursors and mature cells

HSC differentiation gives raise to new cells with a strong clonogenic potential, called hematopoietic progenitors (**Figure 24**). These progenitors are characterized by cultivation technique in semi-solid medium in the presence of growth factors (Dexter et al. 1977; Spangrude et al. 1988). Indeed, in the 1960s, Bradley and Metcalf generated colonies of macrophages and polynuclear cells from bone marrow cells (Bradley and Metcalf 1966). The hematopoietic progenitors as such characterized are called colony forming cells (CFC), colony forming unit (CFU) or burst forming unit (BFU). Different types of progenitors could be characterized, including CFU-GEMM (capable of generating colonies of granulocytes, macrophages, megakaryocytes and erythroid cells), CFU-GM (capable of generating colonies of granulocytes and macrophages) and BFU-E (capable of generating colonies of erythroid cells) (Dingli and Pacheco 2010).

The progenitors differentiate into precursors and represent one of the last stages of hematopoietic cell maturation. These precursors are myeloblasts, promyelocyte basophils, promyelocyte eosinophils, megakaryoblasts and lymphoblasts. They are recognizable by morphological characteristics. Finally, the maturation of the hematopoietic precursors leads to the formation of mature circulating cells, such as granulocytes (essentially neutrophils, but also eosinophils and basophils), monocytes (which further differentiate into macrophages), erythrocytes, thrombocytes and lymphocytes. The latter terminating their differentiation in the bone marrow (B-lymphocytes) or in the thymus (T-lymphocytes) (**Figure 24**) (Dingli and Pacheco 2010).

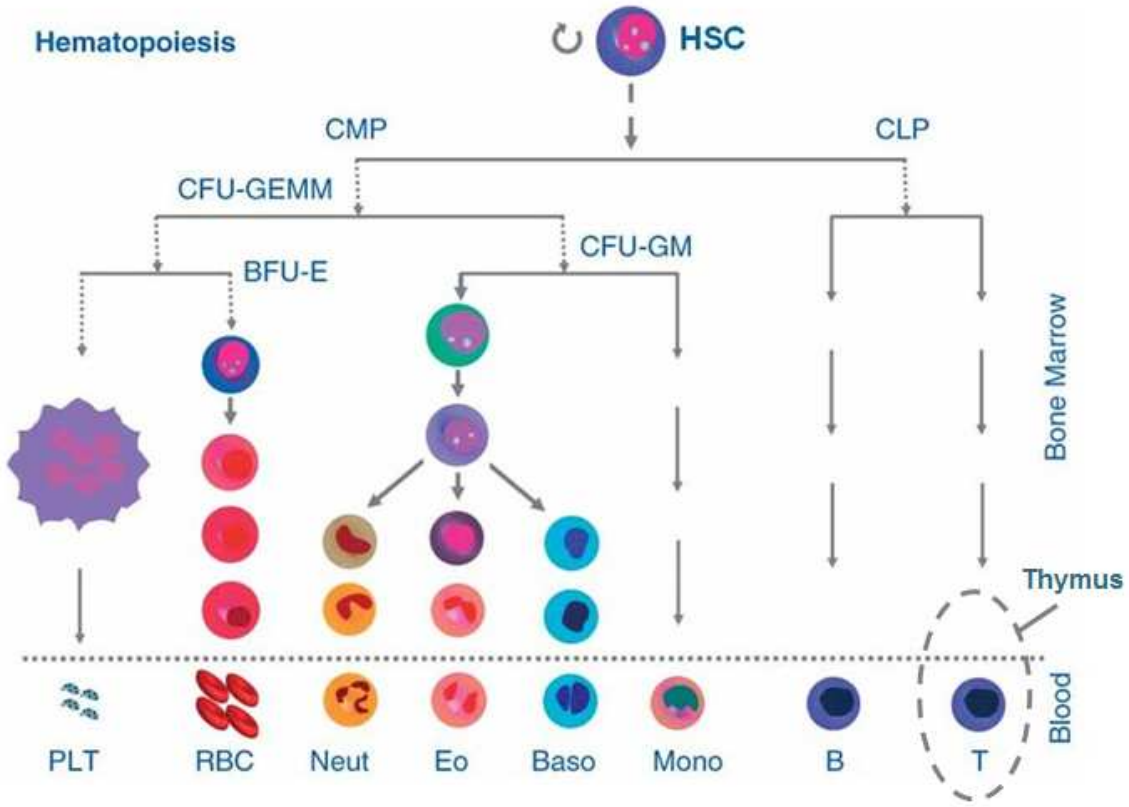

Figure 24. Hematopoiesis has a tree-like structure with the hematopoietic stem cells at the root of the process. Each cell division gives rise to progeny cells that can retain the properties of their parent cell or differentiate. As the progeny move further away from the hematopoietic stem cell (HSC), their pluripotent ability is increasingly restricted. CMP: common myeloid progenitor, CLP: common lymphoid progenitor, CFU-GEMM: granulocyte erythrocyte megakaryocyte monocyte, BFU-E: erythroid burst forming unit, CFU-GM: granulocyte-macrophage colony-forming unit (from Dingli and Pacheco 2010).

8.2.4.Bone hematopoietic niche

Hematopoietic stem cells reside in the bone marrow cavity in a specific microenvironment known as the HSC niche. The hematopoietic niche consists of different stromal cell types such as endothelial cells, fibroblasts, adipocytes and osteoblasts that regulate survival, self-renewal, migration, proliferation and differentiation of HSC (Lam and Adams 2010; Moore 2004).

Osteoblasts have been shown to regulate hematopoiesis by producing a vast array of growth factors and cytokines, important for the maturation of hematopoietic progenitors (Taichman and Emerson 1994, 1998). On the surface of osteoblasts, Angiopoietin-1 regulates HSC number through the activation of Tie-2/Ang-1 signalling pathway, whereas the Notch receptor ligand, Jagged 1, modulates HSC self-renewal (Lemischka and Moore 2003; Zhu and

Emerson 2004). Furthermore, OPN participates in HSC location and is a negative regulator of their proliferation (Lymperi et al. 2008). A study supports the notion that N-cadherin$^+$ osteoblasts are fundamental in the hematopoietic niche (Zhang et al. 2003). Increasing the overall number and function of osteoblasts whithout increasing N-cadherin$^+$ cells is not sufficient to enhance HSC quantity and function. Thus although osteoblasts are indeed a key functional component of the niche, HSC number seems to be correlated with the number of a subset but not the overall number of osteoblasts (Lymperi et al. 2008).

Furthermore, stromal fibroblasts of the bone marrow have been shown to produce a large number of molecules, such as stem cell factor (SCF), granulocyte colony-stimulating factor (G-CSF) and Flt-3 ligand, which are capable to stimulate the proliferation and maturation of hematopoietic progenitors (Lisovsky et al. 1996; Verfaillie 1993). It also seems that hematopoiesis is regulated by endothelial cells and adipocytes, the latter by the action of their leptin and adiponectin production (Laharrague et al. 1998; Yokota et al. 2003).

8.2.5.Flt-3 ligand

Flt3-ligand (fms-like tyrosine kinase 3 ligand) plays a central role in the proliferation, survival, and differentiation of early hematopoietic precursor cells, but also at later stages of hematopoiesis such as early B cell lineage differentiation and expansion of monocytes and immature dendritic cells.

Flt3-ligand is a cell surface transmembrane protein that can be proteolytically processed and released as a soluble protein (McClanahan et al. 1996). It is structurally related to stem cell factor (SCF) and colony stimulating factor (CSF) (Hannum et al. 1994). Despite the widespread expression of Flt3-ligand mRNA, the Flt3-ligand protein has only been found in stromal fibroblasts present in the bone marrow microenvironment and T-lymphocytes (Brasel et al. 1996; Lisovsky et al. 1996). Both the membrane-bound and soluble isoforms of Flt3-ligand are biologically active and stimulate the tyrosine kinase activity of Flt3 receptor Flk2/Flt3 (Rappold et al. 1997). The Flt3 receptor is expressed predominantly on primitive hematopoietic progenitors and is restricted to CD34$^+$ cells lacking lineage-specific markers (Matthews et al. 1991). Flt3-ligand mediated triggering of Flt3 receptor induces a receptor autophosphorylation at tyrosine residues and activation of multiple cytoplasmic molecules (Rosnet et al. 1996).

Administration of Flt3-ligand to mice resulted in expansion of HSC and significant stimulation of hematopoiesis, whereas administration of Flt3-ligand to mice and rabbits subjected to lethal doses of irradiation protected HSC and allowed rapid hematopoietic recovery (Gratwohl et al. 1998; Hudak et al. 1998). Moreover, results of a marked reduction in number of dendritic cells and natural killer cells (NK cells) in mice lacking Flt3-ligand expression indicate that Flt3-ligand is also important for the development and function of the immune system (McKenna et al. 2000).

Regulation of Flt3-ligand is based on intracellular retention of preformed of Flt3-ligand and its release from intracellular stores, depending on the status of the stem cell compartment. During steady-state hematopoiesis, Flt3-ligand is expressed constitutively but little of the cytokine is released by cells. Release of Flt3-ligand may be triggered by stem cell deficiency in the bone marrow. The increase in Flt3-ligand levels reflects a compensatory response whose aim is to restore the HSC compartment and levels return to normal upon hematopoietic recovery. In radiation accidents, the measured Flt3-ligand levels were indicative of the severity of bone marrow aplasia (Bertho et al. 2001; Bertho et al. 2009; Bertho et al. 2008; Huchet et al. 2003; Prat et al. 2006; Wodnar-Filipowicz 2003).

8.3. Immune system

8.3.1. Generalities

The immune system is involved in the regulation of most pathological processes and it is known that impaired immunity promotes disease progression and, in some cases, disease initiation. The immune system is highly susceptible to radiation in addition to other factors.

The immune response includes two types of mechanisms: the non specific immunity or innate immunity and the specific acquired immunity or adaptive immunity. Although few specific, the innate immunity assures an immediate response to an infection. On the other hand, the innate immune response has no memory of antigens encountered, this in contrast to the adaptive immune response. The principal actors of the adaptive immunity are lymphocytes, which use receptors for the recognition of specific antigens. Adaptive immunity has the advantage of an immunological memory, but depends on the innate immunity for initiation and orientation of the response.

Cells involved in the immune system are principally dendritic cells, macrophages and natural killer (NK) cells for the innate immunity and T- and B-lymphocytes for the adaptive immunity. Whatever the immune type activated, the cells can release regulating molecules, which are called cytokines and chemokines. Cytokines are a diverse group of soluble peptides that signal between cells and elicit biological responses, including cell activation, proliferation, growth, differentiation, migration and cytotoxicity (Tarrant 2010). Chemokines are substances that attract cells to migrate in a particular direction (chemotaxis). Like cytokines, they operate via binding to receptors on the outer surface of immune cells (Kidd 2003).

8.3.2. Granulocytes

Neutrophils, basophils and eosinophils are polymorphonuclear granulocytes, named after their nucleus multilobulated shape. The granules present in their cytoplasm contain biochemical mediators that serve inflammatory and immune functions. Moreover, enzymes present in their cytoplasm are capable of destroying microorganisms and catabolyzing debris ingested during phagocytosis (George-Gay and Parker 2003).

Neutrophils are the most abundant type of white blood cells and form an essential part of the innate immune system. Highly motile, they are in response to acute inflammation or infection one of the first to arrive at the site of inflammation. They migrate through the blood vessels and then through interstitial tissue, following chemical signals such as interleukins and leukotrienes. Neutrophils quickly congregate at the site of inflammation and release cytokines which amplify inflammatory reacions by several other cells. In addition neutrophils play a key role in the front line defence against invading pathogens by directly attacking micro-organisms (by phagocytosis or release of granule proteins) (Mantovani et al. 2011; Nathan 2006; Segal 2005; Witko-Sarsat et al. 2000).

Eosinophils circulate in blood and migrate to inflammatory sites in tissues in response to chemokines and leukotrienes. Following activation eosinophils combat parasites and infections by the production and release of granule proteins, enzymes (i.e. elastase), lidid mediators (i.e. eicosanoids), growth factors and cytokines (i.e. interleukins). The granule proteins released by eosinophils can create toxic pores in the membranes of target cells allowing potential entry of other cytotoxic molecules to the cell, can induce the degranulation

by mast cells and can form reactive oxygen species that promote oxidative stress in the target cells, causing cell death by apoptosis and necrosis. Moreover, eosinophils are implicated in antigen presentation to T lymphocytes (Hogan et al. 2008; Rothenberg and Hogan 2006; Shi 2004).

Basophils are the least common type of the white blood cells. They appear in many inflammatory reactions, particularly those that cause allergic symptoms. When activated, basophils degranulate to release histamine, proteoglycans (i.e. heparin), proteolytic enzymes (i.e. elastase), leukotrienes or cytokines (i.e. IL-4) (Schroeder 2009).

8.3.3.Non-granulocytes

Non-granulocytes are white blood cells that do not have granules in their cytoplasm. Inclusive in this group are monocytes/macrophages and lymphocytes.

8.3.3.1. Monocytes/macrophages

Monocytes are the largest of the white blood cells and are young cells found freely circulating in blood. Once the young monocyte leaves the blood stream and enters tissue, it transforms into a mature macrophage. They are usually the first cell to engulf and process the antigen and present it to the immune cells (lymphocytes) in a manner that will stimulate a specific immune response to that particular antigen (George-Gay and Parker 2003).

8.3.3.2. Lymphoid cells

Lymphocytes are also non-granulocytes and are the most numerous circulating white blood cells after neutrophils. There are 2 classes of lymphocytes: T- and B-lymphocytes. Both T- and B-lymphocytes can be sorted into subtypes based on characteristic surface molecules on them called cluster of differentiation (CD).

8.3.3.2.1. T-lymphocytes

The growth of T-lymphocytes from pluripotent stem cells happens by different developmental stages which start in the bone marrow and end in the thymus (Geenen et al. 2003).

During the early stages of differentiation the immature T-lymphocyte cells are double-positive: they express both CD4 and CD8. In a next phase, single-positive $CD4^+$ T lymphocytes are selected by their interaction with MHC class II molecules and the $CD8^+$ T lymphocytes selected on the basis of their interaction with MHC class I molecules (Callard 2007; Geenen et al. 2003; Germain 2002).

During their differentiation, lymphocytes express antigen-specific receptors, called T-cell receptors (TCR) (Nemazee 2000). TCR recognize small peptides consisting of 10 to 12 amino acids presented by antigen presenting cells (APC) (Hennecke and Wiley 2001; Kidd 2003). TCR are associated with a CD3 complex and their simultaneous signals are essential for the activation and proliferation of T cells. T cells that are unable to recognize own major histocompatibility complex (MHC) molecules die by apoptosis and those that do recognize own MHC molecules, receive a signal from the protective epithelial cells in the cortex of the thymus so that they do not undergo apoptosis. This is called the positive selection step in T-lymphocyte differentiation. In a next step, negative selection occurs through an interaction with dendritic cells and macrophages in the medulla of the thymus. The T-lymphocytes that have a high affinity for own MHC molecules (auto-reactive T-lymphocytes) undergo apoptosis (**Figure 25**) (Alam and Gorska 2003).

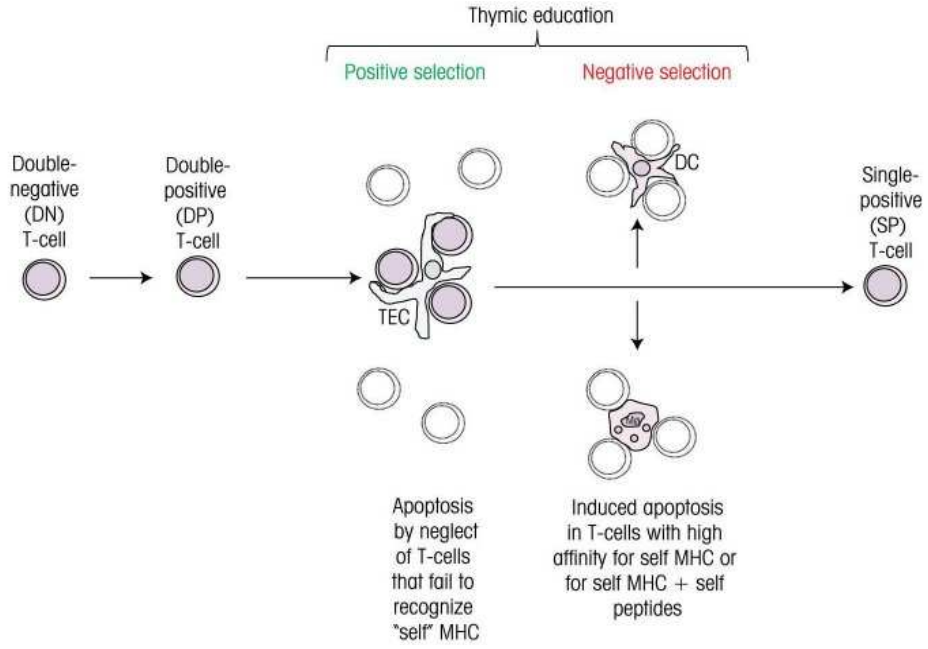

Figure 25. Positive and negative selection steps in T-lymphocyte differentiation (from Delves 2011).

During rearrangement of the gene segments encoding the antigen-specific α/β TCR, certain chromosomal sequences are excised to produce episomal DNA by-products, called TCR

rearrangement excision circles (TRECs) (**Figure 26**). More in detail, the gene segments encoding TCR delta (TCRD) protein chain reside within the TCR alpha (TCRA) locus in human and mice. Functional rearrangement of TCRA gene segments first requires deletion of the TCRD locus. Two elements flanking the TCRD locus preferentially recombine, resulting in deletion of the TCRD locus, the so called TREC (Broers et al. 2002). TRECs are stable, not duplicated during mitosis, and diluted out with each cellular division (Broers et al. 2002). Measurement of TRECs in thymocytes and peripheral blood T cells has been used to study thymus output as a quantitative analysis of thymic T cell production (Castermans et al. 2007; Dion et al. 2007; Geenen et al. 2003; Sempowski et al. 2002).

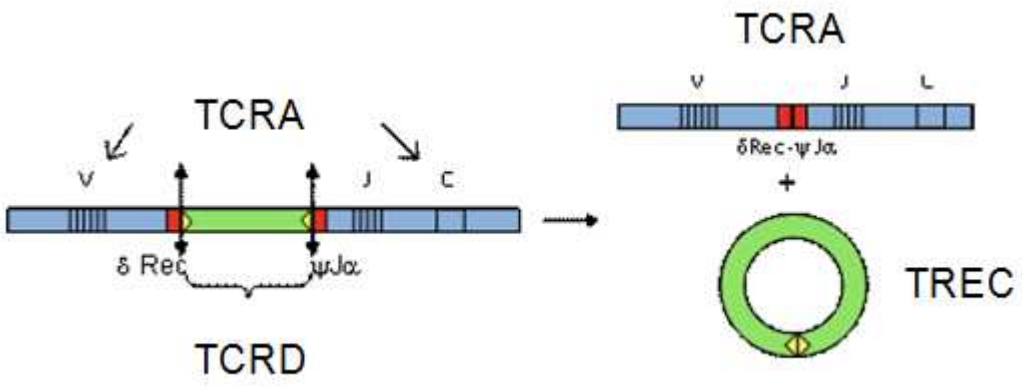

Figure 26. Schematic representation of TCR gene rearrangement (from Delves 2011).

T-lymphocytes play a central role in cell-mediated immunity. Several subsets of T cells exist, each with a distinct function. T cells recognize antigens and modulate the immune response. To enhance contact with antigens, lymphocytes circulate continuously in different tissues and naive T-lymphocytes migrate mainly to the lymph nodes. In order that T-lymphocytes could recognize antigens, exogenous proteins are presented to T-lymphocytes by APC in the context of either class I or class II MHC molecules (**Figure 27**). These APC are mainly monocytes, dendritic cells or B lymphocytes and are able to capture antigens and degrade them by proteosomes (Hennecke and Wiley 2001).

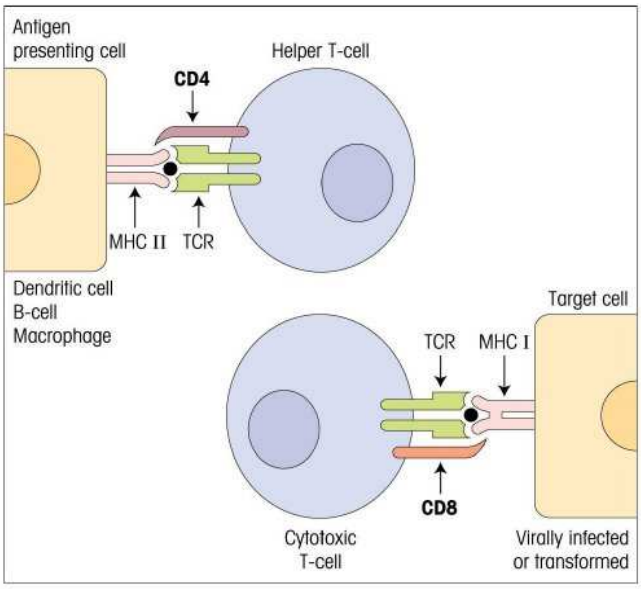

Figure 27. Helper and cytotoxic T-lymphocyte subsets are restriced by MHC class (from Delves 2011).

The $CD4^+$ T-lymphocytes can differentiate into T helper 1 cells (Th1), T helper 2 cells (Th2) or T helper 17 cells (Th17), distinguishable by the profile of their cytokine release **(Figure 28)** (Alam and Gorska 2003). The so called Th1/Th2 balance is further discussed in detail.

Antigen-activated naïve $CD4^+$ T cells may also differentiate into regulatory T cells (Treg). These cells play an essential role in the immune homeostasis. They stimulate or inhibit the functions of other cells involved in the innate and adaptive immune response (Chen et al. 2010; Langier et al. 2010). The specific mechanisms by which these cells act are not yet fully elucidated. Belonging to the group of regulatory T-lymphocytes are $CD4^+CD25^+$ regulatory T-lymphocytes (Treg) and natural killer (NK) cells. $CD4^+CD25^+$ cells represent only a small fraction of the $CD4^+$ T cells and play an important role in the prevention of organ-specific autoimmunity and the maintenance of self tolerance (Sakaguchi et al. 1995).

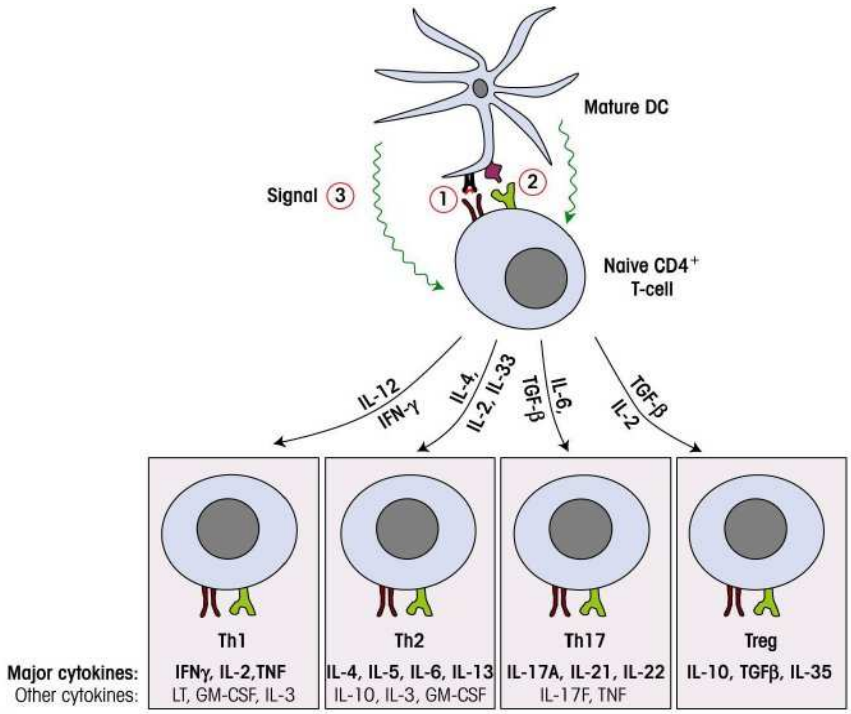

Figure 28. Naive $CD4^+$ T-lymphocytes can undergo polarization to distinct subsets that secrete different cytokine combinations (from Delves 2011).

The $CD8^+$ lymphocytes are known as cytotoxic T lymphocytes. These lymphocytes have perforines and Fas ligand (**Figure 29**). The perforines nestle in the membrane of target cells and forms pores in it (Shresta et al. 1998). Through these pores enter granular enzymes within the cytosol of the target cell leading to apoptosis of the target cell. The Fas ligand binds to its receptor, which leads to apoptosis of the target cell by activation of caspases (Russell and Ley 2002).

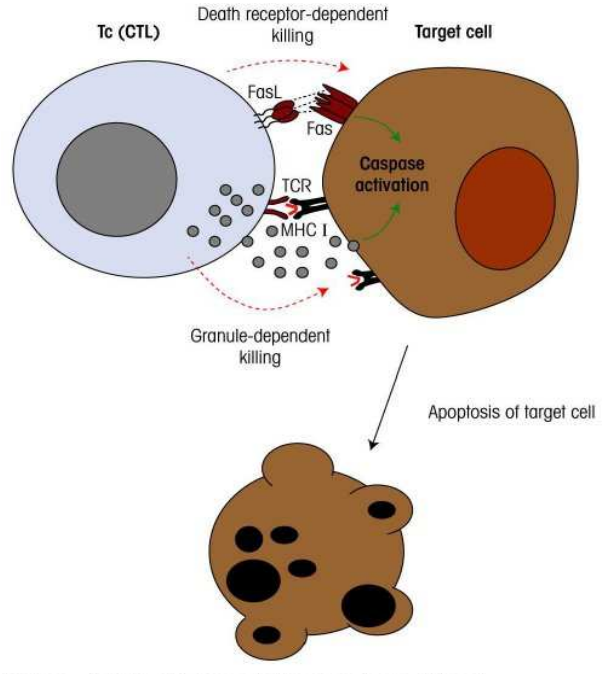

Figure 29. Cytotoxic T-lymphocytes can kill target cells by apoptosis via granule dependent or Fas ligand dependent pathways (from Delves 2011).

8.3.3.2.2. B-lymphocytes

B-lymphocytes play a role in the humoral immune response. These cells make antibodies against antigens, perform the role of APC and eventually develop into memory B cells after activation by antigen interaction.

Like T-lymphocytes B-lymphocytes originate from bone marrow. Unlike T-lymphocytes, these cells undergo their whole differentiation in the bone marrow (Rolink et al. 2006). IL-7 seems to induce the differentiation of common lymphoid progenitors into $CD19^+$ B cell progenitors and initiates the transition of pro-B cells into early pre-B cells. Mature B-lymphocytes bring membrane-bound immunoglobulins (Ig) to expression. Unlike the TCR, B-cell receptors (BCR), which are membrane-bound forms of Ig, recognize directly foreign antigens in the form of large peptides. BCR recognize secondary and tertiary structures and even entire proteins (Delves 2011).

B-lymphocytes leave the bone marrow and are activated in the periphery, but only after contact with an antigen. When B-lymphocytes do not meet antigens, they will die by apoptosis after a few weeks. When a specific antigen binds on the other hand to the BCR, the B-lymphocyte differentiates into a plasmocyte and can produce high quantities of specific antibodies against the antigen (Delves 2011).

Memory B-lymphocytes will bring a much larger and more efficient response after a subsequent exposure to an antigen. Cytokines produced by T cells as IL-4, IL-5, IL-6, IL-2 and IFN-γ can stimulate the proliferation and differentiation of B-lymphocytes into antibody producing plasmocytes. Naive B-lymphocytes produce IgM and IgD on their surface. However, when stimulated, they develop into plasmocytes producing IgG, IgA or IgE (Alam and Gorska 2003).

8.3.4. The immune response

During the first contact with antigen, there is recognition of this antigen by cells of the immune system. This entails an immune response directed against the antigen or a state of tolerance to the same antigen. As mentioned before, the immune response can be cellular or humoral. How the immune response is turned in one or another of these types of answer depends on how the antigen is presented to the lymphocytes. In many cases the response is

mixed cellular and humoral. During the second contact with the antigen, the type of response is largely determined by the effect of the first contact, but the intensity and quality of the immune response is different (**Figure 30**).

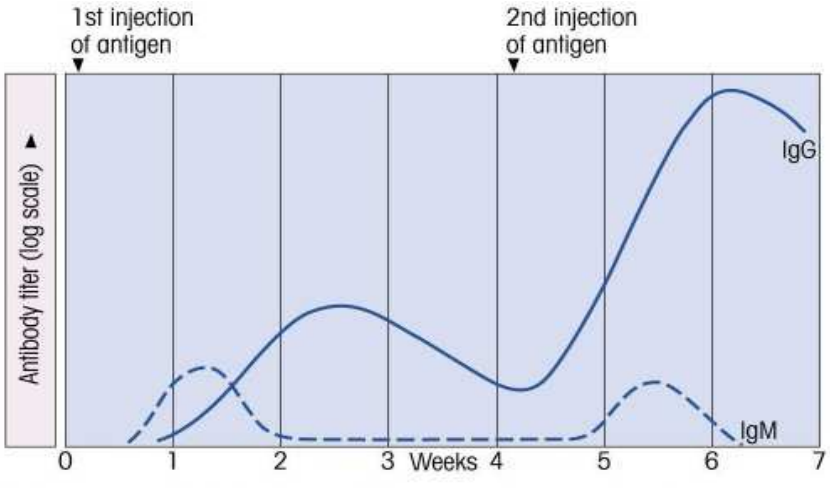

Figure 30. Synthesis of immunoglobulines G (IgG) and M (IgM) in the primary and the secondary responses to antigen (from Delves 2011).

One theory of immune response regulation involves homeostasis between T-helper 1 (Th1) and T-helper 2 (Th2) activity. The Th1/Th2 hypothesis arose from 1986 research suggesting mouse T-helper (Th) cells expressed different cytokines (Mosmann et al. 1986). This hypothesis was adapted to human immunity, with Th1- and Th2- cells directing different immune response pathways (Kidd 2003). Upon receiving signals through the binding of an antigen to the TCR in the presence of polarizing cytokines, the naive Th precursor cells differentiate into Th1 or Th2 effecter cells that are defined by their function and the cytokines they secrete (**Figure 31**).

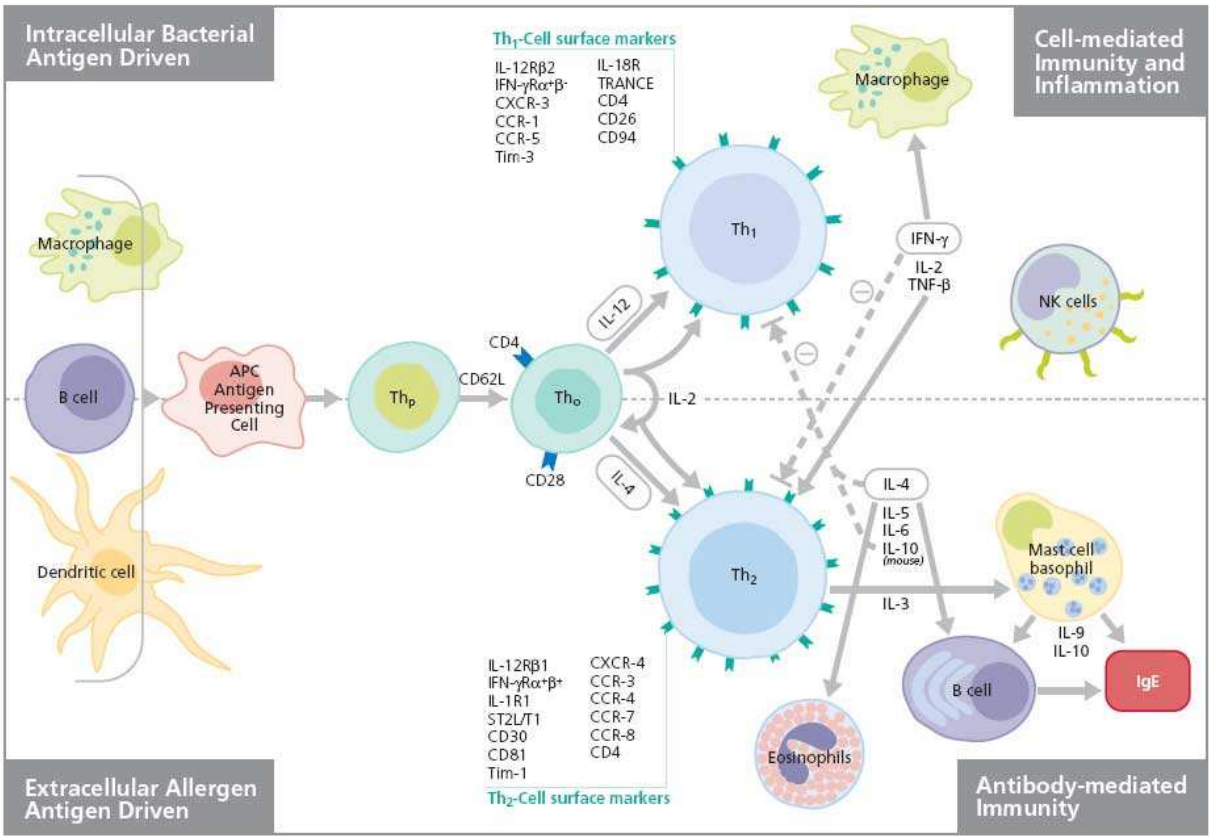

Figure 31. The generation of Th1 and Th2 $CD4^+$ T-cell subsets.

Th1 cells produce large amounts of interferon-gamma (IFN-γ) and also in a smaller extent IL-12 (via Stat4 signalling auto-inducing Th1 development) and IL-2. These cytokines are responsible for cell-mediated immune defence against intracellular pathogens, by activating inflammatory pathways mainly via macrophage activation. They also play a central role in organ-specific autoimmune diseases.

Th2 cells defend the host against extracellular parasites and take part in atopic and allergic reactions. The signature Th2 cytokine is IL-4 (via Stat6 signalling auto-inducing Th2 development) which can be measured early in Th2 development. Other cytokines produced by Th2 lymphocytes include IL-6, IL-10 an IL-13. The cytokines secreted by Th2 cells upregulate antibody formation via B cells and stimulate mast cells and eosinophils (Chakir et al. 2003; Kidd 2003; Szabo et al. 2000; Tarrant 2010; Yamashita et al. 2004).

Furthermore, Th1 and Th2 cells differ by the level of expression of different membrane molecules. The chemokine receptors CCR5 and CXCR3 are expressed on human Th1

lymphocytes, while CCR3 and CCR4 receptors are expressed on Th2 cells (Lebrec et al. 2001).

Among the many signals that influence the development of naive Th cells, two have been suggested to be master regulators of Th1 and Th2 differentiation, respectively expression of the transcription factors T-box expressed in T-cells (T-bet) and Gata-binding protein-3 (Gata3). T-bet is thought to initiate Th1 development, while inhibiting Th2 cell differentiation. Gata-3 plays a role in the development of the Th2 phenotype while inhibiting Th1 cells (Chakir et al. 2003; Szabo et al. 2000; Yamashita et al. 2004).

A key feature of the Th1 and Th2 cells is that they can antagonize each other's actions, either by blocking polarized maturation of the opposite cell type or by blocking its receptor functions (**Figure 32**). For example, IFN-γ secreted by Th1 cells can block the proliferation of Th2 cells, and high concentrations of IL-4 and IL-13 can block the generation of Th1 cells form naïve T cells. However, other immune cell types, like regulatory T cells, can also intervene to block either Th1 or Th2 activity or both (Callard 2007; Kidd 2003). Commitment to Th1 or Th2 cells appears to be final, since efforts to reverse such differentiated cells have not been successful (Callard 2007; Kidd 2003).

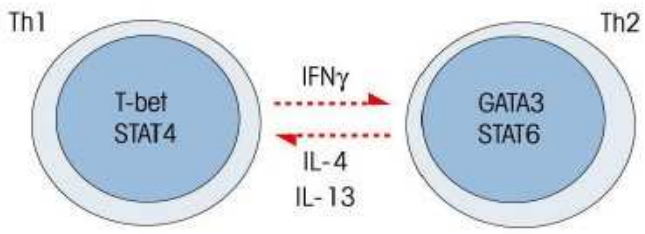

Figure 32. Antagonism between Th1 and Th2 T-lymphocyte subpopulations (modified from Delves 2011).

8.3.5.IFN-γ, IL-4 and IL-7

IFN-γ is produced primarily by T lymphocytes and NK cells. The production of IFN-γ is induced by antigenic challenge and by cytokines such as IL-12. Besides its anti-viral activity, IFN-γ has been shown to play a key role in host defense by exerting antiproliferative, immunoregulatory, and proinflammatory activities. IFN-γ induces the production of cytokines and upregulates the expression of class 1 and 2 MHC antigens. Furthermore, IFN-γ modulates macrophage effector functions and potentiates the secretion of antibodies by B cells. IFN-γ

has also been shown to increase IL-12 induced Th1 development and stimulate HSC to proliferate (Baldridge et al. 2011).

IL-4 is produced primarily by activated T-lymphocytes, but also by mast cells and basophils. This interleukin has multiple immune response-modulating activities on a variety of cell types. IL-4 induces IgE production in B lymphocytes and is an important modulator of the differentiation of precursor Th cells to the Th2 subset (Delves 2011).

In the thymus, IL-7 induces the proliferation of triple negative immature thymocytes, participates in TCR rearrangement, and suppresses CD4 expression in favour of CD8 on single positive T cells. In the periphery, IL-7 contributes to homeostatic proliferation and survival of naive $CD4^+$ and $CD8^+$ T cells and promotes the formation and survival of memory $CD4^+$ and $CD8^+$ T cells (Bradley et al. 2005).

Material and methods

Material and methods

1. In vivo studies

1.1. Animal models

1.1.1. Balb/c mice

Balb/c mice were purchased from Elevage Janvier (Le Genest Saint Isle, France). Before start of experiments a minimal adaptation period of one week was given to the animals. Animals were housed in standard cages and were kept at a constant room temperature (21°C ± 2°C) with a 12-hour daylight cycle (day from 8 AM until 8 PM). In all described experiments animals received *ad libitum* water and standard rodent chow containing a mean calcium concentration of 9 g Ca^{2+}/kg (normal calcium diet, R03-type chow, Safe, Epinay-sur-Orge, France).

The animal care committee of the Institut de Radioprotection et de Sûreté Nucléaire (IRSN) reviewed and approved all the animal experiments, which were conducted in accordance with French regulations for animal experimentation (Ministry of agriculture Act No. 8 7-848, 19 October 1987, modified May 29, 2001).

1.1.2. Contamination of models

Drinking water (Evian, Danone, Paris, France) was contaminated with a ^{90}Sr source ($^{90}SrCl_2$ in 0,1 N HCl, AREVA-CERCA LEA, Pierrelatte, France). The animals were contaminated with through drinking water containing 20 kBq of ^{90}Sr per liter. This concentration was also used in a previous study at our laboratory to determine the biokinetics of ^{137}Cs after chronic contamination (Bertho et al. 2011; Bertho et al. 2010) and represents an expected mean daily intake of 100 Bq per animal. This daily intake is close tot the daily estimated ingestion by populations living on contaminated territories of Chernobyl (Cooper 1992; de Ruig and van der Struijs 1992; Handl et al. 2003; Hoshi et al. 1994). Based upon an assumed daily water consumption of 5 ml per animal per day at adult age, a ^{90}Sr contamination of about 100 Bq per animal per day at adult age was expected.

Contamination of animals was verified by measurement of ^{90}Sr in femurs of sacrificed animals, which is discussed further in detail.

1.1.3.Juvenile model

Two groups of mice were constituted throughout all the experiments. One control group receiving normal drinking water and one group receiving drinking water containing 20 kBq.l^{-1} of ^{90}Sr (CERCA-LEA). Male and female parents received normal or ^{90}Sr containing water starting two weeks before mating and until their date of sacrifice (**Fig 33**). Control and contaminated breeding groups were constituted with one male and two females for one week. Male parents were one week after start of mating anesthetized by intraperiteoneal injection of a mixture of ketamine (Imalgene, Mérial, Villeurbanne, France) and xylazine (Rompun, Bayer Healthcare, Monheim, Germany) and killed by cervical dislocation. Births within breeding groups were carefully recorded. Three weeks after birth, i.e. at the time of weaning, female parents were anesthetized and killed by cervical dislocation. Sexing of the offspring was made and the mice were separated into groups of 6-24 control and 10-24 ^{90}Sr ingesting animals, with a sex ratio of 1:1. In order to avoid possible litter effects, groups of sacrifice were constituted with males and females originating from different litters. Surplus animals were sacrificed. The animals continued to receive normal or ^{90}Sr contaminated drinking water until their sacrifice at the age of 3, 6, 12, 16 or 20 weeks (**Fig 33**) for organ sampling. So the contamination started with parents before mating and continued for offspring until the time of sacrifice. As such, offspring were contaminated by placental transfer during foetal life, by lactation before weaning and by drinking water afterwards.

1.1.4.Adult model

As for the juvenile model, two groups of mice were constituted throughout the experiments. One control group receiving normal drinking water and one group receiving drinking water containing 20 kBq.l^{-1} of ^{90}Sr (CERCA-LEA). Groups of 6 controls and 12 ^{90}Sr ingesting nine-week old mice were formed, with a sex ratio of 1:1. The animals were sacrificed after the same time periods as for the juvenile mouse model, i.e. after 3, 6, 12, 16 or 20 weeks of chronic ingestion (**Fig 33**).

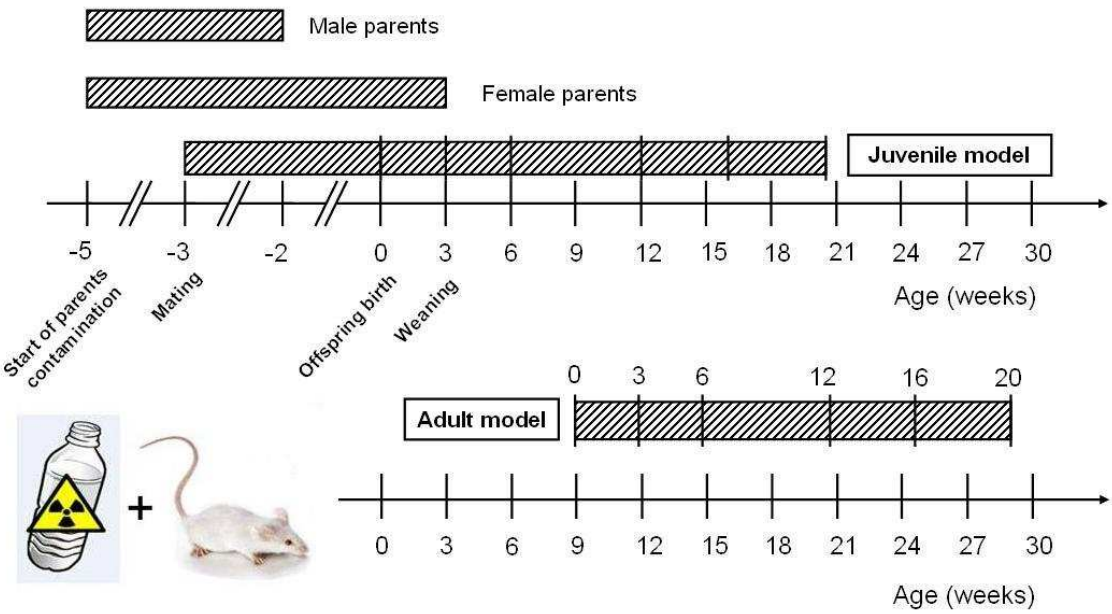

Figure 33. Summary of the ^{90}Sr ingestion schedules (hatched boxes) for the juvenile and the adult mouse model. The time periods of sacrifice of animals are indicated for both models (vertical lines in the hatched boxes).

1.1.5. Vaccination model

The experimental schedule was the same as described for the juvenile model described above, except that at the time of weaning, experimental groups were constituted with male offspring only. The mice were separated into 3 groups of 12 control and 3 groups of 12 ^{90}Sr ingesting male animals. The animals continued to receive normal or ^{90}Sr contaminated drinking water until their sacrifice at the age of 24 weeks (**Fig 34**) for organ sampling.

Response to antigen injection was tested in 3-7 week-old and 20-24 week-old animals. At the age of 3 weeks, 100 µl of tetanus toxin (TT, Pasteur Vaccins, Paris, France, 1:20 dilution in saline) or keyhole limpet hemocyanin (KLH, 0.5 mg.ml^{-1} in saline, Sigma-Aldrich, Saint-Quentin Fallavier, France) were injected intraperitoneally in 12 males from each of the control and ^{90}Sr chronic ingesting groups. A second injection was made at the age of 20 weeks. 12 males from either control or ^{90}Sr chronic ingesting groups were injected with saline (0.9 % NaCl) as an experimental control (placebo group). During 4 weeks after each injection, blood samples were weekly drawn by jugular puncture. At the age of 24 weeks, animals were sacrificed as described above and organs were collected for analysis (**Fig 34**).

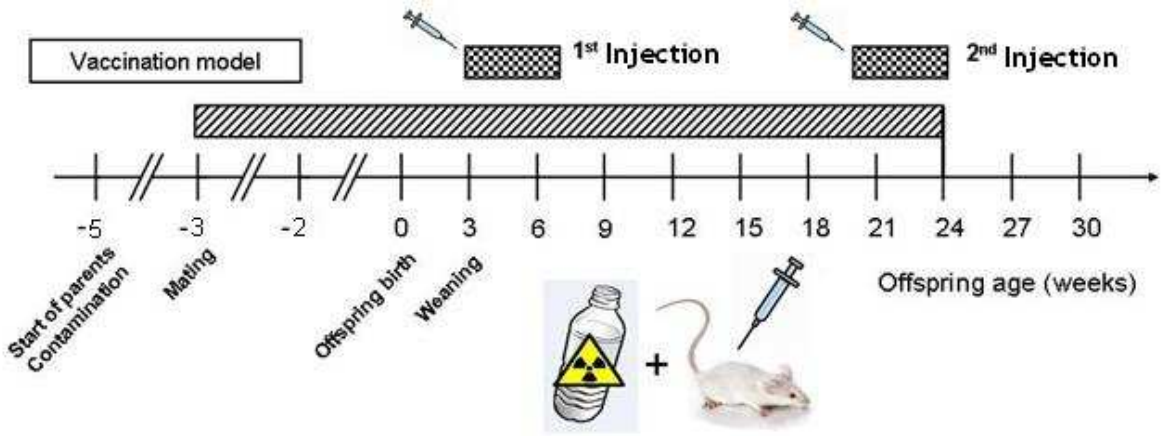

Figure 34. Summary of the ^{90}Sr ingestion schedule (hatched boxes) for the vaccination mouse model. The first injection with tetanus toxin (TT), keyhole limpet hemocyanin (KLH) or saline (placebo) was given at 3 weeks of age and the second injection at 20 weeks of age of animals. During 4 weeks after each injection, blood samples were weekly drawn by jugular puncture (checkered boxes). Animals were sacrificed at 24 weeks of age.

1.2. Methods

1.2.1. Body mass, food and water consumption

A weekly record of individual body weight of each animal was made together with a weekly follow-up record per cage for food and water consumption. For the juvenile model this was done from the time of weaning. The mean food and water consumption per animal and per day was obtained by calculation on the basis of the number of animals per cage.

1.2.2. Organ sampling

For the juvenile model at age of birth, 3, 6, 12, 16 and 20 weeks or for the adult model at 3, 6, 12, 16 and 20 weeks of ^{90}Sr ingestion duration, 6-24 control and 10-24 contaminated animals with equal number of males and females were anesthetized by an intraperiteoneal injection of a mixture of ketamine (Imalgene) and xylazine (Rompun). Blood was drawn by intracardiac puncture using heparinised tubes (Choay, Sanofi Aventis, Paris, France) and the animals were killed by cervical dislocation.

For animals used in the ^{90}Sr biokinetics study, the following organs were collected: skin, liver, spleen, kidneys, digestive tract (from stomach to the rectum), heart, thymus, lungs, skeletal muscle, femurs, central nervous system (CNS). Remaining tissues were separated into two parts: legs, tail, and skin on the one hand, and the remaining upper part of the body (the

carcass) on the other hand. All samples were weighted before ^{90}Sr measurements. Animals used for the determination of ^{90}Sr content at different skeletal sites were sacrificed as described above and internal organs were removed. Carcasses were then treated entirely for 1 hour in boiling water and then overnight at 56°C in the presence of papain (1 mg/ml final concentration, Sigma, Saint Quentin Fallavier, France). Bones were isolated and grouped according to the different skeletal sites under an inverted microscope before ^{90}Sr measurements.

To study the hematopoietic system, blood was drawn from animals as described before and spleen, thymus and femurs were isolated for phenotypical analysis of hematopoietic cells and/or determination of hematopoietic progenitors by the colony forming cell (CFC assay). After flushing the bone marrow of femurs, femurs were weighted and used to verify the presence of ^{90}Sr in bones.

To study the bone physiology, the protocol was modified by isolating both femurs and tibias from animals. One femur was immediately frozen in liquid nitrogen, stored at -80°C and used for genetic expression analysis. The other femur was decalcified with chlorhydric acid (RDC agent, CML, Nemours, France), fixed in 4 % formaldehyde (VWR, Fontenay-sous-Bois, France) and used for histological analysis. The tibias were weighted and used to verify the presence of ^{90}Sr in bones.

For animals used for the study of the immune system, blood was drawn by jugular puncture and spleen, thymus and mesenteric lymph nodes were isolated for genetic and protein expression analysis and phenotypical analysis of cells. Femurs were used to verify the presence of ^{90}Sr in bones as described above.

Blood cell count was performed with a MS-9 (Melet-Schlossing, Osny, France) veterinary automatic blood counter and plasma was isolated by centrifugation of blood at 5000 rounds per minute (rpm) for 5 minutes (min). Obtained plasma was stored at -80°C for subsequent analysis.

1.2.3. ^{90}Sr measurements

To measure ^{90}Sr in organs, these were first calcined at 500°C in an oven during 5 hours. Ashes were dissolved in nitric acid (HNO_3, 67 %) and hydrogen peroxide (H_2O_2, 30 %, both from VWR) in a 2:1 ratio and gently heated until complete evaporation. This step of

dissolution in HNO_3 and H_2O_2 was repeated twice for each sample. This whole procedure was repeated twice. Samples were then redissolved in 1 ml nitric acid (HNO_3, 10 %) by shaking overnight.

Fifteen ml of scintillation liquid was added (Ultima Gold AB, Perkin Elmer, Courtaboeuf, France) to each sample and ^{90}Sr measurements were made with a β counter (TRI-CARB 2700TR Liquid Scintillation Analyzer, Perkin Elmer). ^{90}Sr activity was measured at least one month after organ sampling, the time necessary to reach a secular equilibrium at the time of counting between initial ^{90}Sr content in samples and ^{90}Y. The counting time per sample of organs was 2 hours. The count rate (in counts per minute, cpm) obtained for each sample was converted to activity per mass unit A_m (in $Bq.g^{-1}$) using the following equation:

$$A_m = (CPM_{gross} - CPM_{control})/((60 \times E \times m)/100)$$

where CPM_{gross} is the gross measurement of the sample (cpm), $CPM_{control}$ the mean background cpm of 10 control samples, m the mass of the samples (g) and E the efficiency of ^{90}Sr detection. This efficiency of detection E (%) was determined with the following equation:

$$E = (CPM_{add} - CPM_{gross})/((60 \times A_{add})/100)$$

where CPM_{add} is the gross measurement of the sample after a defined activity of 2Bq of ^{90}Sr was added (cpm) and A_{add} the defined activity of ^{90}Sr added (2 Bq). Organs from control animals were counted under the same conditions.

The whole body specific activity was then calculated as the sum of ^{90}Sr activities (Bq) in all organs divided by the total body weight of the animals (g). The detection limit of ^{90}Sr was between 0,45 Bq and 0,75 Bq per sample depending of the organs.

1.2.4. Metabolic cages

Before sacrifice, animals used for the ^{90}Sr biokinetics study were placed individually in metabolic cages. After an adaptation period feces and urine were collected over a whole period of 48 hours and were measured for ^{90}Sr content.

1.2.5. Transfer rate calculations

1.2.5.1. Daily intestinal absorption ratio

The daily intestinal absorption ratio (*IAR*) of ^{90}Sr was calculated using the following equation:

$$IAR = (I - FE)/I$$

were *I* is the mean daily ^{90}Sr ingestion calculated on the basis of weekly measurements (as described above) in Bq.d^{-1} and *FE* is the measured individual ^{90}Sr excretion through feces in Bq.d^{-1}.

1.2.5.2. Rate of ^{90}Sr accumulation in bones

The rate of ^{90}Sr accumulation in bones $Bq_{\Delta t}$ (in Bq.day^{-1}) was calculated with use of the following equation:

$$Bq_{\Delta t} = (Bq_t - Bq_{t-1})/(\Delta t)$$

where Bq_t and Bq_{t-1} are the total activity (in Bq) of ^{90}Sr measured in bones at the times *t* and *t-1* respectively and Δt the number of days between the two time points *t* and *t-1*.

1.2.6. Calculation of absorbed doses

1.2.6.1. Total body activity, body mass and mass class

For absorbed dose calculation purpose, the ^{90}Sr total body activity of each animal during each time interval was taken to be the mean of the total body activity measured in the animal at the time point of sacrifice and the mean of total body activities measured in all animals euthanized at the previous time point, starting from 0 at the time of mating.

As described earlier, animals were followed up individually for their body mass since weaning (3 weeks old) until their date of sacrifice. As for ^{90}Sr total body activity, the body mass was estimated as the mean of the observed value at the time point of sacrifice for each specific animal and the mean of masses of animals euthanized at the previous time point, starting from 0 at the time of mating.

1.2.6.2. Dose conversion factors used for dose calculation

Dose conversion factors (DCF) expressed in (μGy.day^{-1})/(Bq.kg^{-1}) and used for absorbed dose calculations are indicated in **table**. DCF proposed by the ICRP take into account the daughter products of radionuclides, provided that the half-life of these daughter products is less than 10 days, i.e. only in case secularly equilibrium could be reached during the exposure (ICRP 2008). This is in fact the case for ^{90}Sr, which daughter product, ^{90}Y, has a half-life of 2.7 days.

Radionuclide	Internal exposure	External exposure in an uniformly contaminated soil
^{90}Sr	1.5x10^{-2}	3.0x10^{-9}

Table 6. Dose conversion factors (DCF) used in this study, expressed in (μGy.day^{-1})/(Bq.kg^{-1}), according to ICRP 2008.

For each time of sacrifice *i*, the radiation dose D_i absorbed from the time *i-1* to the time *i* was calculated according to the following formula:

$$D_i = DCF \times T_i \times A_i / M_i$$

where T_i is the time period since previous euthanasia *i-1* expressed in days, A_i and M_i the total body activity and body mass in the time interval *i-1* to *i* in Bq and kg respectively. The total dose absorbed up to a given time point *i* is thus the sum of doses D_j calculated for each time point $j \leq i$.

1.2.7. General biochemical parameters

An automated spectrometric system (Konelab 20, Thermo Electron Corporation, Cergy-Pontoise, France) with the manufacturer's biological chemistry reagents was used to measure levels of calcium (Ca), phosporus (P), alkaline phosphatase (ALP), aspartate aminotransferase (AST), alanine aminotransferase (ALT), creatinine, creatinine kinase and urea in plasma.

1.2.8. Plasma dosages

1.2.8.1. Enzyme linked immunosorbant assays

To evaluate the hematopoietic system, plasma Flt-3 ligand and IL-7 concentrations were measured by commercial available enzyme linked immunosorbant assay (ELISA) following the according manufacturer's recommendations (R&D Systems, London and Abingdon, UK). The detection limits of the tests were 5 $pg.ml^{-1}$ and 15 $pg.ml^{-1}$ respectively.

To evaluate the bone physiology, plasma concentrations of parathyroid hormone (PTH, Immunotopics, San Clemente, CA, USA, detection limit (dl): 3 $pg.ml^{-1}$), 1,25-dihydroxyvitamin D_3 ($1,25(OH)_2D_3$, Immunodiagnostics Systems, Paris, France, dl: 2.5 $pg.ml^{-1}$), bone morphogenetic protein-2 (BMP-2,USCN Life Science Inc., Wuhan, China, dl: 6.7 $pg.ml^{-1}$), osteocalcin (OCN, USCN Life Science Inc., dl: 4.2 $pg.ml^{-1}$), bone-specific alkaline phosphatase (bALP, USCN Life Science Inc., dl: 0.143 U/l), procollagen type 1 N-terminal telopeptide (PINP, Immunodiagnostics Systems, dl: 0.7 $ng.ml^{-1}$), osteoclast-specific tartrate resistant acid phosphatase 5b (TRAP5b, USCN Life Science Inc., dl: 0.29 U/ml) and collagen type 1 C-telopeptide (CTX, Immunodiagnostics Systems, dl: 2 $ng.ml^{-1}$) were measured by commercial available ELISA according to manufacturer's recommendations. Optic density (OD) was measured with a MRX 2 microplate reader (Thermo Labsystems, Palaiseau, France).

1.2.8.2. Immunoglobulin detection

Immunoglobulins (Ig) were measured using specific ELISA tests developed in our laboratory. 96-well plates (Nunc, Dominique Dutcher, Brumath, France) were coated overnight with 100 µl of anti-mouse IgG or IgM (both from Sigma) at a concentration of 10 $\mu g.ml^{-1}$ in 0.1 M sodium carbonate buffer. Wells were then saturated with 100 µl of a 5 $mg.ml^{-1}$ bovine serum albumine (BSA) solution in Tris buffer (TBS, Sigma). After washing with TBS-Tween 0.1%, serial dilutions of plasma (1:1000; 1:3000 and 1:10 000) in TBS were distributed in wells. Control IgG or IgM (both from Sigma) at concentrations of 1; 0.1; 0.01; 0.001 and 0.0001 $\mu g.ml^{-1}$ as well as a negative control were used in each ELISA plate. After 2 hours of incubation, wells were washed and biotinylated anti-IgG or anti-IgM (20 and 100 $ng.ml^{-1}$, respectively, in TBS, both from Sigma) were added for 1 hour. After washing, a streptavidin–peroxidase complex (1:200 dilution in TBS, R&D systems) was incubated for 1 hour, wells

were washed and tetramethylbenzidine (TMB) substrate (BD Biosciences, Le Pont de Claix, France) was added for 30 min. The substrate reaction was stopped by the addition of 2 N H_2SO_4. The OD was read at 490 nm, and concentrations of IgG or IgM were calculated according to a regression analysis made with OD obtained for serial dilutions of control IgG or IgM.

For detection of IgG specific for TT or KLH, the above-described ELISA protocol was used with a modification of the coating step. KLH or TT (10 $\mu g.ml^{-1}$) in carbonate buffer were used for coating ELISA plates, and IgG anti-KLH (BD Biosciences) or IgG anti-TT (Abcam, Paris, France) with serial dilutions (25 down to 0.4 $ng.ml^{-1}$) were used as controls in order to calculate the plasma concentration of specific IgG against TT or KLH.

1.2.9. Phenotypical analysis

Femurs, thymus and spleen from animals were collected and bone marrow was flushed from femurs with a syringe containing α-Minimal Essential Medium Eagle (α-MEM, Invitrogen, Cergy-Pointoise, France). Thymus and spleen were crushed in a Tenbrock's Potter. Cell suspensions were harvested washed, counted and viability was assessed by Trypan Blue (Invitrogen) exclusion.

Suspension of bone marrow, thymic or spleen cells were adjusted to 1×10^6 $cells.ml^{-1}$ in phosphate buffered salt solution (PBS, Invitrogen), supplemented with 0.5 % bovine serum albumin (BSA, Sigma). One hundred microliter of cell suspension was then mixed with pre-defined concentration of a mix of directly coupled specific antibodies as indicated in **Table 7**. Cells were then incubated for 20 min at 4°C. After washing in PBS 0.5 % BSA, cells were then analysed onto a FACSort flow cytometer (BD Biosciences) with at least 10,000 events per point and data was analysed with Cellquest software (BD Biosciences).

Bone Marrow				
Tube number	**FL1**	**FL2**	**FL3**	
1	IgG1-FITC	IgG2b-PE	IgG2a-PECy5	Control
2	CD3e-FITC	CD4-PE	CD8-PECy5	T-lymphocytes
3	CD45-FITC	CD19-PE	-	B-lymphocytes
4	CD45-FITC	CD11b-PE	-	Granulocytes
5	CD45-FITC	CD49b-PE	-	NK cells
6	Lin-FITC	SCA1-PE	c-kit-PECy7	Stem cells
7	Lin-FITC	IgG2b-PE	IgG2a-PECy7	Control

Thymus				
Tube number	**FL1**	**FL2**	**FL3**	
1	IgG1-FITC	IgG2b-PE	IgG2a-PECy5	Control
2	CD3e-FITC	CD4-PE	CD8-PECy5	T-lymphocytes
3	CD44-FITC	CD25-PE	CD8-PECy5	Immature thymic cells
4	CD44-FITC	CD25-PE	CD4-PECy5	Immature thymic cells
5	CD44-FITC	CD25-PE	CD4-PECy5 + CD8-PECy5	Immature thymic cells

Spleen				
Tube number	**FL1**	**FL2**	**FL3**	
1	IgG1-FITC	IgG2b-PE	IgG2a-PECy5	Control
2	CD3e-FITC	CD4-PE	CD8-PECy5	T-lymphocytes
3	CD3e-FITC	CD25-PE	CD4-PECy5	T-regulatory cells
4	CD45-FITC	CD19-PE	-	B-lymphocytes
5	CD45-FITC	CD11b-PE	-	Granulocytes
6	CD45-FITC	CD49b-PE	-	NK cells
7	CD62l-FITC	CD45RB-PE	CD4-PECy5	Naive/Memory cells
8	CD62l-FITC	CD45RB-PE	CD8-PECy5	Naive/Memory cells

Table 7. Mix of antibodies used for phenotypical analysis of hematopoietic cells in the bone marrow, thymus and spleen.

Antibody	Clone	Supplier	Reference
Control FITC (Hamster IgG1)	A19-3	BD Pharmingen	553971
Control PE (Rat IgG2b)	A95-1	BD Pharmingen	553989
Control PE-Cy5 (Rat IgG2a)	R35-95	BD Pharmingen	553931
Control PE-Cy7 (Mouse IgG2a)	G155-178	BD Pharmingen	552868
PE-Cy7 anti mouse CD117 (c-Kit)	2B8	BD Pharmingen	558163
FITC anti-mouse CD44	5035-41.1D	Abcam	ab23557
FITC anti-mouse CD62L (L-Selectin)	MEL-14	Beckman Coulter	732183
FITC anti-mouse CD3	KT3	Beckman Coulter	IM2768
FITC anti-mouse CD45	I3/2.3	Beckman Coulter	732147
AlexaFluor 488 mouse lineage mixture (Lin)		CALTAG	MLM20
PE anti-mouse Ly-6A/E (Sca-1)	D7	Beckman Coulter	732230
PE anti-mouse CD25	PC61	BD Pharmingen	553866
PE anti-mouse CD4 (L3T4)	H129.19	BD Pharmingen	553653
PE anti-mouse CD49b	HMα2	BD Pharmingen	558759
PE anti-mouse CD19	6D6	Beckman Coulter	733273
PE anti-mouse CD11b/Mac1	M1/70	Beckman Coulter	733270
PE anti-mouseCD45RB	C363.16A	Beckman Coulter	732166
PE-Cy5 anti-mouse CD8a	53-6.7	BD Pharmingen	553034
PE-Cy5 anti-mouse CD4 (L3T4)	H129.19	BD Pharmingen	553654

Table 8. Characteristics of antibodies used for phenotypical analysis of hematopoietic cells.

1.2.10. Colony forming cell (CFC) assay

Femurs and spleen from animals were collected and treated as described above. Cells were plated at 2 x 10^5 for spleen cells and 2.5 x 10^4 for bone marrow cells in 1.1 ml of complete methylcellulose medium with cytokines (Stem cell technologies, Vancouver, Canada) in 30 mm diameter petri dishes (Greiner Bio-One, Courtaboeuf, France). Cultures were incubated at 37°C in a humidified atmosphere with 95% air and 5% $C0_2$.

Colony-forming units-granulocyte macrophage (CFU-GM), burst-forming units-erythroid (BFU-E) and CFU-granulocyte erythrocyte monocyte megakaryocyte (CFU-GEMM) were scored on day 12 of culture (**Fig 35**).

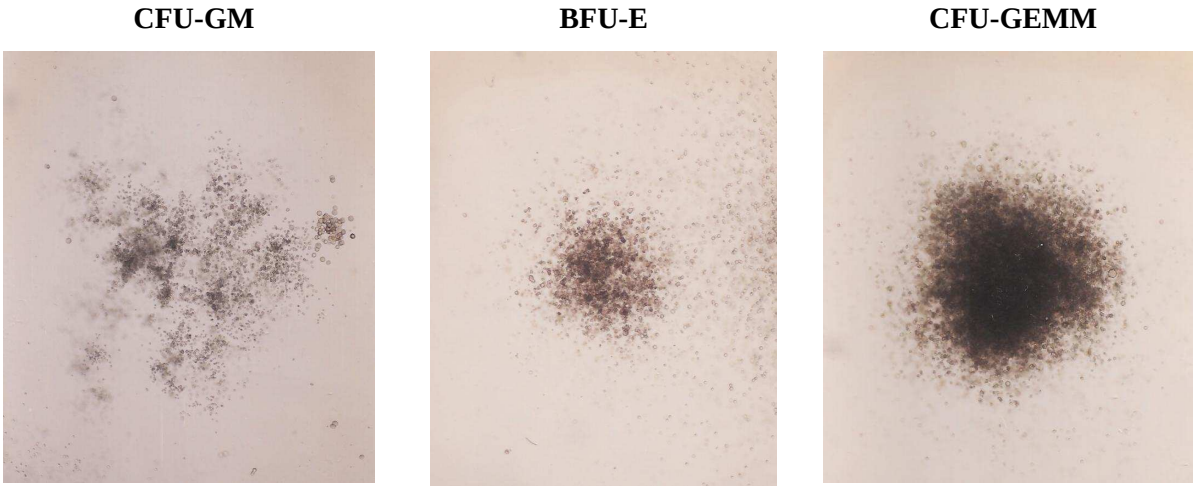

Figure 35. Representative photos of a CFU-GM, BFU-E and CFU-GEMM (60x).

1.2.11. Genetic expression analysis

1.2.11.1. Extraction of messenger RNA

Genetic expression analysis was performed on spleen, mesenteric lymph nodes, thymus and femurs. Except femurs, extraction of RNA was realized with use of a column-based RNA extraction kit (Rneasy Total RNA Isolation kit, Qiagen, Courtaboeuf, France) according to the manufacturer's instructions.

About 30 mg of samples were lysed in 600 µl of a lysis solution containing RLT buffer (buffer containing guanidine-thiocyanate with strong denaturation potential) completed with 1% β-mercaptoethanol. Lysis of samples was performed with use of a ribolyzer-homogenizer (Fastprep, BIO101, QBiogene). After centrifugation (16000g during 3 min), the lysate was harvested and homogenized in 350 µl ethanol 70% in order to increase the specific binding of RNA to the membrane of the column. This mixture was transferred to a mini column containing silicium resin. Then centrifugation took place during 1 min at 16000g. A first wash buffer was applicated on the column and centrifuged 1 min at 16000g. Residual DNA was eliminated by adding DNAse during an incubation step of 15 min. Then a second wash buffer was deposited on the column and centrifugation 1 min at 16000g took place. 25 µl of sterilized RNAse-free water was deposited on the column. A last centrifugation step took place for 1 min at 16000g to recuperate the RNA.

RNA concentration was checked by OD measurement at 230nm (Thermo Scientific NanoDrop 1000, ND-1000 spectrophotometer, Labtech, Palaiseau, France). RNA quality was verified by measurement of the ratio of the OD at 260nm / 280nm (which has to be between 1.75 and 2.1). Integrity of RNA was checked by gel electrophoresis on a 1 % agarose gel in denaturation condition, with ethidium brome for revelation. RNA was conserved at -20°C.

Extraction of RNA from femurs was realized with use of a Trizol reagent (Sigma) according to the manufacturer's instructions. Frozen femurs were pulverized using a T25 Ultra-Turrax (IKA, Staufen, Germany) and total RNA was isolated from bone powder using Trizol reagent. Obtained RNA was purified by RNeasy Total RNA Isolation Kit (Qiagen) as described earlier.

1.2.11.2. Reverse transcription (RT)

1 µg of total RNA was reverse transcribed with random hexamers by use of the high-capacity cDNA Reverse Transcription Kit according to manufacturer's recommendations (Applied Biosystems, Courtaboeuf, France). Synthesis of complementary DNA (cDNA) was performed with 50 units of reversal transcriptase (Multiscribe reverse transcriptase) in a 20 µl reaction buffer (containing RT buffer, Random primer, dNTP, RNase-free water). The steps for reverse transcription include a first step during 10 min at 25°C, a second step during 120 min at 37°C and a third step during 5 min at 85°C. The cDNA samples were conserved at -20°C until their use.

1.2.11.3. Polymerase chain reaction (PCR) in real time

cDNA was amplified with use of forward and reverse primers listed in **Table 9** for genes studied for the bone physiology and in **Table 10** for genes studied for the immune system. Primers used for the amplification of cDNA were inspired from bibliographic study or determined by use of "Primer Express" software (Applied Biosystems). Primers were obtained from Invitrogen-Life Technologies or Applied Biosystems.

Expression of genes was measured by polymerase reaction (PCR) in real time on plates with 96 wells or 384 wells. 5 or 10 ng of cDNA was amplified in duplicates for each reaction using

SYBR Green PCR Master Mix or Taqman fast universal PCR Master Mix (both from Applied Biosystems).

For 96 well plates, it was realized with 5 µl of cDNA diluted at $1/25^{th}$ (10 ng of cDNA) and 20 µl of a mixture with SYBR Mix (polymerase, dNTP, salts, intercalating fluorescent, fluorophore of internal control, Power SYBR Green (Applied Biosystems) or Taqman Mix (83 % v/v), sterilized water (14.5 % v/v) and forward and reverse primers of genes of interest (2.5 % v/v).

For 384 well plates, it was realized with 4 µl of cDNA diluted at $1/50^{th}$ (5 ng of cDNA) and 6 µl of a mixture with SYBR Mix (polymerase, dNTP, salts, intercalating fluorescent, fluorophore of internal control, Power SYBR Green (Applied Biosystems) or Taqman Mix (83 % v/v), sterilized water (14.5 % v/v) and forward and reverse primers of genes of interest (2.5 % v/v).

Amplification and detection of PCR products was performed with the Abi Prism 7900 Sequence Detection System (Applied Biosystems), using the following steps: 50°C during 2 min, 95°C during 10 min to activate AmpliTaq Gold DNA polymerase for 40 cycles of amplification including 15 sec of denaturation at 95°C and 1 min of hybridizing-elongation at 60°C. SYBR green has the characteristics to incorporate on a non specific manner at double strand DNA while emitting fluorescence at 530nm.

The raw, background-subtracted fluorescence data provided was analysed by SDS software (Applied Biosystems). PCR products (using SYBR green technology) were subjected to a melting curve analysis to confirm the specificity of the amplification. The resulting fractional cycle number of the threshold (Ct) was used for transcript quantification. Expression level of each sample was normalized by the expression level of an intern reference gene. Glyceraldehyde 3-phosphate dehydrogenase (GAPDH) has been chosen as the reference gene. Results were normalized to GAPDH transcription to compensate for variation in input RNA amounts and efficiency of reverse transcription. Relative expression to the control group was calculated for each gene by the $2^{-\Delta\Delta Ct}$ method described by Livak et al. (Livak and Schmittgen 2001).

Genes	Forward primer	Reverse primer	Accession number
Runx2	AAATGCCTCCGCTGTTATGAA	GCTCCGGCCCACAAATCT	NM_001145920.1
ALP	CCGATGGCACACCTGCTT	GAGGCATACGCCATCACATG	NM_007431.2
BSP	ACCCCAAGCACAGACTTTTGA	CTTTCTGATCTCCAGCCTTCT	NM_008318.3
OPN	CCCGGTGAAAGTGACTGATTC	ATGGCTTTCATTGGAATTGC	NM_009263.2
OCN	CCGGGAGCAGTGTGAGCTTA	AGGCGGTCTTCAAGCCATACT	NM_007541.2
Coll1	CTTCACCTACAGCACCCTTGTG	CTTGGTGGTTTTGTATTCGATCACT	NM_007742.3
Coll3	TTCCTGAAGATGTCGTTGATGTG	TTTTTGCAGTGGTATGTAATGTTCTG	NM_009930.2
RankL	TCAGCTGATGGTGTATGTCGTTAA	TTCGTGCTCCCTCCTTTCAT	NM_011613.3
OPG	GGGCGTTACCTGGAGATCG	GAGAGAACCCATCTGGACATTT	NM_008764.3
TRAP 5b	GATGACTTTGCCAGTCAGCAGC	GCACATAGCCACACCGTTCTC	NM_007388.3
PTHr	TGGGTCGGTGTCAGAGCAA	CCTGGATGATCCACTTCTTGTG	NM_001083936.1
GAPDH	Product number 4352932-0804021, Applied Biosystems, Courtaboeuf, France		

Table 9. List of genes studied for the bone physiology and the related forward and reverse primers used.

Genes	Forward primer	Reverse primer	Accession number
T-bet	ACCAGAACGCAGAGATCACTCA	CAAAGTTCTCCCGGAATCCTT	NM_019507.2
IFN-γ	AGAGCCAGATTATCTCTTTCTACCTCAG	CCTTTTTCGCCTTGCTGTTG	NM_008337.3
GATA-3	CTACCGGGTTCGGATGTAAGTC	GTTCACACACTCCCTGCCTTCT	NM_008091.3
IL-10	AGAGAAGCATGGCCCAGAAAT	CGCATCCTGAGGGTCTTCA	NM_010548.2
Foxp3	CCCAGGAAAGACAGCAACCTT	TTCTCACAACCAGGCCACTTG	NM_054039.1
GAPDH	Product number 4352932-0804021, Applied Biosystems, Courtaboeuf, France		

Table 10. List of genes studied for the immune system and the related forward and reverse primers used.

1.2.12. T cell excision circle (TREC) detection

5×10^6 thymic cells were used for DNA extraction using a QIAmp DNA Mini Kit (Qiagen). After quality control of DNA by gel electrophoresis in a 0.8 % agarose with 500 $\mu g.ml^{-1}$ ethidium bromide, DNA concentration was adjusted to 12.5 $\mu g.ml^{-1}$.

50 ng of DNA was then used for TREC detection by PCR in real time using Taqman fast universal PCR master mix (Applied Biosystems). For TREC, the following primers were used: sense primer: 5'-CAA GCT GAC AGGGCA GGT TT-3', anti-sense primer: 5'-TGA GCA TGG CAA GCA GTA CC-3'. The reference gene used was the gene encoding for the constant part of the T cell receptor antigen alpha chain (TCRA), with the following primers: sense: 5'-TGA CTC CCA AAT CAA TGT G-3', anti-sense: 5'-GCA GGT GAA GCT TGT CTG-3'. The specificity of the PCR products was controlled using the following probes: FAM-TGC TGG ACA TGA AAG CTA TGG A-TAMRA for TREC, and FAM-TGC TGT GTG CCC TAC CCT GCC C-TAMRA for TCRA.

All amplifications were made on the ABI prism 7900 sequence detection system (Applied Biosystems). Results, expressed as the number of cycles needed to obtain a significant signal for TREC (CtTREC) and for TCRA (CtTCRA), were used for calculating the difference between control and contaminated animals (ΔCtTREC and ΔCtTCRA) at each time point. Results were then normalised by calculating at each time point the ratio according to the following formula: $R = (E_{TREC})^{-\Delta CtTREC} / (E_{TCRA})^{-\Delta CtTCRA}$, where E is the efficiency of the PCR reaction, as determined by the slope of the standard curve made with serial dilutions of DNA.

1.2.13. Protein expression analysis

1.2.13.1. Extraction of total proteins

Total proteins from spleen were extracted with use of a lysis buffer from the Mammalian Cell Lysis Kit (Sigma), using 500 µl of buffer for 10 mg of tissue. The lysis buffer was composed of 250 mM Tris-HCl and 5 mM EDTA Buffer, 750 mM NaCl, 0.5 % SDS lauryl sulphate, 2.5 % deoxycholic acid, 5 % Igepal CA630 and 1 % of cocktail of protease inhibitors.

Samples were homogenized by gentle agitation during 20 min at 4°C and the obtained lysate was refined during 10 sec with a ribolyzer-homogenizer (Fastprep, QBiogene, Illkirch, France). After centrifugation (20 min, 12000 rpm, 4°C), supernatant was harvested and conserved at -80°C.

1.2.13.2. Measure of protein concentration

Protein concentration of samples was determined by Bradford method (Bradford 1976), with a standard curve of bovine serum albumin (BSA) as reference. This method relies on the

characteristic of Coomassie Blue (Protein Assay, Biorad, Marnes la Coquette, France) to change of absorbance from 465nm to 595nm when it is binds to proteins.

1.2.13.3. Protein analysis by western blot method

Proteins of spleen were denaturated (5 min at 95°C) in a laemmli buffer (containing 125 mM Tris-HCl pH 6.8, 20 % glycerol, 4% SDS, 0.02 % bromophenol blue and 10 % β-mercaptoethanol).

40 µg of proteins were deposited on a 12 % SDS-polyacrylamide gel in denaturing conditions. Components of the gel are listed in **Table 11**. After separation, proteins were electro-transferred to a nitrocellulose membrane (Invitrogen) during 2 hours. Aspecific binding sites of the membrane were blocked during 1 hour at room temperature in tris saline buffer (TBS) with 5 % of non-fat dry milk. Then the membrane was incubated with a primary antibody (diluted in TBS with 2 % of non-fat dry milk) overnight at 4°C and afterwards with the corresponding secondary antibody (diluted in TBS with 2 % of non-fat dry milk), coupled at horseradish peroxydase (HRP), during 1 hour at room temperature. The antibodies used are listed in **Table 12**. After each incubation step with an antibody, series of washing with 0.025 % TBS-Tween were realized (5 times 5 min at room temperature). Chemiluminescence (Millipore, Cergy Pontoise, France) permitted to reveal the signal of the immune complexes and these were detected with a CCD camera (Las-3000, Fujifilm, Raytest, France). Reaction intensity was determined by computer-assisted densitometry with use of MultiGauge software (Fujifilm). The intensity of the bands was normalized to the intensity of the protein band of glyceraldehyde 3-phosphate dehydrogenase (GAPDH).

	Stacking gel	**Running gel**
dH_2O	1.4 ml	3.3 ml
Acrylamide	330 µl	4.0 ml
Tris 1,5 M pH 8,8		2.5 ml
Tris 0,5 M pH 6,6	250 µl	
SDS 10 %	20 µl	100 µl
APS 10 %	20 µl	100 µl
Temed	2 µl	4 µl

Table 11. Components of the 12 % polyacrylamide gels used for western blot method.

Protein	Molecular weight (kDa)	Primary antibody		Secondary antibody		
		Ref	Supplier		Ref	Supplier
Tbet	62kDa	4B10 (sc-21749)	Santa Cruz	Goat anti-mouse	sc-2005	Santa Cruz
Gata 3	51kDa	ab-32858	Abcam	Goat anti-rabbit	sc-2004	Santa Cruz
Foxp3	50kDa	ABE75	Millipore	Goat anti-rabbit	sc-2004	Santa Cruz
GAPDH	37kDa	FL335 (sc-25778)	Santa Cruz	Goat anti-rabbit	sc-2004	Santa Cruz

Table 12. Primary and secondary antibodies used for western blot method.

1.2.14. Bone histology and histomorphometric analysis

1.2.14.1. Preparation of samples

After being decalcified with chlorhydric acid (RDC agent, CML), femurs were conserved in formaldehyde 4%. Then femurs were put in cassettes and these were put in an automatic apparatus for dehydration (Tissue-Tek VIP, Sakura, Villeurbanne, France). This apparatus performs different steps to dehydrate samples and includes them in paraffin. The different steps performed are: a step for dehydration which replaces water content of cells by alcohol 100 %, a step which replaces alcohol 100 % by toluene and a final step to replace toluene by paraffin. The different steps and accompanying treatment times are given in **Table 13**.

Solution	Time (minutes)
Formol	10
Ethanol 80 %	10
Ethanol 80 %	25
Ethanol 95 %	10
Ethanol 95 %	25
Ethanol 100 %	25
Butanol	15
Butanol	15
Toluene	40
Xylene	40
Paraffin	15
Paraffin	30
Paraffin	60
Paraffin	60

Table 13. Steps for dehydration of samples.

Femurs were then embedded in paraffin and serial longitudinal sections of 7 µm thick were obtained using a microtome (Microm Microtech, Francheville, France). Sections cut were unfolded in warm water at 37°C and put on glass slides.

1.2.14.2. Removal of paraffin

Removal of paraffin was done with an automatic apparatus (DRS 601, Sakura), following the steps given in **Table 14**.

Solution	Time (minutes)
Xylene	3
Xylene	3
Ethanol 100 %	3
Ethanol 100 %	3
Ethanol 100 %	3
dH_2O	15
Triton X-100 0,1 %	10
dH_2O	5
H_20_2 3 %	10
dH_2O	15

Table 14. Steps for removal of paraffin.

After being deparaffinized, 6 sections per femur were used for modified Trichrome Goldner staining and subsequent quantitative analysis of bone morphometric parameters. Some extra sections were colored by hematoxylin eosin safran (HES) method to examine morphologic structures.

1.2.14.3. Histological staining

1.2.14.3.1. Hematoxylin eosin safran (HES)

This coloration was performed by an automatic apparatus (DRS 601, Sakura) following steps given in **Table 15**.

Solution	Time (minutes)
dH_2O	2
Hematoxylin	15
dH_2O	1,5
dH_2O	1,5
Alcohol HCl 1 %	0,5
dH_2O	0,5
dH_2O	1,5
Lithium carbonate	2
dH_2O	0,5
dH_2O	1,5
Erythrosine 1 %	0,1
dH_2O	0,5
dH_2O	1,5
Ethanol 100 %	1
Ethanol 100 %	1
Safran	4
Ethanol 100 %	0,5
Ethanol 100 %	1
Xylene	1
Xylene	2

Table 15. Steps for hematoxylin eosin safran coloration method.

1.2.14.3.2. Modified trichrome Goldner

Slides were incubated overnight in picric acid (Merck, Darmstadt, Germany) at 4°C and washed afterwards with running tap water. Slides were incubated for 10 min at room temperature with fuchsine (Merck) and rinsed with 1 % acetified water. Then slides were incubated for 5 min at room temperature with phosphomolybdic acid (Merck) and for 10 min at room temperature with Fast Green solution (Sigma). Slides were rinsed with 1% acetified water (Sigma) and dehydrated with 100 % ethanol and methylcyclohexane (VWR) and mounted with Entallan (Merck).

1.2.14.4. Analysis of samples

The distal diaphysis of femurs was examined by a Leica DM4000B light microscope and images were captured using a digital Sony XCD-U100CR camera. Images were analysed with Histolab 7.6 software (Microvision instruments, Evry, France).

Mean thickness of the growth plate per section was determined from 3 measurements (red lines) at set distances along the growth plate. Mean thickness of the growth plate per femur was then determined from 6 sections. Finally growth plate thickness per group was averaged of 8 femurs from different animals in the group.

Furthermore a tissue surface (green contour) restricted in a 2 mm region (yellow line) from the growth plate (which was included) was determined for analysis (**Fig 36 a**). Automated quantification of bone surface in the tissue surface confined was performed by user predefined parameters and the ratio between them (in %) was calculated (**Fig 36 b**). Results were averaged for every femur from 6 sections, giving a bone volume (BV) to tissue volume (TV) ratio. Finally this BV/TV ratio per group was averaged of 8 femurs from different animals in the group.

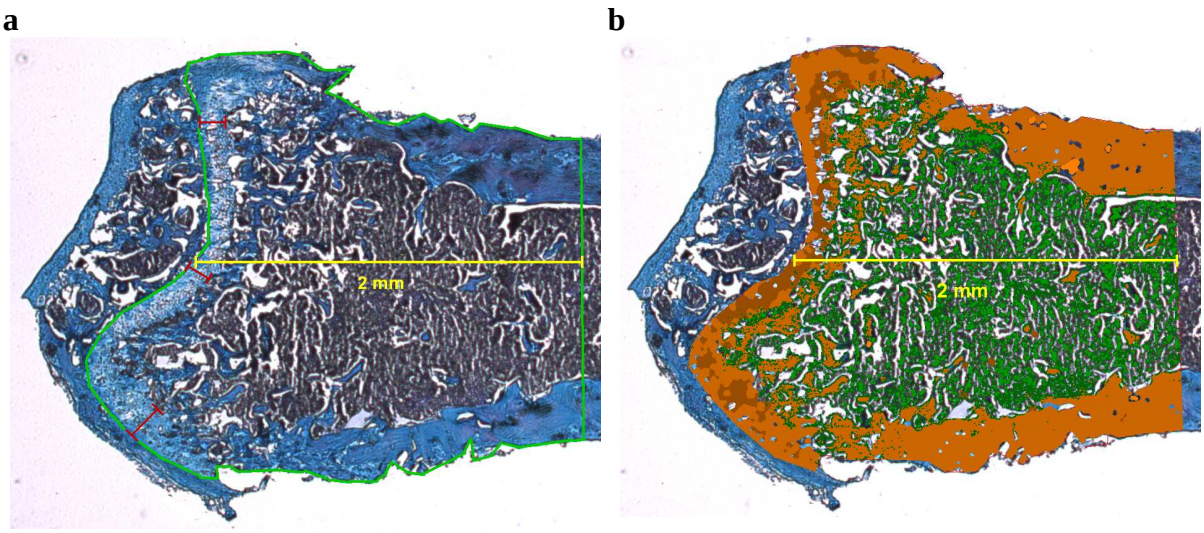

Fig 36. Representative images of bone histology and histomorphometry. **Fig a**: distal diaphysis of femur stained by modified Trichrome Goldner. Mean thickness of the growth plate was determined from 3 measurements (red lines) at set distances along the growth plate and a tissue surface (green contour) restricted in a 2 mm region (yellow line) from the growth plate (which was included) was determined for analysis of bone morphometric parameters. **Fig b**: automated quantification of bone surface in the tissue surface confined was performed by user predefined parameters.

2. In vitro studies

2.1. Cell culture models

2.1.1. Pre-osteoblastic cells

The used cell line MC3T3-E1 is derived from mouse pre-osteoblastic cells. MC3T3-E1 mouse pre-osteoblasts are clonally derived from murine calvariae and this cell line maintains osteoblast phenotype despite repeated subcultivation.

The cells were purchased from ATCC (American Tissue Culture Collection, Illkirch, Strasbourg, France) and had the following references: CRL-2593 MC3T3-E1 for subclone 4 (preosteoblast mouse), CRL-2594 MC3T3-E1 for subclone 14 (bone calvaria mouse), CRL-2596 MC3T3-E1 for subclone 30 (calvaria mouse) and CRL-2595 MC3T3-E1 for subclone 24 (preosteoblast mouse).

Cells were conserved at -150°C. At the moment of cultivation, cells were thawed the fastest as possible and were put in cell culture medium that was previously warmed at 37°C. Cell culture medium used was α-Minimal Essential Medium Eagle (α-MEM, Gibco, Cergy Pontoise, France), supplemented with 1 % penicillin-streptomycin (Gibco), 1 % L-glutamin (Gibco) and 10 % fetal bovine serum (Gibco). Cells were centrifuged during 10 min at 450g. Cell pellet was retaken in new cell culture medium and distributed in cell culture flasks at 20 x 10^3 cells per cm^2. Cells were maintained in culture 75 cm^2 tissue culture flasks at 37°C, in a humidified atmosphere of 95 % O_2 and 5 % CO_2.

2.1.2. Mesenchymal stem cells (MSC)

Mesenchymal stem cells (MSC) are isolated from bone marrow from femurs or subcutaneous and ovarian fat tissue of female Sprague Dawley rats of 7 weeks old. MSC are capable to differentiate into immature osteoblasts in the presence of specific factors (Pittenger et al. 1999). Bone marrow was flushed from femurs with a syringe containing α-MEM cell culture medium (Gibco). Fat tissue was cut in α-MEM cell culture medium and digested under stirring in 0.1 % collagenase type 1 (Sigma) solution during 30 min at 37°C. The obtained cell suspension was filtered with a 100 µm filter and collagenase was neutralized by fresh cell culture medium.

Cells collected were cultivated in cell culture flasks of 75 cm^2, in α-MEM cell culture medium supplemented with 20% of fetal calf serum (Thermo Fisher Scientific, Illkirch, France), 1 % of penicillin/streptavidin (Gibco) and 1 % L-glutamine (Gibco). Cells were kept in culture at 37°C, in a humidified atmosphere of 95 % O_2 and 5 % CO_2. After 24 hours, cell culture medium was removed to eliminate non adherent cells (hematopoietic cells). The adherent cells (MSC) were then washed 3 times in phosphate-buffered saline solution (PBS) (Gibco). Fresh cell culture medium was added and cells were kept in culture at 37 °C, in a humidified atmosphere of 95 % O_2 and 5 % CO_2.

The presence of MSC specific markers (CD90, CD73) and the absence of HSC specific markers (CD45, CD34) were verified by phenotypical analysis. For this, MSC were harvested and the cell density was adjusted to 1 x 10^7 cells per ml with PBS. Then the cells were labelled with the specific markers described above at 4°C in the dark for more than 30 min. Cells were washed once with PBS and then analysed onto a FACSort flow cytometer (BD Biosciences) and data was analysed with Cellquest software (BD Biosciences).

2.1.3. Contamination of cell cultures

^{90}Sr solutions were prepared from a ^{90}Sr source ($^{90}SrCl_2$ in 0,1 N HCl, AREVA-CERCA LEA). For contamination of cell cultures, ^{90}Sr was dissolved in cell culture medium to obtain ^{90}Sr concentrations from 312 Bq/ml up to 100 kBq/ml. The pH of the solutions was verified and adjusted to a neutral pH of 7.

Non radioactive strontium was prepared from strontium dichloride hexahydrate ($SrCl_2$) powder (Sigma), dissolved in deionised and sterilized H_20. The solution was filtered on a 0.22 µm filter and $SrCl_2$ was dissolved in cell culture medium to obtain concentrations from 0.01 mM up to 10 mM.

Some cells used were irradiated with a ^{137}Cs source (IBL 637, Cisbio, Saclay, France). Irradiation of cells was realized in cell culture plates, at room temperature, with a radiation dose of 0.5 Gy for γH2AX foci detection and doses from 0.5 Gy up to 4 Gy for cytotoxic tests. Control cells were treated in the same experimental conditions.

2.2. Methods

2.2.1. Cell cultivation and maintenance

All cells were cultivated in α-MEM (Gibco) cell culture medium supplemented with 10 % of fetal bovine serum (for MC3T3-E1 cell line) (Gibco) or 20 % of fetal calf serum (for MSC) (Thermo Fisher Scientific), 1 % of penicillin/streptavidin (Gibco) and 1 % L-glutamine (Gibco) in an incubator at 37°C, with 95 % of oxygen and 5 % of CO_2.

Cell culture medium was changed twice a week until 80 % of confluence of cells. In this case cells were passaged. For this, cell culture medium was removed from the cell culture flasks and replaced by PBS (Gibco) in order to eliminate cellular debris and cell culture medium containing fetal calf or bovine serum, which could inhibit the action of trypsin. PBS is replaced by a solution of trypsin (Gibco) and incubated with trypsin during 5 minutes at 37°C. After detachment of cells, cells were centrifuged 8 min at 1500 rpm. Cell pellet is retaken in cell culture medium at 37°C and cells were numbered with Trypan blue (Gibco) and seeded at a lower cell density at 5 x 10^3 cells per cm^2 for MC3T3-E1 cells and 1 x 10^3 cells per cm^2 for MSC in new cell culture flasks of 75 cm^2.

For cell culture differentiation and contamination, chemicals were added to fresh cell culture medium.

2.2.2. Cell culture differentiation

Differentiation of cells was induced in cell culture plates of 6, 12 or 24 wells. Differentiation of pre-osteoblastic or mesenchymal stem cells into osteoblasts was induced by addition of specific factors to the cell culture medium: 50 µg/ml ascorbic, 10^{-7} M and 10mM β-glycerophosphate (all from Sigma). The use of this supplemented medium is customary when investigating mineralization properties of cells. Supplemented medium containing ascorbic acid and β-glycerophosphate stimulates greater collagen production and cross-linking. The synthetic glucocorticoid dexamethasone further enhances osteogenesis.

2.2.3. Cell mortality test

Lactate dehydrogenase (LDH) is an enzyme excreted from cells when their cell membrane is damaged. As such, the measurement of this enzyme served to estimate cell mortality. The quantification of LDH in cell lysate is realized with the Cytotoxicity Detection Kit Plus (Roche Diagnostic, Meylan, France) according to the manufacturer's recommendations. Briefly, in a 96 well plate 50µl of reaction mixture was added to 50µl of recuperated cell lysate and this mixture was incubated for 20 min in the dark. 25 µl of a stop solution was added and spectrophotometer analysis was performed at 490 nm and 630 nm. The intensity of the final colour reflected the LDH released from cells.

2.2.4. Cell viability test

The MTT test (Roche Diagnostic) permitted to test viability of cells. The assay is based on the cleavage of the yellow tetrazolium salt MTT (3-(4,5-dimethylthiazol-2-yl)-2,5-diphenyl tetrazolium brome) to purple formazan crystals by metabolic active cells. Briefly, tetrazolium salt MTT was added to the cell culture medium and during different times (24, 48, 72 or 96 hours) this salt was metabolized by the living cells. The obtained colour was homogenized by a buffer solution and the intensity of the final colour reflected the viability of cells in the wells and their cellular metabolic activity. Colour intensity was measured by spectrophotometer analysis at 595 nm and 630 nm.

2.2.5. Differentation assays

2.2.5.1. Alkaline phosphatase activity test

Alkaline phosphatase (ALP) activity was determined using a ALP Assay Kit (Alkaline Phosphatase Blue Microwell Substrate Solution, Sigma) according to the manufacturer's specifications. As a positive control, 10^{-8} M calcitriol (Sigma) was used. Briefly, cell pellets were retaken in 250 µl of PBS supplemented with 0,1 % Triton X-100 (Sigma). Cells were sonicated (100W) during 30 sec and seeded on a 96 well plate. Alkaline substrate solution (5-bromo-4-chloro-3-indolyl phosphate (BCIP) and nitro blue tetrazolium (NBT) was added during 15 min in the dark. A stop solution was added and colour intensity was measured by spectrophotometer analysis at 595 nm. Obtained values were normalized to the protein concentration measured by Bradford method (Bradford 1976).

2.2.5.2. Mineralization tests

Formation of mineralizing plaques was visualized by Von Kossa staining and Alizarin Res S staining techniques.

For Von Kossa staining, cells were rinsed three times in 0,9 % NaCl solution (pH 7,2) and fixed in 4% paraformaldehyde (Sigma) in 0,9 % NaCl solution at room temperature for 10 min. Cells were then rinsed three times in deionised distilled water (dH_2O), incubated with 3 % $AgNO_3$ (Sigma) in the dark for 30 min, and exposed to ultraviolet light for 30 min. Cells were then washed in dH_2O and counterstained with Toluidine Blue (Merck) for 5 min. The total area of nodules (μm^2) per well was analysed with Histolab software (Microvision instruments).

For Alizarin Red S staining, cells washed twice with PBS (pH 7,4) and fixed with ice-cold 70 % ethanol at -20°C for 20 min. Then the plates were washed two times with distilled water and incubated with 40 mM Alizarin Red S (pH 4,2, Sigma) for 10 min at room temperature under gentle agitation. After removing Alizarin Red S solution by aspiration, the cells were then washed thoroughly with deionised water. The cells were subsequently destained for 30 min with 10 % cetylpyridinium chloride (Sigma) in 10 mM sodium phosphate (pH 7). The extracted stain was then transferred to a 96-well plate, and the optical density at 595 nm was measured.

2.2.5.3. Collagen synthesis test

The effects on collagen production were measured by the Sirius Red method. Cell layers were washed with PBS and fixed for 1h in Bouin's fixative. The fixation solution was removed by suction, the wells were washed by immersion in running tap water for 15 min and cell culture plates were dried overnight. 0,1 % Sirius Red F3BA solution (Chroma, Stuttgart, Germany) in satured picric acid was added. After 1 h of staining under gentle agitation, cell layers were washed in running tap water and again in 0,01 N HCl to remove the non-bound dye. Cell morphology was photodocumented and for quantification of collagen content, the dye was dissolved in 0,1 NaOH. The dye solution was transferred to microtiter plates and the optical density was measured at 550 nm.

2.2.6. Immunohistochemical study of γ-H2AX foci

For this study Lab-Tek chamber slides (Nunc, VWR) containing 2 chambers of 4 cm^2 each were used. The immunostaining technique was based on a protocol previously described (Roch-Lefevre et al. 2010) for γ-H2AX immunostaining and foci analysis. Briefly, cells were washed with PBS, and fixed with 2 % paraformaldehyde (PFA, Sigma) for 10 min. Then they were permeabilized with 0,1 % of Triton for 10 min and incubated at 37°C with PBS-BSA 2% for 30 min. Cells were immunostained using a primary monoclonal γ-H2AX antibody (Upstate-Millipore, USA) for 1h at 37°C, washed in PBS, and incubated with a FITC conjugated goat anti-mouse secondary antibody (Sigma) for 1h at 37°C. After extensive washing, slides were mounted with DAPI Vectashield solution (Vector Laboratories, Les Ulis, France) and covered with cover slips. Slides were viewed with an epifluorescence microscope (Provis AX70, Olympus, Japan) and an uncooled CDD camera was used to acquire images. Fields were selected on the basis of DAPI-counterstained nuclei. Image analysis was performed using Cartograph and Histolab software (Microvision instruments). Parameters for focus detection and analysis were maintained constant during all the study and at least 100 cells per condition were analysed.

3. Statistical analysis

All results are presented as mean ± standard deviation (SD) unless otherwise indicated. Comparisons between groups were made with either Student t test or 2-way ANOVA (analysis of variance) test, as indicated in the text. Differences were considered statistically significant for a p value less than 0.05. All statistical analyses were performed using Sigmaplot software (Systat software Inc., San Jose, Ca).

Results

Results

1. Biokinetics of ^{90}Sr

1.1. Reproduction data

We analysed the birth of animals for the whole of our experiences. We had a total of 90 reproduction groups, each consisted of 2 females and 1 male per cage, for each of the control animals and the ^{90}Sr ingesting animals. Despite a similar total number of litters (n=52) for the control and the ^{90}Sr ingesting animals there was no significant difference (Student t test, p = 0.149) in the number of animals per litter at birth between the two groups (**Fig 37**). For the control group, we had a mean of 5.0 ± 2.4 animals per litter and for the ^{90}Sr ingesting group a mean of 5.7 ± 2.8 animals per litter.

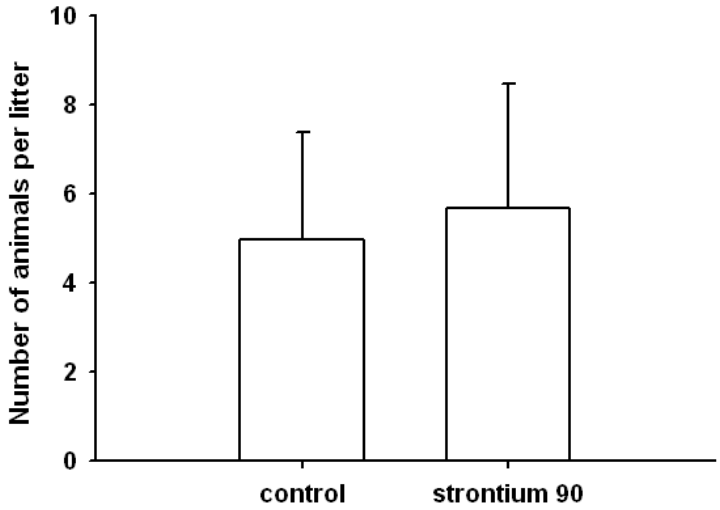

Figure 37. Number of animals per litter for each group of treatment. No significant difference between the two groups was observed by Student t test analysis (p = 0,149). Results are presented as mean ± standard deviation (SD), with n=52 for control mice and ^{90}Sr ingesting mice.

1.2. General health parameters

In order to verify the general health status of our animals, we measured creatin kinase, creatinin, urea, alanine aminotransferase (ALAT) and aspartate aminotransferase (ASAT) levels in blood plasma (data not shown). Overall no significant difference was detected between control and ^{90}Sr ingesting animals (2-way ANOVA analysis, $p>0.05$) with a single exception for creatinin for females at 16 weeks (Student t test, $p<0.001$; 44.2 ± 2.8 µM and 52.7 ± 3.1 µM for control and ^{90}Sr ingesting animals respectively (n=5)).

1.3. Distribution of ^{90}Sr in the juvenile model

1.3.1. Body mass

A regular weight gain was observed for males and females (**Fig 38**). No significant modification of body weight of animals has been observed between control and ^{90}Sr ingesting animals, whatever the age or sex of the offspring (2-way ANOVA analysis, $F_{(1,50)} = 1.06$, non significant (n.s.) for males and $F_{(1, 50)} = 0.017$, n.s. for females), although a dispersion of body weight was observed in males between 16 and 20 weeks of age. The reason for such dispersed body weight in males remains unclear, but time specific statistical analysis (using Student t test) did not showed significant differences. A body weight of 30.7 ± 5.2 g for control males, 28.7 ± 5.2 g for ^{90}Sr ingesting males, 25.8 ± 4.7 g for control females and 25.6 ± 1.6 g for ^{90}Sr ingesting females was reached after 20 weeks of ingestion.

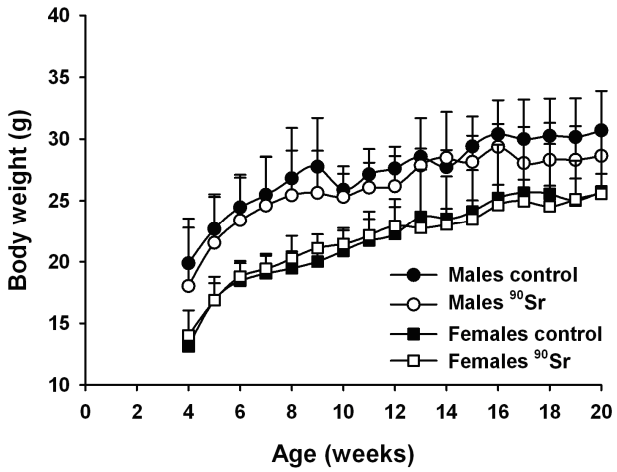

Figure 38. Evolution of the body weight (g) of control and ^{90}Sr ingesting animals from the juvenile model, according to the age and sex of animals. No significant difference between control and ^{90}Sr-ingesting animals was observed (2-way ANOVA test, $F_{(1, 50)} = 1.06$, n.s. for males and $F_{(1, 50)} = 0.017$, n.s. for females). Results are presented as mean ± SD, with n=3 to 9 for control mice and n=6 to 24 for ^{90}Sr ingesting mice, depending on the age.

1.3.2. Water intake and ingestion of ^{90}Sr

A weekly follow-up of food and drinking water consumption per cage was made starting from the time of weaning. The mean food and water intake per animal and per day was obtained by calculation on the basis of the number of animals per cage. Based on these data the corresponding daily ingestion of ^{90}Sr was calculated (**Fig 39**). Results indicated that ^{90}Sr

ingestion increased rapidly the first weeks post-weaning, reaching 68.2 ± 9.7 Bq.animal^{-1}.day^{-1} for males and 71.2 ± 7.7 Bq.animal^{-1}.day^{-1} for females at 6 weeks of chronic ingestion. No significant difference in ^{90}Sr ingestion was observed between males and females, whatever their age (2-way ANOVA analysis, $F_{(1,165)}$ = 1.042, n.s.). The mean daily intake of ^{90}Sr over the whole period of 20 weeks of chronic ingestion was 74.3 ± 14.6 Bq for males and 69.0 ± 11.6 Bq for females. This was lower than the expected ingestion of 100 Bq per animal per day at adult age and was caused by a lower drinking water intake than expected. In fact, the mean daily water intake per animal over the whole period of 20 weeks was 4.6 ± 0.9 ml.day^{-1} for control males, 3.7 ± 0.7 ml.day^{-1} for ^{90}Sr ingesting males, 3.4 ± 0.5 ml.day^{-1} for control females and 3.5 ± 0.6 ml.day^{-1} for ^{90}Sr ingesting females.

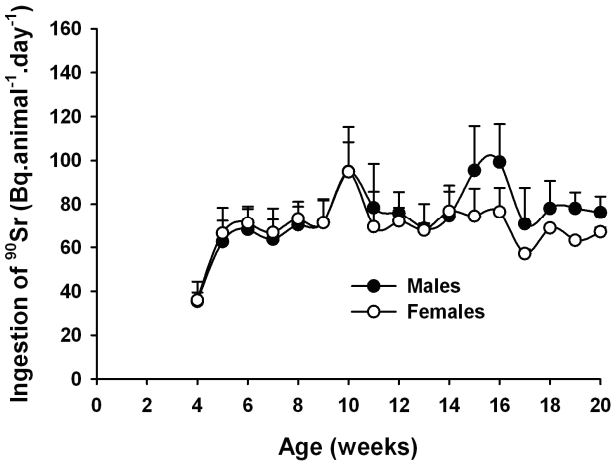

Figure 39. ^{90}Sr intake (Bq.animal^{-1}.day^{-1}) through drinking water, according to the age and sex of animals from the juvenile model. No significant differences were observed between males and females (2-way ANOVA test $F_{(1, 165)}$ = 1.042, n.s.). Results are presented as mean ± SD, with n=3 to 9 for control mice and n=6 to 24 for ^{90}Sr ingesting mice, depending on the age.

1.3.3. ^{90}Sr concentration in femurs

In order to investigate the distribution of ^{90}Sr after chronic ingestion, the ^{90}Sr content was measured in different organs (skin, liver, spleen, kidneys, digestive tract (from stomach to the rectum), heart, thymus, lungs, skeletal muscle, femurs and central nervous system (CNS)) of male and female animals from both control and ^{90}Sr ingestion groups. ^{90}Sr was below detection limit in organs of control animals. The detection limit of ^{90}Sr was between 0.45 Bq and 0.75 Bq per sample. For ^{90}Sr ingesting animals, the highest ^{90}Sr concentrations were found in the bones. It has to be noted that ^{90}Sr content in femurs (**Fig 40**) was measured without separating the bone from the bone marrow. According to the age of animals a

significant increase in ^{90}Sr content in femurs was seen (2-way ANOVA analysis, $F_{(5, 64)}$ = 266.5, p<0.001), reaching at 6 weeks 79.7 ± 9.4 Bq.g^{-1} and 75.4 ± 9.9 Bq.g^{-1} for females and males respectively. At adult age (6 weeks to 20 weeks of offspring), ^{90}Sr content in the femurs seems to be stabilized at 72.6 ± 7.0 Bq.g^{-1} for males and 75.0 ± 2.1 Bq.g^{-1} for females. No significant difference appeared in the evolution of ^{90}Sr in the femurs between males and females (2-way ANOVA analysis, $F_{(1, 64)}$ = 0.521, n.s.) even if a punctual difference was evidenced at 12 weeks old (Student t test, p=0.035).

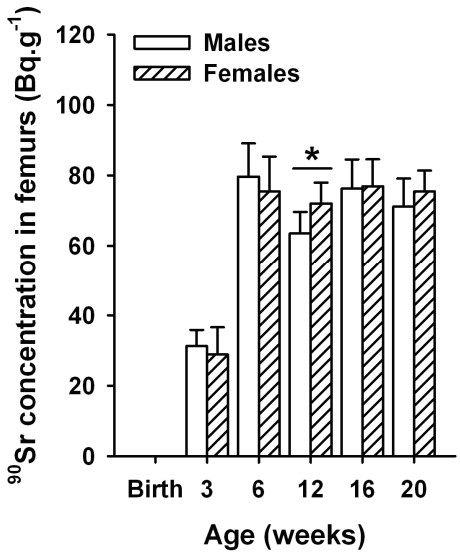

Figure 40. ^{90}Sr concentration (Bq.g^{-1}) in the femurs of ^{90}Sr ingesting animals from the juvenile model, according to the age and sex of animals. All the results are presented as mean ± SD, with n = 6 per group. Time-specific differences between males and females are significant for *: p<0.05 (Student t test).

1.3.4. ^{90}Sr concentration in the digestive tract

^{90}Sr was below the detection limit in all other organs tested (data not shown) with the exception of the digestive tract (**Fig 41**). A significant variation with age was observed (2-way ANOVA analysis, $F_{(5, 64)}$ = 17.3, p<0.001) with a peak of ^{90}Sr content at 12 weeks (3.0 ± 1.8 Bq.g^{-1} for males and 2.0 ± 1.1 Bq.g^{-1} for females) and a decrease afterwards. Again, no significant difference was found between males and females (2-way ANOVA analysis, $F_{(1, 64)}$ = 1.36, n.s.) with the exception of a punctual difference at 12 week-old (p=0.031). In order to delineate more precisely ^{90}Sr location in the digestive tract, ^{90}Sr activity was measured in different segments of the digestive tract, namely the stomach, the small intestine, the caecum and the colon. Results showed that ^{90}Sr was only detectable in the small intestine with a

maximum activity of 0.7 ± 0.3 Bq.g^{-1} both at 6 and 20 weeks and not in other segments (data not shown). Since the villi of the digestive tract are highly prominent in the small intestine, this result suggests that the ^{90}Sr retention was mainly due to a mechanical retention in the villi of the small intestine.

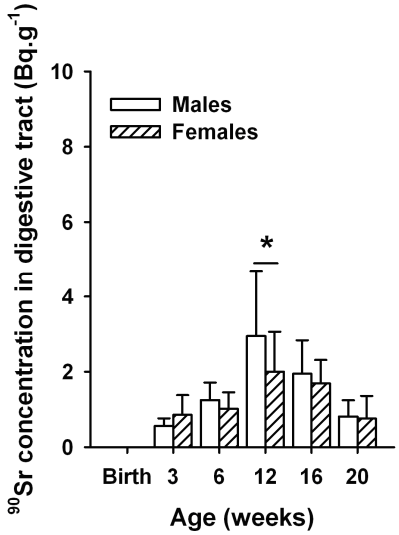

Figure 41. ^{90}Sr concentration (Bq.g^{-1}) in the digestive tract of ^{90}Sr ingesting animals from the juvenile model, according to the age and sex of animals. All the results are presented as mean ± SD, with n = 6 per group. Time-specific differences between males and females are significant for *: p<0.05 (Student t test).

1.3.5. Whole-body ^{90}Sr activity

The mean ^{90}Sr whole body activity (**Fig 42**) was calculated by dividing the sum of all ^{90}Sr activity detected in all organs by the body weight. Results show that between birth and 12 weeks of offspring, a significant increase in the mean whole body activity is seen (2-way ANOVA analysis, $F_{(5, 64)} = 72.32$, $p<0.001$). After 12 weeks of chronic ingestion, the mean whole body activity showed a slight decrease over time for both males and females, down to 4.9 ± 0.6 Bq.g^{-1} for males and 5.6 ± 0.3 Bq.g^{-1} for females at 20 weeks of age of offspring. With the exception of 6 weeks (3.6 ± 2.2 Bq.g^{-1} for males and 2.7 ± 1.6 Bq.g^{-1} for females), the mean whole body activity of females was always higher than for males with significant differences between them at 3 weeks (Student t test, p=0.043) of age of offspring.

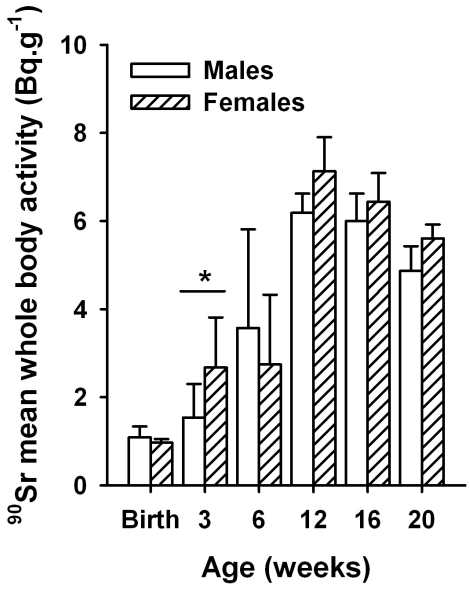

Figure 42. Mean whole body ^{90}Sr activity (Bq.g^{-1}) in ^{90}Sr ingesting animals from the juvenile model, according to age and sex of the animals. All the results are presented as mean ± SD with n = 6 animals per group. A significant evolution of whole body specific activity according to the age of animals was observed (2-way ANOVA test, $F_{(5, 64)}$ = 72.32, p<0.001) but not according to the sex of animals. Time-specific differences between males and females are significant for *: p<0.05 (Student t test).

1.3.6. ^{90}Sr accumulation at different skeletal sites

As ^{90}Sr preferentially accumulates in bones, we investigated if there is a difference in the ^{90}Sr content at the different skeletal sites. We isolated the whole skeleton from animals of 6 and 20 weeks old from the juvenile model by papain treatment. Results showed that the ^{90}Sr uptake in the skeleton depends on both gender ($F_{(1, 150)}$ = 24.4, p<0.001 at 6 weeks and $F_{(1, 120)}$ = 41.9, p<0.001 at 20 weeks) and skeleton site ($F_{(14, 150)}$ = 27.3, p<0.001 at 6 weeks and $F_{(14, 120)}$ = 3.4, p<0.001 at 20 weeks), whatever the age of test. The highest ^{90}Sr accumulation was found in teeth both in males and in females (**Fig 43**) which indeed are continuously growing in rodents, thus accumulating ^{90}Sr over ingestion duration. For other bones, the range of ^{90}Sr concentrations were between 110.7 ± 48.9 Bq.g^{-1} and 154.9 ± 16.8 Bq.g^{-1} for females and between 97.5 ± 14.2 Bq.g^{-1}and 135.5 ± 15.5 Bq.g^{-1} for males at the age of 20 weeks. These variations are in a lower range than the observed variations in humans (Kulp 1960). Overall, higher ^{90}Sr concentrations were consistently found in females as compared to males in all skeleton sites, with the exception of ulna at the age of 20 weeks. One should note that the mean ^{90}Sr concentration is higher in this set of experiments as compared to previous experiments in (**Fig 40**) for the same age. This is due to the difference in the method used to

obtain bones. In fact, bones were isolated by simple dissection and mechanically cleaned (using a scalpel) in previous experiments while in the present experiment bones were isolated by enzymatic treatment which removes completely all soft tissues, including bone marrow and cartilages. However, in both cases females showed higher ^{90}Sr concentration in bones as compared to males.

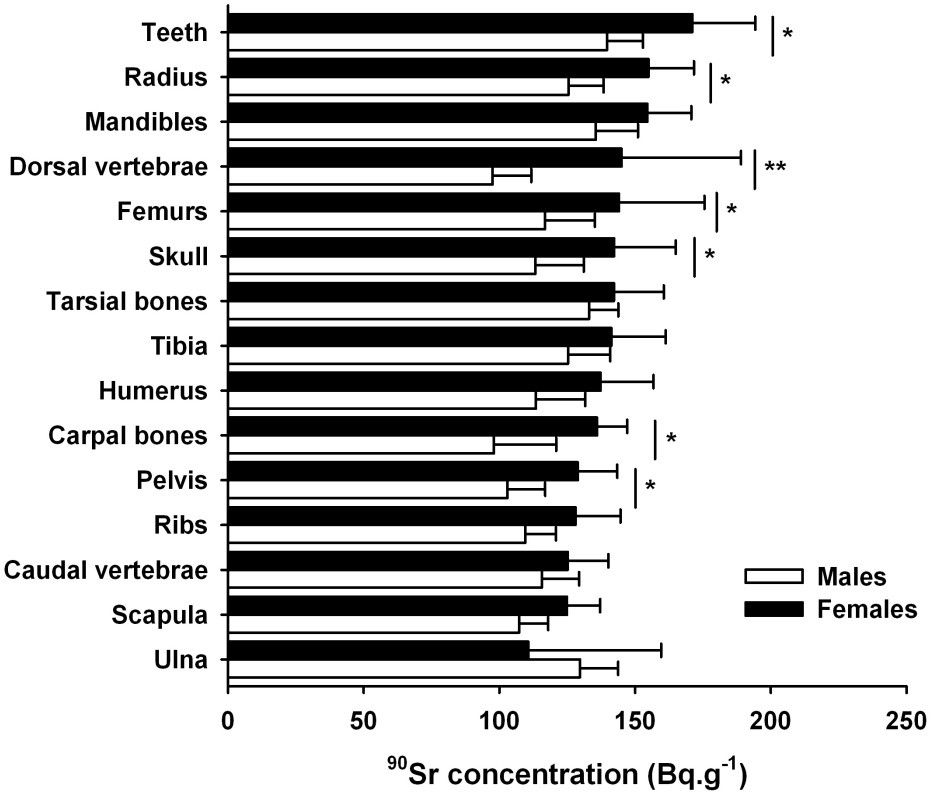

Figure 43. ^{90}Sr content (Bq.g^{-1}) at the different skeletal sites of ^{90}Sr-ingesting male (closed bars) and female (open bars) animals of 20 weeks old of the juvenile model. All the results are presented as mean ± SD of 5 animals per group. Differences between males and females are significant for *: $p<0.05$ and **: $p<0.001$ (Student t test).

1.4. Distribution of ^{90}Sr in the adult model

1.4.1. Body mass

A continuous weight gain was observed for males and females, reaching a body weight of 29.7 ± 1.5 g for control males, 30.0 ± 1.2 g for ^{90}Sr ingesting males, 24.4 ± 0.7 g for control females and 24.2 ± 1.4 g for ^{90}Sr ingesting females after 20 weeks of ingestion duration (**Fig 44**). No significant differences in weight gain between control and ^{90}Sr-ingesting animals was observed (2-way ANOVA analysis, $F_{(1, 444)} = 3.71$ for males and $F_{(1, 444)} = 3.56$ for females, n.s.).

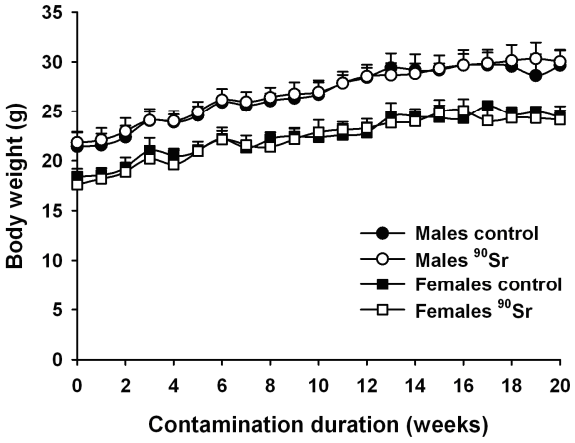

Figure 44. Evolution of the body weight (g) of control (closed symbols) and ^{90}Sr ingesting animals (open symbols) from the adult model, according to the age and sex of animals. No significant difference between control and ^{90}Sr-ingesting animals was observed (2-way ANOVA test, $F_{(1, 444)} = 3.71$, n.s. for males and $F_{(1, 444)} = 3.56$, n.s. for females). Results are presented as mean ± SD with n = 3 to 9 for control mice and n = 6 to 30 for ^{90}Sr ingesting mice.

1.4.2. Water intake and ingestion of ^{90}Sr

The mean calculated daily ingestion of ^{90}Sr per animal was 91.1 ± 16.2 Bq for males and 75.4 ± 14.3 Bq for females over the whole period of 20 weeks of ingestion with a significant higher ^{90}Sr intake by males as compared to females (2-way ANOVA analysis, $F_{(1, 416)} = 192.3$, $p<0.001$) (**Fig 45**). This was due to lower water intake by females. In fact, the mean daily water intake per animal over the whole period of 20 weeks of ingestion was 5.1 ± 1.0 ml.day^{-1} for control males, 4.6 ± 0.8 ml.day^{-1} for Sr-90 ingesting males, 4.0 ± 0.8 ml.day^{-1} for control females and 3.8 ± 0.7 ml.day^{-1} for ^{90}Sr ingesting females (data not shown). As for the juvenile model, the mean daily ^{90}Sr ingestion was lower than envisaged and was caused by an overall lower water intake than expected. One should note that ^{90}Sr intake showed important week-to-week variations, especially in the first 3 weeks of experiment. The reasons for these variations are unclear. Since these variations are linked to variation in water intake, one can propose that this is due to variations in temperature of the animal care that in turn induced variations in water intake by animals. Nevertheless, one also should note that there was no significant difference in water intake between control and ^{90}Sr ingesting animals, and that all animals showed a regular weight gain.

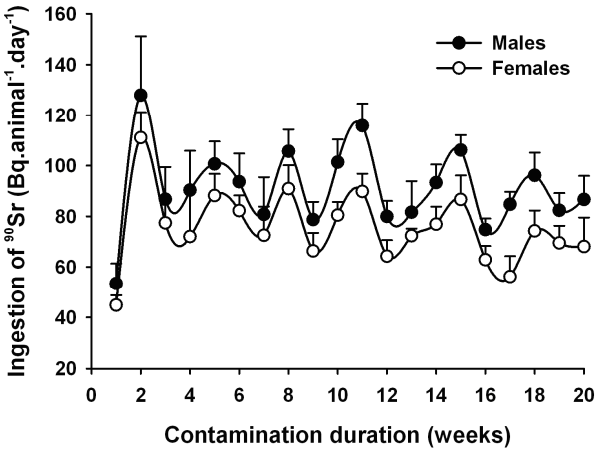

Figure 45. ^{90}Sr intake (Bq.animal^{-1}.day^{-1}) through drinking water according to the age and sex of animals from the adult model. A significant difference in ^{90}Sr intake was observed between males and females (2-way ANOVA test $F_{(1, 416)} = 192.3$, $p<0.001$). Results are presented as mean ± SD with n = 3 to 9 for control mice and n = 6 to 30 for ^{90}Sr ingesting mice.

1.4.3. ^{90}Sr concentration in femurs

A significant continuous increase of ^{90}Sr content in femurs was found (2-way ANOVA analysis, $F_{(4, 50)} = 29.6$, $p<0.001$) (**Fig 46**). At 20 weeks of chronic ingestion, this resulted in a ^{90}Sr concentration of 33.6 ± 5.2 Bq.g^{-1} for males and 39.5 ± 2.8 Bq.g^{-1} for females. 2-way ANOVA analysis did not show overall significant differences between males and females ($F_{(1, 50)} = 1.42$, n.s.), although a significantly higher accumulation was found in females after 20 weeks of ingestion as compared to males (Student t test, $p<0.05$). It has to be noted that after 20 weeks of ingestion the ^{90}Sr content in the femurs from adult animals (36.5 ± 5.1 Bq.g^{-1}) was lower than from juvenile animals (73.6 ± 6.9 Bq.g^{-1}).

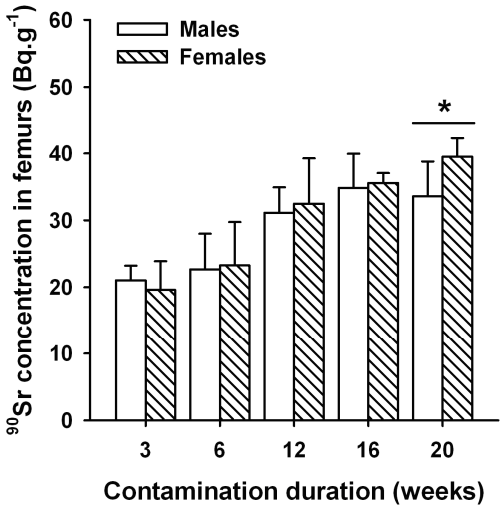

Figure 46. ^{90}Sr concentration (Bq.g^{-1}) in the femurs of contaminated animals from the adult model, according to the age and sex of animals. All the results are presented as mean ± SD with n = 6 animals per point. Time-specific differences between males and females are significant for *: p<0.05 and **: <0.001 (Student t test).

1.4.4. ^{90}Sr concentration in the digestive tract

^{90}Sr was below the detection limit in all other organs tested (data not shown) with the exception of low quantities detected in the digestive tract (**Fig 47**). The mean ^{90}Sr content over the whole 20 weeks period of ingestion duration was 0.3 ± 0.2 Bq.g^{-1} for males and 0.3 ± 0.2 Bq.g^{-1} for females. Significant variation with age was observed (2-way ANOVA analysis, $F_{(4, 50)} = 13.1$, $p<0.001$) with a peak of ^{90}Sr content at 3 weeks (0.6 ± 0.3 Bq.g^{-1} for males and 0.5 ± 0.2 Bq.g^{-1} for females). No significant difference was found between males and females (2-way ANOVA analysis, $F_{(1, 50)} = 2.84$, n.s.). In order to delineate more precisely ^{90}Sr location in the digestive tract, ^{90}Sr activity was measured in different segments of the digestive tract, namely the stomach, the small intestine, the caecum and the colon. Similarly to what was observed in the juvenile model, most of the ^{90}Sr activity was detected in the small intestine (data not shown). The lower ^{90}Sr concentrations found in the adult model as compared to the juvenile model may be due to a better cleaning of the different segments of the digestive tract.

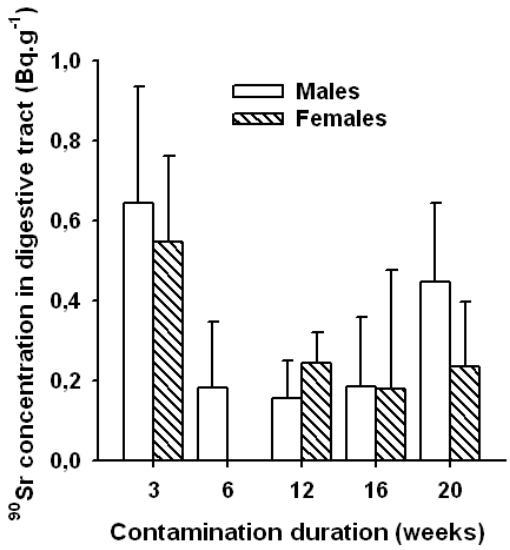

Figure 47. ^{90}Sr concentration (Bq.g^{-1}) in the digestive tract of ^{90}Sr ingesting animals from the adult model, according to the age and sex of animals. All the results are presented as mean ± SD, with n = 6 per group. No significant time-specific differences between males and females were found (Student t test).

1.4.5. Whole-body ^{90}Sr activity

The mean ^{90}Sr whole body activity (**Fig 48**) showed also a continue increase over time (2-way ANOVA analysis, $F_{(4,50)}$ = 90.85, $p<0.001$), with females having systematically and significantly a higher mean whole body activity of ^{90}Sr than males (2-way ANOVA analysis, $F_{(1, 50)}$ = 41.33, $p<0.001$). After 6 weeks of contamination duration, this increase was mainly observed for females, while in males the mean ^{90}Sr whole body activity remained stable. At 20 weeks of contamination duration, a mean content of 2.3 ± 0.4 Bq.g^{-1} for males and 3.7 ± 0.5 Bq.g^{-1} for females was found in their body (Student t test, $p<0.001$).

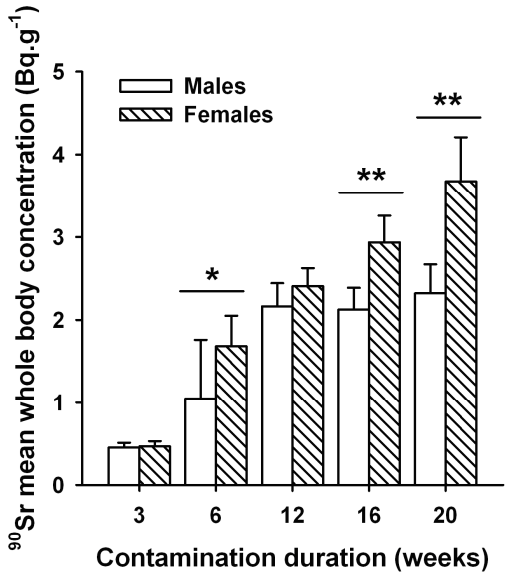

Figure 48. Mean whole body ^{90}Sr concentration (Bq.g^{-1}) of contaminated animals from the adult model, according to the age and sex of animals. All the results are presented as mean ± SD with n = 6 animals per point. Time-specific differences between males and females are significant for *: p<0.05 and **: <0.001 (Student t test).

1.5. Rate of ^{90}Sr accumulation in bones

We calculated the rate of ^{90}Sr accumulation in the bones (Bq.day^{-1}) of animals from both the juvenile and the adult model (**Fig 49**). For both models, an increase in this rate was observed during the first 12 weeks of ingestion, with significantly higher rates for the juvenile than the adult model. At 12 weeks the rate of ^{90}Sr accumulation in the bones was for males 2.5 ± 0.3 Bq.day^{-1} for the juvenile model and 0.8 ± 0.2 Bq.day^{-1} for the adult model (Student t test, p<0.001) and for females 2.6 ± 0.5 Bq.day^{-1} for the juvenile model and 0.5 ± 0.2 Bq.day^{-1} for the adult model (p<0.001). After 12 weeks of ingestion the rate of ^{90}Sr accumulation in the bones decreased for both models, even becoming negative for some time points in the juvenile model. Overall, these facts show that the accumulation of ^{90}Sr in the bones is different during bone growth in the juvenile period and bone remodelling during the adult period.

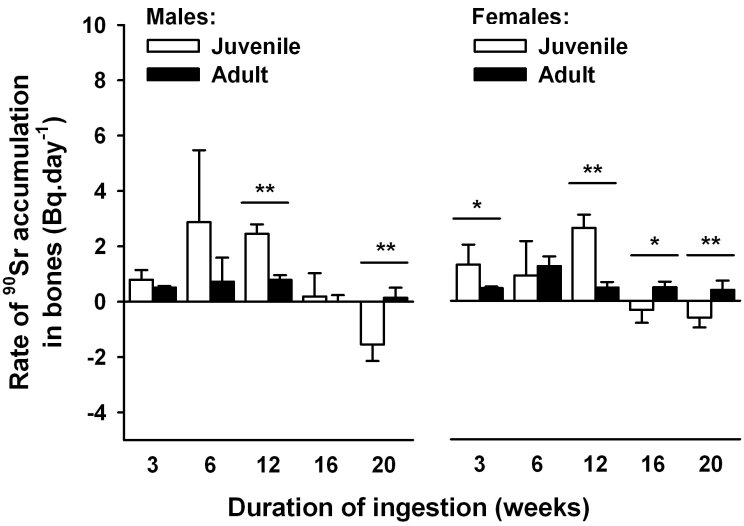

Figure 49. Rate of ^{90}Sr accumulation in the bones of ^{90}Sr-ingesting males (left panel) and females (right panel) from the juvenile (open bars) and adult (closed bars) mouse models. Results are presented as mean ± SD of 6 animals per point. Time-specific differences between juvenile and adults animals are significant for *: $p<0.05$ and **: $p<0.001$ (Student t test).

1.6. Metabolic cage experiment in the adult model

1.6.1. ^{90}Sr concentration in feces

In order to follow the elimination ^{90}Sr during chronic ingestion, animals of the adult model were housed in metabolic cages for 48 hours before euthanasia and their excreta were collected (**Fig 50**). The level of ^{90}Sr elimination through faeces was dependent upon both ingestion duration (2-way ANOVA analysis, $F_{(4, 50)} = 41.4$, $p<0.001$) and sex of animals ($F_{(1, 50)} = 7.1$, $p<0.05$), with a low level of ^{90}Sr excretion at 3 weeks of ingestion.

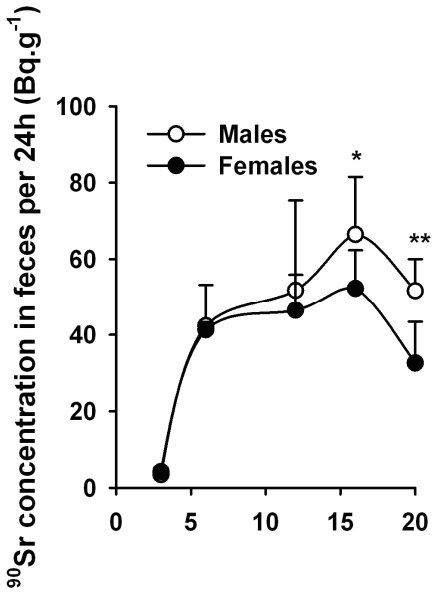

Figure 50. ^{90}Sr excretion during 24 hours in the faeces (Bq.g^{-1}) of ^{90}Sr-ingesting animals from the adult model, according to the age and sex of animals. Results are presented as mean ± SD of 6 animals. Time-specific differences between males and females are significant for *: $p<0.05$ and **: $p<0.001$ (Student t test).

1.6.2. ^{90}Sr concentration in urine

^{90}Sr excretion through urine appeared similar in both gender (2-way ANOVA analysis, $F_{(1,50)} = 4.0$, n.s.) and constant over ingestion duration (2-way ANOVA analysis, $F_{(4,50)} = 2.1$, n.s.), with mean ^{90}Sr contents of 1.1 ± 0.3 Bq.g^{-1} for males and 1.5 ± 0.3 Bq.g^{-1} for females (**Fig 51**).

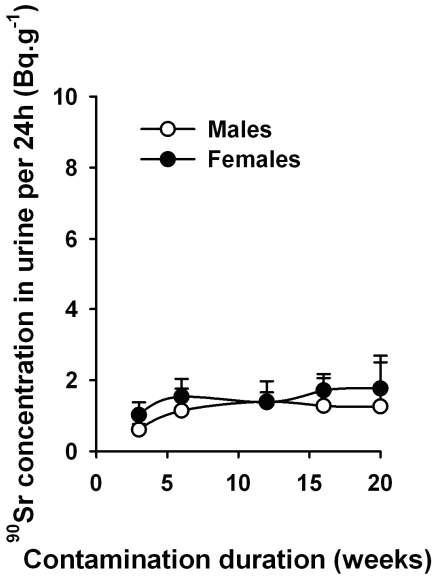

Figure 51. ^{90}Sr excretion during 24 hours in the urine (Bq.g^{-1}) of ^{90}Sr-ingesting animals from the adult model, according to the age and sex of animals. Results are presented as mean ± SD of 6 animals.

1.6.3. Daily intestinal absorption ratio

Starting from these results and the calculated daily ^{90}Sr ingestion we calculated the daily intestinal absorption ratio (IAR) as indicated in the material and methods section. This IAR takes into account both direct ^{90}Sr intestinal uptake and ^{90}Sr actively re-excreted in the intestine, as previously described both in humans and in rodents (Wiseman 1964). Results indicated that for the adult model, the IAR (**Fig 52**) varied according to both the duration of ingestion (2-way ANOVA analysis, $F_{(4, 50)} = 48.1$, $p<0.001$) and the sex of animals ($F_{(1, 50)} = 5.02$, $p<0.05$). The highest IAR was observed at 3 weeks of ingestion and decreased thereafter. This may be explained by a similar direct ^{90}Sr intestinal absorption throughout the experiment, but an increase of active ^{90}Sr re-excretion in the intestine from 6 weeks of ingestion to the end of the experiment. Moreover, gender differences may be explained by increased intestinal absorption of strontium in males, as it was previously suggested in rats and monkeys (Dahl et al. 2001).

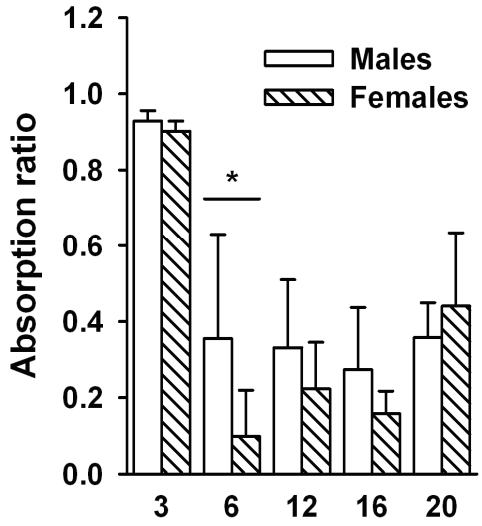

Figure 52. Daily intestinal absorption ratio (IAR) for the adult model calculated as described in the material and methods section. Results are presented as mean ± SD of 6 animals. Time-specific differences between males and females are significant for *: $p<0.05$ (Student t test).

1.7. Calculation of absorbed doses

In order to facilitate the interpretation of observed biological effects, it is of importance to know the absorbed radiation dose due to the chronic ingestion of studied radionuclides. In order to answer this question, we used the mean whole body radionuclide concentration as

previously measured and a model proposed by the ICRP publication 108 (ICRP 2008) to calculate absorbed radiation doses for environmental radiation protection purposes.

The model of the ICRP is based upon three reference plant and nine reference animals, representing most of the ecosystems (ICRP 2008). A simplified geometry was defined for each of these plants and animals. For the rat model, the geometric representation (**Fig 53**) is a solid ellipsoid of 20 cm length and 5 and 6 cm main and secondary diameters, and a mass of 314 g. For each of these organisms, dose conversion factors (DCF) from the whole organism activity concentration to the resulting dose rate were defined in $(\mu Gy.day^{-1})/(Bq.kg^{-1})$ for numerous radionuclides. Several hypotheses were made in addition to the simplified geometry of animals (ICRP 2008). Notably, the organism is considered as a medium of homogeneous density in which the radionuclide is homogeneously distributed.

We used the rat model of ICRP and corresponding DCF for ^{90}Sr, given in the material and methods section, combined with the time-dependant activity concentrations discussed above, in order to calculate absorbed radiation doses from chronic ingestion exposure through ingestion of ^{90}Sr.

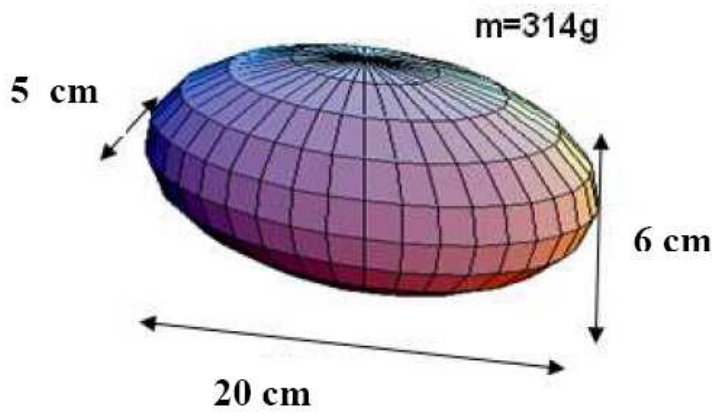

Figure 53. Geometric representation of a rat by the ICRP publication 108 (ICRP 2008).

1.7.1. Absorbed doses during foetal life

Animals are exposed during foetal life to both auto-irradiation due to internal contamination of the foetus and external irradiation due to the internal contamination of the mother. In order to take into account this external irradiation due to the mother, we used DCF corresponding to an external irradiation due to a contaminated soil surrounding the animal together with the

mean body burden of the mother. Thus, as an approximation, the mother is assimilated to a medium of homogeneous density with a homogeneous contamination, as it was previously proposed for modelling radiation doses to the embryo (ICRP 2001).

Mean body burden for the mother obtained was 10.4 ± 2.4 kBq.kg^{-1} for ^{90}Sr. Results (**Fig 54**) show that the total absorbed radiation dose at birth is 0.3 ± 0.1 mGy for animals ingesting ^{90}Sr. For comparison, mean body burden for the mother obtained in a previous study for ^{137}Cs ingestion (Bertho et al. 2010) was 13.8 ± 1.3 kBq.kg^{-1} and results (**Fig 54**) show that the total absorbed radiation dose at birth is 2.3 ± 0.2 mGy for those animals ingesting ^{137}Cs. The results show that the absorbed radiation dose due to internal contamination of the foetus is similar for both radionuclides. By contrast, the contribution to the total dose of external irradiation of the foetus due to the internal contamination of the mother is close to 85% in the case of ^{137}Cs and less than 1% in the case of ^{90}Sr. This is due to the highly penetrating γ-rays emitted by ^{137m}Ba, which was taken into account due to its short half-life (153 seconds) for the establishment of DCF for ^{137}Cs.

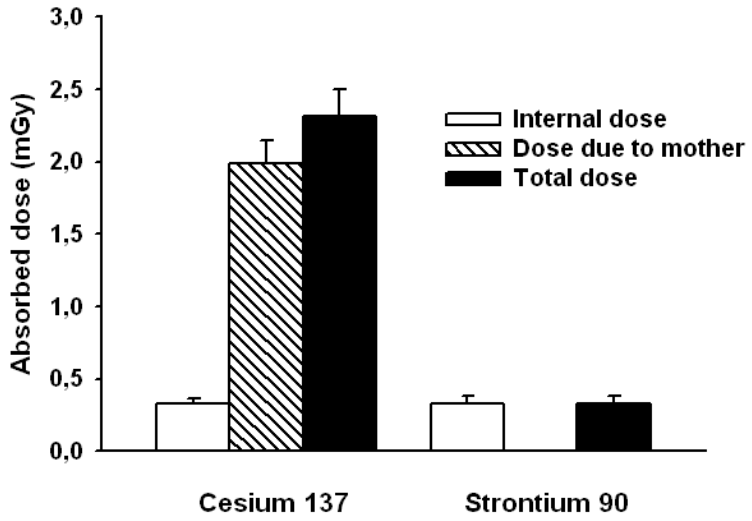

Figure 54. Absorbed doses calculated for foetal life (black bars) and distribution between external dose due to the mother (hatched bars) and dose due to internal irradiation (open bars). Results are presented as mean ± SD of 5 animals.

1.7.2. Whole-body absorbed radiation doses

As shown before, the evolution of body weight of ^{90}Sr ingesting animals of the juvenile mouse model showed a slower body weight increase in females than in males (**Fig 38** and **Fig**

55). Males were significantly heavier than females after 6 weeks and a stabilisation of body weight was observed from 16 weeks. Results show that the evolution of absorbed radiation dose (**Fig 55**) is close to linearity until 20 weeks, when the absorbed radiation dose is up to 9.7 ± 0.1 mGy in males and 10.6 ±0.1 mGy in females (Student t test, $p<0.001$). However, the absorbed radiation dose increases more rapidly in females as compared to males with significant differences appearing as soon as 3 weeks, and mainly after 12 weeks of age. This is linked to the mean ^{90}Sr body burden which increases faster in females than in males (**Fig 42**).

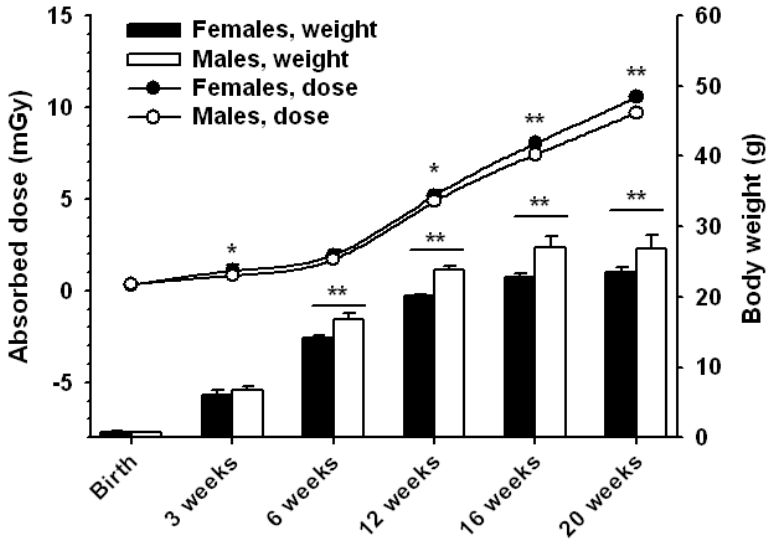

Figure 55. Mean body mass (vertical bar) and body absorbed radiation doses calculated using DCF (circles and lines) for contamination experiments through chronic ingestion of ^{90}Sr for the juvenile mouse model. Results are presented as mean ± SD of 5 animals. Differences between males (white circles and bars) and females (black circles and bars) are significant for *: $p<0.05$ and **: $p<0.001$ (Student t test).

The comparison between ^{90}Sr and ^{137}Cs (data used from Bertho et al. 2010) results for the juvenile mouse model shows that the absorbed dose increases faster in ^{90}Sr ingesting animals than in ^{137}Cs ingesting animals (**Fig 56**), although it is lower at birth. This seems to be linked to the higher energy deposition of beta rays from ^{90}Sr in body tissues as compared to the gamma rays from ^{137}Cs.

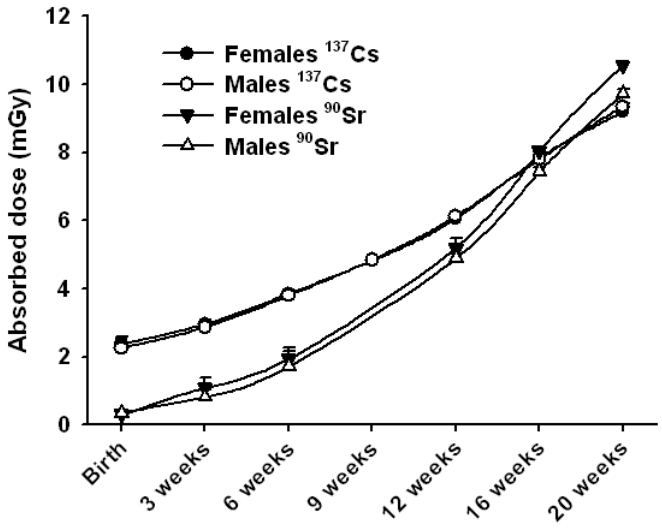

Figure 56. Comparison of body absorbed dose evolution in females (black symbols) and males (white symbols) contaminated by ^{137}Cs (circles) or by ^{90}Sr (triangles). Results are presented as mean ± SD of 5 animals.

For the adult mouse model, body weight results of ^{90}Sr ingesting animals showed an overall higher body weight for males than females (**Fig 44** and **Fig 57**). The evolution of absorbed radiation dose (**Fig 57**) is close to linearity until 20 weeks of ingestion, when the absorbed radiation dose is up to 3.8 ± 0.1 mGy in males and 4.7 ± 0.1 mGy in females (Student t test, $p<0.001$). However, the absorbed radiation dose increases more rapidly in females as compared to males with significant differences appearing at 12 weeks. This is linked to the mean ^{90}Sr body burden which increases faster in females than in males (**Fig 48**).

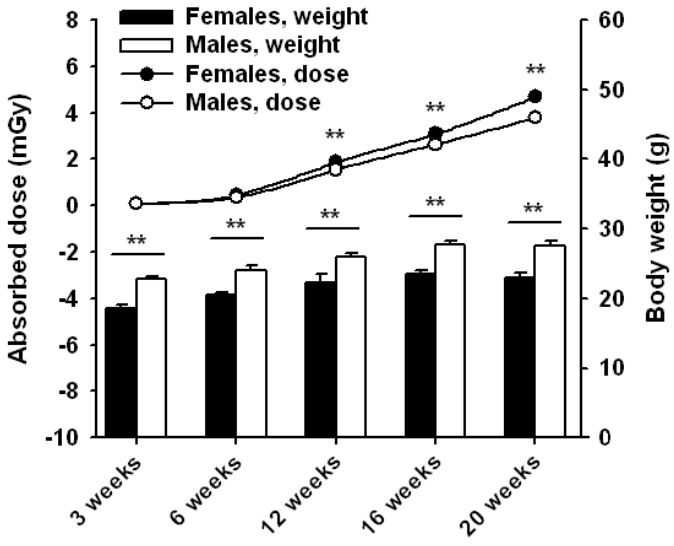

Figure 57. Mean body mass (vertical bar) and body absorbed radiation doses calculated using DCF (circles and lines) for contamination experiments through chronic ingestion of ^{90}Sr for the adult mouse model. Results are presented as mean ± SD of 5 animals. Differences between males (white circles and bars) and females (black circles and bars) are significant for *: $p<0.05$ and **: $p<0.001$ (Student t test).

1.7.3. Validation of the DCF calculation method

In order to confirm the above described dose calculations made with DCF, more sophisticated dose calculations considering cross irradiation of organs were performed by the Laboratory of Internal Dose Evaluation (LEDI, under the direction of E. Blanchardon) of IRSN. To that aim, a mouse voxel (volume x elements) phantom of Stabin et al. (Stabin et al. 2006) was used. This phantom is composed of ten segmented organs and uses specific absorbed fractions of energy (SAF) to calculate absorbed doses.

Calculated body absorbed doses were in the range from 0.3 ± 0.1 mGy at birth up to 9.7 ± 0.1 mGy at 20 weeks of ^{90}Sr ingestion in our juvenile mouse model (**Fig 58**). In order to make a direct comparison between the DCF and SAF calculation methods, the external radiation doses due to the mother during foetal life were omitted as they are negligible for ^{90}Sr (**Fig 54**). 2-way ANOVA analysis showed significant difference between the two calculation methods both for males (circles, $F_{(1,50)} = 31.3$, $p<0.001$) and for females (squares, $F_{(1,50)} = 44.0$, $p<0.001$), especially after 12 weeks of ^{90}Sr ingestion. However, one can note that the body absorbed doses were only slightly overestimated with DCF calculations as compared to SAF calculations and are in this context of absorbed radiation dose calculations insignificant.

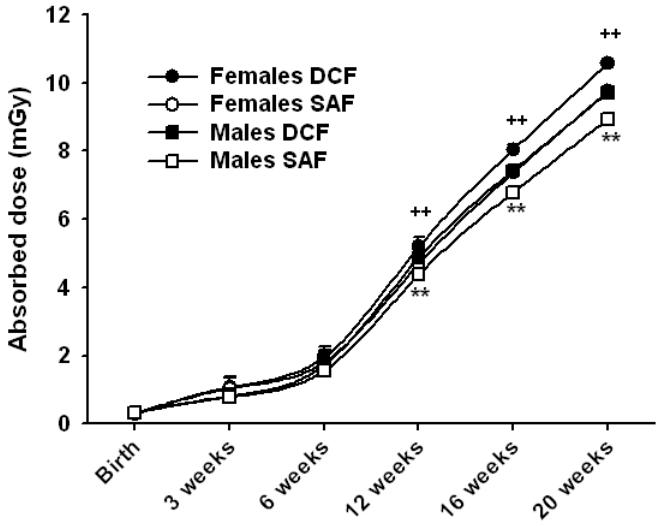

Figure 58. Comparison of two methods for calculation of body absorbed doses by animals contaminated with ^{90}Sr, using either DCF (ICRP 2008) (black symbols) or specific absorbed fractions of energy (Stabin 2006) (white symbols). Results are presented as mean ± SD of 5 animals. Differences at each time point between the two calculation methods for females are significant for *: $p<0.05$ and **: $p<0.001$ and for males for +: $p<0.05$ and ++: $p<0.001$ (Student t test).

1.7.4. Absorbed doses at the skeleton

In collaboration with our laboratory, the LEDI developed a three dimensional mouse voxel phantom to calculate by Monte Carlo simulation absorbed radiation doses for the whole body and more interesting for specific organs after contamination with different radionuclides. This mouse voxel phantom (**Fig 59**) was created from magnetic resonance imaging (MRI) segmentations.

The LEDI calculated for our juvenile mouse model that the absorbed dose is 10.2 mGy for the whole body, which confirms the whole body absorbed dose calculated by us with use of the DCF from the ICRP publication 108 as described above (ICRP 2008). More interesing, the LEDI calculated an absorbed dose of 55.0 mGy for the skeleton in our juvenile mouse model after 20 weeks of chronic ^{90}Sr ingestion.

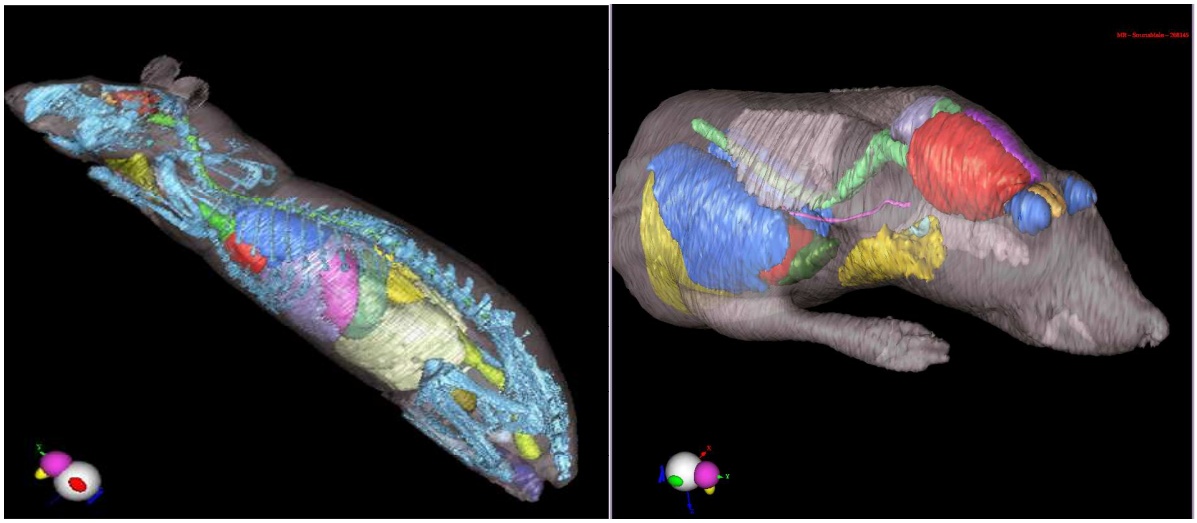

Figure 59. The three dimensional mouse voxel phantom created by the Laboratory of Internal Dose Evaluation (LEDI) from magnetic resonance imaging (MRI) segmentations in order to calculate whole body and specific organ absorbed radiation doses.

2. Effects on the bone physiology

2.1. General plasma parameters

Calcium, phosphorus and alkaline phosphatase (ALP) levels were measured in blood plasma by an automated spectrometric system in blood plasma (**Fig 60**). Time-specific significant differences between control and ^{90}Sr ingesting animals were only observed for calcium at 12 weeks for males ($p=0.021$), for phosphorus at 20 weeks for males ($p=0.020$) and for ALP at birth for males and females (both $p<0.001$) by Student t test analysis. Overall, with the exception of ALP for males (2-way ANOVA analysis, $F_{(1,90)}$, $p<0.001$), these plasma parameters in our juvenile mouse model were not affected by ^{90}Sr chronic ingestion.

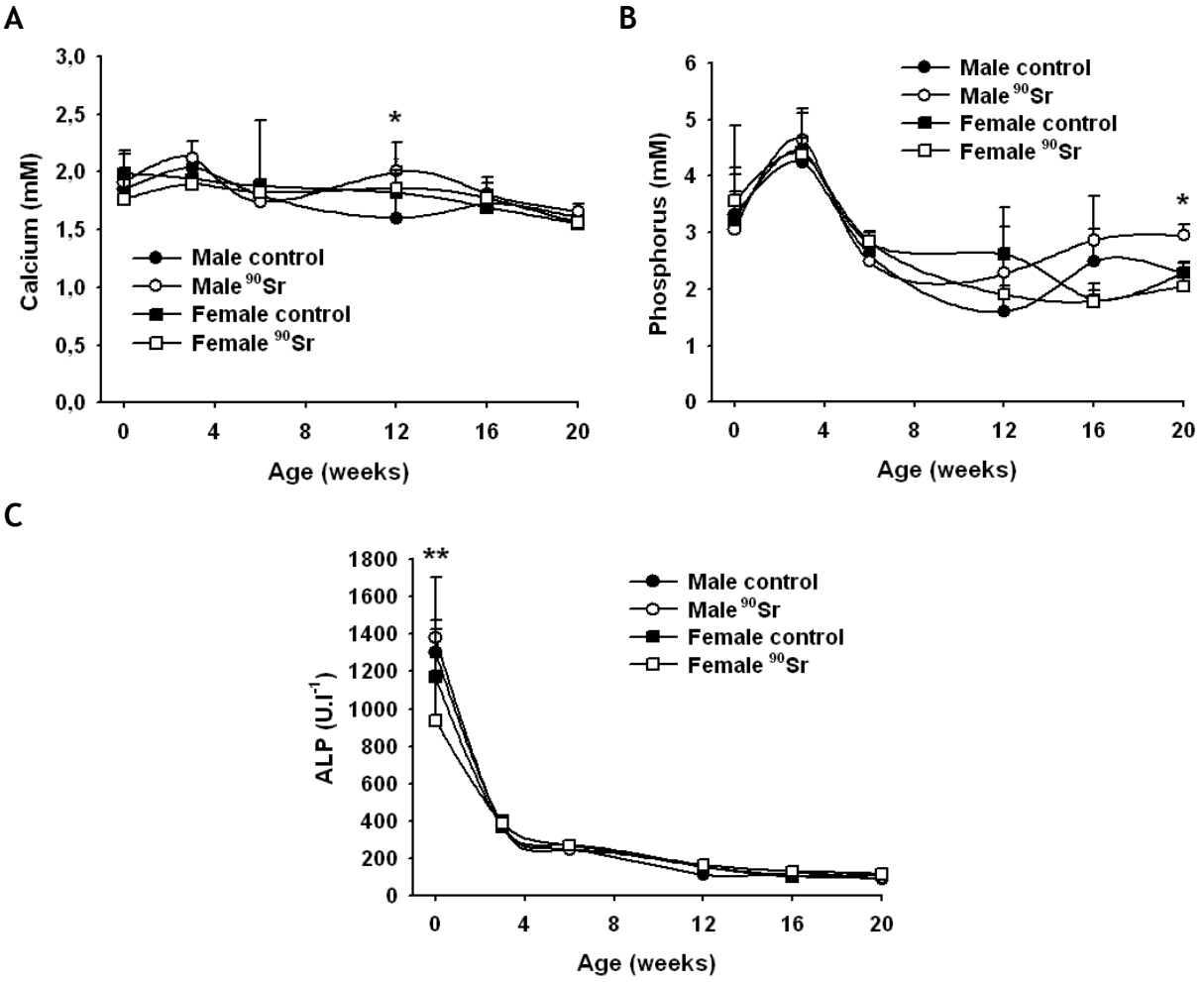

Figure 60. Calcium (mM) **(A)**, phosphorus (mM) **(B)** and alkaline phosphatase (ALP, $U.l^{-1}$) **(C)** levels in blood plasma. Results are presented as mean ± SD of 5 to 17 animals. Time-specific differences between control and ^{90}Sr ingesting males or control and ^{90}Sr ingesting females are significant for *: $p<0.05$ and **: $p<0.001$ (Student t test).

2.2. Bone specific plasma parameters

Specific plasma parameters for the bone physiology were measured by enzyme linked immunosorbant assays at 6 weeks and 20 weeks of age of animals of our juvenile mouse model (**Table 16**). We measured bone specific alkaline phosphatase (bALP), bone morphogenetic protein 2 (BMP2), osteocalcin and procollagen type 1 N-terminal propeptide (PINP) as markers for bone formation and tartrate acid phosphatase 5b (TRAP5b) and C-telopeptide of collagen (CTX) as makers for bone resorption. Moreover parathyroid hormone (PTH) and 1,25-dihydroxyvitamin D3 ($1,25(OH)_2D_3$) were measured, both having multiple roles in the bone physiology as described in the introduction section.

A significant difference for the bone resorption marker CTX was found between control and ^{90}Sr ingesting male animals at 6 weeks (Student t test, p=0.039) and at 20 weeks (Student t test, p=0.023), with ^{90}Sr ingesting males having higher levels of CTX than control males (18.6 ± 3.2 $ng.ml^{-1}$ vs. 15.8 ± 3.7 $ng.ml^{-1}$ at 6 weeks and 9.9 ± 5.8 $ng.ml^{-1}$ vs. 6.4 ± 1.6 $ng.ml^{-1}$ at 20 weeks).

Moreover, we evaluated PINP, CTX and PTH plasma levels over the whole ingestion period for the animals of the juvenile mouse model (**Fig 61**).

A significant decrease in PINP and CTX plasma levels could be observed over time (2-way ANOVA analysis, for example in males for PINP, $F_{(4,77)}$= 102.4, p<0.001 and for CTX, $F_{(4,80)}$= 33.3, p<0.001) however without an effect of contamination status (2-way ANOVA analysis, for example in males for PINP, $F_{(1,77)}$=0.003, p= n.s. and for CTX, $F_{(1,80)}$= 2.5, p= n.s.), despite the earlier mentioned time-specific significant differences at 6 and 20 weeks (Student t test, p=0.039 and p=0.023 respectively) between control and ^{90}Sr ingesting males.

For PTH, an increase in plasma levels could be observed over time (2-way ANOVA analysis, for males, $F_{(4,40)}$= 17.6, p<0.001), with significant differences for males at 12 weeks and 16 weeks (Student t test, p=0.022 and p=0.028 respectively).

Table 16.

	Males				Females			
	6 weeks		20 weeks		6 weeks		20 weeks	
	Control	^{90}Sr	Control	^{90}Sr	Control	^{90}Sr	Control	^{90}Sr
bALP (U/l)	505.1 ± 46.5	480.9 ± 106.9	408.0 ± 70.1	393.4 ± 66.3	471.1 ± 368.6	469.4 ± 91.4	368.5 ± 55.8	371.8 ± 86.8
BMP2 (pg/ml)	1073.1 ± 597.5	863.8 ± 584.8	1268.3 ± 848.7	1256.8 ± 745.9	1182.5 ± 594.8	1037.8 ± 728.7	1151.2 ± 617.9	768.9 ± 822.2
Osteocalcin (pg/ml)	1037.7 ± 193.1	1034.5 ± 139.4	1094.8 ± 223.6	982.8 ± 182.6	881.1 ± 132.3	933.8 ± 215.3	1068.4 ± 151.6	1083.8 ± 124.5
PINP (ng/ml)	26.5 ± 9.9	29.8 ± 12.4	2.2 ± 0.5	2.5 ± 0.8	13.0 ± 4.1	13.6 ± 4.0	1.8 ± 0.5	1.7 ± 0.2
PTH (pg/ml)	173.3 ± 231.5	123.4 ± 113.8	341.9 ± 200.9	522.4 ± 375.5	162.3 ± 127.8	192.5 ± 335.0	234.8 ± 274.7	281.0 ± 305.7
Vitamin D (pg/ml)	38.5 ± 7.8	37.6 ± 7.8	39.0 ± 14.2	38.0 ± 11.2	44.9 ± 18.5	47.5 ± 22.4	46.4 ± 11.6	37.9 ± 10.6
TRAP5b (U/ml)	3.2 ± 4.8	5.3 ± 11.8	6.5 ± 5.9	7.2 ± 8.3	1.7 ± 2.4	3.0 ± 5.9	5.5 ± 5.8	2.4 ± 2.3
CTX (ng/ml)	15.8 ± 3.7	18.6 ± 3.2 ***(p=0.039)**	6.4 ± 1.6	9.9 ± 5.8 ***(p=0.023)**	14.2 ± 2.9	15.6 ± 4.7	6.5 ± 1.3	6.9 ± 1.0

Table. Plasma dosages of bone markers in animals of 6 and 20 weeks old of the juvenile mouse model. bALP : bone specific alkaline phosphatase, BMP2 : bone morphogenetic protein 2, PINP : procollagen type 1 N-terminal propeptide, PTH : parathyroid hormone, TRAP5b : tartrate resistant acid phosphatase 5b, CTX : C-telopeptide of collagen. Results are presented as mean ± standard deviation (SD). Differences between control and ^{90}Sr ingesting animals of the same sex and time point are significant for *: $p<0.05$ (Student t test) and n=7-16.

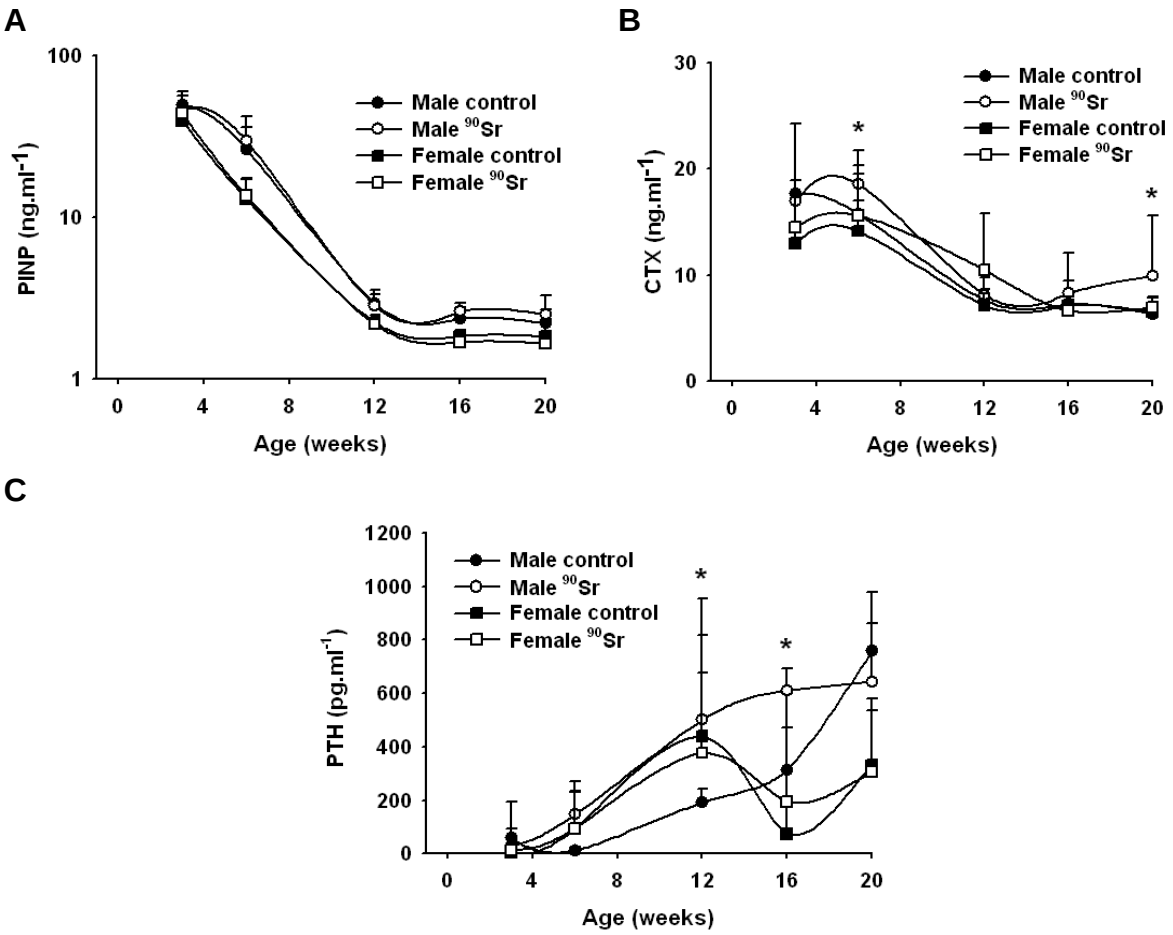

Figure 61. Bone specific plasma parameters procollagen type 1 N-terminal propeptide (PINP) (ng.ml^{-1}) **(A)**, C-telopeptide of collagen (CTX) (ng.ml^{-1}) **(B)** and parathyroid hormone (PTH) (g.ml^{-1}) **(C)** of animals of the juvenile mouse model. Results are presented as mean ± SD of 5 to 16 animals. Time-specific differences between control and ^{90}Sr ingesting males or control and ^{90}Sr ingesting females are significant for *: $p<0.05$ (Student t test).

2.3. Gene expression analysis

Gene expression analysis was performed of genes implicated in the bone formation (runt related transcription factor 2 (Runx2), ALP, bone sialoprotein (BSP), osteopontin (OPN), osteocalcin (OCN), collagen 1 and 3 and in the bone resorption (parathyroid hormone receptor (PTHr), TRAP5b, receptor activator for nuclear factor κ β ligand (RankL) at femurs of 6 and 20 weeks old control and ^{90}Sr ingesting animals of the juvenile mouse model (**Table 17**).

What concerns genes implicated in the bone formation, significant decreases in the expression of ALP (Student t test, $p=0.027$) and OCN (Student t test, $p=0.018$) were observed between

control and ^{90}Sr ingesting animals for males of 6 weeks and for females of 20 weeks of age respectively. For genes implicated in the bone resorption, a significant increase in the expression of RankL (Student t test, p=0.036) was observed for ^{90}Sr ingesting females of 20 weeks of age compared to control females of the same age.

The obtained results of this gene expression analysis are summarized in **Table 18**. At 20 weeks of chronic contamination by ^{90}Sr ingestion, the gene expression balance (at femurs) between bone formation and bone resorption seems to be modified with bone resorption in favour of bone formation.

	^{90}Sr ingesting males		**^{90}Sr ingesting females**	
	Bone formation	**Bone resorption**	**Bone formation**	**Bone resorption**
6 weeks	▼ (*ALP)	▼	-	-
20 weeks	▼	▲ / -	▼ (*OCN)	▲ (*RankL)

Table 17. Summarized table of gene expression analysis at femurs of 6 weeks and 20 weeks old ^{90}Sr ingesting males and females (results are shown for ^{90}Sr ingesting animals in comparison with control animals with same sex and age). ALP: alkaline phosphatase, OCN: osteocalcin and RankL: receptor activator for nuclear factor κ β ligand. Time-specific differences between control and ^{90}Sr ingesting males or control and ^{90}Sr ingesting females are significant for *: $p<0.05$ (Student t test).

Table 18.

		Males				Females			
		6 weeks		20 weeks		6 weeks		20 weeks	
		Control	^{90}Sr	Control	^{90}Sr	Control	^{90}Sr	Control	^{90}Sr
Bone formation	**Runx2**	1.0 ± 0.2	0.7 ±0.2	1.0 ± 0.3	0.9 ± 0.2	1.0 ± 0.2	1.0 ± 0.2	1.0 ± 0.2	0.8 ± 0.2
	ALP	1.0 ± 0.2	0.5 ± 0.1 ***(p=0.027)**	1.0 ± 0.2	0.6 ± 0.3	1.0 ± 0.3	0.8 ± 0.2	1.0 ± 0.2	0.6 ± 0.2
	BSP	1.0 ± 0.2	0.8 ± 0.3	1.0 ± 0.3	0.4 ± 0.5	1.0 ± 0.2	1.1 ± 0.2	1.0 ± 0.3	0.3 ± 0.3
	OPN	1.0 ± 0.2	0.7 ± 0.1	1.0 ± 0.3	0.7 ± 0.4	1.0 ± 0.4	0.7 ± 0.3	1.0 ± 0.3	0.3 ± 0.2
	OCN	1.0 ± 0.2	0.6 ± 0.2	1.0 ± 0.3	0.5 ± 0.4	1.0 ± 0.2	1.2 ± 0.3	1.0 ± 0.2	0.4 ± 0.1 ***(p=0.018)**
	Collagen 1	1.0 ± 0.2	0.7 ± 0.3	1.0 ± 0.3	1.1 ± 1.2	1.0 ± 0.3	1.0 ± 0.2	1.0 ± 0.3	0.6 ± 0.2
	Collagen 3	1.0 ± 0.2	0.8 ± 0.3	1.0 ± 0.3	1.0 ± 0.2	1.0 ± 0.2	1.1 ± 0.2	1.0 ± 0.3	0.5 ± 0.2
Bone resorption	**PTHr**	1.0 ± 0.2	0.5 ± 0.2	1.0 ± 0.2	0.9 ± 0.2	1.0 ± 0.2	0.9 ± 0.2	1.0 ± 0.2	0.6 ± 0.2
	TRAP5b	1.0 ± 0.2	0.6 ± 0.2	1.0 ± 0.2	1.0 ± 0.2	1.0 ± 0.4	0.6 ± 0.2	1.0 ± 0.3	0.6 ± 0.2
	RankL	1.0 ± 0.2	0.7 ± 0.3	1.0 ± 0.3	1.5 ± 0.6	1.0 ± 0.3	1.2 ± 0.2	1.0 ± 0.3	2.9 ± 1.4 ***(p=0.036)**
	OPG	1.0 ± 0.2	0.8 ± 0.4	1.0 ± 0.3	1.1 ± 0.3	1.0 ± 0.2	1.1 ± 0.3	1.0 ± 0.2	1.2 ± 0.3

Table. Expression of genes implicated in the bone formation and bone resorption in the femurs of 6 and 20 weeks old animals of the juvenile mouse model. Runx2 : runt related transcription factor 2 ALP : alkaline phosphatase, BSP : bone sialoprotein, OPN : osteopontin, OCN : osteocalcin, PTHr : parathyroid hormone receptor, TRAP5b : tartrate resistant acid phosphatase 5b, RankL : receptor activator for nuclear factor κ B ligand. Results are presented as mean ± standard error of mean (SEM). Differences between control and ^{90}Sr ingesting animals of the same sex and time point are significant for *: $p<0.05$ (Student t test) and n=10-12.

2.4. Bone histomorphometry

In this report bone histomorphometry results are presented for femurs from 20 weeks old animals of the juvenile mouse model.

Firstly we used hematoxylin eosin safran (HES) staining to evaluate the overall structure of the femur area used for further histomorphometry analysis, i.e. the distal femur end (**Fig 62**). Collagenous structures are colored in orange, cell nuclei in blue and cytoplasm in red. Cortical bone is colored in orange, as the bone matrix is mainly composed of type I collagen. The growth plate appears in dark purple as this area is made up of newly synthesized bone and chondrocytes whose nuclei are revealed in blue by HES staining. The growth plate is at the boundary between the epiphyseal and metaphyseal part of the bone. The bone marrow cells have their nucleus stained blue and their cytoplasm stained red resulting in an overall purple color of the bone marrow space.

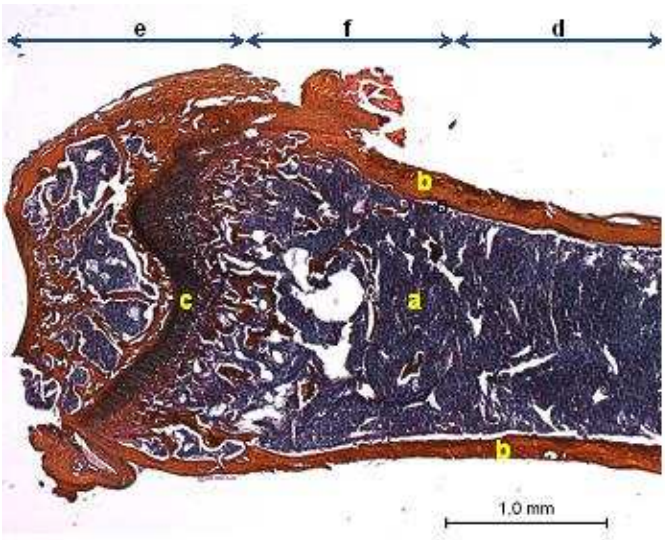

Figure 62. Longitudinal section of a femur after HES staining (2.5x). We can distinguish the bone marrow (**a**) surrounded on both sides by cortical bone (**b**) and distally by the growth plate (**c**). The diaphysis (**d**), epiphysis (**e**) and metaphysis (**f**) are also shown.

As decribed in the material and methods section, we quantified after modified trichrome Goldner staining the bone tissue volume (BV) in a total tissue volume (TV) defined in a 2 mm region from the growth plate with Histolab software (**Fig 63**). After automated analysis, orange and brown colors defined by Histolab are superimposed on the bone tissue area, while

green color is superimposed on the bone marrow area. The obtained analysed image is consistent with a HES stained femur section.

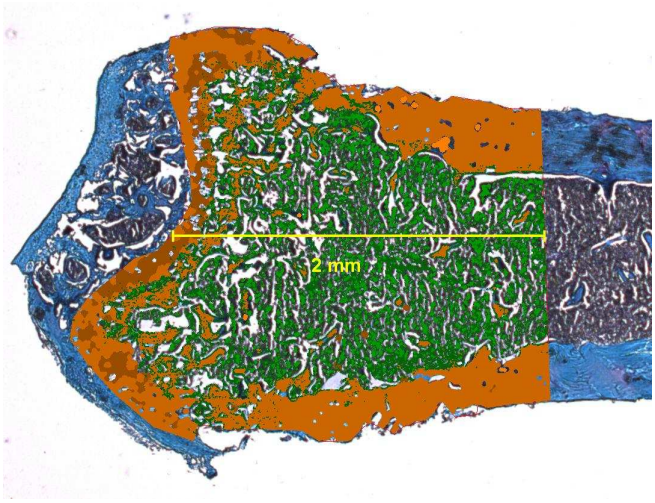

Figure 63. Longitudinal section of a femur stained with modified trichrome Goldner and analysed by Histolab software (2.5x). Bone tissue is shown in orange and brown colors, bone marrow is shown in green color.

2.4.1. Total surface analysed

To perform the histomorphometry analysis, it was necessary to ensure that the total surface (TV) analysed for each femur was the same for all groups (**Fig 64**). Overall, the average total surface analysed per animal for all four groups was 22.4 ± 1.0 mm^2 and no significant differences between the control and ^{90}Sr ingesting animals were observed (Student t test, for males p=0.328 and for females p= 0.164). As such, the study could be performed without the risk of bias in the delimitation of the area of interest.

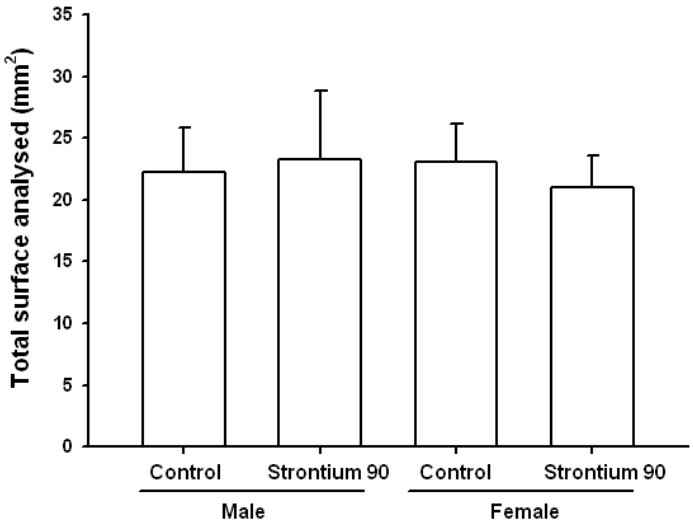

Figure 64. The average total surface (TV) analysed (mm^2) per animal for each group of 20 weeks old animals of the juvenile mouse model. After comparing the groups by Student t test analysis, no significant differences were observed ($p>0.05$). Results are presented as mean ± standard deviation (SD), with n=8.

2.4.2. Growth plate thickness

The thickness of the growth plate is expressed as the mean for all animals of each group determined from three measurements at set distances along the growth plate per slide. Overall, the average growth plate thickness per animal for all four groups was 142.6 ± 4.6 µm and no significant differences were observed between the control and ^{90}Sr ingesting animals (Student t test, for males p=0.195 and for females p=0.695) (**Fig 65**).

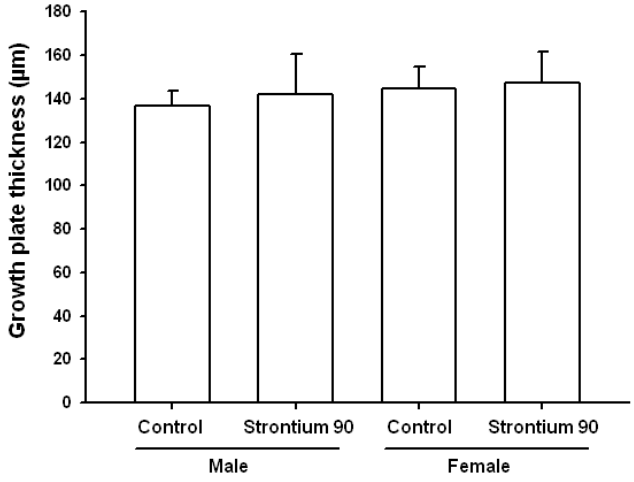

Figure 65. The average growth plate thickness (µm) per animal for each group of 20 weeks old animals of the juvenile mouse model. After comparing the groups by Student t test analysis, no significant differences were observed ($p>0.05$). Results are presented as mean ± standard deviation (SD), with n=8.

2.4.3. BV/TV ratio

No significant differences were observed between the control and ^{90}Sr ingesting animals for the bone volume to tissue volume (BV/TV) ratio (Student t test, for males p=0.803 and for females p=0.350). Overall, the average BV/TV ratio per animal for all four groups was 35.9 ± 2.0 % (**Fig 66**).

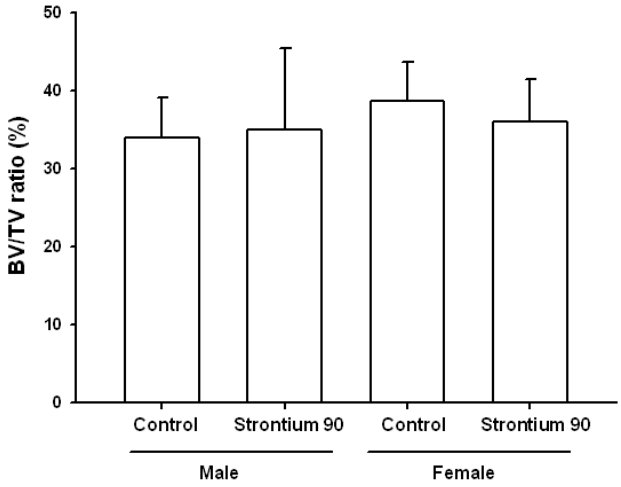

Figure 66. The average bone volume (BV) to tissue volume (TV) ratio (%) per animal for each group of 20 weeks old animals of the juvenile mouse model. After comparing the groups by Student t test analysis, no significant differences were observed (p>0.05). Results are presented as mean ± standard deviation (SD), with n=8.

3. Effects on the hematopoietic system

3.1. Blood cell count

Blood cell count was made in offspring of the juvenile mouse model, with differential for white blood cells, lymphocytes, monocytes, granulocytes, red blood cells and blood platelets. Moreover hemoglobin and hematocrit levels were measured. Overall, with the exception for white blood cells (Student t test, p=0.030) (**Fig 67**) and lymphocytes (Student t test, p=0.013) (data not shown) of males of 12 weeks old, we did not detect any significant difference between control groups and ^{90}Sr ingesting groups by 2-way ANOVA analysis (p>0.05), taking into account possible effects of age. A significant increase in red blood cell number (2-way ANOVA analysis, for males $F_{(55, 825)}$= 157.3, p<0.001 and for females $F_{(56, 993)}$= 38.5, p<0.001) and blood platelets number (2-way ANOVA analysis, for males $F_{(56, 801)}$= 6.6, p<0.001 and for females $F_{(54, 981)}$= 6.2, p<0.001) was observed with increasing age, mainly

before age of 6 weeks. This increase in both red blood cells and blood platelets corresponds to the development of the hematopoietic system during the post-natal life in the mouse.

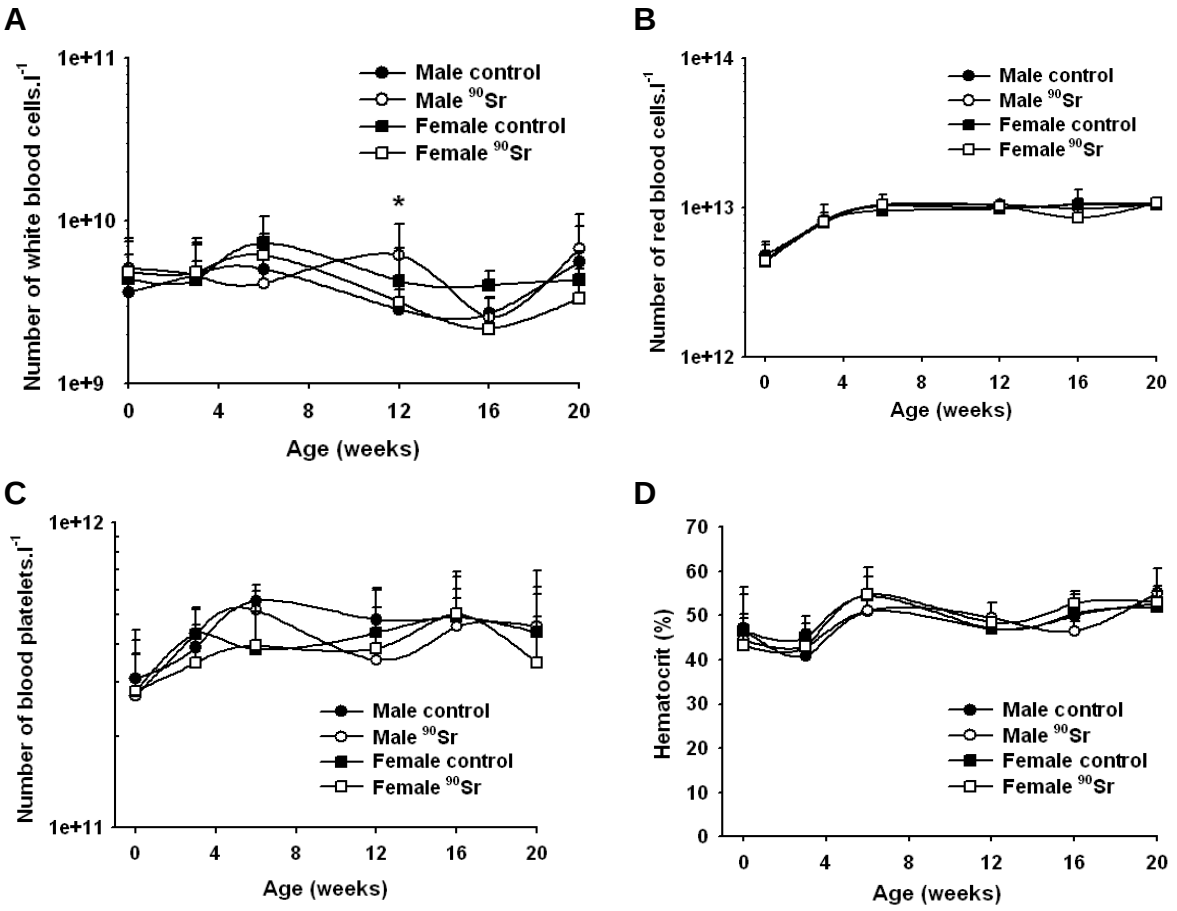

Figure 67. Evolution of the number (per liter) of white blood cells (**A**), red blood cells (**B**), blood platelets (**C**) and and hematocrit (%) level (**D**) in control and ^{90}Sr ingesting animals. All the results are presented as mean ± SD, with 5 to 14 animals per group. Time-specific differences between control and ^{90}Sr ingesting males or control and ^{90}Sr ingesting females are significant for *: $p<0.05$ (Student t test).

3.2. Flt3-ligand

We used plasma Flt3-ligand concentration as a biological indicator of bone marrow function (Prat et al. 2006). The highest concentrations were observed at birth, with a significant decrease with increasing age of the animals (2-way ANOVA analysis, for males $F_{(5,47)}= 47.3$, $p<0.001$ and for females $F_{(5,47)}= 51.1$, $p<0.001$) (**Fig 68**). For females at birth a significant difference was found in plasma Flt3-ligand concentration between control and ^{90}Sr ingesting animals (Student t test, $p<0.001$).

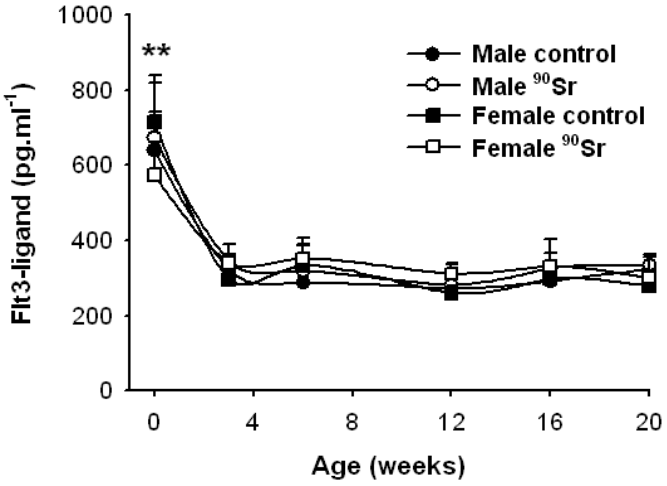

Figure 68. Evolution of Flt3-ligand concentration ($pg.ml^{-1}$) in blood plasma of animals of the juvenile mouse model. All the results are presented as mean ± SD, with 5 animals per group. Time-specific differences between control and ^{90}Sr ingesting males or control and ^{90}Sr ingesting females are significant for **: $p<0.001$ (Student t test).

3.3. Phenotypic analysis of bone marrow cells

We evaluated the hematopoietic system by phenotypic analysis of the following bone marrow cells: $Lin^-C\text{-}kit^+SCA\text{-}1^+$ early progenitors and stem cells, $CD3^+CD4^+$ and $CD3^+CD8^+$ T lymphocytes and $CD45^+CD19^+$ B lymphocytes (**Fig 69**).

For all cell populations studied, significant differences over time were observed (2-way ANOVA analysis, $p<0.001$), without influence of the contamination status of animals (2-way ANOVA analysis, $p>0.05$). Indeed, only punctual differences between control and ^{90}Sr ingesting animals were observed in the percentage of $Lin^-C\text{-}kit^+SCA\text{-}1^+$cells for males at 6 and 16 weeks (Student t test, $p=0.003$ and $p=0.012$ respectively) and for females at 16 weeks (Student t test, $p=0.041$); in $CD3^+CD4^+$ T helper lymphocytes for females at 16 weeks (Student t test, $p=0.002$); in $CD3^+CD8^+$ T cytotoxic lymphocytes for males and females at 6 weeks (Student t test, $p<0.001$ and $p=0.010$ respectively); and in $CD45^+CD19^+$ B lymphocytes for males and females at 16 weeks (Student t test, $p=0.005$ and $p=0.028$ respectively) and females at 20 weeks (Student t test, $p=0.021$).

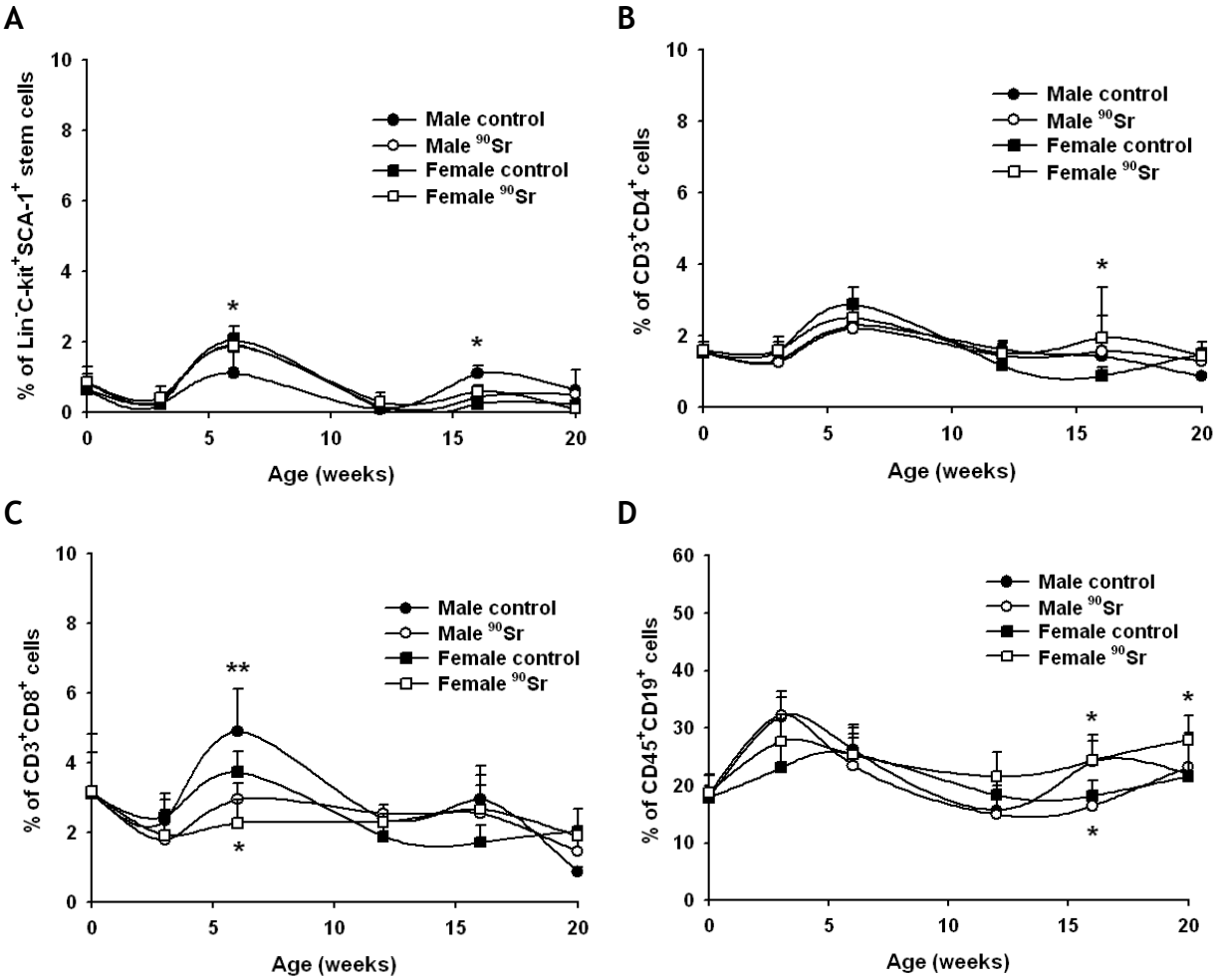

Figure 69. Phenotypical analysis of bone marrow cells of animals of the juvenile mouse model. Percent $Lin^-C\text{-}kit^+SCA\text{-}1^+$ early progenitor and stem cells (**A**), $CD3^+CD4^+$ T helper lymphocytes (**B**), $CD3^+CD8^+$ T cytotoxic lymphocyes (**C**) and $CD45^+CD19^+$ B lymphocytes (**D**). All the results are presented as mean ± SD, with 5 animals per group. Time-specific differences between control and ^{90}Sr ingesting males or control and ^{90}Sr ingesting females are significant for *: $p<0.05$ and **: $p<0.001$ (Student t test).

3.4. Colony-forming cells

As a functional test we evaluated the frequency of colony forming cells (CFCs) in the bone marrow and the spleen by a methylcellulose CFC assay. A significant difference in the number of the progenitors was observed over time (2-way ANOVA analysis, p<0,001) without influence of the contamination status of animals (2-way ANOVA analysis, p>0,05) (**Fig 70**). However, some time-specific significant differences between control and ^{90}Sr ingesting animals could be observed. For the bone marrow assays significant differences were observed for colony-forming units-granulocyte erythrocyte monocyte macrophage (CFU-GEMM) of females at birth and for males at 6 weeks (Student t test, p=0,030 and p=0,045

respectively); for CFU-granulocyte macrophage (CFU-GM) of females at 16 weeks (Student t test, p=0,007); and for burst-forming units-erythroid (BFU-E) of males at 6 weeks and females at 16 weeks (Student t test, p<0,001 and p=0,045 respectively). For the spleen assays significant differences were observed for CFU-GEMM of females at birth and at 3 weeks (Student t test, p=0,007 and p=0,033 respectively) and of males at birth (Student t test, p<0,001); and for CFU-GM of females at 12 weeks (Student t test, p=0,039).

It should be noted that the number of cells harvested from femurs and spleen of animals were not significantly different between control and ^{90}Sr ingesting animals (data not shown), indicating that the absolute number of CFCs remained unchanged in ^{90}Sr ingesting animals when compared to the control animals.

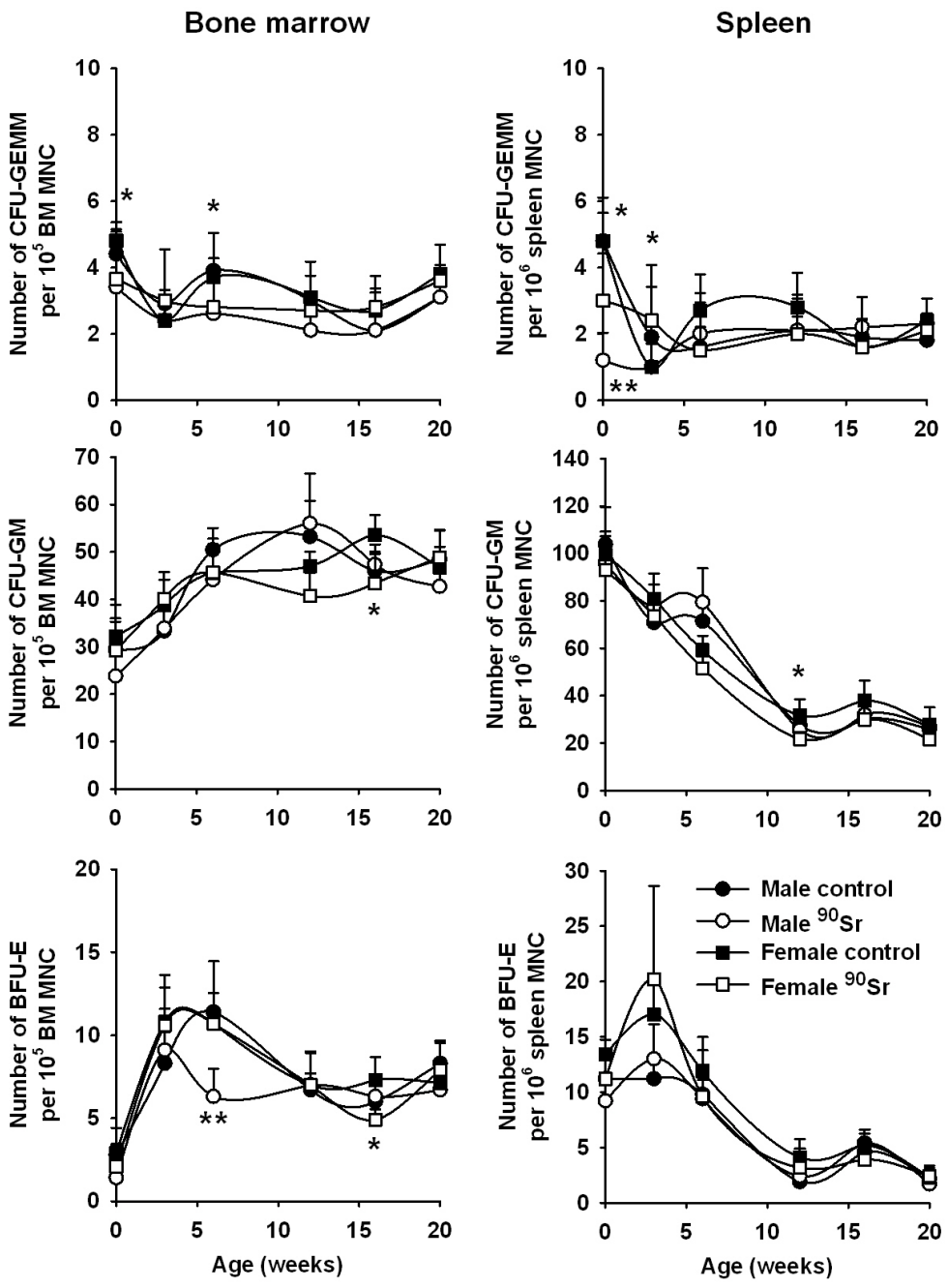

Figure 70. Colony forming cells (CFCs) in the bone marrow and spleen of animals of the juvenile mouse model. CFU-GEMM: colony-forming units-granulocyte erythrocyte monocyte macrophage; CFU-GM: colony-forming units-granulocyte macrophage and BFU-E: burst-forming units-erythroid. The number of progenitors are given for the bone marrow per 10^5 plated bone marrow cells and for the spleen per 10^6 plated spleen cells. All the results are presented as mean ± SD, with 5 animals per group. Time-specific differences between control and ^{90}Sr ingesting males or control and ^{90}Sr ingesting females are significant for *: $p<0.05$ and **: $p<0.001$ (Student t test).

4. Effects on the immune system

4.1. Steady-state immune system

4.1.1. Thymus parameters

4.1.1.1. Phenotypic analysis of thymic cells

Results showed (**Fig 71**) some time-specific significant differences between control and ^{90}Sr ingesting animals for the T lymphocyte subsets tested, i.e. $CD4^-CD8^-$ double negative thymocytes, $CD4^+CD8^+$ double positive thymocytes, $CD4^+CD8^-$ T helper lymphocytes and $CD4^-CD8^+$ T cytotoxic lymphocytes. Indeed, time-specific significant differences were observed between control and ^{90}Sr ingesting animals for $CD4^+CD8^+$ cells of males at 6 weeks and at 16 weeks (Student t test, $p=0.026$ and $p=0.002$ respectively), for $CD4^+CD8^-$ cells of males and females at 16 weeks (Student t test, both $p<0.001$) and for $CD4^-CD8^+$ cells of males at 6 weeks (Student t test, $p=0.011$). However, there was no overall significant variation according to either the ^{90}Sr ingestion status or the age of animals as demonstrated by 2-way ANOVA analysis ($p>0.05$). As a result, the $CD4^+/CD8^+$ ratio seemed not to be affected by chronic ingestion of ^{90}Sr.

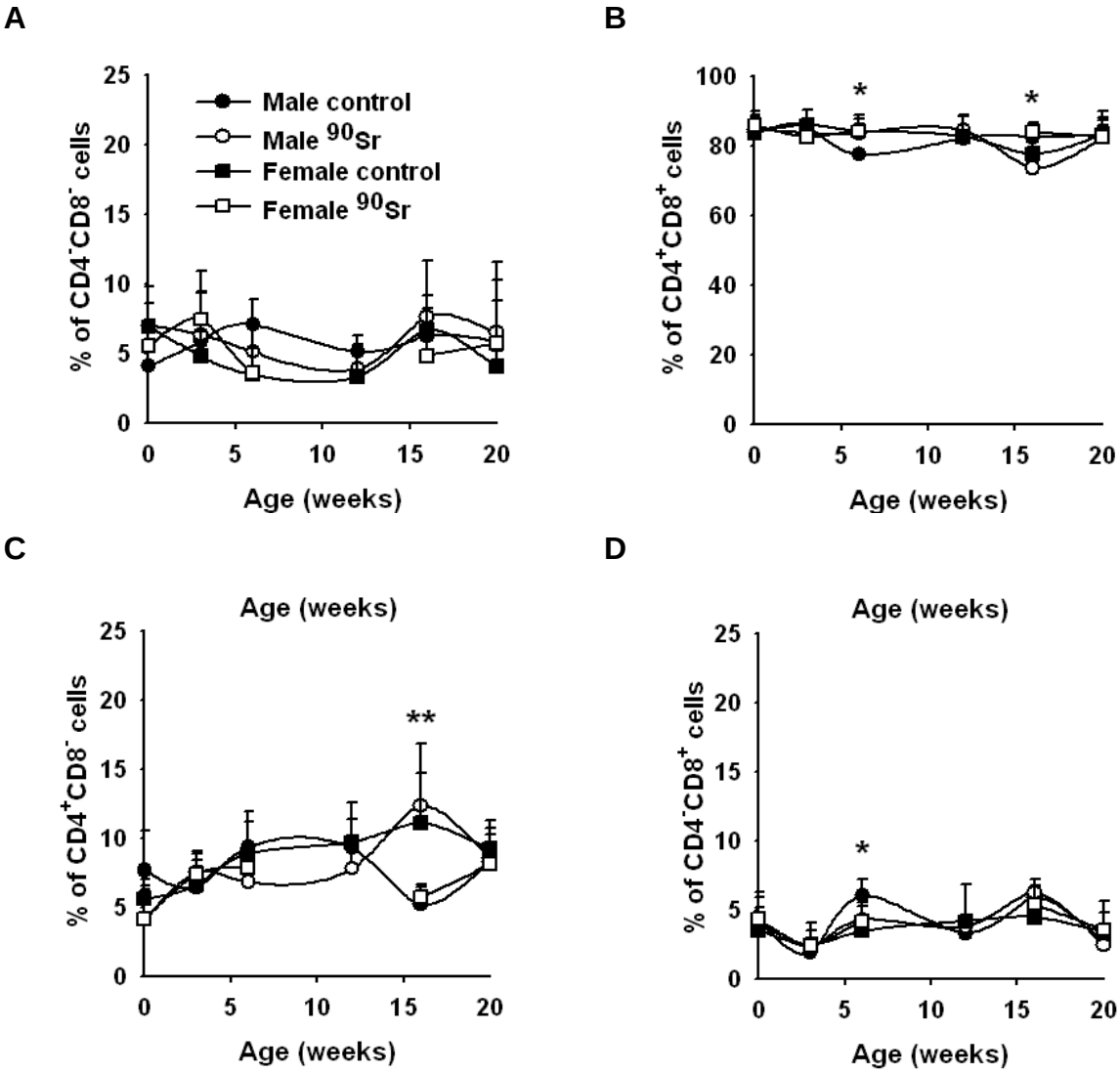

Figure 71. Phenotypical analysis of thymic cells of animals of the juvenile mouse model. Percent $CD4^-CD8^-$ double negative thymocytes (**A**), $CD4^+CD8^+$ double positive thymocytes (**B**), $CD4^+CD8^-$ T helper lymphocytes (**C**) and $CD4^-CD8^+$ T cytotoxic lymphocytes (**D**). All the results are presented as mean ± SD, with 5 animals per group. Time-specific differences between control and ^{90}Sr ingesting males or control and ^{90}Sr ingesting females are significant for *: $p<0.05$ and **: $p<0.001$ (Student t test).

4.1.1.2. TRECs

We used T cell excision circle (TREC) detection as an indicator of T cell receptor gene rearrangement, which is a central process during T lymphocyte differentiation. No significant variation of the ratio of TRECs (**Fig 72**) was observed in comparison with the reference dotted line, indicating that the frequency of TRECs was not significantly different between control and ^{90}Sr ingesting animals.

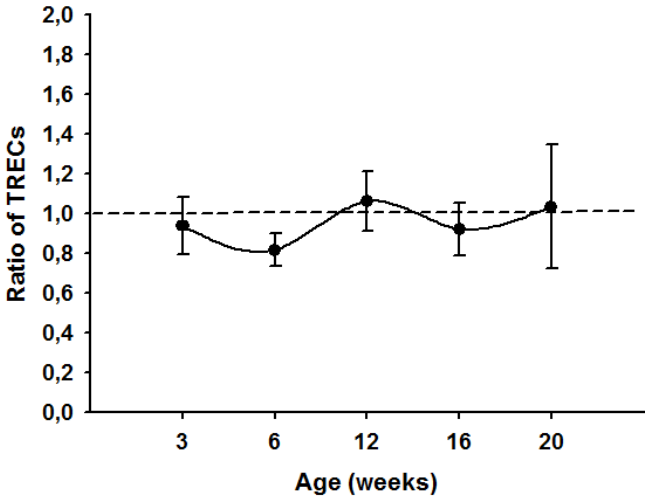

Figure 72. Ratio of T cell excision circles (TRECs) in thymic cells. All the results are presented as mean ± SD, with n= 9-10.

4.1.2.Blood parameters

4.1.2.1. Interleukin-7

Interleukin-7 (IL-7) concentration in plasma (**Fig 73**) was used as a bio-indicator of T cell homeostasis. There was a significant influence of the age of animals on IL-7 concentration (2-way ANOVA analysis, males: $F_{(5,44)} = 7.8$, $p<0.001$ and females: $F_{(5,46)} = 11.1$, $p<0.001$). No influence of the contamination status of animals was observed (2-way ANOVA analysis, $p>0.05$), with a time-specific exception at birth for males (Student t test, $p=0.002$).

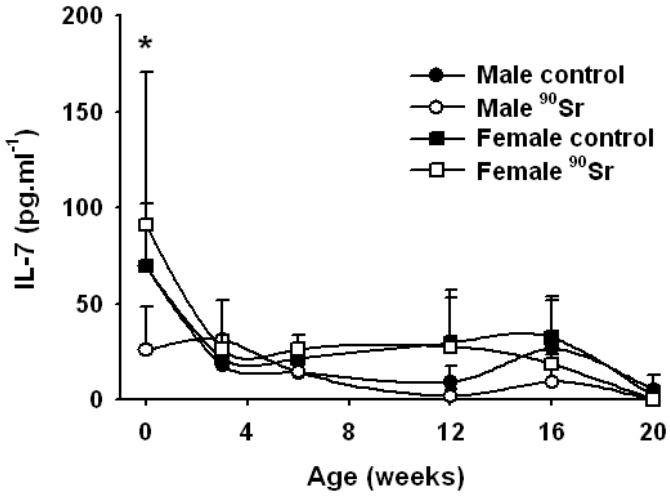

Figure 73. Evolution of IL-7 concentration ($pg.ml^{-1}$) in blood plasma of animals of the juvenile mouse model. All the results are presented as mean ± SD, with 2 to 5 animals per group. Time-specific differences between control and ^{90}Sr ingesting males or control and ^{90}Sr ingesting females are significant for *: $p<0.05$ (Student t test).

4.1.2.2. Immunoglobulins G and M

Circulating immunoglobulins G (IgG) and M (IgM) (**Fig 74**) were measured as indicators of B lymphocyte function. No significant differences between control and ^{90}Sr ingesting animals were observed, although a significant evolution of IgG and IgM levels according to the age of animals was observed by 2-way ANOVA analysis ($p<0.001$). This suggests that the main immune function of B lymphocytes, i.e. immunoglobulin production, was not affected by chronic ingestion of ^{90}Sr.

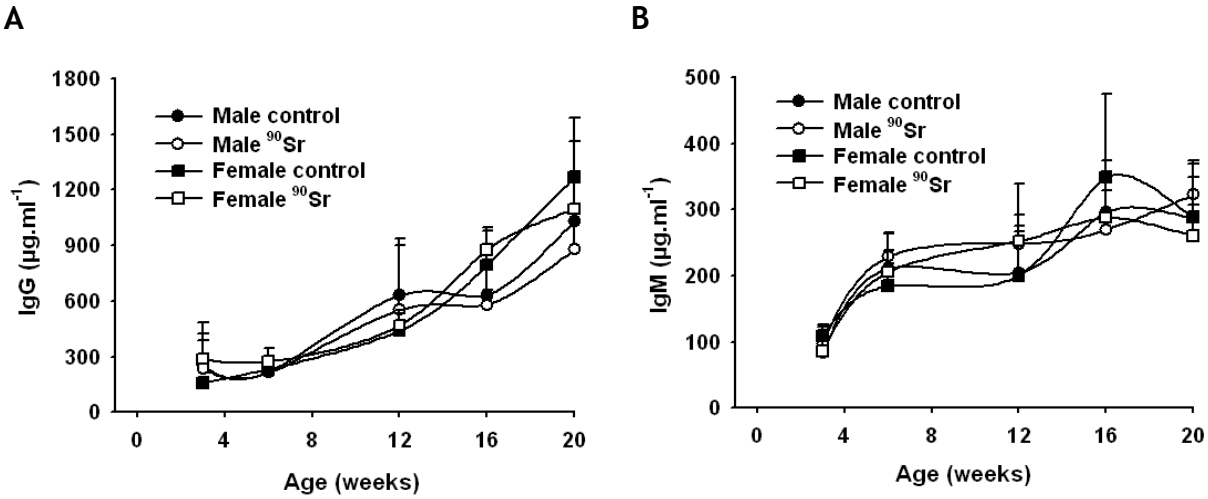

Figure 74. Immunoglobulins G (IgG) (A) and M (IgM) (B) levels ($\mu g.ml^{-1}$) in blood plasma of control and ^{90}Sr ingesting animals of the juvenile mouse model. No significant differences were observed between control and ^{90}Sr ingesting animals for the same age and sex. Results are presented as the mean ± SD of 5 animals per group.

4.1.3. Spleen parameters

4.1.3.1. Phenotypic analysis of spleen cells

Phenotypic analysis of spleen cells showed (**Fig 75**) some significant differences between control and ^{90}Sr ingesting animals for the cell populations tested, i.e. $CD3^+CD4^+$ T helper lymphocytes, $CD3^+CD8^+$ T cytotoxic lymphocytes, $CD45^+CD19^+$ B lymphocytes and $CD3^+CD4^+CD25^+$ T regulatory cells. Indeed, time-specific significant differences were observed between control and ^{90}Sr ingesting animals for $CD3^+CD4^+$ cells of females at 3 weeks (Student t test, $p=0.029$) and of males at 12 weeks and 20 weeks (Student t test, $p=0.003$ and $p=0.033$ respectively); for $CD3^+CD8^+$ cells of females at 3 weeks (Student t test, $p=0.005$) and of males at 12, 16 and 20 weeks (Student t test, $p=0.002$, $p=0.030$ and $p=0.005$ respectively); for $CD45^+CD19^+$ cells of males at 6 weeks (Student t test, $p<0.001$) and

females at 6 weeks and 12 weeks (Student t test, p=0.024 and p=0.022 respectively); and for $CD3^+CD4^+CD25^+$ cells of females at 16 weeks (Student t test, p<0.001) and males at 20 weeks (Student t test, p<0.001). However, there was no overall significant difference between control and ^{90}Sr ingesting animals for all the cell populations tested, as demonstrated by 2-way ANOVA analysis. As a result, the $CD4^+/CD8^+$ ratio seemed not to be affected by chronic ingestion of ^{90}Sr.

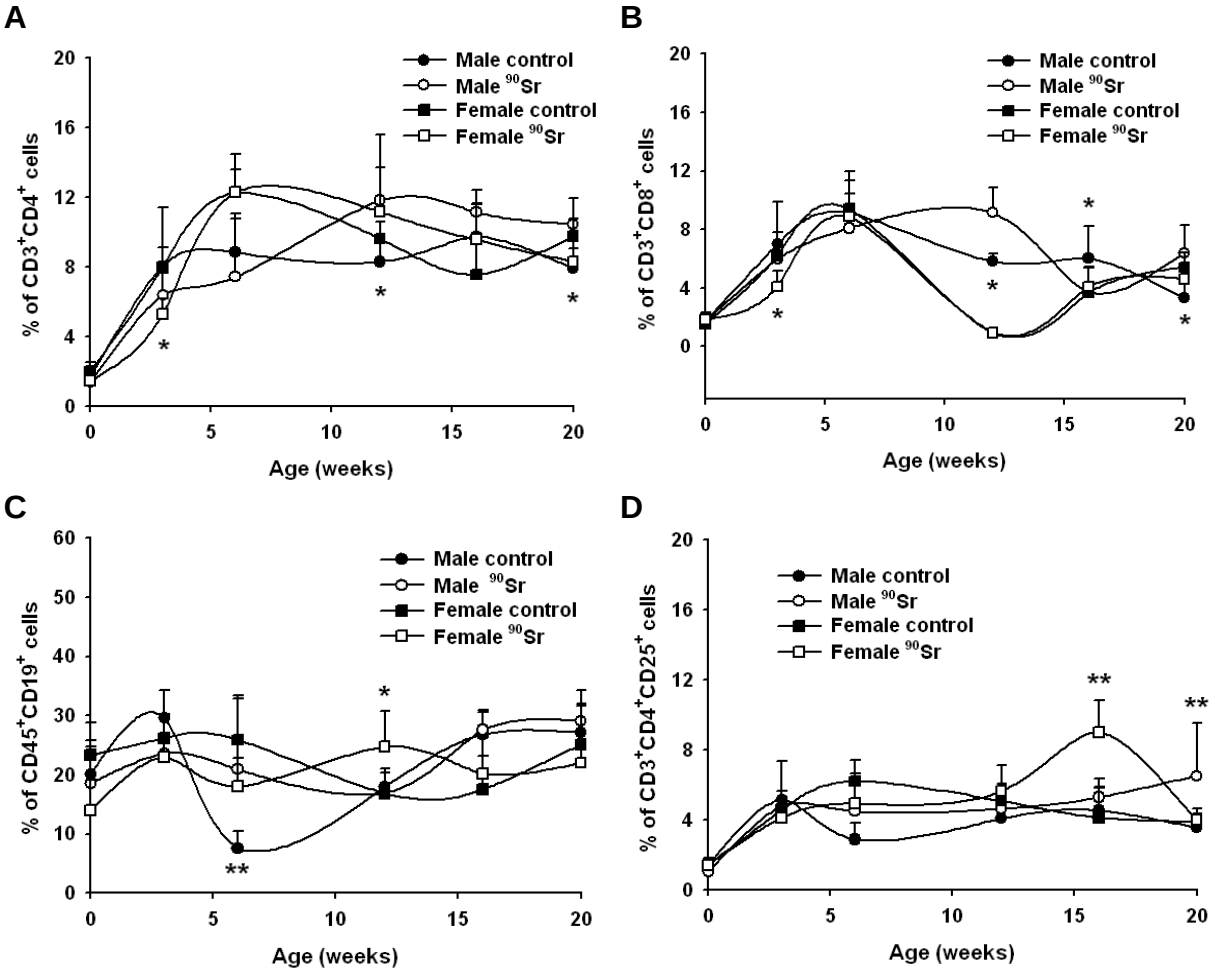

Figure 75. Phenotypical analysis of spleen cells of animals of the juvenile mouse model. Percent $CD3^+CD4^+$ T helper lymphocytes (**A**), $CD3^+CD8^+$ T cytotoxic lymphocytes (**B**), $CD45^+CD19^+$ B lymphocytes (**C**) and $CD3^+CD4^+CD25^+$ T regulatory cells (**D**). All the results are presented as mean ± SD, with 5 animals per group. Time-specific differences between control and ^{90}Sr ingesting males or control and ^{90}Sr ingesting females are significant for *: p<0.05 and **: p<0.001 (Student t test).

4.2. Immune response to KLH and TT antigens

4.2.1. Specific immunoglobulins

We used a vaccine challenge experiment as a functional test to study the immune system of our animals. Tetanus toxin (TT) and keyhole limpet hemocyanin (KLH) antigens were used, both classically used in toxicological experiments. This experiment was made with 3 week old control and ^{90}Sr ingesting animals. Two antigen injections were made, the first one at 3 weeks of age and the second one at 20 weeks of age in order to evaluate both the primary and secondary vaccine response. The concentration of IgG and IgM specific for either TT or KLH was followed for 4 weeks after each injection. Results (**Fig 76**) indicated that very low levels of specific immunoglobulins for either TT or KLH were found in placebo injected animals, either form the control group or from the ^{90}Sr ingesting group, throughout the experiment and without any significant evolution according to time (2-way ANOVA analysis, $p>0.05$). In antigen injected groups a time dependent increase in plasma concentration of specific IgG or IgM against TT or KLH was observed by 2-way ANOVA analysis ($p<0.001$). Furthermore specific time point significant differences were observed especially for IgG specific to TT between control and ^{90}Sr ingesting TT vaccinated animals (2-way ANOVA analysis $F_{(1,175)} = 12.9$, $p<0.001$).

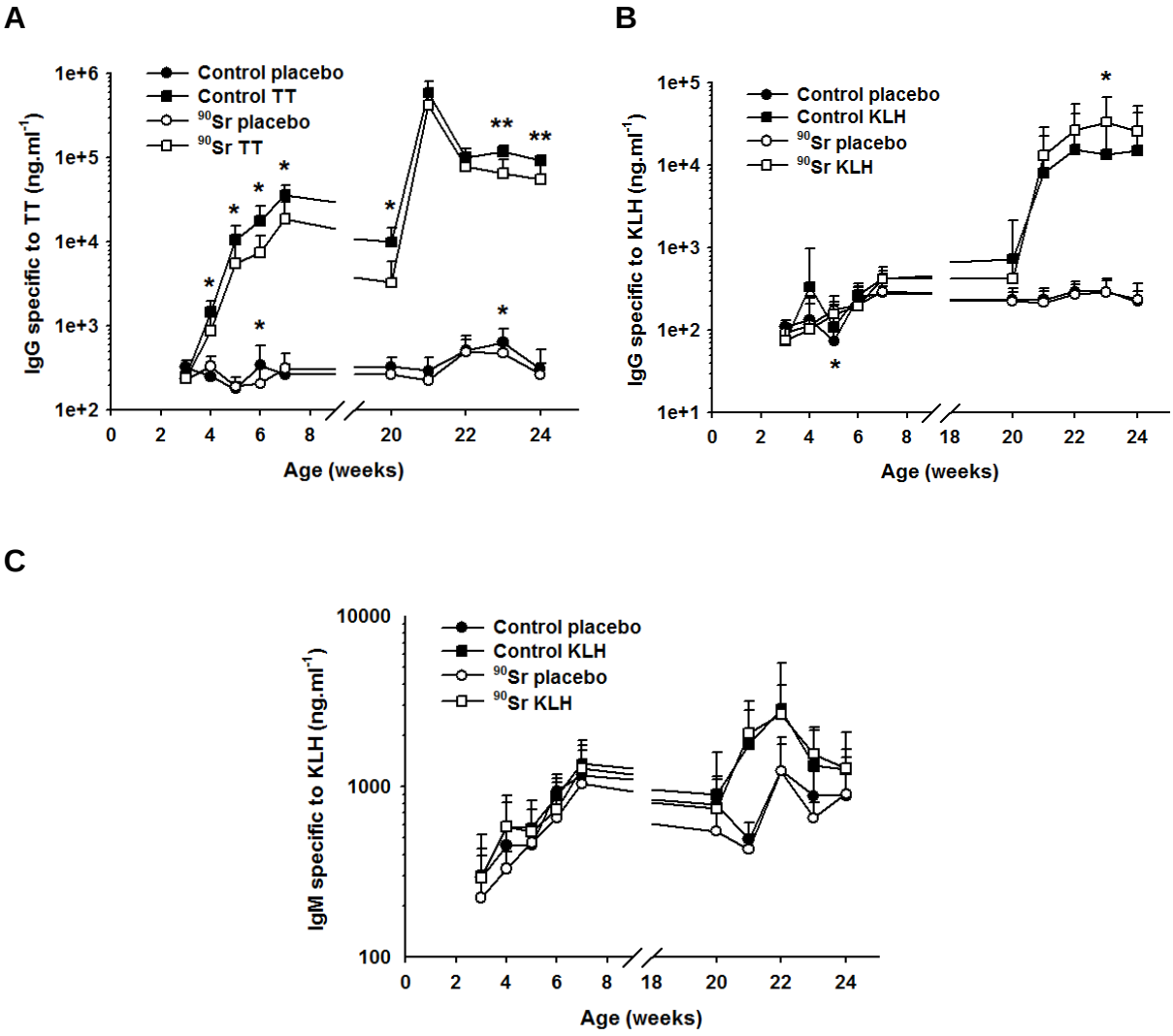

Figure 76. Specific immunoglobulin response of control and ^{90}Sr ingesting male animals injected with either tetanus toxin (TT) or keyhole limpet hemocyanin (KLH) or saline (placebo). Results were analysed separately for saline, TT or KLH injected animals using a 2-way ANOVA test. Each point is the mean ± SD from 12 animals. Time-specific significant differences are indicated for *: $p<0.05$ and **: $p<0.001$.

4.2.2.Phenotypical analysis of spleen cells

Phenotypical analysis of spleen cells (**Fig 77**) of vaccinated animals at 24 weeks was performed for the following cell populations: $CD3^+CD4^+$ T helper lymphocytes, $CD3^+CD8^+$ T cytotoxic lymphocytes, $CD4^+CD25^+$ T regulatory cells and $CD45^+CD19^+$ B lymphocytes. Significant differences were observed for $CD3^+CD4^+$ cells between control and ^{90}Sr ingesting TT vaccinated animals (Student t test, $p=0.044$) and for $CD45^+CD19^+$ cells also between control and ^{90}Sr ingesting TT vaccinated animals (Student t test, $p=0.009$).

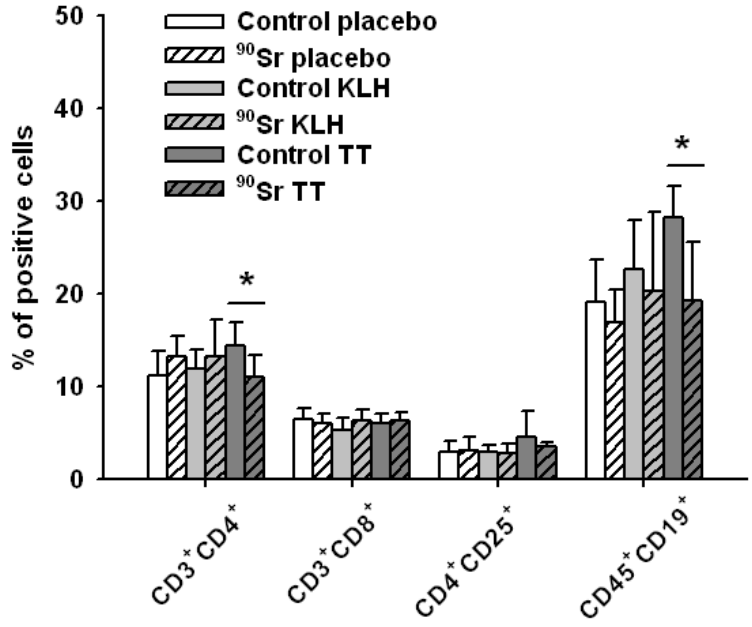

Figure 77. Phenotypical analysis of spleen cells of control and ^{90}Sr ingesting animals injected with either saline (placebo), keyhole limpet hemocyanin (KLH) or tetanus toxin (TT). Percent $CD3^+CD4^+$ T helper lymphocytes, $CD3^+CD8^+$ T cytotoxic lymphocytes, $CD4^+CD25^+$ T regulatory cells and $CD45^+CD19^+$ B lymphocytes in the spleen are given for each group. All the results are presented as mean ± SD, with 6 animals per group. Differences between groups are significant for *: $p<0.05$ (Student t test).

4.2.3. Gene expression analysis

Gene expression analysis of genes implicated in the differentiation of naive $CD4^+$ T lymphocytes towards T helper 1 cells (Th1), T helper 2 cells (Th2) or T regulatory cells (Treg) was performed at the spleen of control and ^{90}Sr ingesting animals of 24 weeks of age **(Fig 78)**. For Th1 cells we analysed the gene expression of T-box expressed in T cells (Tbet) and interferon gamma (IFNg), for Th2 cells the gene expression of Gata-binding protein 3 (Gata3) and interleukin-10 (IL-10) and for Treg cells the gene expression of Forkhead box P3 (FoxP3). For all genes we observed significant differences by Student t test analysis ($p<0.05$) between control and ^{90}Sr ingesting KLH or TT vaccinated animals, with very significant decreases in both Tbet and Gata3 gene expression for ^{90}Sr ingesting KLH and TT vaccinated animals compared to control KLH and TT vaccinated animals (Student t test, $p<0.001$).

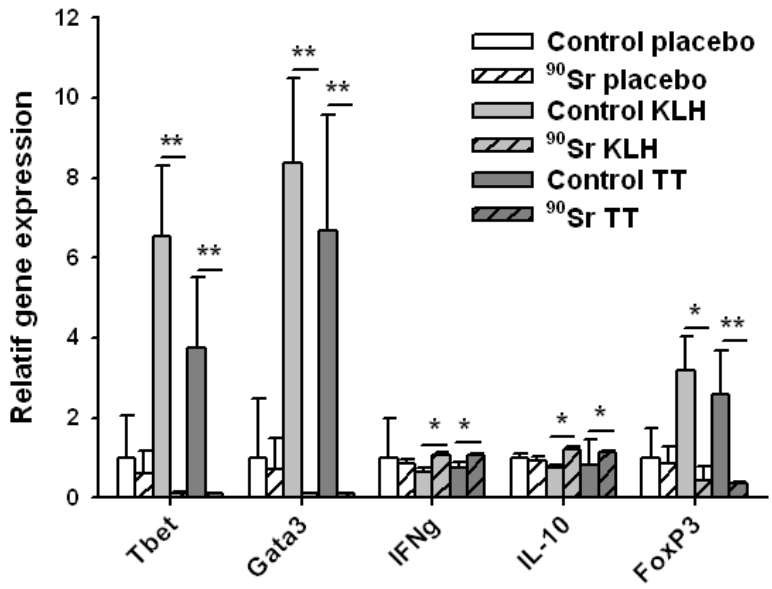

Figure 78. Expression of genes implicated in the differentiation of naive $CD4^+$ T lymphocytes towards T helper 1 cells (Th1), T helper 2 cells (Th2) or T regulatory cells (Treg) at the spleen of 24 weeks male animals injected with either saline (placebo), keyhole limpet hemocyanin (KLH) or tetanus toxin (TT). Tbet: T-box expressed in T cells, Gata3: Gata-binding protein 3, IFNg: interferon gamma, IL-10: interleukin-10, FoxP3: forkhead box P3. Expression of genes for all groups is relative to the control placebo group and GAPDH is used as reference gene. Results are presented as mean ± standard error of mean (SEM). Differences between groups are significant for *: $p<0.05$ and **:$p<0.001$ (Student t test) and n=8-11.

4.2.4.Protein expression analysis

Moreover we analysed the expression of Tbet, Gata3 and FoxP3 at the protein level in the spleen of control and ^{90}Sr ingesting animals of 24 weeks of age **(Fig 79)**. For KLH and TT vaccinated animals we found a decrease in Tbet protein levels for ^{90}Sr ingesting animals compared to control animals, although this decrease was only statistically significant for ^{90}Sr ingesting TT vaccinated animals (Student t test, $p=0.023$). On the other hand, for Gata3 and FoxP3 no significant differences were found between control and ^{90}Sr ingesting animals, whatever the vaccination status of the animals (Student t test, $p>0.05$).

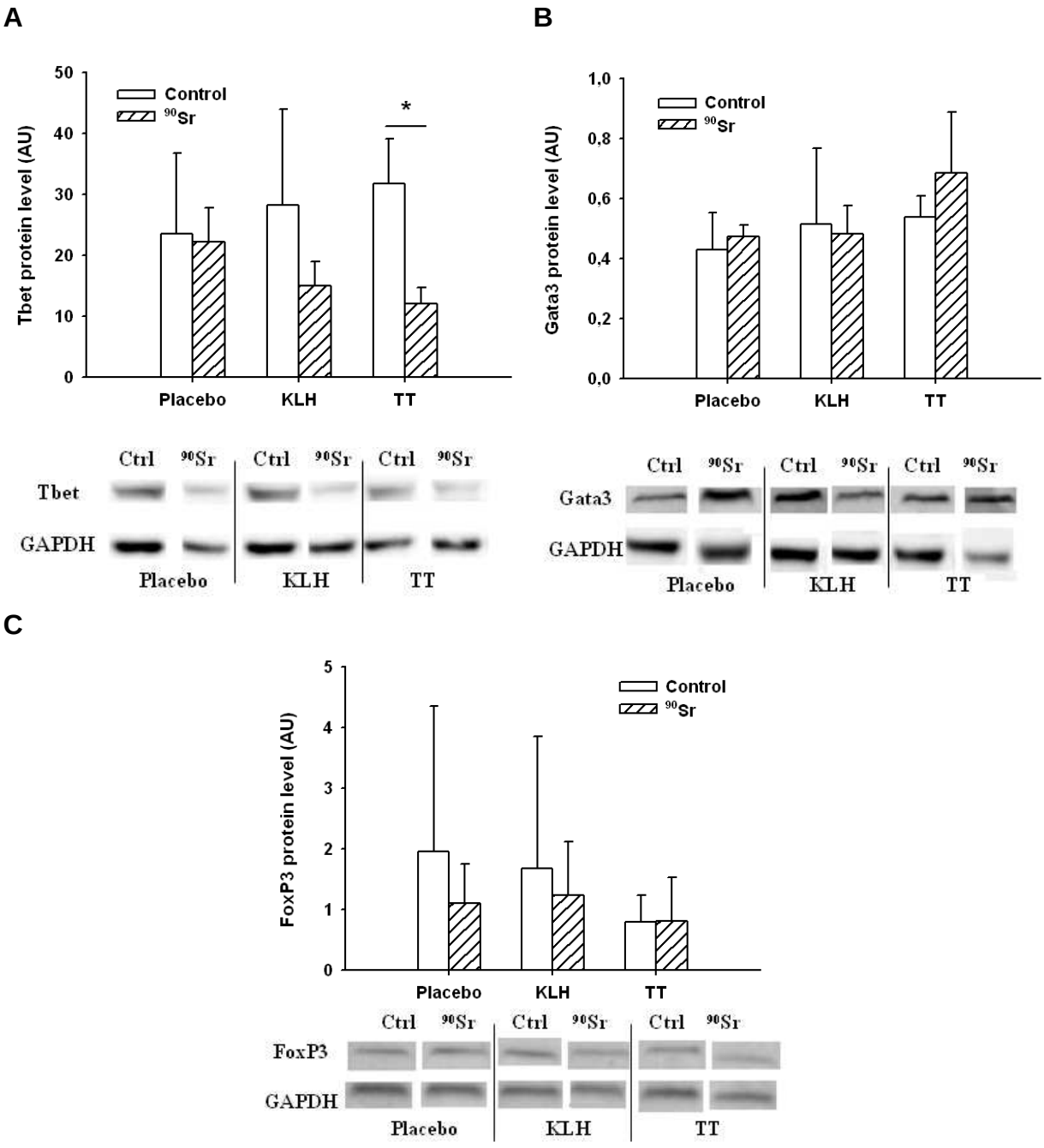

Figure 79. Protein expression levels of Tbet **(A)**, Gata3 **(B)** and FoxP3 **(C)** in the spleen of control and ^{90}Sr ingesting male animals of 24 weeks injected with either saline (placebo), keyhole limpet hemocyanin (KLH) or tetanus toxin (TT). Representative images of protein bands are shown for each group. Protein levels were normalized to the protein level of glyceraldehyde 3-phosphate dehydrogenase (GAPDH). Results are presented as mean ± SD. Differences between groups are significant for *: $p<0.05$ (Student t test) and n=5-6.

5. Cell culture models

To examine the mechanisms of action of ^{90}Sr we used the pre-osteoblastic MC3T3-E1 cell line. This cell line has been shown to be a viable model for exploring the molecular mechanisms of osteoblast proliferation, maturation and differentiation (Gal et al. 2000). It has been shown that MC3T3-E1 cultured in the presence of ascorbic acid and β-glycerophosphate display a time-dependent and sequential expression of osteoblast characteristics analogous to the bone formation process in vivo. The cells actively replicate, express alkaline phosphatase (ALP) activity and synthetize a collagenous extracellular matrix which progressively undergoes mineralization (Barbara et al. 2004; Quarles et al. 1992).

5.1. Differentiation potential

To validate the previous mentioned studies we investigated the differentiation potential of pre-osteoblastic MC3T3-E1 clone 4 cells in the presence of ascorbic acid (AA) and β-glycerophosphate (BglyP). Moreover we investigated the effects of non-radioactive $^{88}SrCl_2$ on bone matrix mineralization, collagen synthesis and alkaline phosphatase activity.

5.1.1. Bone matrix mineralization

We examined by Von Kossa staining bone matrix mineralization of MC3T3-E1 clone 4 cells treated with cell culture medium alone (control), medium supplemented with 10 mM $^{88}SrCl_2$ or medium supplemented with AA + BglyP during 7, 10 and 14 days (**Fig 80**). A significant increase over time in bone matrix mineralization was only observed for MC3T3-E1 clone 4 cells treated with AA + BglyP.

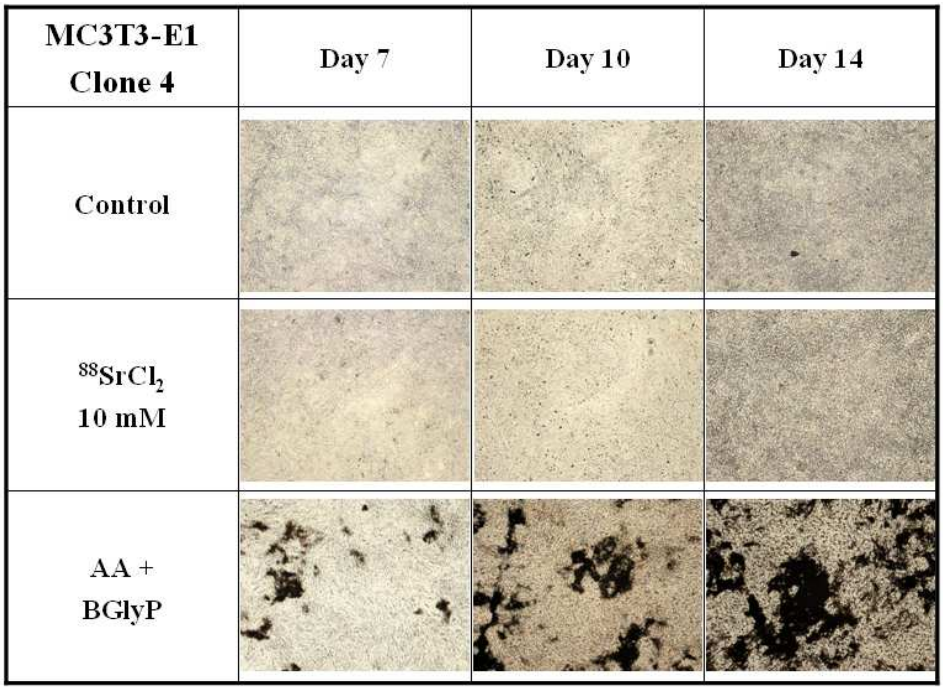

Figure 80. Representative images (10x) of Von Kossa staining of MC3T3-E1 clone 4 cell cultures after 7, 10 and 14 days of treatment with cell culture medium alone (control), medium supplemented with 10 mM $^{88}SrCl_2$ or 50µg/ml acid ascorbic (AA) + 10 mM β-glycerophosphate (BglyP).

Bone matrix mineralization was also examined by Alizarin Red S staining (**Fig 81**). An increase in mineralization was again only observed for MC3T3-E1 clone 4 cells treated with AA + BglyP. The presence of $^{88}SrCl_2$ in cell culture medium at the concentration of 10 mM didn't seem to affect bone mineralization in our experiments.

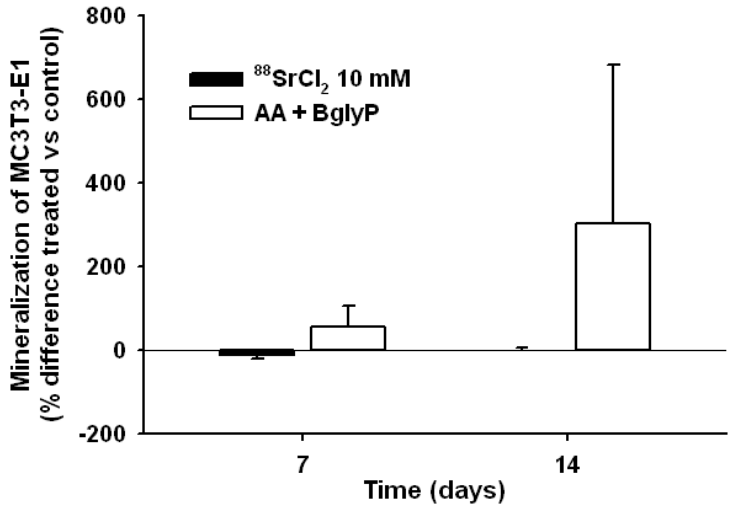

Figure 81. Mineralization (% difference treated vs control) of MC3T3-E1 clone 4 cell cultures after 7 and 14 days of treatment with cell culture medium supplemented with 10 mM $^{88}SrCl_2$ or 50µg/ml acid ascorbic (AA) + 10 mM β-glycerophosphate (BglyP). Results are presented as mean ± SD of 2 independent experiments.

5.1.2. Collagen synthesis

Collagen synthesis was examined by Sirius Red staining (**Fig 82**). The presence of 10 mM $^{88}SrCl_2$ in cell culture medium didn't stimulate collagen synthesis by MC3T3-E1 clone 4 cells. However collagen synthesis was increased for all other conditions tested, i.e. cell culture medium supplemented with AA, AA + 10 mM $^{88}SrCl_2$ or AA + BglyP.

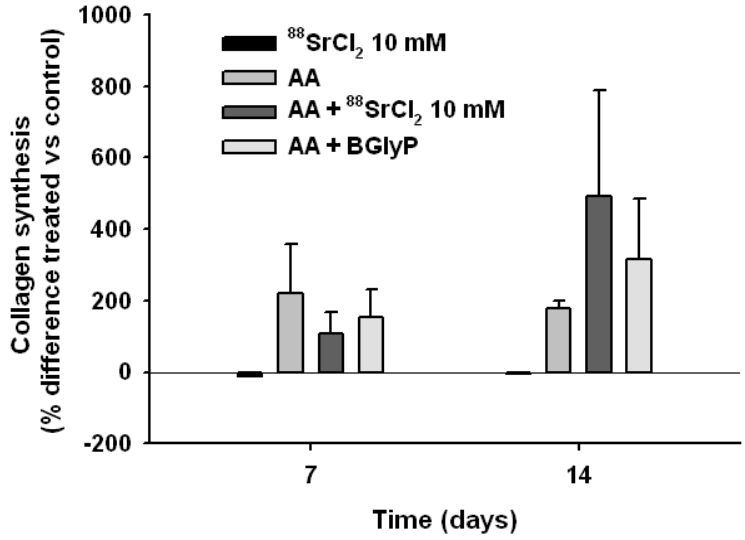

Figure 82. Collagen synthesis (% difference treated vs control) of MC3T3-E1 clone 4 cell cultures after 7 and 14 days of treatment with cell culture medium supplemented with 10 mM $^{88}SrCl_2$, 50µg/ml acid ascorbic (AA), 50µg/ml AA + 10 mM $^{88}SrCl_2$ or 50µg/ml AA + 10 mM β-glycerophosphate (BglyP). Results are presented as mean ± SD of 4 independent experiments.

5.1.3. Alkaline phosphatase activity

We examined alkaline phosphatase (ALP) activity between 3 and 21 days of MC3T3-E1 clone 4 cells in the presence of 10 mM $^{88}SrCl_2$ in cell culture medium (supplemented with AA + Bglyp) (**Fig 83**). A significant increase in ALP activity was observed between 3 and 10 days and declined slightly afterwards. However, no significant difference was observed in ALP activity of the cells contaminated with $^{88}SrCl_2$ and supplemented cell culture medium alone in this experiment.

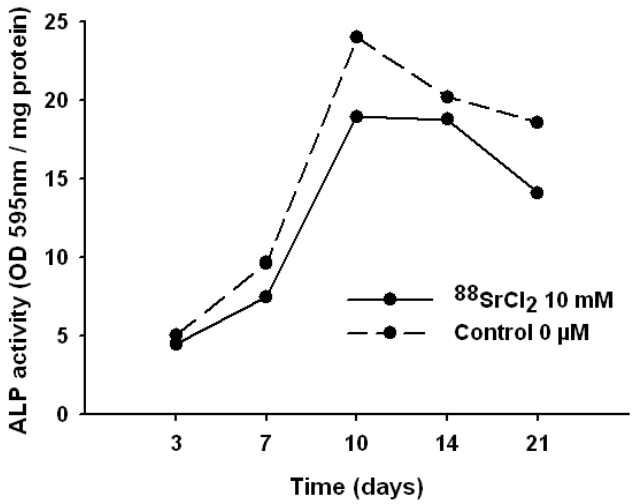

Figure 83. Effect of 10 mM $^{88}SrCl_2$ on alkaline phosphatase (ALP) activity (OD at 595nm / mg protein) by MC3T3-E1 clone 4 cells at 3, 7, 10, 14 and 21 days of treatment. Results are presented of 1 experiment.

5.2. Cell mortality and viability

Our results of bone matrix mineralization, collagen synthesis and alkaline phosphatase activity tests confirmed that MC3T3-E1 cells cultured in the presence of AA and BglyP display a time-dependent and sequential expression of osteoblast characteristics analogous to the bone formation process in vivo. However, $^{88}SrCl_2$ in cell culture medium at a concentration of 10 mM didn't have any influence on the differentiation potential of this cell line.

In a next step we investigated if ^{90}Sr has an influence on the cell mortality (**Fig 84**) and cell viability (**Fig 85**) of the MC3T3-E1 clone 4 cells. We used different concentrations of ^{90}Sr (from 3.125 $kBq.ml^{-1}$ to 100 $kBq.ml^{-1}$) in cell culture medium but didn't observe any significant modification on the mortality and viability of MC3T3-E1 clone 4 cells in the presence of ^{90}Sr.

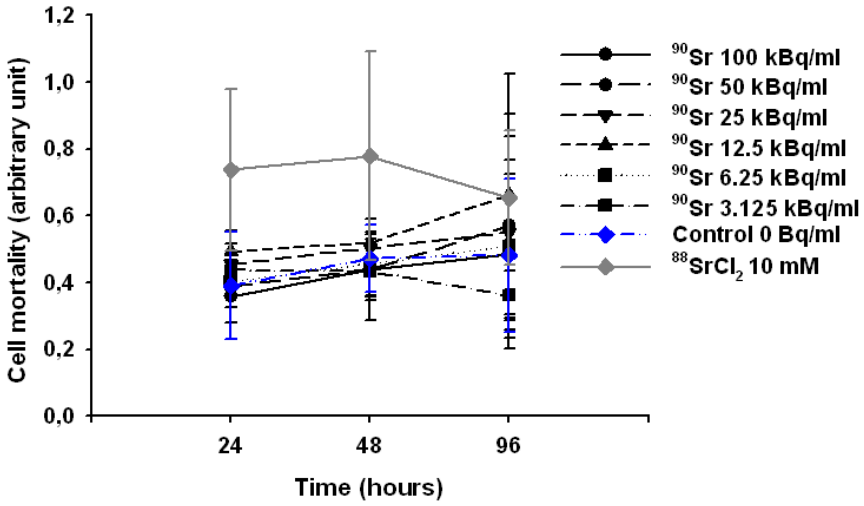

Figure 84. Effect of different concentrations of ^{90}Sr (3.125 kBq/ml up to 100 kBq/ml) and 10 mM $^{88}SrCl_2$ on the cell mortality (measured by the release of lactate dehydrogenase (LDH)) of MC3T3-E1 clone 4 cells after 24, 48 and 96 hours treatment with ^{90}Sr or $^{88}SrCl_2$. Results are presented as mean ± SD of 4 independent experiments.

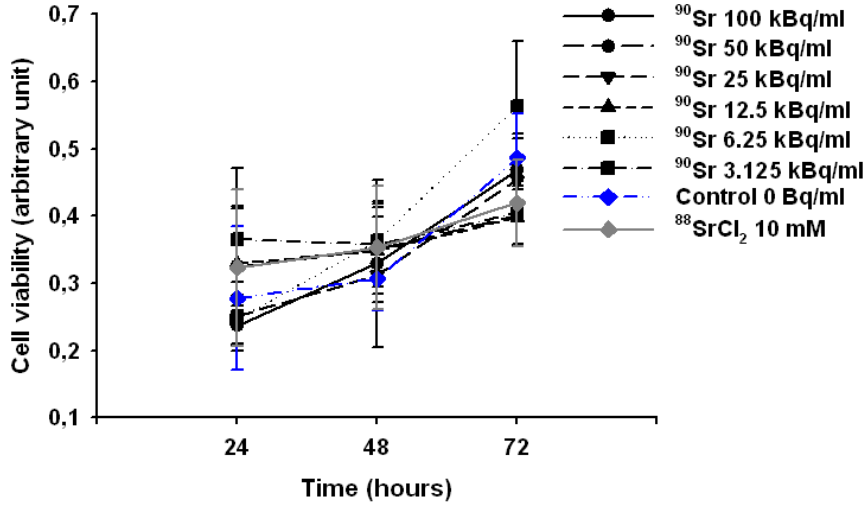

Figure 85. Effect of different concentrations of ^{90}Sr (3.125 kBq/ml up to 100 kBq/ml) and 10 mM $^{88}SrCl_2$ on the cell viability (measured by MTT assay) of MC3T3-E1 clone 4 cells after 24, 48 and 96 hours treatment with ^{90}Sr or $^{88}SrCl_2$. Results are presented as mean ± SD of 4 independent experiments.

5.3. γ-H2AX foci

In preliminary experiments we detected γ-H2AX foci, as markers of DNA double-strand breaks (DSB), in MC3T3-E1 clone 4 cells that were irradiated with a dose of 0.5 Gy and foci per cell were counted after 30 minutes (**Fig 86**). One has to note that the number of γ-H2AX foci in control non-irradiated cells was higher, i.e. 7.6 ± 3.6 foci per cell for the 3 experiments taken together, than normally expected for non-irradiated cells. For the irradiated cells 13.3 ±

5.6 foci per cell were observed for the 3 experiments taken together. This higher number of γ-H2AX foci indicates more DNA double-strand breaks in irradiated cells.

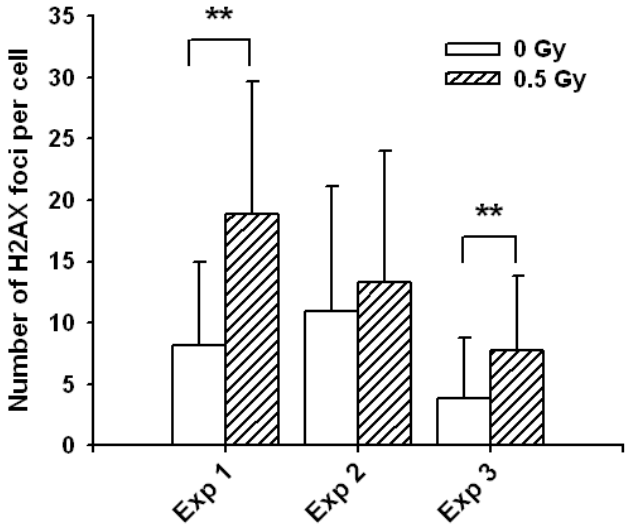

Figure 86. Number of γ-H2AX foci per cell of MC3T3-E1 clone 4 cells irradiated at a dose of 0.5 Gy for 3 independent experiments. Results are presented as mean ± SD of 100 evaluated cells per condition. Differences between control (0 Gy) and irradiated (0.5 Gy) groups are significant for **:$p<0.001$ (Student t test).

Because of the observed high number of γ-H2AX foci already present in the control MC3T3-E1 clone 4 cells, we decided to use for further experiments mesenchymal stem cells (MSC).

We repeated the above described experiment (irradiation at 0.5 Gy) (**Fig 87**) and observed a lower number of γ-H2AX foci for the control MSC than for the MC3T3-E1 cells (1.0 ± 0.1 foci per cell for both experiments vs. 7.6 ± 3.6 foci per cell respectively). Furthermore, a higher number of γ-H2AX foci were observed for the irradiated MSC (3.0 ± 1.0 foci per cell for both experiments) compared to the control MSC.

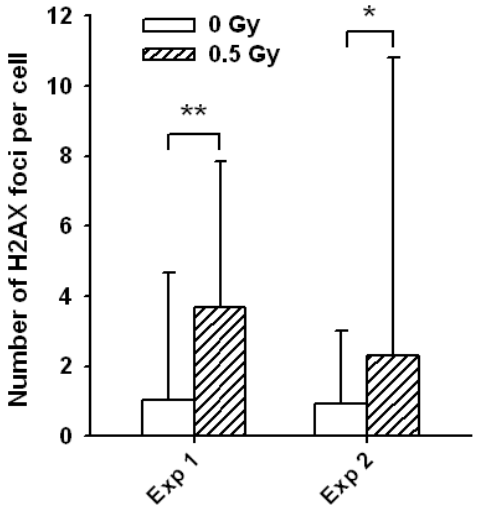

Figure 87. Number of γ-H2AX foci per cell of MSC irradiated at a dose of 0.5 Gy for 2 independent experiments. Results are presented as mean ± SD of 100 evaluated cells per condition. Differences between control (0 Gy) and irradiated (0.5 Gy) groups are significant for *:p<0.05 and **:p<0.001 (Student t test).

Finally we evaluated γ-H2AX foci in MSC after ^{90}Sr contamination. MSC were contaminated by 1 kBq.ml^{-1} or 10 kBq.ml^{-1} during 30 minutes, 24 hours or 72 hours (**Fig 88**). Experiments showed more γ-H2AX foci in ^{90}Sr contaminated MSC than control MSC for almost all experiences. This demonstrates the induction of DNA double-strand breaks in MSC cells by radiation of ^{90}Sr. However, at longer exposure times to ^{90}Sr present in cell culture medium (i.e. 72 hours), fewer γ-H2AX foci per cell were observed and thus indicating DSB reparation.

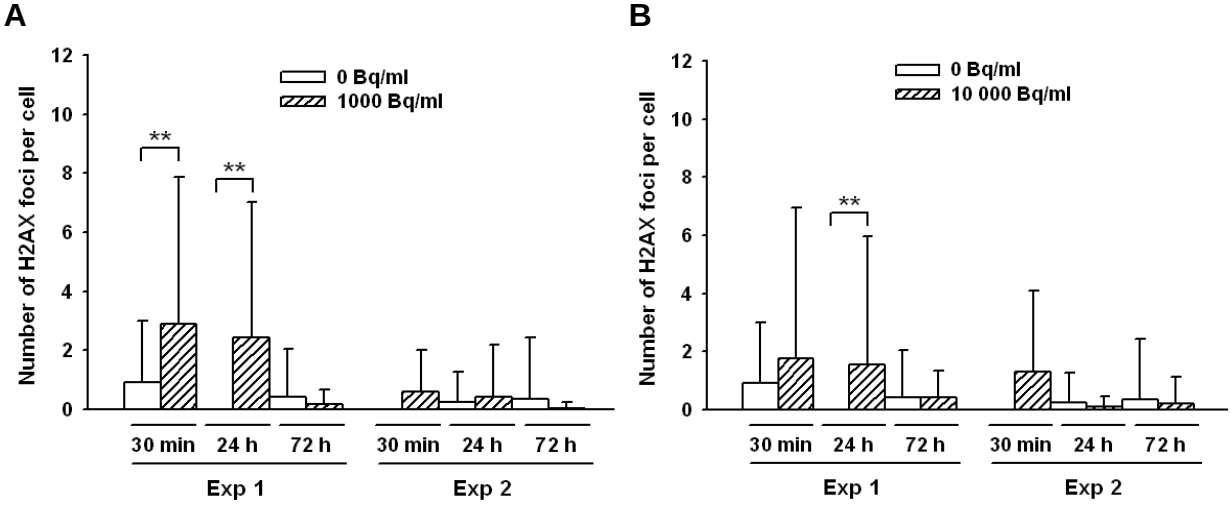

Figure 88. Number of γ-H2AX foci per cell of MSC contaminated with 1 kBq/ml of ^{90}Sr (**A**) and 10 kBq/ml of ^{90}Sr (**B**) after 30 minutes, 24 hours and 72 hours of ^{90}Sr contamination. Results for 2 independent experiments and presented as mean ± SD of 100 evaluated cells per condition. Differences between control and ^{90}Sr contaminated groups are significant for **:p<0.001 (Student t test).

Discussion

Discussion

For several years the research program ENVIRHOM at our laboratory has been dedicated to the study of non-cancerous effects of chronic ingestion of low quantities of radionuclides. The type of contamination used, i.e. chronic ingestion, was chosen because it is representative to the mode of contamination for populations living on radionuclide contaminated territories after nuclear accidents. These accidents led to the dispersion of many radionuclides in the environment. On the long term, two radionuclides remain important for chronic contamination by ingestion, ^{137}Cs and ^{90}Sr (Fairlie 2007; Kashparov et al. 2001). Indeed, several studies showed that due to the Chernobyl accident important populations are already chronically exposed to small amounts of ^{137}Cs and ^{90}Sr by ingestion, although studies showed a reduction of radionuclide ingestion with time (Cooper 1992; de Ruig and van der Struijs 1992; Hoshi et al. 1994; UNSCEAR 2000).

The first studies conducted at our laboratory were focused on the effects of chronic ^{137}Cs contamination by ingestion. These studies showed that the contamination induced some modifications in various physiological systems of rodent models used. For instance, a modification of sleep-wake cycles in rats (Lestaevel et al. 2006) was demonstrated, which may be associated with a neuro-inflammatory reaction (Lestaevel et al. 2008). Also modifications on the cardio-vascular system (decrease in arterial pressure) (Gueguen et al. 2008), the vitamin D metabolism (decrease of active vitamin D3 in plasma) (Tissandie et al. 2006; Tissandie et al. 2009), the cholesterol metabolism (increase in different cytochromes intervening in the transformation of cholesterol and bile acids) (Racine et al. 2010; Racine et al. 2009; Souidi et al. 2006) and the steroid hormone metabolism (Grignard et al. 2008) were shown. However, most of the observed modifications are at the molecular level (such as gene expression modifications or variation in protein synthesis) without any major consequences on health status of animals (Lestaevel et al. 2010). By contrast, studies on the hematopoietic and immune systems showed no modifications after chronic ingestion of ^{137}Cs (Bertho et al. 2011; Bertho et al. 2010).

Overall, results obtained showed that chronic ingestion of ^{137}Cs has limited effects on animal physiology. Furthermore modifications on the hematopoietic and immune systems as observed for populations living on contaminated territories, as described in the introduction

section, were not observed. Thus it was suggested that these observed effects were due to other radionuclides than ^{137}Cs and we decided to investigate the effects of chronic ^{90}Sr contamination by ingestion.

The effects of ^{90}Sr after administration by injection, inhalation or ingestion have been under study for several decades using laboratory animals (Book et al. 1982). Most of these studies were performed using large animals, mainly beagle dogs and involved a relatively short period of administration, by single injection, multiple injections, or inhalation, or longer periods of administration, by ingestion. However, the bulk of these studies mainly investigated cancerous effects after ^{90}Sr contamination at high quantities of this radionuclide.

1. ^{90}Sr biokinetics

We used a juvenile and adult mouse model and contamination was performed by drinking water containing a ^{90}Sr concentration of 20 $kBq.l^{-1}$, as previously used by Bertho et al. (Bertho et al. 2011; Bertho et al. 2010). This concentration corresponds to a daily ingestion of ^{90}Sr by populations living on contaminated territories of Chernobyl, mainly by consumption of dairy products and mushrooms (de Ruig and van der Struijs 1992; Hoshi et al. 1994). Indeed, we expected that animals used in our study ingested on average 5 ml of water per day, which gives a ^{90}Sr contamination of 100 Bq per day. Our results showed that for our animals the daily ^{90}Sr intake ranged from 40 Bq up to 91 Bq per animal, depending on its age and gender. Thus our protocol of chronic contamination through ingestion appears as representative of what is going on in contaminated territories.

We detected ^{90}Sr mainly in bones is in agreement with other experimental studies in various animal models (Gillett et al. 1992; Lloyd et al. 1976; Raabe et al. 1981) including rats (Gran 1960; Nilsson 1970a, b) and in accordance with the biokinetic model of strontium previously proposed by the ICRP (ICRP 1993; Leggett 1992; Lloyd et al. 1976). The juvenile and the adult models showed very different patterns of ^{90}Sr accumulation in bones. The rate of ^{90}Sr uptake in bones was rapid during the first weeks of offspring's life, reaching a plateau level afterwards at adult age. A plateau level of ^{90}Sr accumulation at adult age was also observed in a study with beagles which ingested chronically ^{90}Sr from in utero to 1.5 years of age (Parks et al. 1984).

As shown by Book et al., this high rate of ^{90}Sr accumulation is correlated with bone growth (Book et al. 1982). Moreover, it has previously been demonstrated that the level of strontium uptake is limited by calcium availability (Apostoaei 2002; Hollriegl et al. 2006a; Hollriegl et al. 2006b; Hoshi et al. 1994). In fact, in the present study the animals received a diet with normal levels of calcium, thus limiting the absorption of strontium. Other studies showed that, due to their chemical similarities, strontium and calcium share similar transport system mechanisms across the intestinal wall and are absorbed competitively (Apostoaei 2002; Hoshi et al. 1994). A study by Sugihira et al. showed that the ratio of Sr/Ca accumulation in bones was higher during young ages, possibly due to a higher efficiency of Sr absorption by the small intestine early in life (Sugihira et al. 1990). These mechanisms may explain both the rapid increase in ^{90}Sr accumulation at young ages and the plateau level at the adult age observed in the juvenile model. Further they suggest that ^{90}Sr accumulation in bones may be limited even in immature skeletons that have the high calcium turnover associated with early life.

By contrast, in our adult mouse model, a continuous increase of ^{90}Sr content in the bones was found during the 20 weeks of chronic ^{90}Sr ingestion and no plateau level was reached. This is probably due to the low level of daily ingestion which may not allow reaching equilibrium between ingestion, excretion and bone accumulation, but also to the limitation to 20 weeks of ingestion duration. Furthermore, the reduced rate of ^{90}Sr uptake in our adult model is in accordance with other studies showing that ^{90}Sr uptake in adult bones is mainly linked to bone remodelling (Dahl et al. 2001; Momeni et al. 1976a; Momeni et al. 1976b).

In all the other organs tested (blood, liver, spleen, kidneys, thymus, heart, lungs, CNS, muscles, skin), ^{90}Sr was below the detection limit. In fact, since previous studies showed that more than 90% of absorbed strontium is accumulated in bones (ICRP 1993), this indicates that, according to the daily rate of ^{90}Sr intestinal absorption between 0.1 and 0.4 in our models, less than 3.5 Bq may be found in all other organs than the skeleton. This estimation strongly suggests that, once ^{90}Sr is present in the liver, kidney and/or blood, the ^{90}Sr concentration is below the detection limit in our models.

Nevertheless, small amounts of ^{90}Sr were found in the digestive tract. Measure of ^{90}Sr content in different segments of the digestive tract (stomach, small intestine, caecum and large intestine) of animals of both models showed that ^{90}Sr was only detectable in the small

intestine and not in the other segments. This suggests rather a weak trapping of ^{90}Sr in the villi of the intestinal mucosa than a real accumulation in the intestinal tissue, as previously described for uranium ingestion (Dublineau et al. 2007; Dublineau et al. 2005). However, this local retention may have influence on the inflammatory status of the intestine due to ^{90}Sr irradiation, similarly to the inflammatory reaction observed in a rat model of uranium ingestion (Dublineau et al. 2007).

Furthermore, gender differences were observed in ^{90}Sr uptake. For both models higher ^{90}Sr contents were found in the bones of females as compared to males. This difference between males and females was observed whatever the skeletal site tested at the age of 6 and 20 weeks. It is well known that bone remodelling is under the dependency of hormonal cycles in females (Chiu et al. 1999; Hotchkiss and Brommage 2000; Kalyan and Prior 2010) and this may explain the observed discrepancy in ^{90}Sr accumulation in bones between females and males, despite the lower ^{90}Sr intestinal absorption in females as compared to males. Especially the oestrogen hormone seems to be involved in the regulation of the bone physiology. Indeed, a study showed that osteoblasts express oestrogen receptors, which once activated promote osteoblast differentiation (Marie 2001).

Differences in ^{90}Sr content were also observed according to the different skeletal sites. Previously a study with monkeys who were chronically contaminated by ^{90}Sr ingestion for 26 weeks showed that the incorportation of ^{90}Sr into bone depended upon skeletal site. Differences in ^{90}Sr content were observed in the femoral diaphysis, lumbar vertebra and iliac crest (Dahl et al. 2001). A difference in skeletal retention was also observed in beagles following ingestion or injection of ^{90}Sr (Momeni et al. 1976a; Momeni et al. 1976b). The variations in uptake of Sr between various skeletal sites may depend on differences in local bone turnover and regional blood flow (Dahl et al. 2001).

Our results confirmed that the skeleton is the preferential site of storage of ^{90}Sr along the course of a long term chronic ingestion. We also showed that the incorporation of ^{90}Sr was age, gender and skeletal site dependant and this must be taken into account in future studies on the potential effects of ^{90}Sr chronic ingestion on the long term.

2. Absorbed ^{90}Sr doses

We calculated absorbed radiation doses based upon dose conversion factors (DCF) for a rat model published by the ICRP (ICRP 2008).

Results show that the application of these DCF in our experiments with chronic contamination through ingestion of ^{90}Sr allowed calculating absorbed radiation doses between 0.3 ± 0.1 mGy and 10.6 ± 0.1 mGy. More precisely, after 20 weeks of ^{90}Sr ingestion, they were 9.7 ± 0.1 mGy for males and 10.6 ± 0.1 mGy for females in the juvenile model and 3.8 ± 0.1 mGy for males and 4.7 ± 0.1 mGy for females in the adult model. As such, absorbed radiation doses to the whole body due to the chronic ^{90}Sr intake and accumulation in bones remained low in our model.

However, the setup of DCF relies on some hypotheses. The first one is the simplified geometry of animals and their environment. This is a major limitation, since energy deposition in living tissues depends on the source-target geometry. In fact, the model used for a rat representation is a solid ellipsoid with a length of 20 cm, diameters of 6 and 5 cm, and a mass of 315 g. This is approximately 12 fold larger than an adult mouse. The DCF model considers also that plants and animals are made of a medium of homogeneous density in which radionuclides are homogeneously distributed (ICRP 2008). Obviously, results from biokinetic experiments demonstrate that radionuclides are heterogeneously distributed. Indeed, ^{90}Sr for example seems to be strictly localized in bones (Synhaeve et al. 2011; Dahl et al. 2001) and ^{137}Cs content varies from 2 kBq.kg^{-1} in the skin up to 30 kBq.kg^{-1} in striated muscles in the adult mouse (Bertho et al. 2010). Tissue density on itself also varies, although in lesser proportions, from less dense tissues such as lungs up to more dense tissues such as bones and teeth.

The use of a soil uniformly contaminated surrounding the animal as a substitute to calculate the external radiation dose due to the mother during foetal life is another important limitation. Other limitations are parameters linked to animal housing such as the litter contamination, the presence of the bottle of drinking water containing the radionuclide in the upper part of the cage and the cross irradiation of animals by neighbours. Litter contamination may be taken into account by using DCF proposed for a superficially contaminated ground (ICRP 2008),

but other parameters would need additional modelling. However, due to the short distance travelled by β particles emitted by ^{90}Sr, the external radiation doses due to these parameters seems to be negligible in the case of ^{90}Sr contamination experiments, as it was the case for external irradiation due to the contamination of the mother during fetal life. On the other hand, they may induce a significant external irradiation in the case of ^{137}Cs contamination experiments. This hypothesis is supported by the calculation of external radiation doses during foetal life due to mother contamination.

However, we were able to verify that the use of the rat model proposed by the ICRP as a surrogate for the mouse does not induce large uncertainties on the calculation of mean whole body absorbed radiation doses for ^{90}Sr and ^{137}Cs used in our studies. In fact, by using a method of dose calculation based upon specific absorption fractions (SAF) previously established in a mouse voxel phantom by Stabin et al. (Stabin et al. 2006) we observed a good correlation between the doses estimated by the DCF and SAF methods. Moreover, in collaboration with our laboratory, a three dimensional mouse voxel phantom was created by the Laboratory of Internal Dose Evaluation (LEDI). By Monte Carlo simulation they calculated for our juvenile mouse model an absorbed dose of 10.2 mGy for the whole body after 20 weeks of ^{90}Sr chronic ingestion, which confirms the whole body absorbed dose at the same time point calculated by us with use of the DCF. Overall, the DCF calculated absorbed radiation doses to the whole body were very similar to the values obtained with the mouse voxel phantom of the LEDI. In conclusion, the DCF calculation method allows estimating in a simple and rapid way whole body radiation doses absorbed by laboratory rodents in contamination experiments on the long term, provided that data on organ mass and biokinetics are available.

Furthermore, absorbed radiation doses for specific organs could be calculated by the LEDI with use of their mouse voxel phantom. As expected, the absorbed dose for the skeleton was much higher than other tissues and reached 55.0 mGy for our juvenile mouse model after 20 weeks of ^{90}Sr ingestion. Consequently, potential health effects of ^{90}Sr chronic ingestion may be observed on the bone physiology and also the hematopoietic system, due to the location of the hematopoietic stem cells close to the bone (Calvi et al. 2003; Howard and Clarke 1970; Taichman 2005). Indeed, a dosimetric model described that much higher radiation doses may arise to hematopoietic stem cells due to the proximity of bone (Eckerman and Stabin 2000).

As the bone marrow is the main anatomical site of B lymphocyte differentiation, potential effects may be observed on the immune system.

For our mouse models absorbed radiation doses to the whole body remained low. On the other hand, absorbed doses for the skeleton were much higher and could have an impact on bone physiology as well as on the hematopoietic and immune systems.

The use of a juvenile mouse model to study potential effects of ^{90}Sr contamination by chronic ingestion on the bone, hematopoietic and immune systems seemed to be of particular interest because the absorbed radiation is higher. The hematopoietic and immune systems which mainly develop during late fetal and post-natal life and juveniles show an enhanced sensitivity towards many toxic compounds including radionuclides (Blakley 2005; Hoyes et al. 2000; Lindop and Rotblat 1962; Preston 2004). Moreover, their lifespan makes them the primary targets for potential long-term effects.

3. Effects on the bone physiology

Different phases of the skeletal development were studied to estimate the effects of a chronic ^{90}Sr contamination by ingestion on the bone physiology during bone growth and bone maturity. For this purpose, we analysed calcium, phosphate and alkaline phosphatase (ALP) plasma levels but also more specific biochemical markers of bone turnover in plasma which allowed us estimating the processes of bone formation and bone resorption. We evaluated also plasma concentrations of the calciotropic hormones 1,25-$(OH)_2$ vitamin D3 and parathyroid hormone (PTH) which both influence bone metabolism by playing a crucial role in the regulation of calcium and phosphate homeostasis (Baek and Kang 2009; Morgan 2001). Finally on femurs, expression analysis of genes involved in the bone formation and resorption and a morphological study by histomorphometry were performed.

First of all, we didn't observe a modification in calcium and phosphate plasma levels for ^{90}Sr ingesting animals compared to control animals. Neither were the plasma levels of 1,25-$(OH)_2$ vitamin D3 and PTH modified, which by acting on the intestine, bone and kidney, strictly regulate the plasma concentrations of these elements important in bone mineral status (Baek and Kang 2009; Brzoska and Moniuszko-Jakoniuk 2005a, b; Garnero et al. 2003; Tissandie et al. 2006).

On the other hand, significant increased plasma levels of the bone resorption marker C-telopeptide degradation products from type 1 collagen (CTX) were observed in ^{90}Sr ingesting males at the age of 6 and 20 weeks. Previously in rat models, it was shown that an increased concentration of CTX in plasma is associated to an enhanced degradation of bone matrix (Brzoska and Moniuszko-Jakoniuk 2005a, b; Garnero et al. 2003). Surprisingly this effect was observed in males and not in females. The latter have in fact a skeleton which is supposed to be more susceptible to damage resulting from variations in calcium levels associated to hormonal cycles, pregnancy, lactation cycles or postmenopausal changes in the hormone profile (Riis 1996; Xing and Boyce 2005). By contrast, bone formation markers measured in plasma, i.e. bone-specific ALP, bone morphogenetic protein 2 (BMP2) and procollagen 1 N-terminal propeptide (PINP) were not modified according to the contamination status of animals, either in males or females.

At the same time points, i.e. during skeletal growth and at maturity, we observed a significant decrease in the bone formation activating genes ALP and osteocalcin (OCN) and a significant increase in the bone resorption gene RANKL in femurs of ^{90}Sr ingesting animals.

The results of plasma markers of bone turnover and gene expression at femurs may indicate that ^{90}Sr accelerates the age related loss of bone mass by enhancing the rate of bone turnover. Indeed, if bone resorption is enhanced and bone formation impaired, the amount of bone that is lost by continuously occurring bone resorption is incompletely restored by bone formation and as such results in a net bone loss. We thus looked at bone morphology at the age of 20 weeks of animals. Nevertheless, at the morphological level, we could not observe differences in growth plate thickness and ratio of bone volume to tissue volume between ^{90}Sr ingesting animals and control animals of 20 weeks of age. However, we cannot exclude that at later time points morphological changes at the bone tissue level can be observed for ^{90}Sr ingesting animals.

At 20 weeks of chronic ^{90}Sr contamination by ingestion bone specific plasma markers and gene expression balance at femurs between bone formation and bone resorption seemed to be modified with bone resorption in favour of bone formation. At the same time point no modifications at the morphological level could be observed. However, it is not excluded that they could be observed at later time points.

In conclusion, as we observed a modification in the balance between bone formation and bone resorption at the gene expression level and plasma level at 20 weeks of chronic ^{90}Sr contamination by ingestion, it would be interesting complete to study the effects at the morphological level at later time points and complete this study by immunohistology, bone microarchitecture and bone strength measurements.

4. Effects on the hematopoietic system

As mentioned before, potential health effects of ^{90}Sr chronic ingestion may be observed on the hematopoietic system due to the location of the hematopoietic stem cells in the bone marrow close to the bone (Calvi et al. 2003; Porter and Calvi 2008; Taichman 2005). Moreover, it is known that the hematopoietic system is one of the most radiosensensitive tissues and as such the effects of external irradiation or radionuclide accumulation have already been studied on hematopoietic stem cells (HSC) (Bertho et al. 2010; Dainiak 2002; Svoboda and Klener 1972; Svoboda et al. 1985).

As such it has been shown that irradiation induces an important reduction in the number of HSC and hematopoietic progenitors in the bone marrow. However, as the hematopoietic cells don't have all the same activation status (resting vs. proliferating), they don't have all the same radiosensitivity. Indeed, HSC located in the niche are in general quiescent and as such relatively radioresistant. On the other hand, hematopoietic progenitors are highly proliferating, making them more radiosensitive. On the opposite, hematopoietic precursor cells and differentiated mature hematopoietic cells, with the exception of lymphocytes, are less proliferating and consequently more radioresistant. Furthermore, irradiation of medullar stroma cells affects regulation of hematopoiesis by modification of the expression of growth factors (Dainiak 2002; Fliedner et al. 1988; Gothot et al. 1997; Laver 1989). Thus, the hypothesis of an indirect effect of strontium accumulation in bones on HSC early hematopoiesis is substantiated by current knowledge.

We investigated the influence of a chronic ^{90}Sr ingestion on the hematopoietic system by analysing blood cell counts, plasma Flt3-ligand concentration (as a biological marker of bone marrow function) (Prat et al. 2006), progenitor frequencies in the bone marrow and spleen (reflecting the general status of hematopoiesis) (Grande and Bueren 2004) and phenotypical analysis of bone marrow cells.

With the exception of some punctual time-specific differences, we did not detect significant differences between control animals and ^{90}Sr ingesting animals in terms of the parameters measured. Moreover, we did not observe significant differences between males and females. However, one can note that Flt3-ligand was significantly decreased in ^{90}Sr ingesting females at birth. This result could indicate a modified hematopoiesis but was not confirmed by phenotypical analysis of $Lin^{-}C\text{-}kit^{+}SCA\text{-}1^{+}$ cells in the bone marrow nor by progenitor frequency both in the bone marrow an in the spleen.

By contrast, significant differences over time (without influence of the contamination status of animals) were observed for some parameters, associated with normal development of the hematopoietic system during post-natal life (Tavian and Peault 2005). This was for instance the case for Flt3-ligand concentration, red blood cell count and progenitor frequencies in the bone marrow and the spleen.

Although the parameters used in this study could be not sufficiently sensitive to detect subtle variations in the homeostasis of hematopoiesis, our results strongly suggest that a chronic ^{90}Sr intake does not induce a significant modification of the hematopoietic system.

As discussed before, effects on the bone physiology were observed after chronic ^{90}Sr ingestion. Surprisingly for the hematopoietic system this was not the case. Different reasons can explain this discrepancy. Firstly, strontium and calcium are both without any known chemical toxicity (Dahl et al. 2001; Leggett 1992; Pors 2004). Thus the potential toxic effect may be exclusively linked to the emission of ionizing radiation by ^{90}Sr. Secondly, the ^{90}Sr concentration used in this study was low, with corresponding radiation doses to the contaminated animals also being low, i.e. 10 mGy for the whole body and 55 mGy for the skeleton after 20 weeks of chronic ^{90}Sr ingestion. Such radiation doses are possibly insufficient to induce cell death in detectable amounts when compared to the background. Thirdly, the hematopoietic system is a hierarchically organized physiological system that is able to produce from a reduced pool of stem cells large numbers of mature and functional cells per day (Blank et al. 2008; Ceredig et al. 2009). Consequently, the hematopoietic system is able to respond to stressful situations, such as exposure to external high dose irradiation, that lead to significant cell loss (Grande and Bueren 2004; Prat et al. 2006). In a similar way, the hematopoietic system may also be able to respond to an internal exposure with low doses from ingested ^{90}Sr. However, more sensitive methods should be used in order to confirm this.

For instance by looking in situ at the HSC in the niche or performing plasma dosages of specific growth factors of hematopoiesis like stromal cell derived factor 1 (SDF-1) erythropoietin (EPO), thrombopoietin (TPO) or stem cell factors (SCF) (Tarasova et al. 2011; Wognum et al. 2003).

Our results suggest that chronic ingestion of ^{90}Sr at low concentrations does not induce a significant change in bone marrow function of mice.

5. Effects on the immune system

We studied potential effects of chronic ^{90}Sr intake on the immune system as earlier studies suggested that chronic ingestion of long lived radionuclides in humans may be responsible for modifications in thymic physiology (Yarilin et al. 1993), in immunoglobulin levels in blood (Titov et al. 1995) and in blood lymphocyte subsets (Vykhovanets et al. 2000). Moreover, other studies demonstrated a link between the bone and immune systems by molecular and cellular interactions, for instance between lymphocytes and osteoclasts (Hanada et al. 2011; Takayanagi 2007). Furthermore, it has been shown that osteoblasts and mesenchymal stem cells (MSC) can interact with cells of both the innate and adaptive immune systems, leading to the modulation of several of their effector functions (Lorenzo 2000; Lorenzo et al. 2008; Uccelli et al. 2008; Zhu et al. 2007).

First of all we analysed T-lymphocyte differentiation by phenotypical analysis of thymic cells and intrathymic T cell differentiation by TREC evaluation, being an indicator of TCR gene rearrangement (Broers et al. 2002; Ciofani and Zuniga-Pflucker 2007; Sempowski et al. 2002). In fact, in a previous study it was proposed that T-lymhocyte deficiencies observed in victims of the Chernobyl accident were due to a modification of intrathymic T-lymphocyte differentiation (Yarilin et al. 1993). Our results showed no modifications for the T-lymphocyte subsets tested and for TRECs after chronic ingestion of ^{90}Sr.

We then looked at mature T lymphocytes in the spleen of contaminated animals. Analysis of various T-lymphocyte subsets and the associated $CD4^+/CD8^+$ T-lymphocyte ratio are indeed frequently used methods for evaluating the immune status in various situations including long term effects of chronic low dose external irradiation or internal contamination (Chang et al. 1999a; Chang et al. 1999b; Vykhovanets et al. 2000). However, percentage of T-lymphocyte

subsets and $CD4^+/CD8^+$ T-lymphocyte ratio were not affected by the chronic ingestion of ^{90}Sr in our mouse model.

Furthermore, we evaluated interleukin-7 (IL-7) plasma levels as an indicator of T cell homeostasis (Bradley et al. 2005). Also for this parameter no significant differences were observed between control and ^{90}Sr ingesting animals.

Phenotypic analysis of B lymphocytes in the spleen together with determination of circulating immunoglobulins G (IgG) and M (IgM) in the plasma provided a global analysis of B lymphocyte lineage as were previously used in a study of atomic bomb survivors and a study of children exposed to the Chernobyl fallout (Fujiwara et al. 1994; Titov et al. 1995). In our mouse model with chronic ingestion of ^{90}Sr on the long term however, neither B lymphocyte numbers nor IgG or IgM concentrations were affected.

Our results show no major effects on the steady state immune system of mice after chronic ingestion of ^{90}Sr at low concentrations.

Although we didn't observe a major modification on T- and B-lymphocyte populations, we cannot formerly exclude that potential effects of chronic ^{90}Sr intake might include induction of accelerated ageing of the immune system that could be observed at later time points. In fact, some time-specific changes were observed in ^{90}Sr ingesting animals for the parameters tested, for instance in the percentage of T helper and T cytotoxic cell populations in the spleen at different time points and in IL-7 plasma level at birth.

Furthermore, one can note that significant increases in the percentage of $CD3^+CD4^+CD25^+$ T regulatory lymphocytes (Treg) were observed for ^{90}Sr ingesting animals at the age of 16 weeks and 20 weeks. Tregs are known to negatively regulate the immune response from B, T and NK cells and to control the autoimmune response (Jager and Kuchroo 2010). As such, an increase in the percentage of Tregs may suggest a reduced response to antigens. Thus, although no major changes were observed in the steady-state immune system, we hypothesized that ^{90}Sr contamination could induce functional changes in the immune system.

In order to answer to this question, we investigated the immune response to a vaccine challenge. We performed this functional test with the specific antigens tetanus toxin (TT) and

keyhole limpet hemocyanin (KLH), which are classically used in toxicology experiments (Luster et al. 1993; Luster et al. 1992).

For the circulatory immunoglobulins, we observed significant decreases in the levels of IgG specific to TT for ^{90}Sr ingesting TT vaccinated animals compared to control TT vaccinated animals. Moreover, phenotypic analysis of spleen cells revealed significant decreases in the percentage of $CD3^+CD4^+$ T helper lymphocytes and $CD45^+CD19^+$ B lymphocytes for these animals.

Based on these facts we evaluated if the Th1/Th2 immune response balance was modified after antigen challenge. First of all we examined in the spleen the expression of genes implicated in the differentiation of naive $CD4^+$ T-lymphocytes towards T Th1, Th2 or Treg cells. We found significant decreases for the genes T-box expressed in T-cells (T-bet) (Th1), Gata-binding protein-3 (Gata3) (Th2) and Forkhead box P3 (Treg) for ^{90}Sr ingesting TT or KLH vaccinated animals compared to control TT or KLH vaccinated animals. At the protein level the significant decrease in T-bet expression for ^{90}Sr ingesting TT vaccinated animals compared to control TT vaccinated animals was confirmed. This ensemble of results gives an indication of a modified Th1/Th2 balance and even an immunosuppressive effect of ^{90}Sr.

In conclusion, the vaccination challenge test with TT and KLH to evaluate the functionality of the immune system after stimulation with antigens showed a significant decrease in specific immunoglobulins, an impaired B-lymphocyte differentiation and a possible change in the Th1/Th2 balance in the spleen in vaccinated animals. This suggests an indirect effect of the ^{90}Sr accumulation in the bones of animals on their immune system and this effect could be due to the irradiation of bone marrow cells by ^{90}Sr.

A functional test with vaccine challenge demonstrated that the chronic ingestion of ^{90}Sr in the long term modifies the ability of the immune system to respond to an antigenic stimulation.

To complete this study, it would be interesting to evaluate this immune response also at the spleen after the first injection with antigens and compare these results with the above described results after the second injection with antigens. We could complete our study by evaluating the Th1/Th2 balance at the spleen at 3 weeks (before vaccination), at 7 weeks (end

of first vaccination) and at 20 weeks (before second vaccination). Furthermore this study can be extended by phenotypical and histological analysis of bone marrow cells, histological evaluation of B cells at the spleen and bone marrow, and to confirm our results by measurement of Th1 and Th2 cytokine levels in the spleen.

6. ^{90}Sr mechanistic effects

To examine the mechanisms of action of ^{90}Sr we used the pre-osteoblastic MC3T3-E1 cell line, which was previously used for exploring the molecular mechanisms of osteoblast proliferation, maturation and differentiation (Davis et al. 2000; Gal et al. 2000; Wang et al. 1999). As such it has been shown that MC3T3-E1 cultured in the presence of ascorbic acid (AA) and β-glycerophosphate (BglyP) display a time-dependent and sequential expression of osteoblast characteristics which are analogous to the processes during bone formation in vivo. For instance, the MC3T3-E1 cells actively replicate, express alkaline phosphatase (ALP) activity and synthetize a collagenous extracellular matrix which progressively undergoes mineralization (Barbara et al. 2004; Quarles et al. 1992).

To validate these characteristics we investigated the differentiation potential of MC3T3-E1 clone 4 cells in the presence of AA and BglyP as described above. Moreover we investigated the effects of non-radioactive $^{88}SrCl_2$ on bone matrix mineralization, collagen synthesis and alkaline phosphatase activity. Our results of bone matrix mineralization, collagen synthesis and alkaline phosphatase activity tests confirmed that MC3T3-E1 cells cultured in the presence of AA and BglyP display a time-dependent and sequential expression of osteoblast characteristics (Al-Jallad et al. 2006; Davis et al. 2000; Dudziak et al. 2000; Gal et al. 2000; Nakano et al. 2007; Quarles et al. 1992). However, $^{88}SrCl_2$ in cell culture medium at a concentration of 10 mM in our study didn't have any influence on the differentiation potential of this cell line. By contrast, in studies using MC3T3-E1 cells and comparable concentrations of non-radioactive strontium ranelate, increased ALP activity and collagen synthesis could be demonstrated (Barbara et al. 2004; Nie and Richardson 2009; Quarles et al. 1992). Thus, the chemical form of strontium coupled with ranelate appears crucial for its activity on the bone physiology. This in turn may suggest that ^{90}Sr has only a radiation toxicity in vivo and may explain that we observe an effect of ^{90}Sr on bone resorption in vivo.

What concerns the action of ^{90}Sr on MC3T3-E1 clone 4 cells, we investigated first if ^{90}Sr had an influence on the cell mortality and cell viability of these cells. We used different concentrations of ^{90}Sr (up to 100 $kBq.ml^{-1}$) in cell culture medium but couldn't observe any significant modification on the mortality and viability of MC3T3-E1 clone 4 cells in the presence of ^{90}Sr at the concentrations used. By contrast, it has previously been shown that MC3T3-E1 cells are sensitive to ionizing radiation and that their cell survival and proliferation can in consequence be affected (Dudziak et al. 2000; Gal et al. 2000; Gevorgyan et al. 2008; Szymczyk et al. 2004).

On the other hand, in some preliminary experiments with MC3T3-E1 clone 4 cells that were irradiated with a dose of 0.5 Gy we detected an increase in phosphorylated H2AX (γ-H2AX) foci, which are early markers of DNA double-strand breaks (DSB) (MacPhail et al. 2003; Roch-Lefevre et al. 2010). However, the number of γ-H2AX foci in control non-irradiated cells was higher than normally expected for non-irradiated cells. This may be due to the facts that MC3T3-E1 cells continuously proliferate and the knowledge that γ-H2AX foci appear during cell division (MacPhail et al. 2003; Roch-Lefevre et al. 2010).

Because of the observed high number of γ-H2AX foci already present in the control MC3T3-E1 clone 4 cells, we decided to use MSC for further experiments. Indeed, we observed a lower number of γ-H2AX foci for the control MSC than for the MC3T3-E1 cells. Furthermore, in these MSC we confirmed a higher number of γ-H2AX foci in irradiated cells than control cells.

Ultimately we evaluated γ-H2AX foci in MSC after ^{90}Sr contamination. Results showed more γ-H2AX foci in ^{90}Sr contaminated MSC than control MSC. This demonstrated the induction of DNA double-strand breaks in MSC by radiation of ^{90}Sr. However, one can note that at longer exposure times to ^{90}Sr present in cell culture medium, less γ-H2AX foci per cell were observed and was probably associated to DSB reparation.

In vitro results didn't show an influence of chronic ^{90}Sr contamination on pre-osteoblastic MC3T3-E1 cell line viability, mortality or differentiation potential at the concentrations of ^{90}Sr used. On the other hand, more γ-H2AX foci in MSC were observed after chronic ^{90}Sr contamination, indicating an increase in DNA double strand breaks by ^{90}Sr.

It is necessary to confirm results of our study by performing supplementary experiments under the same conditions. In addition, it would be interesting to detect DSB repair proteins such as ATM and MRE11 (Czornak et al. 2008; Garner and Costanzo 2009) to confirm our interpretation of results.

7. Perspectives

In this study we used a single concentration of ^{90}Sr in drinking water. Our results showed that the daily intake of ^{90}Sr in was in agreement with estimates of daily ingestion by humans living on contaminated territories (Cooper 1992; de Ruig and van der Struijs 1992; Hoshi et al. 1994). Moreover, the ^{90}Sr ingestion resulted in ^{90}Sr contents in the skeleton similar to those measured in human bones (Shagina et al. 2003b; Tolstykh et al. 2011b; Tolstykh et al. 2011a). We thus assumed that our mouse models of chronic ^{90}Sr ingestion are representative for the situation of people living in contaminated territories.

Nevertheless in the radioprotection context, it would be interesting to perform a dose response study to determine at what concentration of ^{90}Sr ingestion a No Observable Adverse Effect Level (NOAEL) is reached, i.e. the highest concentration of ^{90}Sr chronic ingestion at which no effects on the studied physiological systems are observed. Moreover, from a toxicological viewpoint, a dose response study with higher doses of ^{90}Sr would be interesting to confirm the conclusions formulated on the basis of our obtained results.

One can remark that the length of follow-up in our study may not be representative of the existing situation of populations living in contaminated territories. In fact, effects of ^{90}Sr could be cumulative and may lead to the appearance of late bone, hematopoietic or immune defects as it was observed for chronic ^{90}Sr ingesting beagles, swine or rats (Clarke et al. 1972; Dungworth et al. 1969; Howard and Clarke 1970; White et al. 1993; Zapol'skaya et al. 1974). Indeed, we cannot exclude that chronic ^{90}Sr ingestion might for instance induce an acceleration of hematopoietic aging that may be observed at later time points. However, the choice of a 20 week duration of ^{90}Sr intake in our study was based upon the hypothesis that this duration would be sufficient to observe eventual effects due to early exposure. This is based on the fact that during fetal and early post-natal life the hematopoietic and immune systems are highly sensitivity to many toxic agents including radionuclides (Blakley 2005; Gran 1960; Hoyes et al. 2000; Lindop and Rotblat 1962; MacDonald 1962; Preston 2004;

Ruhmann et al. 1963; Verfaillie 1993). In fact, in accordance with other studies (Gran 1960; MacDonald 1962; Ruhmann et al. 1963; von Zallinger and Tempel 1998), we observed a passage of ^{90}Sr through the placenta during fetal life as ^{90}Sr was detected in offspring at birth. Moreover, as far as mice and humans are comparable in such a simple way, our duration of contamination corresponds to approximately 30 % of human life expectancy, including the early period of life (Quinn 2005).

Moreover one can remark that in our study we used a single contaminant in a controlled environment and that this represents a simplification of existing situations. Indeed, we cannot exclude that a combination of radionuclides, including for example ^{90}Sr, ^{137}Cs and ^{134}Cs, may have different effects on the physiological systems studied. Moreover, this mouse model takes into account only one exposure route. By contrast, human populations in contaminated territories are exposed to both external and internal irradiation (Kuzmenok et al. 2003; Yarilin et al. 1993). This induces an uncertainty about the level of either external exposure or internal contamination. However a recent study based on long term external and internal radiation exposure measurements of residents around Chernobyl indicated that the proportion of effective doses from internal contamination is (increasingly) more important as body burdens are decreasing more slowly than the external exposure (Bernhardsson et al. 2011). Furthermore, other studies used also estimates of exposure based upon soil and food contamination data and did not include whole body counting for example (Chernyshov et al. 1997; Titov et al. 1995; Vykhovanets et al. 2000). However, we agree that it would be interesting to use a mix of different radionuclides in drinking water for our mouse model, eventually in combination with heavy metals or other chemical pollutants, in order to be more relevant to the post accident situation.

What concerns the effects of chronic ^{90}Sr ingestion on the bone physiology and immune system, it was surprising that we observed effects at the low dose and dose rate in our study, even taking in account the exposure over long term. As discussed before, the whole absorption radiation dose of our animals was on average 10 mGy after 20 weeks of chronic ^{90}Sr intake, which correspond to a dose rate of about 3 µGy per hour. However, others have also shown effects on the immune system of mice at low dose and dose rate irradiation, i.e. by a reduced percentage of $CD4^+$ and $CD8^+$ T lymphocytes in lymph nodes and spleen or a decreased level of immunoglobulins, both after long term γ irradiation at 10 cGy per year (Courtade et al. 2001; Lacoste-Collin et al. 2007). Moreover in studies at our laboratory, other

physiological systems were shown to be modified by chronic ^{137}Cs intake at low dose (Gueguen et al. 2008; Lestaevel et al. 2006; Racine et al. 2010a; Souidi et al. 2006; Tissandie et al. 2006).

The mechanisms by which the accumulation of ^{90}Sr in bones conducts to a reduced ability of the immune system to respond to external stimuli remain to be elucidated. However, one can propose a putative mechanism based upon the fact that MSC and osteoblasts, which are both key regulators of early hematopoiesis, are situated at the site of ^{90}Sr accumulation (**Fig 89**). Thus we cannot exclude that local irradiation of MSC and/or osteoblasts conduct not only to a disregulation of the bone physiology but also of the regulation of early hematopoiesis. This is supported by our preliminary observation of γ-H2AX foci in MSC and osteoblasts cultured in the presence of ^{90}Sr. As well, one cannot exclude that ^{90}Sr irradiates HSC in the endosteal niche. As a result, we expect that this low level and localized irradiation by ^{90}Sr may induce changes in B cell differentiation and/or early T cell differentiation. Although in our study not visible on main parameters of the immune system such as phenotypic analysis, this may induce functional changes in the immune response. Furthermore, it can not be exlcuded that the differentation of other cells of hematopoietic origin may be affected by ^{90}Sr. In this context the differentiation of dendritic cells and macrophages may be changed, wich may alter their antigen presenting capacity and as such modify the immune response.

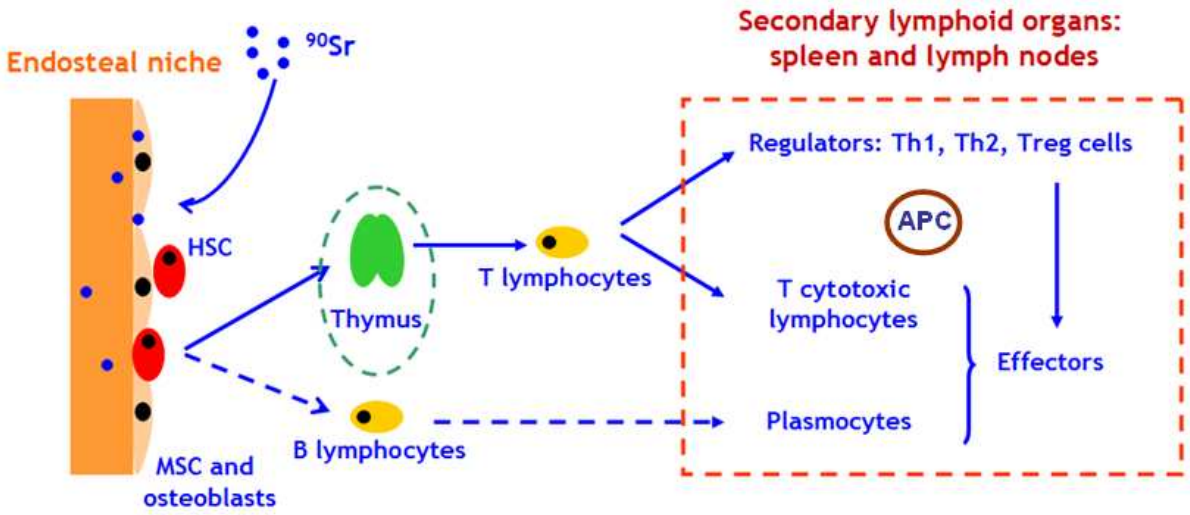

Figure 89. Illustration for hypothesis of ^{90}Sr mechanisms.

The mechanistic effects of ^{90}Sr could be elucidated by: DNA damage detection *in situ* (on bone marrow slides) by γ-H2AX foci and phosphorylated ATM and MRE11 foci detection

(Czornak et al. 2008; Garner and Costanzo 2009; Suzuki et al. 2006); study of apoptosis of stromal cells in the bone marrow; histological examination of the endosteal HSC niche by quantification of nestin^{+} or SDF-1^{+} mesenchymal stem cells and CXCR4 expressing hematopoietic cells (Martin et al. 2003; Nagasawa et al. 2011); and follow-up of B lymphocyte differentiation according to the age of animals by quantification of IgM^{+}, IgD^{+} and CD20^{+} pre-B cells in the bone marrow and spleen (Chu et al. 2006). Marcrophage and dendritic cell populations could be investigated by quantification of respectively CD68^{+}CD14^{+} and CD80^{+}CD40^{+} cells in the spleen (Vremec and Shortman 1997; Wang et al. 2009).

In conclusion, our results suggest that the accumulation of ^{90}Sr in bone after chronic ^{90}Sr ingestion is responsible for changes in the bone and immune systems. Our results help to improve the knowledge on non cancerous consequences after chronic exposure to small quantities of radionuclides discharged accidentally. According to the physiological systems tested we observed various levels of response, from the bone marrow in which no significant effect was observed, to the immune system in which a major effect was observed. Thus biological effects of chronic contamination may vary not only according to the radionuclide concentration, but also according to the physiological system. It is important to continue this work as it is of major interest for the public health, shown by the nuclear accidents of Chernobyl and more recently of Fukushima, at which many long remaining radionuclides, including ^{90}Sr, were released into the environment. Nowadays questions about the health consequences of these accidents remain, and this even 25 years after the Chernobyl accident.

List of scientific publications and presentations

List of scientific publications and presentations

Scientific publications accepted or submitted

Biokinetics of (90)Sr after chronic ingestion in a juvenile and adult mouse model.

Synhaeve N, Stefani J, Tourlonias E, Dublineau I, Bertho JM.

Radiat Environ Biophys. 2011 Nov; 50 (4): 501-11. Epub 2011 Jun 18.

Radiation doses from chronic ingestion of Cs-137 or Sr-90 by mice.

Bertho JM, Synhaeve N, Miloudi H, Stefani J, Desbree A, Blanchardon E, Dublineau I.

Radioprotection. 2011. (Submitted)

Scienfic publications in preparation

Influence of chronic 90Sr contamination by ingestion on the mouse bone and hematopoietic systems.

Other publications

Influence of Sr-90 chronic ingestion on blood and bone marrow parameters in a juvenile mouse model.

Synhaeve N, Stefani J, Grandcolas L, Bertho JM

Toxicology Letters. 2011 Aug; 205S: S54 (OS9-7).

Biokinetics of Sr-90 after chronic ingestion in a juvenile and adult mouse model.

Synhaeve N, Stefani J, Tourlonias E, Bertho JM

Toxicology Letters. 2011 Aug; 205S: S136 (P1250).

Oral presentations

Ingestion chronique de strontium-90: biocinétique, doses absorbées et effets sur les systèmes immunitaire et hématopoïétique.

Sirlaf, 10ème Colloque International de Radiobiologie Fondementale et Appliquée, Anglet, France, 11-16 Sept 2011

Influence of 90Sr chronic ingestion on blood and bone marrow parameters in a juvenile mouse model.

Eurotox, the 47th congress of the European Toxicology Societies, Paris, France, 28-31 Aug 2011.

Biocinétique du Sr-90 après ingestion chronique chez la souris et effets sur les systèmes hématopoïétique et immunitaire.

Journées de l'Ecole doctorale ED425, Châtenay-Malabry, France, 23-24 May 2011.

Influence d'une contamination chronique par ingestion de Sr-90 sur les systèmes hématopoïétique et osseux.

Journées des thèses de l'IRSN, Arles, France, 21-24 Sept 2010.

Poster presentations

Biokinetics of Sr-90 after chronic ingestion in a juvenile and adult mouse model.

Eurotox, the 47th congress of the European Toxicology Societies, Paris, France, 28-31 Aug 2011.

Comparaison des doses absorbées après contamination par ingestion chronique de Cs-137 ou de Sr-90.

SFRP, Congrès National de Radioprotection, Tours, France, 21-23 June 2011.

Biokinetics of Sr-90 in a mouse model of chronic ingestion and effects on the hematopoietic system and bone physiology.

ERR, the 38th annual meeting of the European Radiation Research Society, Stockholm, Sweden, 5-9 Sept 2010.

Fluctuating asymmetry as a tool to compare relative toxicity of radionuclides.

ERR, the 38th annual meeting of the European Radiation Research Society, Stockholm, Sweden, 5-9 Sept 2010.

Biocinétique du Sr-90 après ingestion chronique chez la souris et effets sur les systèmes hématopoïétique et osseux.

Journées de l'Ecole doctorale ED425, Orsay, France, 25-26 May 2010.

Evaluation de l'asymétrie fluctuante comme marqueur de toxicité de différents radionucléides après ingestion chronique.

9eme colloque international de radiobiologie fondomentale et appliqué, Annecy, France, 20-25 Sept 2009.

Biocinétique du Sr-90 après ingestion chronique et influence sur des ostéoblastes de souris.

Journées des thèses de l'IRSN, Aussois, France, 28-1 Sept-Oct 2009.

References

References

Ahmet-Camcioglu N, Okman-Kilic T, Durmus-Altun G, Ekuklu G, Kucuk M (2009) Effects of strontium ranelate, raloxifene and misoprostol on bone mineral density in ovariectomized rats. European journal of obstetrics, gynecology, and reproductive biology

Akleyev AV, Dimov GP, Varfolomeyeva TA (2010) Late effects in hemopoiesis and bone tissue among people with incorporated osteotropic isotope 90Sr. Health physics 98 (6):819-824

Al-Jallad HF, Nakano Y, Chen JL, McMillan E, Lefebvre C, Kaartinen MT (2006) Transglutaminase activity regulates osteoblast differentiation and matrix mineralization in MC3T3-E1 osteoblast cultures. Matrix Biol 25 (3):135-148

Alam R, Gorska M (2003) 3. Lymphocytes. The Journal of allergy and clinical immunology 111 (2 Suppl):S476-485

Ammann P (2006) Strontium ranelate: a physiological approach for an improved bone quality. Bone 38 (2 Suppl 1):15-18

Andrews RG, Singer JW, Bernstein ID (1989) Precursors of colony-forming cells in humans can be distinguished from colony-forming cells by expression of the CD33 and CD34 antigens and light scatter properties. The Journal of experimental medicine 169 (5):1721-1731

Apostoaei AI (2002) Absorption of strontium from the gastrointestinal tract into plasma in healthy human adults. Health physics 83 (1):56-65

Apostoaei AI, Miller LF (2004) Uncertainties in dose coefficients from ingestion of 131I, 137Cs, and 90Sr. Health physics 86 (5):460-482

Assimakopoulos PA, Divanes K, Pakou AA, Stamoulis KC, Mantzios AS, Nikolaou E (1995) Radiostrontium transfer to sheep's milk as a result of soil ingestion. The Science of the total environment 172 (1):17-20

ATSDR (2004) Toxicological profile for strontium. US Public health service. Agency for toxic substances an disease registry., Atlanta.

Baek KH, Kang MI (2009) Biomarkers of bone and mineral metabolism following bone marrow transplantation. Advances in clinical chemistry 49:99-120

Bain SD, Jerome C, Shen V, Dupin-Roger I, Ammann P (2009) Strontium ranelate improves bone strength in ovariectomized rat by positively influencing bone resistance determinants. Osteoporos Int 20 (8):1417-1428

Baldridge MT, King KY, Goodell MA (2011) Inflammatory signals regulate hematopoietic stem cells. Trends in immunology 32 (2):57-65

Balonov MI (1997) Health impacts of large releases of radionuclides. Internal exposure of populations to long-lived radionuclides released into the environment. Ciba Foundation symposium 203:120-133; discussion 133-140

Barbara A, Delannoy P, Denis BG, Marie PJ (2004) Normal matrix mineralization induced by strontium ranelate in MC3T3-E1 osteogenic cells. Metabolism: clinical and experimental 53 (4):532-537

Baron R, Tsouderos Y (2002) In vitro effects of S12911-2 on osteoclast function and bone marrow macrophage differentiation. European journal of pharmacology 450 (1):11-17

Baum CM, Weissman IL, Tsukamoto AS, Buckle AM, Peault B (1992) Isolation of a candidate human hematopoietic stem-cell population. Proceedings of the National Academy of Sciences of the United States of America 89 (7):2804-2808

Bedford J, Harrison GE, Raymond WH, Sutton A (1960) The metabolism of strontium in children. British medical journal 1 (5173):589-592

Benjamin SA, Hahn FF, Chieffelle TL, Boecker BB, Hobbs CH (1975) Occurrence of hemangiosarcomas in beagles with internally deposited radionuclides. Cancer research 35 (7):1745-1755

Bernhardsson C, Zvonova I, Raaf C, Mattsson S (2011) Measurements of long-term external and internal radiation exposure of inhabitants of some villages of the Bryansk region of Russia after the Chernobyl accident. The Science of the total environment 409 (22):4811-4817

Bertho JM, Frick J, Demarquay C, Laporte JP, Aigueperse J, Gorin NC, Gourmelon P (2001) Le Flt3-ligand plasmatique, un bio-indicateur pronostique de l'atteinte radio-induite à la moelle osseuse. Radioprotection 36:303-315

Bertho JM, Roy L, Souidi M, Benderitter M, Bey E, Racine R, Fagot T, Gourmelon P (2009) Initial evaluation and follow-up of acute radiation syndrome in two patients from the Dakar accident. Biomarkers 14 (2):94-102

Bertho JM, Louiba S, Faure MC, Tourlonias E, Stefani J, Siffert B, Paquet F, Dublineau I (2010) Biodistribution of (137)Cs in a mouse model of chronic contamination by ingestion and effects on the hematopoietic system. Radiation and environmental biophysics 49 (2):239-248

Bertho JM, Faure MC, Louiba S, Tourlonias E, Stefani J, Siffert B, Paquet F, Dublineau I (2011) Influence on the mouse immune system of chronic ingestion of 137Cs. J Radiol Prot 31 (1):25-39

Bertho JM, Roy L, Souidi M, Benderitter M, Gueguen Y, Lataillade JJ, Prat M, Fagot T, De Revel T, Gourmelon P (2008) New biological indicators to evaluate and monitor radiation-induced damage: an accident case report. Radiation research 169 (5):543-550

Blakley B, Blakley, PM. (2005) Developmental immunotoxicology in rodent species. In: Tryphonas H FM, Blakley BR, Smits JEG, Brousseau P (ed) Investigative immunotoxicology. Taylor and Francis, Londen, pp 183-196

Blank U, Karlsson G, Karlsson S (2008) Signaling pathways governing stem-cell fate. Blood 111 (2):492-503

Boanini E, Torricelli P, Fini M, Bigi A (2011) Osteopenic bone cell response to strontium-substituted hydroxyapatite. Journal of materials science

Bolsunovsky A, Dementyev D (2011) Evidence of the radioactive fallout in the center of Asia (Russia) following the Fukushima Nuclear Accident. Journal of environmental radioactivity

Bonfield TL, Caplan AI (2010) Adult mesenchymal stem cells: an innovative therapeutic for lung diseases. Discovery medicine 9 (47):337-345

Bonnet D (2003) Hematopoietic stem cells. Birth Defects Res C Embryo Today 69 (3):219-229

Book SA, Spangler WL, Swartz LA (1982) Effects of lifetime ingestion of 90Sr in beagle dogs. Radiation research 90 (2):244-251

Boudiffa M, Wade-Gueye NM, Guignandon A, Vanden-Bossche A, Sabido O, Aubin JE, Jurdic P, Vico L, Lafage-Proust MH, Malaval L (2010) Bone sialoprotein deficiency impairs osteoclastogenesis and mineral resorption in vitro. J Bone Miner Res 25 (12):2669-2679

Boxall SA, Cook GP, Pearce D, Bonnet D, El-Sherbiny YM, Blundell MP, Howe SJ, Leek JP, Markham AF, de Wynter EA (2009) Haematopoietic repopulating activity in human cord blood CD133+ quiescent cells. Bone marrow transplantation 43 (8):627-635

Boyce BF, Xing L (2007) Biology of RANK, RANKL, and osteoprotegerin. Arthritis research & therapy 9 Suppl 1:S1

Bradford MM (1976) A rapid and sensitive method for the quantitation of microgram quantities of protein utilizing the principle of protein-dye binding. Analytical biochemistry 72:248-254

Bradley LM, Haynes L, Swain SL (2005) IL-7: maintaining T-cell memory and achieving homeostasis. Trends in immunology 26 (3):172-176

Bradley TR, Metcalf D (1966) The growth of mouse bone marrow cells in vitro. The Australian journal of experimental biology and medical science 44 (3):287-299

Brasel K, McKenna HJ, Morrissey PJ, Charrier K, Morris AE, Lee CC, Williams DE, Lyman SD (1996) Hematologic effects of flt3 ligand in vivo in mice. Blood 88 (6):2004-2012

Braux J, Velard F, Guillaume C, Bouthors S, Jallot E, Nedelec JM, Laurent-Maquin D, Laquerriere P (2011) A new insight into the dissociating effect of strontium on bone resorption and formation. Acta biomaterialia 7 (6):2593-2603

Broers AE, Meijerink JP, van Dongen JJ, Posthumus SJ, Lowenberg B, Braakman E, Cornelissen JJ (2002) Quantification of newly developed T cells in mice by real-time quantitative PCR of T-cell receptor rearrangement excision circles. Experimental hematology 30 (7):745-750

Brzoska MM, Moniuszko-Jakoniuk J (2005a) Bone metabolism of male rats chronically exposed to cadmium. Toxicology and applied pharmacology 207 (3):195-211

Brzoska MM, Moniuszko-Jakoniuk J (2005b) Disorders in bone metabolism of female rats chronically exposed to cadmium. Toxicology and applied pharmacology 202 (1):68-83

Callard RE (2007) Decision-making by the immune response. Immunology and cell biology 85 (4):300-305

Calvi LM, Adams GB, Weibrecht KW, Weber JM, Olson DP, Knight MC, Martin RP, Schipani E, Divieti P, Bringhurst FR, Milner LA, Kronenberg HM, Scadden DT (2003) Osteoblastic cells regulate the haematopoietic stem cell niche. Nature 425 (6960):841-846

Canalis E, Hott M, Deloffre P, Tsouderos Y, Marie PJ (1996) The divalent strontium salt S12911 enhances bone cell replication and bone formation in vitro. Bone 18 (6):517-523

Cao L, Bu R, Oakley JI, Kalla SE, Blair HC (2003) Estrogen receptor-beta modulates synthesis of bone matrix proteins in human osteoblast-like MG63 cells. Journal of cellular biochemistry 89 (1):152-164

Casarett GW, Tuttle LW, Baxter RC (1962) Pathology of imbibed ^{90}Sr in rats and monkeys. . In: Dougherty J, Mays et al. (ed) Some aspects of internal radiation: proceedings of a

symposium held at Homestead, Heber, Utah, 8-11 May, 1961. Pergamon Press, New York, NY, pp pp. 329-336

Castermans E, Morrhaye G, Marchand S, Martens H, Moutschen M, Baron F, Beguin Y, Geenen V (2007) [Clinical evaluation of thymic function]. Revue medicale de Liege 62 (11):675-678

Cecchi X, Wolff D, Alvarez O, Latorre R (1987) Mechanisms of Cs+ blockade in a Ca2+-activated K+ channel from smooth muscle. Biophysical journal 52 (5):707-716

Ceredig R, Rolink AG, Brown G (2009) Models of haematopoiesis: seeing the wood for the trees. Nature reviews 9 (4):293-300

Chakir H, Wang H, Lefebvre DE, Webb J, Scott FW (2003) T-bet/GATA-3 ratio as a measure of the Th1/Th2 cytokine profile in mixed cell populations: predominant role of GATA-3. Journal of immunological methods 278 (1-2):157-169

Chang WP, Hwang JS, Hung MC, Hu TH, Lee SD, Hwang BF (1999a) Chronic low-dose gamma-radiation exposure and the alteration of the distribution of lymphocyte subpopulations in residents of radioactive buildings. International journal of radiation biology 75 (10):1231-1239

Chang WP, Lin YP, Hwang PT, Tang JL, Chen JY, Lee SD (1999b) Persistent leucocyte abnormalities in children years after previous long-term low-dose radiation exposure. British journal of haematology 106 (4):954-959

Chen Z, Lin F, Gao Y, Li Z, Zhang J, Xing Y, Deng Z, Yao Z, Tsun A, Li B (2010) FOXP3 and RORgammat: transcriptional regulation of Treg and Th17. International immunopharmacology 11 (5):536-542

Cherenko SM, Larin OS, Gorobeyko MB, Sichynava RM (2004) Clinical analysis of thyroid cancer in adult patients exposed to ionizing radiation due to the Chernobyl nuclear accident: 5-year comparative investigations based on the results of surgical treatment. World journal of surgery 28 (11):1071-1074

Chernyshov VP, Vykhovanets EV, Slukvin, II, Antipkin YG, Vasyuk AN, Strauss KW (1997) Analysis of blood lymphocyte subsets in children living on territory that received high amounts of fallout from Chernobyl accident. Clinical immunology and immunopathology 84 (2):122-128

Chiu KM, Ju J, Mayes D, Bacchetti P, Weitz S, Arnaud CD (1999) Changes in bone resorption during the menstrual cycle. J Bone Miner Res 14 (4):609-615

Choudhary S, Huang H, Raisz L, Pilbeam C (2008) Anabolic effects of PTH in cyclooxygenase-2 knockout osteoblasts in vitro. Biochemical and biophysical research communications 372 (4):536-541

Christodouleas JP, Forrest RD, Ainsley CG, Tochner Z, Hahn SM, Glatstein E (2011) Short-Term and Long-Term Health Risks of Nuclear-Power-Plant Accidents. The New England journal of medicine

Chu PG, Loera S, Huang Q, Weiss LM (2006) Lineage determination of CD20- B-Cell neoplasms: an immunohistochemical study. American journal of clinical pathology 126 (4):534-544

Chumak A, Thevenon C, Gulaya N, Guichardant M, Margitich V, Bazyka D, Kovalenko A, Lagarde M, Prigent AF (2001) Monohydroxylated fatty acid content in peripheral blood mononuclear cells and immune status of people at long times after the Chernobyl accident. Radiation research 156 (5 Pt 1):476-487

Chung UI, Kawaguchi H, Takato T, Nakamura K (2004) Distinct osteogenic mechanisms of bones of distinct origins. J Orthop Sci 9 (4):410-414

Ciofani M, Zuniga-Pflucker JC (2007) The thymus as an inductive site for T lymphopoiesis. Annual review of cell and developmental biology 23:463-493

Civin CI, Strauss LC, Brovall C, Fackler MJ, Schwartz JF, Shaper JH (1984) Antigenic analysis of hematopoiesis. III. A hematopoietic progenitor cell surface antigen defined by a monoclonal antibody raised against KG-1a cells. J Immunol 133 (1):157-165

Clarke B (2008) Normal bone anatomy and physiology. Clin J Am Soc Nephrol 3 Suppl 3:S131-139

Clarke WJ, Busch RH, Hackett PL (1972) Strontium-90 effects in swine: a summary to date. AEC Symp Ser 25:242-258

Clarke WJ, Palmer RF, Howard EB, Hackett PL, Thomas JM (1970) Strontium-90: effects of chronic ingestion on farrowing performance of miniature swine. Science (New York, NY 169 (945):598-600

Coetzee M, Haag M, Kruger MC (2009) Effects of arachidonic acid and docosahexaenoic acid on differentiation and mineralization of MC3T3-E1 osteoblast-like cells. Cell biochemistry and function 27 (1):3-11

Cohen MM, Jr. (2006) The new bone biology: pathologic, molecular, and clinical correlates. American journal of medical genetics 140 (23):2646-2706

Cohn SH, Lippincott SW, Gusmano EA, Robertson JS (1963) Comparative kinetics of Ca47 and Sr85 in man. Radiation research 19:104-119

Comar CL, Russell RS, Wasserman RH (1957) Strontium-calcium movement from soil to man. Science (New York, NY 126 (3272):485-492

Cooper E, Zeiller, E., Ghods-Esphahani, A., Makarewicz, M., Schelenz, R., Frindik, O., Heilgeist, M., Kalus, W. (1992) Radioactivity in food and total diet samples collected in selected settlements in the USSR. Journal of environmental radioactivity 17:147-157

Cortet B (2010) Use of Strontium as a Treatment Method for Osteoporosis. Current osteoporosis reports

Coulombe J, Faure H, Robin B, Ruat M (2004) In vitro effects of strontium ranelate on the extracellular calcium-sensing receptor. Biochemical and biophysical research communications 323 (4):1184-1190

Courtade M, Caratero A, Jozan S, Pipy B, Caratero C (2001) Influence of continuous, very low-dose gamma-irradiation on the mouse immune system. International journal of radiation biology 77 (5):587-592

Cragle RG, Stone WH, Bacon JA, Wykoff MH (1969) Effects of large doses of orally ingested strontium-90 on young cattle. Radiation research 37 (2):415-422

Cristy M (1981) Active bone marrow distribution as a function of age in humans. Physics in medicine and biology 26 (3):389-400

Czornak K, Chughtai S, Chrzanowska KH (2008) Mystery of DNA repair: the role of the MRN complex and ATM kinase in DNA damage repair. Journal of applied genetics 49 (4):383-396

Dahl SG, Allain P, Marie PJ, Mauras Y, Boivin G, Ammann P, Tsouderos Y, Delmas PD, Christiansen C (2001) Incorporation and distribution of strontium in bone. Bone 28 (4):446-453

Dainiak N (2002) Hematologic consequences of exposure to ionizing radiation. Experimental hematology 30 (6):513-528

Danet GH, Luongo JL, Butler G, Lu MM, Tenner AJ, Simon MC, Bonnet DA (2002) C1qRp defines a new human stem cell population with hematopoietic and hepatic potential. Proceedings of the National Academy of Sciences of the United States of America 99 (16):10441-10445

Davis J, Cook ND, Pither RJ (2000) Biologic mechanisms of 89SrCl2 incorporation into type I collagen during bone mineralization. J Nucl Med 41 (1):183-188

de Ruig WG, van der Struijs TD (1992) Radioactive contamination of food sampled in the areas of the USSR affected by the Chernobyl disaster. The Analyst 117 (3):545-548

Degteva MO, Kozheurov VP, Vorobiova MI (1994) General approach to dose reconstruction in the population exposed as a result of the release of radioactive wastes into the Techa River. The Science of the total environment 142 (1-2):49-61

Delannoy P, Bazot D, Marie PJ (2002) Long-term treatment with strontium ranelate increases vertebral bone mass without deleterious effect in mice. Metabolism: clinical and experimental 51 (7):906-911

Delves P (2011) Riott's essential immunology. 12th edn. Wiley-Blackwell, Oxford

Dempster DW, Cosman F, Parisien M, Shen V, Lindsay R (1993) Anabolic actions of parathyroid hormone on bone. Endocrine reviews 14 (6):690-709

Dexter TM, Allen TD, Lajtha LG (1977) Conditions controlling the proliferation of haemopoietic stem cells in vitro. Journal of cellular physiology 91 (3):335-344

Dick JE, Bhatia M, Gan O, Kapp U, Wang JC (1997) Assay of human stem cells by repopulation of NOD/SCID mice. Stem cells (Dayton, Ohio) 15 Suppl 1:199-203; discussion 204-197

Dingli D, Pacheco JM (2010) Modeling the architecture and dynamics of hematopoiesis. Wiley interdisciplinary reviews 2 (2):235-244

Dion ML, Sekaly RP, Cheynier R (2007) Estimating thymic function through quantification of T-cell receptor excision circles. Methods in molecular biology (Clifton, NJ 380:197-213

Disthabanchong S, Radinahamed P, Stitchantrakul W, Hongeng S, Rajatanavin R (2007) Chronic metabolic acidosis alters osteoblast differentiation from human mesenchymal stem cells. Kidney international 71 (3):201-209

Downie ED, Macpherson S, Ramsden EN, Sissons HA, Vaughan J (1959) The effect of daily feeding of 90 Sr to rabbits. British journal of cancer 13:408-423

Dublineau I, Grandcolas L, Grison S, Baudelin C, Paquet F, Voisin P, Aigueperse J, Gourmelon P (2007) Modifications of inflammatory pathways in rat intestine following chronic ingestion of depleted uranium. Toxicol Sci 98 (2):458-468

Dublineau I, Grison S, Baudelin C, Dudoignon N, Souidi M, Marquette C, Paquet F, Aigueperse J, Gourmelon P (2005) Absorption of uranium through the entire gastrointestinal tract of the rat. International journal of radiation biology 81 (6):473-482

Dudziak ME, Saadeh PB, Mehrara BJ, Steinbrech DS, Greenwald JA, Gittes GK, Longaker MT (2000) The effects of ionizing radiation on osteoblast-like cells in vitro. Plastic and reconstructive surgery 106 (5):1049-1061

Dungworth DL, Goldman M, Switzer J, McKelvie DH (1969) Development of a myeloproliferative disorder in beagles continuously exposed to 90Sr. Blood 34 (5):610-632

Duque G, El Abdaimi K, Macoritto M, Miller MM, Kremer R (2002) Estrogens (E2) regulate expression and response of 1,25-dihydroxyvitamin D3 receptors in bone cells: changes with aging and hormone deprivation. Biochemical and biophysical research communications 299 (3):446-454

Duque G, Macoritto M, Dion N, Ste-Marie LG, Kremer R (2005) 1,25(OH)2D3 acts as a bone-forming agent in the hormone-independent senescence-accelerated mouse (SAM-P/6). American journal of physiology 288 (4):E723-730

Eckerman KF, Stabin MG (2000) Electron absorbed fractions and dose conversion factors for marrow and bone by skeletal regions. Health physics 78 (2):199-214

Euratom (2000) Report 2000/473. Official journal of the European Communities. Luxembourg

Fabbri S, Piva G, Sogni R, Fusconi G, Lusardi E, Borasi G (1994) Transfer kinetics and coefficients of 90Sr, 134Cs, and 137Cs from forage contaminated by Chernobyl fallout to milk of cows. Health physics 66 (4):375-379

Fairlie I (2007) Dispersal, deposition and collective doses after the Chernobyl disaster. Medicine, conflict, and survival 23 (1):10-30

Fina L, Molgaard HV, Robertson D, Bradley NJ, Monaghan P, Delia D, Sutherland DR, Baker MA, Greaves MF (1990) Expression of the CD34 gene in vascular endothelial cells. Blood 75 (12):2417-2426

Finkel M (1960) Life Shortening and Production of Tumors by Strontium-90. Science (New York, NY 132 (3440):1681-1682

Fliedner TM, Nothdurft W, Steinbach KH (1988) Blood cell changes after radiation exposure as an indicator for hemopoietic stem cell function. Bone marrow transplantation 3 (2):77-84

Froidevaux P, Geering JJ, Valley JF (2006) 90Sr in deciduous teeth from 1950 to 2002: the Swiss experience. The Science of the total environment 367 (2-3):596-605

Fu L, Tang T, Miao Y, Hao Y, Dai K (2009) Effect of 1,25-dihydroxy vitamin D3 on fracture healing and bone remodeling in ovariectomized rat femora. Bone 44 (5):893-898

Fujita M (1965) Absorption of Strontium-90 in Man. Health physics 11:47-50

Fujiwara S, Carter RL, Akiyama M, Akahoshi M, Kodama K, Shimaoka K, Yamakido M (1994) Autoantibodies and immunoglobulins among atomic bomb survivors. Radiation research 137 (1):89-95

Gal TJ, Munoz-Antonia T, Muro-Cacho CA, Klotch DW (2000) Radiation effects on osteoblasts in vitro: a potential role in osteoradionecrosis. Archives of otolaryngology--head & neck surgery 126 (9):1124-1128

Galle P (1982) Métabolisme et toxicité du Strontium. In: Toxiques nucléaires. Masson, Paris, pp 78-102

Galle P (1997) Métabolisme et toxicité du Strontium. In: Toxiques nucléaires. 2e edition edn. Masson, Paris, pp 105-122

Garner E, Costanzo V (2009) Studying the DNA damage response using in vitro model systems. DNA repair 8 (9):1025-1037

Garnero P, Ferreras M, Karsdal MA, Nicamhlaoibh R, Risteli J, Borel O, Qvist P, Delmas PD, Foged NT, Delaisse JM (2003) The type I collagen fragments ICTP and CTX reveal distinct enzymatic pathways of bone collagen degradation. J Bone Miner Res 18 (5):859-867

Gass ML, Kagan R, Kohles JD, Martens MG (2008) Bone turnover marker profile in relation to the menstrual cycle of premenopausal healthy women. Menopause (New York, NY 15 (4 Pt 1):667-675

Geenen V, Poulin JF, Dion ML, Martens H, Castermans E, Hansenne I, Moutschen M, Sekaly RP, Cheynier R (2003) Quantification of T cell receptor rearrangement excision circles to estimate thymic function: an important new tool for endocrine-immune physiology. The Journal of endocrinology 176 (3):305-311

Geoffroy V, Chappard D, Marty C, Libouban H, Ostertag A, Lalande A, de Vernejoul MC (2010) Strontium ranelate decreases the incidence of new caudal vertebral fractures in a growing mouse model with spontaneous fractures by improving bone microarchitecture. Osteoporos Int

George-Gay B, Parker K (2003) Understanding the complete blood count with differential. J Perianesth Nurs 18 (2):96-114; quiz 115-117

Germain RN (2002) T-cell development and the CD4-CD8 lineage decision. Nature reviews 2 (5):309-322

Gevorgyan A, Sukhu B, Alman BA, Bristow RG, Pang CY, Forrest CR (2008) Radiation effects and radioprotection in MC3T3-E1 mouse calvarial osteoblastic cells. Plastic and reconstructive surgery 122 (4):1025-1035

Gillett NA, Pool RR, Taylor GN, Muggenburg BA, Boecker BB (1992) Strontium-90 induced bone tumours in beagle dogs: effects of route of exposure and dose rate. International journal of radiation biology 61 (6):821-831

Gillett NA, Muggenburg BA, Boecker BB, Griffith WC, Hahn FF, McClellan RO (1987a) Single inhalation exposure to 90SrCl2 in the beagle dog: late biological effects. Journal of the National Cancer Institute 79 (2):359-376

Gillett NA, Muggenburg BA, Boecker BB, Hahn FF, Seiler FA, Rebar AH, Jones RK, McClellan RO (1987b) Single inhalation exposure to 90SrCl2 in the beagle dog: hematological effects. Radiation research 110 (2):267-288

Gothot A, Pyatt R, McMahel J, Rice S, Srour EF (1997) Functional heterogeneity of human CD34(+) cells isolated in subcompartments of the G0 /G1 phase of the cell cycle. Blood 90 (11):4384-4393

Graf B, Lafuma J (1963) [Effects of Contamination by Strontium-90 in Growing Rats]. International journal of radiation biology and related studies in physics, chemistry, and medicine 7:601-617

Gran FC (1960) Studies on calcium and strontium-90 metabolism in rats. Acta physiologica Scandinavica Supplementum 48 (167):1-109

Grande T, Bueren JA (2004) A new approach to evaluate the total reserve of hematopoietic progenitors after acute irradiation. Radiation research 162 (4):397-404

Gratwohl A, John L, Baldomero H, Roth J, Tichelli A, Nissen C, Lyman SD, Wodnar-Filipowicz A (1998) FLT-3 ligand provides hematopoietic protection from total body irradiation in rabbits. Blood 92 (3):765-769

Grignard E, Gueguen Y, Grison S, Lobaccaro JM, Gourmelon P, Souidi M (2008) In vivo effects of chronic contamination with 137 cesium on testicular and adrenal steroidogenesis. Archives of toxicology 82 (9):583-589

Gueguen Y, Lestaevel P, Grandcolas L, Baudelin C, Grison S, Jourdain JR, Gourmelon P, Souidi M (2008) Chronic contamination of rats with 137 cesium radionuclide: impact on the cardiovascular system. Cardiovascular toxicology 8 (1):33-40

Hanada R, Hanada T, Sigl V, Schramek D, Penninger JM (2011) RANKL/RANK-beyond bones. Journal of molecular medicine (Berlin, Germany) 89 (7):647-656

Handl J, Beltz D, Botsch W, Harb S, Jakob D, Michel R, Romantschuk LD (2003) Evaluation of radioactive exposure from 137Cs in contaminated areas of Northern Ukraine. Health physics 84 (4):502-517

Hannum C, Culpepper J, Campbell D, McClanahan T, Zurawski S, Bazan JF, Kastelein R, Hudak S, Wagner J, Mattson J, et al. (1994) Ligand for FLT3/FLK2 receptor tyrosine kinase regulates growth of haematopoietic stem cells and is encoded by variant RNAs. Nature 368 (6472):643-648

Harrison DE (1980) Competitive repopulation: a new assay for long-term stem cell functional capacity. Blood 55 (1):77-81

Harrison GE, Carr TE, Sutton A (1967) Distribution of radioactive calcium, strontium, barium and radium following intravenous injection into a healthy man. International journal of radiation biology and related studies in physics, chemistry, and medicine 13 (3):235-247

Haylock DN, Nilsson SK (2006) Osteopontin: a bridge between bone and blood. British journal of haematology 134 (5):467-474

Hennecke J, Wiley DC (2001) T cell receptor-MHC interactions up close. Cell 104 (1):1-4

Hirose K, Takatani S, Aoyama M (1993) Wet deposition of radionuclides derived from the Chernobyl accident. J Atmos Chem 17:61-71

Hogan SP, Rosenberg HF, Moqbel R, Phipps S, Foster PS, Lacy P, Kay AB, Rothenberg ME (2008) Eosinophils: biological properties and role in health and disease. Clin Exp Allergy 38 (5):709-750

Hole DJ, Gillis CR, Sumner D (1993) Childhood cancer in birth cohorts with known levels of strontium-90. Health reports / Statistics Canada, Canadian Centre for Health Information = Rapports sur la sante / Statistique Canada, Centre canadien d'information sur la sante 5 (1):39-43

Hollriegl V, Li WB, Oeh U (2006a) Human biokinetics of strontium--part II: Final data evaluation of intestinal absorption and urinary excretion of strontium in human subjects after stable tracer administration. Radiation and environmental biophysics 45 (3):179-185

Hollriegl V, Li WB, Oeh U, Roth P (2006b) Methods for assessing gastrointestinal absorption of strontium in humans by stable tracer techniques. Health physics 90 (3):232-240

Hopkins BJ, Casarett GW, Baxter RC, Tuttle LW (1966) A roentgenographic study of terminal pathological changes in skeletons of strontium-90 treated rats. Radiation research 29 (1):39-49

Hoshi M, Yamamoto M, Kawamura H, Shinohara K, Shibata Y, Kozlenko MT, Takatsuji T, Yamashita S, Namba H, Yokoyama N, et al. (1994) Fallout radioactivity in soil and

food samples in the Ukraine: measurements of iodine, plutonium, cesium, and strontium isotopes. Health physics 67 (2):187-191

Hotchkiss CE, Brommage R (2000) Changes in bone turnover during the menstrual cycle in cynomolgus monkeys. Calcified tissue international 66 (3):224-228

Howard EB, Clarke WJ (1970) Induction of hematopoietic neoplasms in miniature swine by chronic feeding of strontium-90. Journal of the National Cancer Institute 44 (1):21-38

Howard EB, Jannke CC (1970) Immunosuppressive effect of chronic Strontium-90 administration to miniature swine. Experientia 26 (7):785

Howard EB, Clarke WJ, Karagianes MT, Palmer RF (1969) Strontium-90-induced bone tumors in miniature swine. Radiation research 39 (3):594-607

Hoyes KP, Hendry JH, Lord BI (2000) Modification of murine adult haemopoiesis and response to methyl nitrosourea following exposure to radiation at different developmental stages. International journal of radiation biology 76 (1):77-85

Huchet A, Belkacemi Y, Frick J, Prat M, Muresan-Kloos I, Altan D, Chapel A, Gorin NC, Gourmelon P, Bertho JM (2003) Plasma Flt-3 ligand concentration correlated with radiation-induced bone marrow damage during local fractionated radiotherapy. International journal of radiation oncology, biology, physics 57 (2):508-515

Hudak S, Leach MW, Xu Y, Menon S, Rennick D (1998) Radioprotective effects of flk2/flt3 ligand. Experimental hematology 26 (6):515-522

Hughes DE, Dai A, Tiffee JC, Li HH, Mundy GR, Boyce BF (1996) Estrogen promotes apoptosis of murine osteoclasts mediated by TGF-beta. Nature medicine 2 (10):1132-1136

ICRP (1979) Limits for Intakes of Radionuclides. In: Annals of the ICRP, vol 2. Pergamon Pess, Oxford,

ICRP (1993) Age-dependent doses to members of the public from intake of radionuclides, part 2. Ingestion dose coefficients. Publication 67. In: Annals of the ICRP, vol 23. vol 3-4. Pergamon press, Oxford,

ICRP (2001) Doses to the embryo and fetus from intakes of radionuclides by the mother. In: Annals of the ICRP, vol 31. Pergamon Press, Oxford, pp 1-518

ICRP (2006) Human alimentary tract model for radiological protection. Publication 100. In: Annals of the ICRP, vol 36. vol 1-2. Pergamon press, Oxford,

ICRP (2008) Environmental protection: the concept and use of reference animals and plants. Annals of the ICRP 38 (4-6):1-242

Jager A, Kuchroo VK (2010) Effector and regulatory T-cell subsets in autoimmunity and tissue inflammation. Scandinavian journal of immunology 72 (3):173-184

Kalyan S, Prior JC (2010) Bone changes and fracture related to menstrual cycles and ovulation. Critical reviews in eukaryotic gene expression 20 (3):213-233

Kargacin B, Kostial K (1982) The influence of various ingredients of rat food on the absorption of radiostrontium in rats. Arhiv za higijenu rada i toksikologiju 33 (2):185-191

Kashparov VA, Lundin SM, Khomutinin YV, Kaminsky SP, Levchuk SE, Protsak VP, Kadygrib AM, Zvarich SI, Yoschenko VI, Tschiersch J (2001) Soil contamination with 90Sr in the near zone of the Chernobyl accident. Journal of environmental radioactivity 56 (3):285-298

Kidd P (2003) Th1/Th2 balance: the hypothesis, its limitations, and implications for health and disease. Altern Med Rev 8 (3):223-246

Komori T (2006) Regulation of osteoblast differentiation by transcription factors. Journal of cellular biochemistry 99 (5):1233-1239

Komori T (2009) Regulation of bone development and extracellular matrix protein genes by RUNX2. Cell and tissue research

Kossenko MM (1996) Cancer mortality in the exposed population of the Techa River area. World health statistics quarterly 49 (1):17-21

Kossenko MM, Izhevsky PV, Degteva MO, Akleev AV, Vyushkova OV (1994) Pregnancy outcome and early health status of children born to the Techa River population. The Science of the total environment 142 (1-2):91-100

Kossenko MM, Degteva MO, Vyushkova OV, Preston DL, Mabuchi K, Kozheurov VP (1997) Issues in the comparison of risk estimates for the population in the Techa River region and atomic bomb survivors. Radiation research 148 (1):54-63

Kulev YD, Polikarpov GG, Prigodey EV, Assimakopoulos PA (1994) Strontium-90 concentrations in human teeth in south Ukraine, 5 years after the Chernobyl accident. The Science of the total environment 155 (3):215-219

Kulp JL, Schulert AR, Hodges EJ (1960) Strontium-90 in man. IV. Science (New York, NY 132:448-454

Kuzmenok O, Potapnev M, Potapova S, Smolnikova V, Rzheutsky V, Yarilin AA, Savino W, Belyakov IM (2003) Late effects of the Chernobyl radiation accident on T cell-mediated immunity in cleanup workers. Radiation research 159 (1):109-116

Lacoste-Collin L, Jozan S, Cances-Lauwers V, Pipy B, Gasset G, Caratero C, Courtade-Saidi M (2007) Effect of continuous irradiation with a very low dose of gamma rays on life span and the immune system in SJL mice prone to B-cell lymphoma. Radiation research 168 (6):725-732

Laharrague P, Larrouy D, Fontanilles AM, Truel N, Campfield A, Tenenbaum R, Galitzky J, Corberand JX, Penicaud L, Casteilla L (1998) High expression of leptin by human bone marrow adipocytes in primary culture. Faseb J 12 (9):747-752

Lam BS, Adams GB (2010) Hematopoietic stem cell lodgment in the adult bone marrow stem cell niche. International journal of laboratory hematology 32 (6 Pt 2):551-558

Langier S, Sade K, Kivity S (2010) Regulatory T cells: The suppressor arm of the immune system. Autoimmunity reviews 10 (2):112-115

Laver J (1989) Radiobiological properties of human hematopoietic and stromal marrow cells. International journal of cell cloning 7 (4):203-212

Lawson J (1994) Catalog of known and putative nuclear explosions from unclassified sources. Oklahoma Geological Survey Observatory, Oklahoma, US

Lebrec H, Kerdine S, Gaspard I, Pallardy M (2001) Th(1)/Th(2) responses to drugs. Toxicology 158 (1-2):25-29

Leeuwenkamp OR, van der Vijgh WJ, Husken BC, Lips P, Netelenbos JC (1990) Human pharmacokinetics of orally administered strontium. Calcified tissue international 47 (3):136-141

Leggett RW (1992) A generic age-specific biokinetic model for calcium-like elements. Radiat Protect Dosim 41 (2):183-198

Leggett RW, Eckerman KF, Williams LR (1982) Strontium-90 in bone: a case study in age-dependent dosimetric modeling. Health physics 43 (3):307-322

Leggett RW, Williams LR, Melo DR, Lipsztein JL (2003) A physiologically based biokinetic model for cesium in the human body. The Science of the total environment 317 (1-3):235-255

Lemischka IR, Moore KA (2003) Stem cells: interactive niches. Nature 425 (6960):778-779

Lestaevel P, Grandcolas L, Paquet F, Voisin P, Aigueperse J, Gourmelon P (2008) Neuro-inflammatory response in rats chronically exposed to (137)Cesium. Neurotoxicology 29 (2):343-348

Lestaevel P, Dhieux B, Tourlonias E, Houpert P, Paquet F, Voisin P, Aigueperse J, Gourmelon P (2006) Evaluation of the effect of chronic exposure to 137Cesium on sleep-wake cycle in rats. Toxicology 226 (2-3):118-125

Lestaevel P, Racine R, Bensoussan H, Rouas C, Gueguen Y, Dublineau I, Bertho JM, Gourmelon P, Jourdain JR, Souidi M (2010) Césium 137 : propriétés et effets biologiques après contamination interne. Médecine Nucléaire 34 (2):108-118

Li WB, Hollriegl V, Roth P, Oeh U (2006) Human biokinetics of strontium. Part I: intestinal absorption rate and its impact on the dose coefficient of 90Sr after ingestion. Radiation and environmental biophysics 45 (2):115-124

Li WB, Hollriegl V, Roth P, Oeh U (2008) Influence of human biokinetics of strontium on internal ingestion dose of 90Sr and absorbed dose of 89Sr to organs and metastases. Radiation and environmental biophysics 47 (2):225-239

Li Z, Li L (2006) Understanding hematopoietic stem-cell microenvironments. Trends in biochemical sciences 31 (10):589-595

Lindop PJ, Rotblat J (1962) The age factor in the susceptibility of man and animals to radiation. I. The age factor in radiation sensitivity in mice. The British journal of radiology 35:23-31

Lisovsky M, Braun SE, Ge Y, Takahira H, Lu L, Savchenko VG, Lyman SD, Broxmeyer HE (1996) Flt3-ligand production by human bone marrow stromal cells. Leukemia 10 (6):1012-1018

Livak KJ, Schmittgen TD (2001) Analysis of relative gene expression data using real-time quantitative PCR and the 2(-Delta Delta C(T)) Method. Methods (San Diego, Calif 25 (4):402-408

Lloyd RD, Mays CW, Atherton DR, Taylor GN, Van Dilla MA (1976) Retention and skeletal dosimetry of injected 226Ra, 228Ra, and 90Sr in bealges. Radiation research 66 (2):274-287

Lorenzo J (2000) Interactions between immune and bone cells: new insights with many remaining questions. The Journal of clinical investigation 106 (6):749-752

Lorenzo J, Horowitz M, Choi Y (2008) Osteoimmunology: interactions of the bone and immune system. Endocrine reviews 29 (4):403-440

Luster MI, Portier C, Pait DG, White KL, Jr., Gennings C, Munson AE, Rosenthal GJ (1992) Risk assessment in immunotoxicology. I. Sensitivity and predictability of immune tests. Fundam Appl Toxicol 18 (2):200-210

Luster MI, Portier C, Pait DG, Rosenthal GJ, Germolec DR, Corsini E, Blaylock BL, Pollock P, Kouchi Y, Craig W, et al. (1993) Risk assessment in immunotoxicology. II. Relationships between immune and host resistance tests. Fundam Appl Toxicol 21 (1):71-82

Lymperi S, Horwood N, Marley S, Gordon MY, Cope AP, Dazzi F (2008) Strontium can increase some osteoblasts without increasing hematopoietic stem cells. Blood 111 (3):1173-1181

MacDonald N, Hutchinson, DL., Hepler, M. (1962) The bidirectional transport of radiostrontium across the primate placenta. Radiation research 17:752-766

Mackie EJ, Ahmed YA, Tatarczuch L, Chen KS, Mirams M (2008) Endochondral ossification: how cartilage is converted into bone in the developing skeleton. The international journal of biochemistry & cell biology 40 (1):46-62

MacPhail SH, Banath JP, Yu Y, Chu E, Olive PL (2003) Cell cycle-dependent expression of phosphorylated histone H2AX: reduced expression in unirradiated but not X-irradiated G1-phase cells. Radiation research 159 (6):759-767

Mangano JJ, Sherman JD (2011) Elevated in vivo strontium-90 from nuclear weapons test fallout among cancer decedents: a case-control study of deciduous teeth. Int J Health Serv 41 (1):137-158

Mangano JJ, Gould JM, Sternglass EJ, Sherman JD, McDonnell W (2003) An unexpected rise in strontium-90 in US deciduous teeth in the 1990s. The Science of the total environment 317 (1-3):37-51

Mantovani A, Cassatella MA, Costantini C, Jaillon S (2011) Neutrophils in the activation and regulation of innate and adaptive immunity. Nature reviews 11 (8):519-531

Marie P (2001) Différenciation, fonction et contrôle de l'ostéoblaste. Médecine/Sciences 17 (12):1252-1259

Marie PJ (1984) Effect of stable strontium on bone metabolism in rats. In: Priest ND (ed) Metals in bone. MTP Press, Lancaster, England,

Marie PJ (2006) Strontium ranelate: a physiological approach for optimizing bone formation and resorption. Bone 38 (2 Suppl 1):S10-14

Marie PJ (2009) Bone cell-matrix protein interactions. Osteoporos Int 20 (6):1037-1042

Marie PJ, Ammann P, Boivin G, Rey C (2001) Mechanisms of action and therapeutic potential of strontium in bone. Calcified tissue international 69 (3):121-129

Martin C, Burdon PC, Bridger G, Gutierrez-Ramos JC, Williams TJ, Rankin SM (2003) Chemokines acting via CXCR2 and CXCR4 control the release of neutrophils from the bone marrow and their return following senescence. Immunity 19 (4):583-593

Martinez-Agosto JA, Mikkola HK, Hartenstein V, Banerjee U (2007) The hematopoietic stem cell and its niche: a comparative view. Genes & development 21 (23):3044-3060

Masuyama R, Stockmans I, Torrekens S, Van Looveren R, Maes C, Carmeliet P, Bouillon R, Carmeliet G (2006) Vitamin D receptor in chondrocytes promotes osteoclastogenesis and regulates FGF23 production in osteoblasts. The Journal of clinical investigation 116 (12):3150-3159

Matthews W, Jordan CT, Wiegand GW, Pardoll D, Lemischka IR (1991) A receptor tyrosine kinase specific to hematopoietic stem and progenitor cell-enriched populations. Cell 65 (7):1143-1152

McClanahan T, Culpepper J, Campbell D, Wagner J, Franz-Bacon K, Mattson J, Tsai S, Luh J, Guimaraes MJ, Mattei MG, Rosnet O, Birnbaum D, Hannum CH (1996) Biochemical and genetic characterization of multiple splice variants of the Flt3 ligand. Blood 88 (9):3371-3382

McClellan RO, Kerr ME, Bustard LL (1963) Reproductive performance of female miniature swine ingesting strontium-90 daily. Nature 197:670-671

McKenna HJ, Stocking KL, Miller RE, Brasel K, De Smedt T, Maraskovsky E, Maliszewski CR, Lynch DH, Smith J, Pulendran B, Roux ER, Teepe M, Lyman SD, Peschon JJ (2000) Mice lacking flt3 ligand have deficient hematopoiesis affecting hematopoietic progenitor cells, dendritic cells, and natural killer cells. Blood 95 (11):3489-3497

Moller AP, Mousseau TA (2006) Biological consequences of Chernobyl: 20 years on. Trends in ecology & evolution (Personal edition) 21 (4):200-207

Momeni MH, Jow N, Bradley E (1976a) 90Sr-90Y dose distribution in beagles: injection relative to ingestion. Health physics 30 (1):3-19

Momeni MH, Williams JR, Jow N, Rosenblatt LS (1976b) Dose rates, dose and time effects of 90Sr + 90Y and 226Ra on beagle skeleton. Health physics 30 (5):381-390

Moore KA (2004) Recent advances in defining the hematopoietic stem cell niche. Current opinion in hematology 11 (2):107-111

Morgan SL (2001) Calcium and vitamin D in osteoporosis. Rheumatic diseases clinics of North America 27 (1):101-130

Morohashi T, Sano T, Yamada S (1994) Effects of strontium on calcium metabolism in rats. I. A distinction between the pharmacological and toxic doses. Japanese journal of pharmacology 64 (3):155-162

Morrison SJ, Kimble J (2006) Asymmetric and symmetric stem-cell divisions in development and cancer. Nature 441 (7097):1068-1074

Morrison SJ, Shah NM, Anderson DJ (1997) Regulatory mechanisms in stem cell biology. Cell 88 (3):287-298

Mosmann TR, Cherwinski H, Bond MW, Giedlin MA, Coffman RL (1986) Two types of murine helper T cell clone. I. Definition according to profiles of lymphokine activities and secreted proteins. J Immunol 136 (7):2348-2357

Moysich KB, McCarthy P, Hall P (2011) 25 years after Chernobyl: lessons for Japan? The lancet oncology 12 (5):416-418

Muck K, Sinojmeri M, Whilidal H, Steger F (2001) The long-term decrease of 90Sr availability in the environment and its transfer to man after a nuclear fallout. Radiation protection dosimetry 94 (3):251-259

Müller J (1966) Stydy of internal contamination with strontium-90 and radium-226 in man in relation to clinical findings. Health physics 12:993-1006

Nagaoka H, Mochida Y, Atsawasuwan P, Kaku M, Kondoh T, Yamauchi M (2008) 1,25(OH)2D3 regulates collagen quality in an osteoblastic cell culture system. Biochemical and biophysical research communications 377 (2):674-678

Nagasawa T, Omatsu Y, Sugiyama T (2011) Control of hematopoietic stem cells by the bone marrow stromal niche: the role of reticular cells. Trends in immunology 32 (7):315-320

Nakano Y, Addison WN, Kaartinen MT (2007) ATP-mediated mineralization of MC3T3-E1 osteoblast cultures. Bone 41 (4):549-561

Nathan C (2006) Neutrophils and immunity: challenges and opportunities. Nature reviews 6 (3):173-182

Nemazee D (2000) Receptor selection in B and T lymphocytes. Annual review of immunology 18:19-51

Nie H, Richardson RB (2009) Radiation dose to trabecular bone marrow stem cells from (3)H, (14)C and selected alpha-emitters incorporated in a bone remodeling compartment. Physics in medicine and biology 54 (4):963-979

Nilsson A (1970) Pathologic effects of different doses of radiostrontium in mice. Changes in the haematopoietic system. Acta radiologica: therapy, physics, biology 9 (6):528-544

Nilsson A, Book SA (1987) Occurrence and distribution of bone tumors in beagle dogs exposed to 90Sr. Acta oncologica (Stockholm, Sweden) 26 (2):133-138

Nilsson SK, Johnston HM, Whitty GA, Williams B, Webb RJ, Denhardt DT, Bertoncello I, Bendall LJ, Simmons PJ, Haylock DN (2005) Osteopontin, a key component of the hematopoietic stem cell niche and regulator of primitive hematopoietic progenitor cells. Blood 106 (4):1232-1239

Okada S, Nakauchi H, Nagayoshi K, Nishikawa S, Miura Y, Suda T (1992) In vivo and in vitro stem cell function of c-kit- and Sca-1-positive murine hematopoietic cells. Blood 80 (12):3044-3050

Osawa M, Hanada K, Hamada H, Nakauchi H (1996) Long-term lymphohematopoietic reconstitution by a single CD34-low/negative hematopoietic stem cell. Science (New York, NY 273 (5272):242-245

Outola I, Saxen RL, Heinavaara S (2009) Transfer of 90Sr into fish in Finnish lakes. Journal of environmental radioactivity 100 (8):657-664

Paasikallio A, Rantavaara A, Sippola J (1994) The transfer of cesium-137 and strontium-90 from soil to food crops after the Chernobyl accident. The Science of the total environment 155 (2):109-124

Palmer RF, Thompson RC (1961) Discrimination in intestinal absorption of strontium and calcium. Proceedings of the Society for Experimental Biology and Medicine Society for Experimental Biology and Medicine (New York, NY 108:296-300

Papworth DG, Vennart J (1984) The uptake and turnover of 90Sr in the human skeleton. Physics in medicine and biology 29 (9):1045-1061

Parks NJ, Book SA, Pool RR (1984) Squamous cell carcinoma in the jaws of beagles exposed to 90Sr throughout life: beta flux measurements at the mandible and tooth surfaces and a hypothesis for tumorigenesis. Radiation research 100 (1):139-156

Peremyslova LM, Kostiuchenko VA, Popova I, Safronova NG (2009) [Radioecological situation in the Iset riverside settlements]. Radiatsionnaia biologiia, radioecologiia / Rossiiskaia akademiia nauk 49 (6):714-720

Perez AV, Picotto G, Carpentieri AR, Rivoira MA, Peralta Lopez ME, Tolosa de Talamoni NG (2008) Minireview on regulation of intestinal calcium absorption. Emphasis on molecular mechanisms of transcellular pathway. Digestion 77 (1):22-34

Pi M, Quarles LD (2004) A novel cation-sensing mechanism in osteoblasts is a molecular target for strontium. J Bone Miner Res 19 (5):862-869

Pi M, Faber P, Ekema G, Jackson PD, Ting A, Wang N, Fontilla-Poole M, Mays RW, Brunden KR, Harrington JJ, Quarles LD (2005) Identification of a novel extracellular cation-sensing G-protein-coupled receptor. The Journal of biological chemistry 280 (48):40201-40209

Pittenger MF, Mackay AM, Beck SC, Jaiswal RK, Douglas R, Mosca JD, Moorman MA, Simonetti DW, Craig S, Marshak DR (1999) Multilineage potential of adult human mesenchymal stem cells. Science (New York, NY 284 (5411):143-147

Pors NS (2004) The biological role of strontium. Bone 35 (3):583-588

Porter RL, Calvi LM (2008) Communications between bone cells and hematopoietic stem cells. Archives of biochemistry and biophysics 473 (2):193-200

Prat M, Demarquay C, Frick J, Dudoignon N, Thierry D, Bertho JM (2006) Use of flt3 ligand to evaluate residual hematopoiesis after heterogeneous irradiation in mice. Radiation research 166 (3):504-511

Pratt CW (1957) Observations on osteogenesis in the femur of the foetal rat. Journal of anatomy 91 (4):533-544

Preston RJ (2004) Children as a sensitive subpopulation for the risk assessment process. Toxicology and applied pharmacology 199 (2):132-141

Prysyazhnyuk A, Gristchenko V, Fedorenko Z, Gulak L, Fuzik M, Slipenyuk K, Tirmarche M (2007) Twenty years after the Chernobyl accident: solid cancer incidence in various groups of the Ukrainian population. Radiation and environmental biophysics 46 (1):43-51

Putyatin YV, Seraya TM, Petrykevich OM, Howard BJ (2006) Comparison of the accumulation of (137)Cs and (90)Sr by six spring wheat varieties. Radiation and environmental biophysics 44 (4):289-298

Quarles LD (2008) Endocrine functions of bone in mineral metabolism regulation. The Journal of clinical investigation 118 (12):3820-3828

Quarles LD, Yohay DA, Lever LW, Caton R, Wenstrup RJ (1992) Distinct proliferative and differentiated stages of murine MC3T3-E1 cells in culture: an in vitro model of osteoblast development. J Bone Miner Res 7 (6):683-692

Quinn R (2005) Comparing rat's to human's age: how old is my rat in people years? Nutrition (Burbank, Los Angeles County, Calif 21 (6):775-777

Raabe OG, Parks NJ, Book SA (1981a) Dose-response relationships for bone tumors in beagles exposed to 226Ra and 90Sr. Health physics 40 (6):863-880

Raabe OG, Book SA, Parks NJ, Chrisp CE, Goldman M (1981b) Lifetime studies of 226Ra and 90Sr toxicity in beagles--a status report. Radiation research 86 (3):515-528

Racine R, Grandcolas L, Blanchardon E, Gourmelon P, Veyssiere G, Souidi M (2010a) Hepatic cholesterol metabolism following a chronic ingestion of cesium-137 starting at fetal stage in rats. Journal of radiation research 51 (1):37-45

Racine R, Grandcolas L, Grison S, Gourmelon P, Gueguen Y, Veyssiere G, Souidi M (2009) Molecular modifications of cholesterol metabolism in the liver and the brain after chronic contamination with cesium 137. Food Chem Toxicol 47 (7):1642-1647

Racine R, Grandcolas L, Grison S, Stefani J, Delissen O, Gourmelon P, Veyssiere G, Souidi M (2010b) Cholesterol 7alpha-hydroxylase (CYP7A1) activity is modified after chronic ingestion of depleted uranium in the rat. The Journal of steroid biochemistry and molecular biology 120 (1):60-66

Ramos CA, Venezia TA, Camargo FA, Goodell MA (2003) Techniques for the study of adult stem cells: be fruitful and multiply. BioTechniques 34 (3):572-578, 580-574, 586-591

Rappold I, Ziegler BL, Kohler I, Marchetto S, Rosnet O, Birnbaum D, Simmons PJ, Zannettino AC, Hill B, Neu S, Knapp W, Alitalo R, Alitalo K, Ullrich A, Kanz L, Buhring HJ (1997) Functional and phenotypic characterization of cord blood and bone marrow subsets expressing FLT3 (CD135) receptor tyrosine kinase. Blood 90 (1):111-125

Renaud P, Beaugelin C, Maubert H, Ledenvic P (1999) Les retombés en France de l'accident de Tchernobyl: Conséquences radioécologiques et dosimétriques. EDP Sciences, Paris

Riis BJ (1996) The role of bone turnover in the pathophysiology of osteoporosis. British journal of obstetrics and gynaecology 103 Suppl 13:9-14; discussion 14-15

Roch-Lefevre S, Mandina T, Voisin P, Gaetan G, Mesa JE, Valente M, Bonnesoeur P, Garcia O, Voisin P, Roy L (2010) Quantification of gamma-H2AX foci in human lymphocytes: a method for biological dosimetry after ionizing radiation exposure. Radiation research 174 (2):185-194

Rolink AG, Massa S, Balciunaite G, Ceredig R (2006) Early lymphocyte development in bone marrow and thymus. Swiss medical weekly 136 (43-44):679-683

Rosnet O, Buhring HJ, deLapeyriere O, Beslu N, Lavagna C, Marchetto S, Rappold I, Drexler HG, Birg F, Rottapel R, Hannum C, Dubreuil P, Birnbaum D (1996) Expression and signal transduction of the FLT3 tyrosine kinase receptor. Acta haematologica 95 (3-4):218-223

Rothenberg ME, Hogan SP (2006) The eosinophil. Annual review of immunology 24:147-174

Ruhmann AG, Stover BJ, Brizzee KR, Atherton DR (1963) Placental Transfer of Strontium in Rats. Radiation research 20:484-492

Russell JH, Ley TJ (2002) Lymphocyte-mediated cytotoxicity. Annual review of immunology 20:323-370

Ryabokon NI, Smolich, II, Kudryashov VP, Goncharova RI (2005) Long-term development of the radionuclide exposure of murine rodent populations in Belarus after the Chernobyl accident. Radiation and environmental biophysics 44 (3):169-181

Sakaguchi S, Sakaguchi N, Asano M, Itoh M, Toda M (1995) Immunologic self-tolerance maintained by activated T cells expressing IL-2 receptor alpha-chains (CD25). Breakdown of a single mechanism of self-tolerance causes various autoimmune diseases. J Immunol 155 (3):1151-1164

Samadfam R, Xia Q, Miao D, Hendy GN, Goltzman D (2008) Exogenous PTH and endogenous 1,25-dihydroxyvitamin D are complementary in inducing an anabolic effect on bone. J Bone Miner Res 23 (8):1257-1266

Schroeder JT (2009) Basophils beyond effector cells of allergic inflammation. Advances in immunology 101:123-161

Segal AW (2005) How neutrophils kill microbes. Annual review of immunology 23:197-223

Sekitani Y, Hayashida N, Karevskaya IV, Vasilitsova OA, Kozlovsky A, Omiya M, Yamashita S, Takamura N (2010) Evaluation of (137)Cs body burden in inhabitants of Bryansk Oblast, Russian Federation, where a high incidence of thyroid cancer was observed after the accident at the Chernobyl nuclear power plant. Radiation protection dosimetry 141 (1):36-42

Sempowski GD, Gooding ME, Liao HX, Le PT, Haynes BF (2002) T cell receptor excision circle assessment of thymopoiesis in aging mice. Molecular immunology 38 (11):841-848

Senyuk OF, Kavsan VM, Muller WE, Schroder HC (2002) Long-term effects of low-dose irradiation on human health. Cellular and molecular biology (Noisy-le-Grand, France) 48 (4):393-409

Shagina NB, Tolstykh EI, Degteva MO (2003a) Improvements in the biokinetic model for strontium with allowance for age and gender differences in bone mineral metabolism. Radiation protection dosimetry 105 (1-4):619-622

Shagina NB, Tolstykh EI, Zalyapin VI, Degteva MO, Kozheurov VP, Tokareva EE, Anspaugh LR, Napier BA (2003b) Evaluation of age and gender dependences of the rate of strontium elimination 25-45 years after intake: analysis of data from residents living along the Techa river. Radiation research 159 (2):239-246

Shi HZ (2004) Eosinophils function as antigen-presenting cells. Journal of leukocyte biology 76 (3):520-527

Shibata S, Yamashita Y (2001) An ultrastructural study of osteoclasts and chondroclasts in poorly calcified mandible induced by high doses of strontium diet to fetal mice. Ann Anat 183 (4):357-361

Shibata T, Shira-Ishi A, Sato T, Masaki T, Masuda A, Hishiya A, Ishikura N, Higashi S, Uchida Y, Saito MO, Ito M, Ogata E, Watanabe K, Ikeda K (2002) Vitamin D hormone inhibits osteoclastogenesis in vivo by decreasing the pool of osteoclast precursors in bone marrow. J Bone Miner Res 17 (4):622-629

Shresta S, Pham CT, Thomas DA, Graubert TA, Ley TJ (1998) How do cytotoxic lymphocytes kill their targets? Current opinion in immunology 10 (5):581-587

Shutov VN, Travnikov IG, Bruk GY, Golikov VY, Balonov MI, Howard BJ, Brown J, Strand P, Kravtsova EM, Gavrilov AP, Kravtsova OS, Mubasarov AA (2002) Current contamination by 137Cs and 90Sr of the inhabited part of the Techa river basin in the Urals. Journal of environmental radioactivity 61 (1):91-109

Sila-Asna M, Bunyaratvej A, Maeda S, Kitaguchi H, Bunyaratavej N (2007) Osteoblast differentiation and bone formation gene expression in strontium-inducing bone marrow mesenchymal stem cell. The Kobe journal of medical sciences 53 (1-2):25-35

Simmons PJ, Torok-Storb B (1991) CD34 expression by stromal precursors in normal human adult bone marrow. Blood 78 (11):2848-2853

Souidi M, Tissandie E, Grandcolas L, Grison S, Paquet F, Voisin P, Aigueperse J, Gourmelon P, Gueguen Y (2006) Chronic contamination with 137cesium in rat: effect on liver cholesterol metabolism. International journal of toxicology 25 (6):493-497

Spangrude GJ, Heimfeld S, Weissman IL (1988) Purification and characterization of mouse hematopoietic stem cells. Science (New York, NY 241 (4861):58-62

Srivastava S, Weitzmann MN, Cenci S, Ross FP, Adler S, Pacifici R (1999) Estrogen decreases TNF gene expression by blocking JNK activity and the resulting production of c-Jun and JunD. The Journal of clinical investigation 104 (4):503-513

Srivastava S, Weitzmann MN, Kimble RB, Rizzo M, Zahner M, Milbrandt J, Ross FP, Pacifici R (1998) Estrogen blocks M-CSF gene expression and osteoclast formation by regulating phosphorylation of Egr-1 and its interaction with Sp-1. The Journal of clinical investigation 102 (10):1850-1859

Stabin MG, Peterson TE, Holburn GE, Emmons MA (2006) Voxel-based mouse and rat models for internal dose calculations. J Nucl Med 47 (4):655-659

Stamoulis KC, Assimakopoulos PA, Ioannides KG, Johnson E, Soucacos PN (1999) Strontium-90 concentration measurements in human bones and teeth in Greece. The Science of the total environment 229 (3):165-182

Sugihira N, Kobayashi E, Suzuki KT (1990) Age-related changes in strontium to calcium ratios in rat tissues. Biological trace element research 25 (1):79-88

Suzuki K, Okada H, Yamauchi M, Oka Y, Kodama S, Watanabe M (2006) Qualitative and quantitative analysis of phosphorylated ATM foci induced by low-dose ionizing radiation. Radiation research 165 (5):499-504

Svoboda V, Klener V (1972) Effect of incorporated 226 Ra on colony forming units of bone marrow and spleen in mice. Acta radiologica: therapy, physics, biology 11 (5):472-480

Svoboda V, Sedlak A, Bubenikova D, Kotaskova Z, Truxova O (1985) Self-renewal capacity of murine hemopoietic stem cells under internal contamination with 239Pu and 241Am. Radiation and environmental biophysics 24 (3):203-209

Synhaeve N, Stefani J, Tourlonias E, Dublineau I, Bertho JM (2011) Biokinetics of (90)Sr after chronic ingestion in a juvenile and adult mouse model. Radiation and environmental biophysics 50 (4): 501-11

Szabo SJ, Kim ST, Costa GL, Zhang X, Fathman CG, Glimcher LH (2000) A novel transcription factor, T-bet, directs Th1 lineage commitment. Cell 100 (6):655-669

Szilvassy SJ, Cory S (1993) Phenotypic and functional characterization of competitive long-term repopulating hematopoietic stem cells enriched from 5-fluorouracil-treated murine marrow. Blood 81 (9):2310-2320

Szymczyk KH, Shapiro IM, Adams CS (2004) Ionizing radiation sensitizes bone cells to apoptosis. Bone 34 (1):148-156

Taichman RS (2005) Blood and bone: two tissues whose fates are intertwined to create the hematopoietic stem-cell niche. Blood 105 (7):2631-2639

Taichman RS, Emerson SG (1994) Human osteoblasts support hematopoiesis through the production of granulocyte colony-stimulating factor. The Journal of experimental medicine 179 (5):1677-1682

Taichman RS, Emerson SG (1998) The role of osteoblasts in the hematopoietic microenvironment. Stem cells (Dayton, Ohio) 16 (1):7-15

Takahashi N, Sasaki T, Tsouderos Y, Suda T (2003) S 12911-2 inhibits osteoclastic bone resorption in vitro. J Bone Miner Res 18 (6):1082-1087

Takatsuji T, Sato H, Takada J, Endo S, Hoshi M, Sharifov VF, Veselkina, II, Pilenko IV, Kalimullin WA, Masyakin VB, Kovalev AI, Yoshikawa I, Okajima S (2000) Relationship between the 137Cs whole-body counting results and soil and food contamination in farms near Chernobyl. Health physics 78 (1):86-89

Takayanagi H (2007) Osteoimmunology: shared mechanisms and crosstalk between the immune and bone systems. Nature reviews 7 (4):292-304

Taooka Y, Takeichi N, Noso Y, Kawano N, Apsalikov KN, Hoshi M (2006) Increased T-cell receptor mutation frequency in radiation-exposed residents living near the Semipalatinsk nuclear test site. Journal of radiation research 47 Suppl A:A179-181

Tarasova A, Haylock D, Winkler D (2011) Principal signalling complexes in haematopoiesis: Structural aspects and mimetic discovery. Cytokine & growth factor reviews

Tarrant JM (2010) Blood cytokines as biomarkers of in vivo toxicity in preclinical safety assessment: considerations for their use. Toxicol Sci 117 (1):4-16

Tavian M, Peault B (2005) The changing cellular environments of hematopoiesis in human development in utero. Experimental hematology 33 (9):1062-1069

Terstappen LW, Huang S, Safford M, Lansdorp PM, Loken MR (1991) Sequential generations of hematopoietic colonies derived from single nonlineage-committed CD34+CD38- progenitor cells. Blood 77 (6):1218-1227

Thompson DL, Lum KD, Nygaard SC, Kuestner RE, Kelly KA, Gimble JM, Moore EE (1998) The derivation and characterization of stromal cell lines from the bone marrow of p53-/- mice: new insights into osteoblast and adipocyte differentiation. J Bone Miner Res 13 (2):195-204

Till JE, Mc Culloch EA (1961) A direct measurement of the radiation sensitivity of normal mouse bone marrow cells. Radiation research 14:213-222

Tissandie E, Gueguen Y, Lobaccaro JM, Aigueperse J, Souidi M (2006) [Vitamin D: metabolism, regulation and associated diseases]. Med Sci (Paris) 22 (12):1095-1100

Tissandie E, Gueguen Y, Lobaccaro JM, Grandcolas L, Grison S, Aigueperse J, Souidi M (2009) Vitamin D metabolism impairment in the rat's offspring following maternal exposure to (137)cesium. Archives of toxicology

Titov LP, Kharitonic GD, Gourmanchuk IE, Ignatenko SI (1995) Effects of radiation on the production of immunoglobulins in children subsequent to the Chernobyl disaster. Allergy Proc 16 (4):185-193

Tolstykh EI, Peremyslova LM, Shagina NB, Degteva MO (2010) [90Sr in residents of the Iset riverside settlements]. Radiatsionnaia biologiia, radioecologiia / Rossiiskaia akademiia nauk 50 (1):90-97

Tolstykh EI, Shagina NB, Degteva MO, Anspaugh LR, Napier BA (2011a) Does the cortical bone resorption rate change due to (90)Sr-radiation exposure? Analysis of data from Techa Riverside residents. Radiation and environmental biophysics

Tolstykh EI, Shagina NB, Peremyslova LM, Degteva MO, Phipps AW, Harrison JD, Fell TP (2008) Reconstruction of (90)Sr intake for breast-fed infants in the Techa riverside settlements. Radiation and environmental biophysics 47 (3):349-357

Tolstykh EI, Degteva MO, Peremyslova LM, Shagina NB, Shishkina EA, Krivoshchapov VA, Anspaugh LR, Napier BA (2011b) Reconstruction of long-lived radionuclide intakes for techa riverside residents: strontium-90. Health physics 101 (1):28-47

Toyoda S, Hino Y, Romanyukha AA, Tarasov O, Pivovarov SP, Hoshi M (2010) 90Sr in mammal teeth from contaminated areas in the former Soviet Union measured by imaging plates. Health physics 98 (2):352-359

Tsumaki N, Yoshikawa H (2005) The role of bone morphogenetic proteins in endochondral bone formation. Cytokine & growth factor reviews 16 (3):279-285

Uccelli A, Moretta L, Pistoia V (2008) Mesenchymal stem cells in health and disease. Nature reviews 8 (9):726-736

UNSCEAR (2000) Annex J: Exposures and effects of the Chernobyl accident. Sources and effects of ionizing radiation. United Nations, New-York

UNSCEAR (2011) Annex D: Health effects due to radiation from the Chernobyl accident. Sources and effects of ionizing radiation. United Nations, New-York

Vaaraniemi J, Halleen JM, Kaarlonen K, Ylipahkala H, Alatalo SL, Andersson G, Kaija H, Vihko P, Vaananen HK (2004) Intracellular machinery for matrix degradation in bone-resorbing osteoclasts. J Bone Miner Res 19 (9):1432-1440

Valverde P, Zhang J, Fix A, Zhu J, Ma W, Tu Q, Chen J (2008) Overexpression of bone sialoprotein leads to an uncoupling of bone formation and bone resorption in mice. J Bone Miner Res 23 (11):1775-1788

Verfaillie CM (1993) Soluble factor(s) produced by human bone marrow stroma increase cytokine-induced proliferation and maturation of primitive hematopoietic progenitors while preventing their terminal differentiation. Blood 82 (7):2045-2053

von Zallinger C, Tempel K (1998) Transplacental transfer of radionuclides. A review. Zentralblatt fur Veterinarmedizin 45 (10):581-590

Vremec D, Shortman K (1997) Dendritic cell subtypes in mouse lymphoid organs: cross-correlation of surface markers, changes with incubation, and differences among thymus, spleen, and lymph nodes. J Immunol 159 (2):565-573

Vykhovanets EV, Chernyshov VP, Slukvin, II, Antipkin YG, Vasyuk A, Colos V (2000) Analysis of blood lymphocyte subsets in children living around Chernobyl exposed

long-term to low doses of cesium-137 and various doses of iodine-131. Radiation research 153 (6):760-772

Wang D, Christensen K, Chawla K, Xiao G, Krebsbach PH, Franceschi RT (1999) Isolation and characterization of MC3T3-E1 preosteoblast subclones with distinct in vitro and in vivo differentiation/mineralization potential. J Bone Miner Res 14 (6):893-903

Wang Y, Cui X, Tai G, Ge J, Li N, Chen F, Yu F, Liu Z (2009) A critical role of activin A in maturation of mouse peritoneal macrophages in vitro and in vivo. Cellular & molecular immunology 6 (5):387-392

Warabi S, Tachibana Y, Kumegawa M, Hakeda Y (2001) Dexamethasone inhibits bone resorption by indirectly inducing apoptosis of the bone-resorbing osteoclasts via the action of osteoblastic cells. Cytotechnology 35 (1):25-34

Wasserman RH (1963) Over-all aspects of calcium and strontium absorption. In: The transfer of calcium and strontium across biological membranes. Academic Press, New York, pp 85-95

White RG, Raabe OG, Culbertson MR, Parks NJ, Samuels SJ, Rosenblatt LS (1993) Bone sarcoma characteristics and distribution in beagles fed strontium-90. Radiation research 136 (2):178-189

WHO (2011) Guidelines for drinking-water quality, fourth edition. 4th edition. World Health Organisation, Geneva

Widdowson EM, Slater JE, Harrison GE, Sutton A (1960) Absorption, excretion, and retention of strontium by breast-fed and bottle-fed babies. Lancet 2 (7157):941-944

Windahl SH, Andersson N, Chagin AS, Martensson UE, Carlsten H, Olde B, Swanson C, Moverare-Skrtic S, Savendahl L, Lagerquist MK, Leeb-Lundberg LM, Ohlsson C (2009) The role of the G protein-coupled receptor GPR30 in the effects of estrogen in ovariectomized mice. American journal of physiology 296 (3):E490-496

Wiseman G (1964) Calcium, Strontium, Magnesium and Phosphate. In: Absorption from the intestine. Academic press, New York, pp 235-240

Witko-Sarsat V, Rieu P, Descamps-Latscha B, Lesavre P, Halbwachs-Mecarelli L (2000) Neutrophils: molecules, functions and pathophysiological aspects. Laboratory investigation; a journal of technical methods and pathology 80 (5):617-653

Wodnar-Filipowicz A (2003) Flt3 ligand: role in control of hematopoietic and immune functions of the bone marrow. News Physiol Sci 18:247-251

Wognum AW, Eaves AC, Thomas TE (2003) Identification and isolation of hematopoietic stem cells. Archives of medical research 34 (6):461-475

Wright DE, Bowman EP, Wagers AJ, Butcher EC, Weissman IL (2002) Hematopoietic stem cells are uniquely selective in their migratory response to chemokines. The Journal of experimental medicine 195 (9):1145-1154

Wu J, Glimcher LH, Aliprantis AO (2008) HCO3-/Cl- anion exchanger SLC4A2 is required for proper osteoclast differentiation and function. Proceedings of the National Academy of Sciences of the United States of America 105 (44):16934-16939

Xing L, Boyce BF (2005) Regulation of apoptosis in osteoclasts and osteoblastic cells. Biochemical and biophysical research communications 328 (3):709-720

Xu F, Zhang X, Liu J, Fan M (1997) [The effects of strontium in drinking water on growth and development of rat bone]. Wei sheng yan jiu = Journal of hygiene research 26 (3):172-178

Yahata T, Ando K, Sato T, Miyatake H, Nakamura Y, Muguruma Y, Kato S, Hotta T (2003) A highly sensitive strategy for SCID-repopulating cell assay by direct injection of primitive human hematopoietic cells into NOD/SCID mice bone marrow. Blood 101 (8):2905-2913

Yamashita M, Ukai-Tadenuma M, Miyamoto T, Sugaya K, Hosokawa H, Hasegawa A, Kimura M, Taniguchi M, DeGregori J, Nakayama T (2004) Essential role of GATA3 for the maintenance of type 2 helper T (Th2) cytokine production and chromatin remodeling at the Th2 cytokine gene loci. The Journal of biological chemistry 279 (26):26983-26990

Yarilin AA, Belyakov IM, Kusmenok OI, Arshinov VY, Simonova AV, Nadezhina NM, Gnezditskaya EV (1993) Late T cell deficiency in victims of the Chernobyl radiation accident: possible mechanisms of induction. International journal of radiation biology 63 (4):519-528

Yokota T, Meka CS, Kouro T, Medina KL, Igarashi H, Takahashi M, Oritani K, Funahashi T, Tomiyama Y, Matsuzawa Y, Kincade PW (2003) Adiponectin, a fat cell product, influences the earliest lymphocyte precursors in bone marrow cultures by activation of the cyclooxygenase-prostaglandin pathway in stromal cells. J Immunol 171 (10):5091-5099

Yoshitake H, Rittling SR, Denhardt DT, Noda M (1999) Osteopontin-deficient mice are resistant to ovariectomy-induced bone resorption. Proceedings of the National Academy of Sciences of the United States of America 96 (14):8156-8160

Zallone A (2006) Direct and indirect estrogen actions on osteoblasts and osteoclasts. Annals of the New York Academy of Sciences 1068:173-179

Zapol'skaya NA, Borisova VV, Zhorno LU (1974) Comparison of the biological effects of strontium-90, cesium-137, iodine-131, and external radiation. In: Third internat congress of the internat radiation protection association. US Atomic Energy Commission, Springfield, VA, pp pp. 147-152

Zhang J, Niu C, Ye L, Huang H, He X, Tong WG, Ross J, Haug J, Johnson T, Feng JQ, Harris S, Wiedemann LM, Mishina Y, Li L (2003) Identification of the haematopoietic stem cell niche and control of the niche size. Nature 425 (6960):836-841

Zhu J, Emerson SG (2004) A new bone to pick: osteoblasts and the haematopoietic stem-cell niche. Bioessays 26 (6):595-599

Zhu J, Garrett R, Jung Y, Zhang Y, Kim N, Wang J, Joe GJ, Hexner E, Choi Y, Taichman RS, Emerson SG (2007) Osteoblasts support B-lymphocyte commitment and differentiation from hematopoietic stem cells. Blood 109 (9):3706-3712

Ziegler BL, Valtieri M, Porada GA, De Maria R, Muller R, Masella B, Gabbianelli M, Casella I, Pelosi E, Bock T, Zanjani ED, Peschle C (1999) KDR receptor: a key marker defining hematopoietic stem cells. Science (New York, NY 285 (5433):1553-1558

Le Strontium 90 (^{90}Sr) est un radionucléide d'origine anthropogénique, relâché en grandes quantités dans l'environnement à la suite d'essais nucléaires aériens ou d'accidents d'installations nucléaires. Le ^{90}Sr persiste à long terme dans l'environnement, ce qui conduit à la contamination chronique par ingestion de populations des territoires contaminés. L'induction de tumeurs osseuses liées à la fixation du ^{90}Sr a été largement décrite. Par contre, l'occurrence d'effets non cancéreux est beaucoup moins connue. Nous avons utilisé un modèle murin avec une contamination chronique par ingestion d'eau contenant 20 kBq/l de ^{90}Sr. Une étude de biocinétique a confirmé l'accumulation de ^{90}Sr dans les os, avec un taux d'accumulation plus rapide durant la croissance osseuse. Cette accumulation est plus élevée dans les os des femelles que chez les males. Les doses absorbées au corps entier varient de 0.33 ± 0.06 mGy (naissance) à 10.6 ± 0.1 mGy (20 semaines). La dose au squelette peut aller jusqu'à 55 mGy. L'ingestion de ^{90}Sr induit une modification de l'expression des gènes impliqués induisant à un déséquilibre favorisant la résorption osseuse, mais sans répercussion sur la morphologie de l'os. Aucun effet majeur n'a été observé pour le système hématopoïétique. Par contre, des modifications mineures du système immunitaire ont été observées. Afin d'évaluer la fonctionnalité du système immunitaire, un test de vaccination avec les antigènes TT et KLH a été utilisé. Les résultats montrent chez les animaux contaminés une diminution significative de la production d'immunoglobulines spécifiques, une modification de la balance Th1/Th2 dans la rate et une différenciation lymphoïde B perturbée. Ces résultats permettent de mieux comprendre certaines des conséquences non cancéreuses de l'exposition chronique à faible dose à des radionucléides à demi-vie longue pouvant être rejetés accidentellement.

Mots clés : ^{90}Sr, ingestion chronique, faible dose, biocinétique, physiologie osseuse, système hématopoïétique, système immunitaire

Strontium 90 (^{90}Sr) is a radionuclide of anthropogenic origin released in large quantities in the environment as a result of nuclear atmospheric tests or accidents at nuclear facilities. ^{90}Sr persists on a long-term basis in the environment, leading to chronic contamination by ingestion of populations living on contaminated territories. The induction of bone tumours associated with the fixation of ^{90}Sr has been widely described. However, the occurrence of non-cancer effects is much less known. We used a mouse model with chronic contamination by ingestion of water containing 20 kBq/l of ^{90}Sr. A biokinetic study confirmed the accumulation of ^{90}Sr in the bones, with an increased rate of accumulation during bone growth. This accumulation was higher in the bones of females than in males. The whole-body absorbed doses ranged from 0.33 ± 0.06 mGy (birth) to 10.6 ± 0.1 mGy (20 weeks). The absorbed dose for the skeleton was up to 55 mGy. Ingestion of ^{90}Sr induced a change in the expression of genes inducing an imbalance in favour of bone resorption, but without effect on bone morphology. No significant effect was observed for the hematopoietic system. On the other hand, minor modifications were observed for the immune system. To evaluate the functionality of the immune system, a vaccination test with TT and KLH antigens was used. Results showed in contaminated animals a significant decrease in the production of specific immunoglobulins, changes in the Th1/Th2 balance in the spleen and a disrupted B lymphocyte differentiation. These results improve the understanding of some of the non-cancerous consequences of chronic exposure at low dose of radionuclides with a long half-life, which can be accidentally released.

Keywords : ^{90}Sr, chronic ingestion, low dose, biokinetics, bone physiology, hematopoietic system, immune system